Generation of synthesis gas for fuels and chemicals production

Tunå, Per

2013

Generation of synthesis gas for fuels and chemicals production

Per Tunå

Department of Chemical Engineering
Lund University, Sweden
2013

LUND
UNIVERSITY

Academic thesis which, by due permission of the Faculty of Engineering of Lund University will be publicly defended on 31st of May at 1 pm in Lecture hall K:B at the Centre for Chemistry and Chemical Engineering, Getingevägen 60, Lund, for a degree of Doctor of Philosophy in Chemical Engineering.

The faculty opponent is Dr. Christiaan van der Meijden,
Biomass Energy Engineering, The Netherlands

Generation of synthesis gas for fuels and chemicals production

Printed by Media Tryck, Lund University, Lund 2013

Department of Chemical Engineering
Lund University
P.O. Box 124
SE-221 00 Lund, SWEDEN

ISBN 978-91-7422-321-7

Abstract

Many scientists believe that the oil production will peak in the near future, if the peak has not already occurred. Peak oil theories and uncertain future oil deliveries have stimulated interest in alternative sources of fuel and chemicals. This interest has been enhanced by concerns about energy security and about the climate change caused by emissions of carbon dioxide. The result has been increased interest in substituting fossil fuels with renewable energy sources such as wind, solar and biomass. However, this has proved particularly difficult in the transportation sector.

The most likely source of renewable hydrocarbon fuels for transportation is biomass. It comes in many forms, none of which are suitable for direct use in internal combustion engines and gas turbines. Thus the biomass has to be refined to convert its energy into a more usable form. The most versatile conversion of biomass is thermochemical conversion via gasification and downstream synthesis, which allows the production of both fuels and chemicals.

In the biomass gasification process, a gasifier converts the solid biomass into a gaseous product known as producer gas. The producer gas contains the desired components carbon monoxide and hydrogen, but it also contains water, carbon dioxide, lower hydrocarbons, tars and impurities that need to be removed from the gas. Reforming the tars and hydrocarbons in producer gas is difficult because of the amount of sulphur present.

This thesis investigates the use of reverse-flow reactors to reform the tars and hydrocarbons in biomass generated producer gas.. Reverse-flow reactors operate by periodically reversing the direction of flow to enable high levels of heat recovery. The high heat recovery enables non-catalytic reformers to be operated at efficiencies near that of catalytic reformers. The operation of reverse-flow reactors is investigated experimentally in a tar-cracking reactor using dolomite as bed material and also theoretically using computer models. The investigations show that reverse-flow reactors have great potential, offering a chemically robust alternative to conventional reformers when operating on sulphur-containing biomass-generated

producer gas. Furthermore, operation of reverse-flow tar crackers using dolomite as bed material is an efficient and viable solution for tar removal and syngas boosting.

The producer gas also contains ammonia in varying amounts depending on the gasifier's operating parameters and feedstock. Ammonia can be a poison for catalysts and, if the producer gas is burnt, will produce elevated levels of NO_X in the flue gas. The selective catalytic oxidation of ammonia in synthesis gas was thus also investigated by experiments on a model synthesis gas.

This thesis also covers mass and energy balance calculations to determine the efficiency and economics of synthetic fuels and chemicals plants. Several possible plant configurations were investigated, both stand-alone and integrated. The integration of a pulp and paper mill with a fuel synthesis plant is a very likely scenario as the biomass logistics are already located on-site. Another possible integration scenario involves steel plants, where large quantities of energy-rich gases are handled as off-gases in coke production. Utilisation of this off-gas coupled with biomass gasification was also investigated.

In the stand-alone plants, the difference between reverse-flow reformers and conventional non-catalytic reformers was investigated as front-ends to well-head gas upgrading to produce crude oil via the Fischer-Tropsch synthesis. Furthermore a well-to-wheel comparison of synthetic natural gas, methanol, ethanol, dimethyl ether, Fischer-Tropsch diesel and synthetic gasoline was performed. The comparison used woody biomass as feedstock and computed mass and energy balances for complete plants from gasifier to fuel as well as for lignocellulosic ethanol production by fermentation. Efficiency in regard to feedstock to travel distance (Well-to-Wheel) and the cost of transportation was also investigated.

Ammonia is one of the most valuable chemicals for modern agriculture. Current production is almost entirely based on fossil fuels. Thus small-scale production of ammonia from renewable feedstocks was also investigated.

List of publications

This thesis is based on the work reported in the following. Papers I through III are focused on reverse-flow reforming reactors. Paper IV focuses on selective catalytic oxidation of ammonia. Papers V through IX are focused on system studies of the production of synthetic fuel and chemicals.

I. *Modeling of Reverse-Flow Partial-Oxidation Process for Gasifier Product Gas Upgrading*, P. Tunå, H. Svensson, J. Brandin, Proceedings of the Fifth International Conference on Thermal Engineering: Theory and Applications May 10-14, 2010, Marrakesh, Morocco

II. *Modeling of soot formation during partial oxidation of producer gas,* H. Svensson, P. Tunå, C. Hulteberg, J. Brandin, *Fuel* 106 (2013) 271–278

III. *Regenerative reverse-flow reactor system for cracking of producer gas tars*, P. Tunå, F. Bauer, C. Hulteberg, L. Malek, Submitted

IV. *Selective Catalytic Oxidation of Ammonia by Nitrogen Oxides in a Model Synthesis Gas,* P. Tunå, J. Brandin, Fuel 105 (2013) 331–337

V. *Techno-Economic Assessment of Non-Fossil Ammonia Production*, P. Tunå, C. Hulteberg, S. Ahlgren, Submitted

VI. *Woody biomass-based transportation fuels: A comparative techno-economic study*, P. Tunå, C. Hulteberg, Submitted

VII. *A new process for well-head gas upgrading,* P. Tunå, C. Hulteberg, Journal of Natural Gas Science and Engineering 13 (2013) 1-6

VIII. *Synergies from combined pulp & paper and fuel production,* P. Tunå, C. Hulteberg, J. Hansson, A. Åsblad, E. Andersson, Biomass and Bioengineering 40 (2012) 174–180

IX. *Methanol production form steel-work off-gases and biomass based synthesis gas,* J. Lundgren, T. Ekbom, C. Hulteberg, M. Larsson, C.E. Grip, L. Nilsson, P. Tunå, submitted for publication in *Applied Energy*

My contributions to the papers

I. I wrote the simulation software and developed the model. I also wrote most of the paper.

II. I performed the simulations on the dynamic model and wrote parts of the paper.

III. I designed and built the reactor, analysis equipment and control equipment/software. I designed and performed the experiments and wrote part of the paper.

IV. I performed the experiments and wrote most of the paper.

V. I made the computer models for the mass and energy balances and wrote part of the paper.

VI. I planned the study, created the computer models for the mass and energy balances, and wrote most of the paper.

VII. I made the computer models and wrote parts of the paper.

VIII. I made the computer models for the synthetic fuel plant. I wrote parts of the paper.

IX. I made the computer models for the methanol plant. I wrote parts of the paper.

Populärvetenskaplig sammanfattning

Dagens samhälle är mycket beroende av fordonsbränslen och kemikalier som producerats av råolja. Framtidens tillgång på råolja är oviss, det enda som är säkert är att det är en ändlig resurs. Användningen av olja bidrar dessutom till koldioxidutsläpp till atmosfären. För att säkra framtida tillförsel av energi och kemikalier till samhället och för att uppnå ett mer klimatneutralt samhälle behöver råoljan ersättas med förnybara och hållbara råvaror. Förädlingen av biomassa till drivmedel och kemikalier är ett av alternativen för att uppnå ett fossilfritt samhälle. Förädlingen kan ske antingen via termokemisk eller via biokemisk omvandling. Den termokemiska omvandlingen är den mest flexibla med avseende på möjliga produkter och har dessutom högre verkningsgrad. Termokemisk omvandling av biomassa, som kan vara träflis eller jordbruksrester, kan användas för att producera syntetiska fordonsbränslen, plaster och gummi. En av de termokemiska omvandlingsprocesserna börjar med en förgasare som producerar en energirik gas som kallas syntesgas vilken sedan kan användas för att syntetisera flytande eller gasformiga produkter. Produktgasen från förgasaren innehåller förutom kolmonoxid och vätgas även kolväten, tjäror, koldioxid, vatten samt en del andra föroreningar. Av föroreningarna i gasen är tjärorna det största problemet då de kan förstöra värmeväxlare och annan utrustning.

I detta arbete studerades bland annat apparatur som kan öka verkningsgraden i förädlingen av biomassa till produkter såsom drivmedel och kemikalier. Högre verkningsgrader i processerna leder till mer produkt per råvara och därmed lägre specifika produktionskostnader. En av arbetets huvuddelar är fokuserat på utrustning för att omvandla tjäror och andra kolväten i gas producerad av en förgasare. Den här delen består dels av experimentellt arbete utfört på Institutionen för Kemiteknik och av datormodeller. Resultaten visar på mycket hög omsättning av föroreningarna i gasen med en hög energieffektivitet.

Processerna som används i omvandlingen av biomassa till fordonsbränslen och kemikalier används idag till stor del i naturgasbaserade anläggningar för framställning av bland annat metanol, ammoniak och råmaterial för plasttillverkning. För att biomassabaserad tillverkning ska kunna konkurera med

naturgasbaserad tillverkning och för att använda en begränsad råvara på bästa sätt krävs hög verkningsgrad i processerna.

Datormodeller över tillverkningsanläggningar för framställning av drivmedel och kemikalier kan användas för att beräkna hur mycket produkt som kan produceras från en given mängd råvara, verkningsgrad och vad produktionskostnaden blir för produkten. Ett flertal modeller har konstruerats och använts i detta arbete för att utreda verkningsgrader och kostnader för framställning av olika drivmedel och kemikalier. Tillverkning av följande produkter har studerats; metanol, dimetyleter, syntetisk bensin, syntetisk diesel, syntetisk naturgas samt ammoniak. Resultaten visar att den termokemiska omvandlingen till syntetiska fordonsbränslen har en betydligt högre energiverkningsgrad än etanol tillverkad via biokemisk omvandling av träflis. Samtliga fordonsbränslen tillverkade via termokemisk omvandling har dessutom en lägre produktionskostnad än etanol framställt via biokemisk omvandling. Produktionen av ammoniak från förnyelsebara råvaror har också studerats och visar på en produktionskostnad som kan konkurrera med fossilbaserad ammoniak.

Resultaten av det här arbetet visar på att förnyelsebara fordonsbränslen och kemikalier kan vara konkurrenskraftiga med dagens fossilbaserade alternativ.

Acknowledgements

When I started my PhD studies I did not fully realise what it meant. There have been a lot of people around me that helped me during the years and I would like to express my gratitude to all of you, but the following people deserve special acknowledgments:

Hans T. Karlsson, thank you for your support during the years.

Jan Brandin, thank you for the nice discussions and the time we had at the Department of Chemical Engineering and for always having a positive attitude. See you in Vienna over a schnitzel and a glass of white wine.

Special thank you goes to Christian Hulteberg. Without you I would not have made it this far.

Thank you Laura for being an excellent roommate and for all the funny conversations and discussions we have had.

My gratitude goes out to my colleagues at the Department of Chemical Engineering and especially to Helena and Fredric. You have all contributed to making my five years a wonderful experience.

I also want to thank all the people I have collaborated with in the various papers for the excellent teamwork.

Tack min goa familj för ert stöd! Det har varit fantastiskt.

Lisa. Du är underbar!

Table of Contents

1 Introduction

The industrial world has been using fossil energy for over a century. Coal was the first fossil fuel to be used on a large scale for the production of steam in industry. Coal was also used to heat homes and to produce town gas, a mixture of carbon monoxide, hydrogen and lower hydrocarbons that was distributed to be used as cooking gas. Since then coal has been used mostly for power production, but also for the production of fuels and chemicals via gasification. Gasification will be covered in detail in 2.2 (p. 10).

1.1 Crude oil

The widespread availability of cheap, abundant energy was not realised until the start of large-scale oil production early in the 20th century. Since then, oil has been the most important commodity for modern society. Oil is used for everything from powering cars to the production of plastics and fine chemicals.

The first oil crisis occurred in October 1973. The price of oil rose from $15 to $45 (2009 US$) per barrel (bbl) by 1974. In 1979 the price of oil increased even further as a result of the Iranian revolution and the political decision in the USA to stop all imports of oil from Iran. This caused the second oil crisis, which was further exacerbated by the Iran-Iraq war, starting in September 1980 and ending in 1988. The price of oil went from $45 in 1979 to over $75 per bbl in 1981, with a peak of over $95 (Figure 1).

During both oil crises the world demand for crude oil declined as a result of higher prices, but also because crude oil, which was once thought of as an endless supply of energy, was starting to show its limits. The decline in consumption was also an effect of better energy conservation and increased use of alternative energy sources

such as nuclear energy and natural gas. At the same time crude production increased, resulting in the 1980s oil glut (increased supply with steady or declining demand) with prices of crude again down to around $25 per bbl. The price of crude remained somewhat constant until just before the financial crisis in 2008, when the price peaked at over $145 per bbl. After the financial crisis started to affect businesses, the price fell to around $45 per bbl. The oil price recovered quickly, and three years later it was again above $100 per bbl. It is worth noting that the two major oil trading classifications, Brent, which is oil from the North Sea, and West Texas Intermediate (WTI) have historically traded at the same price. However, in recent years the prices have diverged, and are currently (2013) Brent is trading at around $110 and WTI at $95 per bbl. The reason for this divergence is an oversupply of crude oil in the USA caused by increased energy supply, mostly from Canadian tar sands and shale gas, but also due to the US crude oil export embargo (Energy Policy and Conservation Act of 1975). The export of refined products such as gasoline and diesel is allowed, but with limited refinery capacity and increased crude oil supply, a decrease in crude prices could be expected.

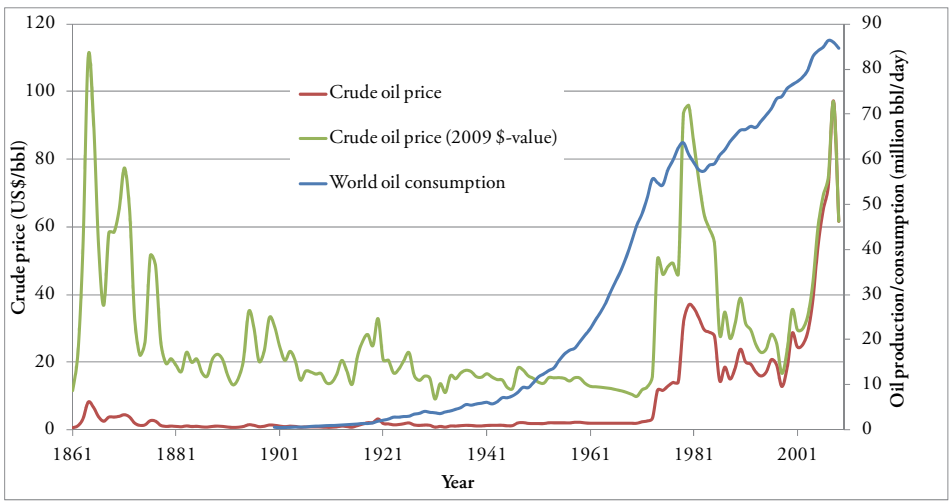

Figure 1: Oil price from 1861 and oil consumption from 1900 to 2009.

The 2008 peak in crude prices, while production was at an all-time high, may be an indication that peak oil has been reached and that the world's oil production is now in decline. However, it is worth noting that crude prices are heavily influenced

by speculation and future demand, and are not only an indication of current usage. World oil consumption is currently (2013) at around 80–85 million bbl per day. There is currently no substitute for oil, given the amount of energy and materials consumed daily. There are, however, alternatives to crude that can be used to produce synthetic oils, fuels and chemicals. In the short term, synthetic fuels and chemicals will allow an increase in both energy and material consumption; later they will enable a phase-out of expensive crude.

1.2 Replacing oil

The production of synthetic oils and fuels started in Germany during the Second World War. Germany was short of oil wells but had abundant reserves of coal. Large underground plants where built during the war and produced most of the gasoline and diesel used by the German army. The technology used was either Fischer-Tropsch synthesis (see 3.1.1, p. 55) or direct coal liquefaction. During the apartheid era in South Africa, there was an oil embargo against the regime. The same technology used by the Germans during the war was used in South Africa to produce fuels and chemicals from coal. The companies producing the synthetic fuels and chemicals in South Africa, Sasol and PetroSA, are still active in the production of synthetic fuels even though the oil embargo has been lifted.

In recent years, large-scale gas-to-liquid (GTL) plants have been built in natural gas-rich countries such as Qatar. The Pearl GTL plant in Qatar has a GTL production of 140 000 bbl per day from an input of 1 600 million standard cubic feet per day (mmscfd). Producing synthetic fuels and chemicals from natural gas is better, both from an environmental (lower CO_2 emissions) and chemical perspective (cleaner feedstock) than producing it from coal.

Ideally, synthetic fuels should be produced from biomass. Unlike coal and natural gas, biomass is renewable. This enables more sustainable production, assuming sustainable management of the feedstock such as forests. Without sustainable resource management, biomass should not be considered a sustainable feedstock. Biomass, however, has numerous problems such as logistics, various impurities and a chemical composition not found in coal or natural gas, with the result that it

requires different catalysts and purifying methods than coal and natural gas. Furthermore, biomass has a lower energy density than oil or coal. It is therefore even more important to preserve as much of the energy as possible by utilising processes that are as efficient as possible. Plants producing synthetic fuels and chemicals using biomass as feedstock are not only converting solids into gaseous or liquid products, they are also concentrating the energy. Due to the logistics problems with biomass, smaller plants (less than 500 MW) are more practical when using biomass as raw material. However, smaller plants have a negative effect on the economies of scale, which makes the product more expensive to produce.

1.3 Aim and scope

The aim of this work is to suggest improvements to critical parts of gas conditioning and outline the processes involved in producing synthetic fuels and chemicals from various feedstocks via thermochemical conversion. A large part of gas cleaning is devoted to the most critical conditioning steps for synthesis gas generated from biomass, namely removing tars and hydrocarbons in sulphur-rich environments. About half of the work in this thesis was directed to the development of models and experimental reforming/tar cracking reactors for reverse-flow operation. Reverse-flow methodology is of particular interest for biomass applications in which sulphur and tars are a major concern, particularly in reforming operations. Reverse-flow reactors offer improved efficiency over traditional unidirectional flow reactors, allowing non-catalytic reactors to operate nearly as efficiently as catalytic reactors without suffering from catalyst deactivation. Experiments were also performed on a new system for the removal of ammonia from synthesis gas at elevated temperatures (>300 °C). Selective catalytic oxidation of ammonia from synthesis gas at elevated temperatures can be beneficial for applications where the synthesis gas is burnt directly, for example in a gas turbine, as this reduces the emissions of NO_X to the environment.

The remaining work focused mostly on the development of thermodynamic models using flowsheeting software to evaluate different systems for the production of fuels and chemicals. Starting from an energy source such as woody biomass or

natural gas, the systems were evaluated for matters such as process efficiency and the cost of producing the end product. The synthetic fuels and chemicals considered include methanol, dimethyl ether, Fischer-Tropsch diesel, synthetic natural gas, synthetic gasoline and ammonia. The plants were evaluated both as stand-alone plants and integrated with other industries such as pulp and paper mills and steel plants.

1.4 Outline of this thesis

This thesis follows the same outline as a plant for synthetic fuel production. First there is a general description of how synthesis gas is produced from solid feedstocks via gasification and from natural gas via reforming. The production of synthesis gas is followed by the critical step of gas conditioning, in which some of the work performed by the author will be described in more detail. Matters dealt with include reverse-flow partial oxidation for secondary reforming and reverse-flow prereforming for tar cracking. Gas conditioning also includes the necessary steps for downstream synthesis such as water-gas shift. The removal of ammonia by selective catalytic oxidation is included in the gas conditioning.

A review of the fuel and chemical syntheses follows the chapters on gas-conditioning, and covers operating parameters, catalysts used, and constraints such as chemical equilibrium.

A chapter on system studies and the various configurations investigated in the papers that are the basis of this thesis follows the description of the different syntheses.

The thesis ends with conclusions on the gas-conditioning configurations presented in the previous chapters and a discussion of the fuels and chemicals considered in the papers.

2 Production of synthesis gas

Synthesis gas or syngas is the name given to gas mixtures containing carbon monoxide (CO) and hydrogen (H_2). Syngas can also contain carbon dioxide (CO_2) and other components such as water (H_2O).

2.1 Overview

Syngas is among the most important building blocks used in the chemical industry. Almost any hydrocarbon can be produced from syngas (Figure 2). Among the more common are methanol and methane.

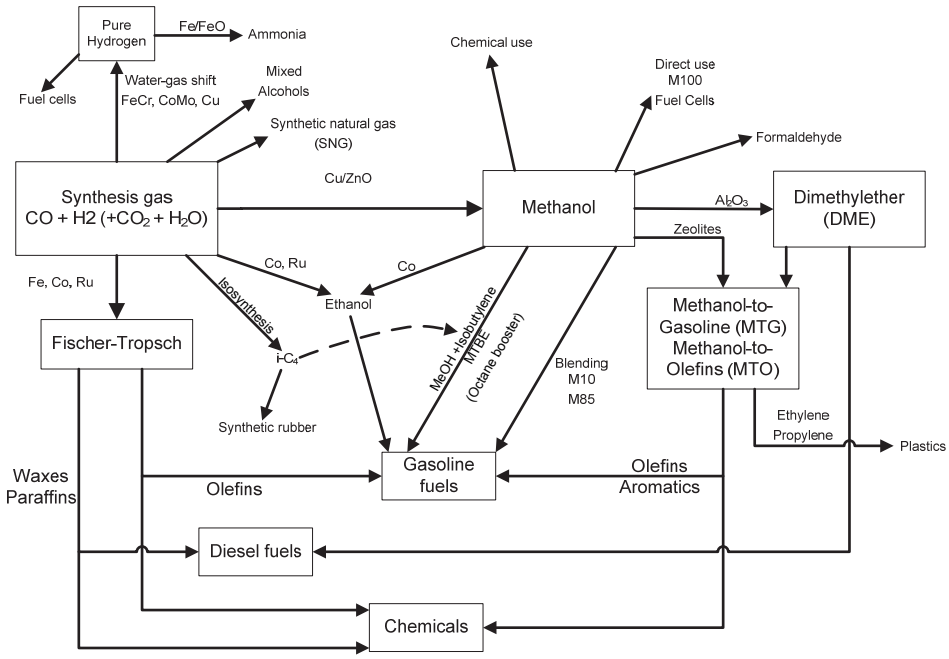

Figure 2: Products from synthesis gas and methanol.

2.1 Overview

Methane produced from syngas is usually called synthetic natural gas (SNG). Syngas is also the intermediate when the desired product is H_2 and the feedstock contains carbon.

As can be seen in Figure 2, all products normally produced from crude oil or natural gas can be produced by chemical synthesis using syngas as the building block. Gasoline and diesel are fuels with definitions not based on their chemical composition but rather on their physical properties, such as boiling and flash point. The octane rating of gasoline is empirical and based on its actual performance in an internal combustion (IC) engine. This means that as long as the synthetic fuel matches the properties of crude oil-based gasoline or diesel, at least low-level blending is possible. Figure 2 also shows products or intermediates that are very important chemicals for our daily life, including ammonia, methanol, formaldehyde and plastic monomers.

The production of fuels and chemicals from synthesis gas via gasification usually follows the scheme shown in Figure 3. If methane obtained either from natural gas or from biogas is used as feedstock, the process starts with removal of sulphur followed by reforming. Depending on the feedstock and end product, different reforming techniques are required (see 2.3; p. 17).

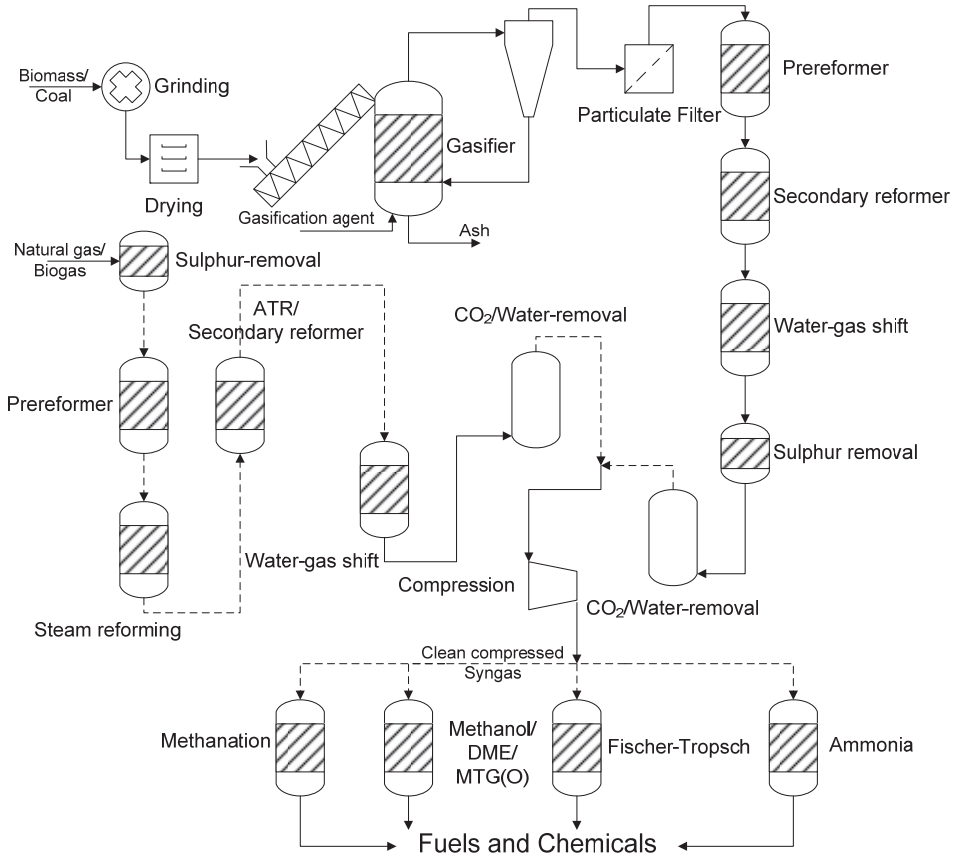

Figure 3: Production of fuels and chemicals from gasification of biomass/coal or reforming of natural gas and downstream processing.

When starting with a solid feedstock such as biomass or coal, the feedstock needs to be gasified. Before gasification the feedstock may need to be ground or pulverised (this is usually the case with coal). The fineness of the particles depends on the type of gasifier. Drying is the next step and is required for most biomass gasification plants. Some gasifiers have the drying integrated into the gasifier reactor vessel.

After gasification the product is a gas, called producer gas, which is full of impurities that need to be removed prior to synthesis. The producer gas also usually needs to have the ratio between H_2 and CO before synthesis. Both H_2:CO

adjustment and removal of impurities are performed in the process known as gas conditioning.

2.2 Gasification

All carbon-containing feedstocks such as coal, heavy oils or biomass that can be combusted can be gasified into synthesis gas. In the gasifier several reactions take place, but the overall reaction can be summarised by reaction (1).

$$C_aH_bO_cN_d + O_2/H_2O/N_2 \rightarrow CO + H_2 + C_xH_yO_z + CO_2 + H_2O + NH_3 + N_2 \quad (1)$$

The solid carbon is partially oxidised with a gasification agent that can be oxygen (O_2), air, steam (H_2O) or a combination of them all. For most gasifiers, $C_xH_yO_z$ consists of mostly methane with some lower hydrocarbons such as ethane and ethylene. Depending on the feedstock used and the operating parameters, the gas can also contain heavier hydrocarbons such as benzene, toluene and naphthalenes. Hydrocarbons heavier than benzene are often referred to as tars.

Gasification is a process that occurs in several steps: drying, pyrolysis, oxidation and reduction. The gasification reactions require heat, which must be supplied to the reactor to maintain the desired temperature. Heat can be supplied either directly by combusting a part of the fuel (autothermal) or indirectly (allothermal). Indirect heating is usually achieved either by heat transfer through the reactor wall or by transfer of heated bed material from another reactor (combustor).

Types of Gasifier

There are several different types of gasifiers, distinguished by the way they convert the fuel. Most operate on coal or heavy oils, but most types can also operate on any carbon-containing feedstock such as biomass. Data for the most common types of gasifier are presented below.

2.2.1 Fixed bed gasifier

Fixed bed gasifiers (sometimes denoted moving bed) are the most common type of gasifier worldwide due to the simplicity of the design. They are also more tolerant with regard to fuel particle size and moisture content than fluidised bed and entrained flow gasifiers. They can be used in a wide range of applications from small-scale biomass gasifiers to large-scale coal gasifiers.

Fixed bed gasifiers have a 'fixed' bed of solid fuel that moves through the gasifier as the solid feedstock is converted into gas. They are divided into downdraft, updraft and crossdraft gasifiers depending on how the gas flows relative to the bed (Figure 4).

In downdraft or co-current gasifiers, the gasification agent flows downwards, in the same direction as the bed is moving. As it exits the gasifier, the producer gas flows through an oxidation zone where tars and hydrocarbons are cracked, yielding a gas with a relatively low tar content. For wood, the tar yield is typically less than 1 wt-% of the dry wood feed [1]. Downdraft gasifiers produce a syngas with a relatively high temperature as the outlet is near the oxidation zone. The high temperature of the producer gas means that downdraft gasifiers have lower efficiency than updraft gasifiers.

In updraft gasifiers, the gasification agent is injected at the bottom of the gasifier. The temperature is highest at the bottom and decreases towards the top. The relatively low temperature at the top allows for the use of rather moist feedstock (< 50 wt-% moisture) compared to downdraft gasifiers (around 20 wt-% moisture) [2]. The produced gas is cooler than the gas produced by a downdraft gasifier, which increases efficiency. However, the gas also contains more tars as it has not passed through an oxidation zone (see Figure 4). Wood-fed updraft gasifiers can have tar yields as high as 12 wt-% of the dry wood feed (almost 20 wt-% of the carbon in the wood feed) [1]. Typical temperatures in the oxidation zone are 800–1000 °C depending on the fuel [3, 4]. The Lurgi Gas Generator is an updraft-type gasifier developed in the 1930s by Lurgi. It is a pressurised coal gasifier operating on feedstocks with a particle size of 13–25 or 25–50 mm, depending on feedstock. The pressure in Lurgi Gas Generators is 25–35 bar [3].

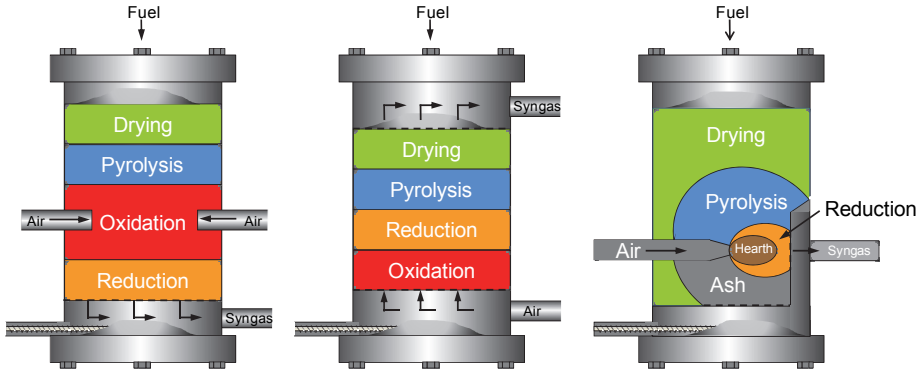

Figure 4: Fixed bed gasifiers. From left to right, downdraft, updraft and crossdraft.

In crossdraft gasifiers, the gasification agent is injected on one side of the gasifier and the outlet is on the opposite side. The reduction zone in a crossdraft gasifier is on the edge nearest the outlet. Drying and pyrolysis occur higher up in the vessel. This results in a high temperature producer gas with a relatively high tar content as the gas does not pass through an oxidation zone before exiting the reactor [5].

Table 1 presents the differences in particulates, tars and lower hydrocarbons for updraft and downdraft fixed bed gasifiers.

Table 1: Tars and particulates from fixed bed gasifiers [6].

Reactor type	Fixed bed (downdraft)	Fixed bed (updraft)
$C_2H_4 + C_3H_6$ [vol-%]	0.2–0.4	1–2.5
Tars [g/Nm^3]	0.05–0.5	10–100
Particulates [g/m^3]	0.1–10	0.1–1.0

Fixed bed gasifiers can produce large amounts of tars and lower hydrocarbons, as shown in Table 1. Tar is not always unwanted in the producer gas. For example, a woodchip updraft gasifier at Harboore in Denmark is used to produce gas with a high tar content (80 g/Nm^3) to be used for heat and power generation. The tar is separated from the gas and used to increase the plant output in the district heating grid during periods of high load (peak-shaving) [7].

2.2.2 Fluidised bed gasifier

Fluidised beds have a more uniform temperature distribution in the reactor than fixed beds, with the result that there are no defined zones (such as drying). This necessitates more stringent pretreatment requirements for the moisture content of the feedstock. As the feedstock must fluidise, there are also more stringent pretreatment requirements regarding particle size.

Fluidising bed gasifiers can be defined as having either a bubbling or a circulating fluidised bed, depending on how the bed moves in the reactor.

In circulating fluidised bed (CFB) gasifiers the bed material circulates between the gasifier and a cyclone where ash and particles are separated from the producer gas and returned to the gasifier. Ashes are typically removed from the returning bed material before entering the gasifier. The gasification agent is injected at the bottom of the reactor at high speed, causing the bed to lift. The bed material is usually a mineral with properties such as high heat capacity, catalytic activity in tar cracking, or adsorption of certain species such as potassium. The bed material in CFBs must have a high mechanical strength to avoid the circulation grinding down the material too quickly.

The bed in bubbling fluidised bed gasifiers (BFB) is much the same as in CFBs, except that there is no circulation to a cyclone. The bed is almost lifted by the gasification agent, but not as much as in a CFB. The gasification agent flows through the bed in bubbles that cause the bed to move or bubble. The reported tar content in gas produced in fluidising bed gasifiers ranges from 1–3 to over 40 g/Nm^3 when using woody biomass as feedstock [1, 2, 8, 9]. Baker et al. have reported tar yields from steam-blown fluidised bed gasifiers, such as those used in twin-bed allothermal gasification, ranging from 4 wt-% up to as high as 15 wt-% of the dry wood feed, depending on operating temperature and feedstock [1]. Boerrigter et al. reported tar yields ranging from 0.5 to 40 g/Nm^3 for the MILENA and Güssing FICFB allothermal gasifiers (see Table 2). Baker et al. concluded that oxygen-blown gasifiers typically produce less tar than air-blown gasifiers [1], possibly due to the higher local temperatures in oxygen-blown gasifiers.

Boerrigter et al. did not draw the same conclusion and presented data that showed higher tar yields for pressurised gasifiers [9].

The major operational difficulty with fluidising beds is the potential for slagging, or melting of the ash in the feedstock. Slagging is mostly a biomass-related problem that can be avoided by lower bed temperatures. However, lowering temperatures decreases the carbon conversion and thus the energy efficiency of the gasifier. (In some entrained flow gasifiers, slagging is wanted as the melted ash protects the reactor wall from the reducing environment and high temperatures).

The Winkler fluidised bed gasifier is a coal-fed gasifier that was developed in the 1920s. The particle size of the coal feed is smaller than 8 mm. The Winkler gasifier was originally an atmospheric gasifier, but has evolved and pressures can go up to 10 bar [3].

The gas composition from three different fluidised bed gasifiers is presented in Table 2. The Värnamo gasification plant located in southern Sweden is a pressurised oxygen-blown fluidised bed. The MILENA gasifier at ECN in Petten, the Netherlands, is a pressurised allothermal fluidised bed gasifier. Lastly, the FICFB, or Fast Internally Circulated Fluidised Bed, in Güssing is a dual fluidised bed gasifier consisting of one combustor and one gasifier.

Table 2: Fluidised bed gasifier gas composition on dry basis.

Component	Värnamo [10]	MILENA [9]	Güssing FICFB [9]
CO [vol-%]	19	40–43	20–30
CO_2 [vol-%]	45	10–12	15–25
H_2 [vol-%]	19	15–20	30–45
CH_4 [vol-%]	13	15–17	8-12
C_2H_4 [vol-%]	2.6	5–6	1–3
NH_3 [vppm]	4800	500–1000	500–1000
Tars [g/Nm^3]	25–30	40	0.5–1.5
H_2S [vppm]	160	40–100	50–120

2.2.3 Entrained flow gasifier

Entrained flow gasifiers are high throughput reactors with low residence times and high temperatures. In an entrained flow gasifier a very fine powdered fuel is injected into the reactor vessel along with oxygen or oxygen and steam. A high temperature is obtained (1600–1900 °C) and therefore short residence times are sufficient to achieve high carbon conversions (90–99 %) allowing the reactors to have high throughput [3]. In most cases the high temperature results in a gas free from tars and hydrocarbons.

The high performance of the entrained flow gasifier comes at the expense of fuel pretreatment requirements. A very fine powder is required (around 0.1 mm) for most gasifiers to allow fluidisation of the solid feedstock [11]. This constraint on the feedstock makes it difficult to use unprocessed biomass. Torrefaction, a thermal process that produces charcoal from wood, has been proposed as a solution to address the fluidisation properties of biomass and to make it more thermally stable [12]. The entrained flow gasifier is the most common gasification reactor operating worldwide on a large scale. Among the most common entrained flow gasifiers are Koppers-Totzek (coal), Shell (coal) and Texaco (low grade fuels, such as heavy residual oil and other refinery by-products) [3].

Table 3 presents the producer gas composition of a biomass entrained flow gasifier. Although no sulphur is shown in the table (not reported in the original data), almost all of the sulphur in the biomass should end up in the gas, with only small amounts remaining in the ashes. As the entrained flow gasifier produces a gas with almost no hydrocarbons, organic sulphur should be almost non-existent, and all the sulphur should be present as either H_2S and COS.

Table 3: Entrained flow gasifier producer gas composition (dry) [9].

Component	Composition
CO [vol-%]	41
CO_2 [vol-%]	15
H_2 [vol-%]	21
H_2O [vol-%]	22
CH_4 [vol-%]	0
$C_2H_4 + C_3H_6$ [vol-%]	0
Tars [g/Nm^3]	0
Particulates [g/m^3]	–

2.2.4 Molten media and supercritical gasifiers

The last type of gasifier is the molten media reactor in which the feedstock is dispersed in a molten carrier. The carrier generally provides heat for the gasification and can participate in the gasification if it contains catalytically active species such as nickel or iron. The major advantages of molten media reactors are the high heat transfer rates, as the molten media is the heat source, and the ability of the molten media to absorb contaminants in the feedstock, mainly sulphur and alkalis. Molten media reactors can have a high temperature depending on the molten media and can accept most feedstocks. The disadvantage is that the processes must handle the molten media. For molten salts this can become very troublesome as the media are highly corrosive [13].

Under supercritical conditions (T > 374.8 °C, P > 221 bar) water reacts with biomass to produce a gas rich in hydrogen and methane. The water self-dissociates to form both H_3O^+ and OH^- ions that act as catalysts for converting the biomass into gas [14]. Gas composition from supercritical water gasification of biomass below 400 °C typically has high methane (CH_4) and CO_2 content and low H_2 content [14-16]. Above 400 °C the H_2 content increases and the CH_4 content decreases [15]. CO content during supercritical gasification at a temperature below 600 °C is several orders of magnitude lower than H_2, CO_2 and CH_4 [15, 16]. This

gas composition has an unfavourable H_2:CO ratio for downstream chemical synthesis, which requires a H_2:CO ratio of 2-3:1.

The advantage of supercritical gasification is its ability to use wet biomass (> 70 wt-% water content) that would be too costly to dry for traditional gasifiers. This enables supercritical gasifiers to use feedstocks such as manure or sewage sludge. However, these feedstocks are already often used as feedstocks in anaerobic digestion for the production of biogas.

2.3 Reforming

Reforming is a process very similar to gasification, in which a gaseous or liquid feedstock is converted into synthesis gas.

$$CH_4 + H_2O \rightleftharpoons CO + 3H_2 \qquad \Delta H^0_{298} = +206\text{kJ/mol} \qquad (2)$$

$$CO + H_2O \rightleftharpoons CO_2 + H_2 \qquad \Delta H^0_{298} = -41\text{kJ/mol} \qquad (3)$$

$$C_nH_m + nH_2O \rightleftharpoons nCO + (n + \tfrac{1}{2}m)H_2 \qquad \Delta H^0_{298} = +1175\text{kJ/mol (for n-}C_7H_{15}\text{)} \ [17] \qquad (4)$$

$$CH_4 + 2O_2 \rightarrow CO_2 + 2H_2O \qquad \Delta H^0_{298} = -890\text{kJ/mol} \qquad (5)$$

$$CH_4 + \tfrac{1}{2}O_2 \rightarrow CO + 2H_2 \qquad \Delta H^0_{298} = -36\text{kJ/mol} \qquad (6)$$

$$CH_4 + CO_2 \rightleftharpoons 2CO + 2H_2 \qquad \Delta H^0_{298} = +247\text{kJ/mol} \qquad (7)$$

Reactions (2–4) are basically the same as for gasification, except that in reforming both the reactant and product are gases. Reforming is highly endothermic as can be seen by the standard enthalpy of change for reactions (2, 4 and 7) above. Reaction (7) is also known as dry reforming and is a combination of reactions (1 and 2). Furthermore, reforming is equilibrium bound and high temperatures (> 800 °C) are required for adequate conversions of methane. Higher pressures are desired for increased throughputs but are unfavourable for the equilibrium, necessitating even higher temperatures as shown in Figure 5. In most cases downstream processes are

operated at high pressures and having the product gas already pressurised is better for overall efficiency.

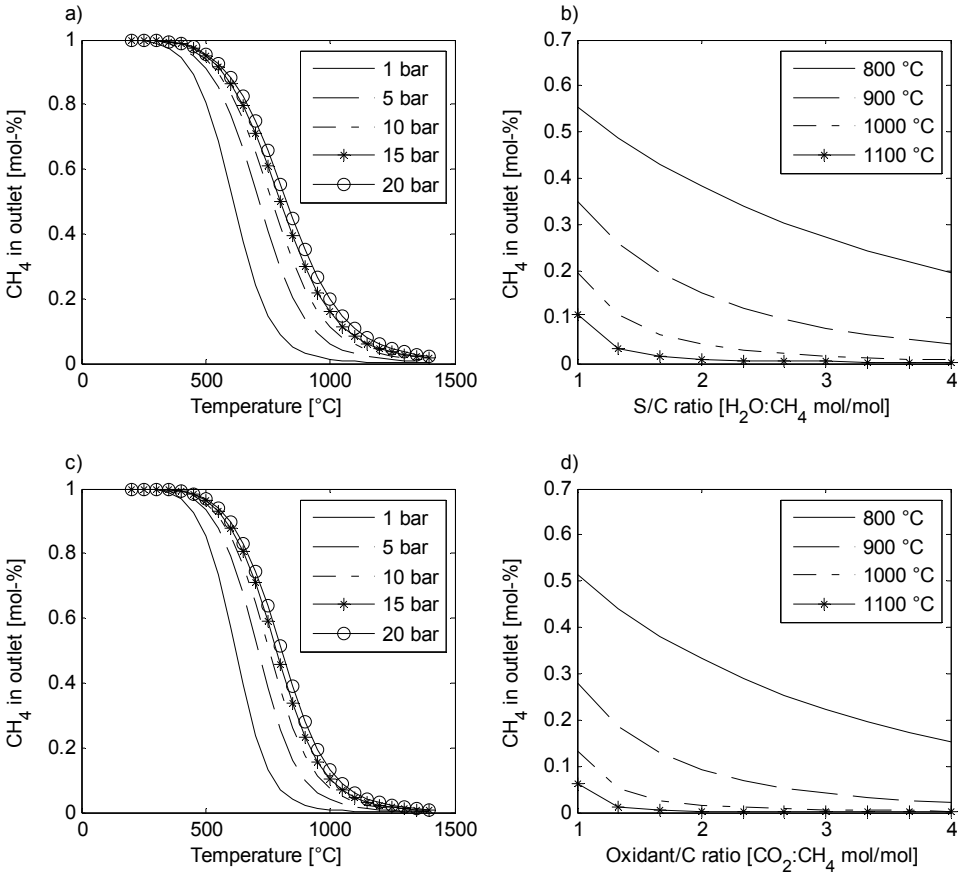

Figure 5: Equilibrium for CH_4 as a function of temperature and pressure. For a) the CH_4:H_2O ratio is 1:1, for b) and d) the pressure is 20 bar and for c) the CH_4:CO_2 ratio is 1:1.

Figure 5 shows the equilibrium of CH_4 and H_2O/CO_2 for different pressures, temperatures and varying amounts of oxidant. Comparing b) and d) shows that CO_2 reforming has higher conversions than steam reforming as can be seen from the lower CH_4 content in the outlet for any given temperature. The figure does not show the coke formation that would be a problem for gas mixtures containing only CH_4 and CO_2.

Reforming is usually divided into three processes: steam reforming or steam methane reforming (SR/SMR), autothermal reforming (ATR) and partial oxidation (POX). Partial oxidation is usually a non-catalytic process, but there is also a catalytic partial oxidation process (CPO). Natural gas is the primary feedstock in industrial reformers. Steam reforming is the dominant technology for industrial hydrogen production, either pure for direct use for example in ammonia synthesis, or as part of synthesis gas in the production of methanol [18]. Reformers have different reactor designs as can be seen in Figure 6. Steam reformers use air as oxidant, but other reformers can be run on air, enriched air or oxygen, depending on the desired syngas composition.

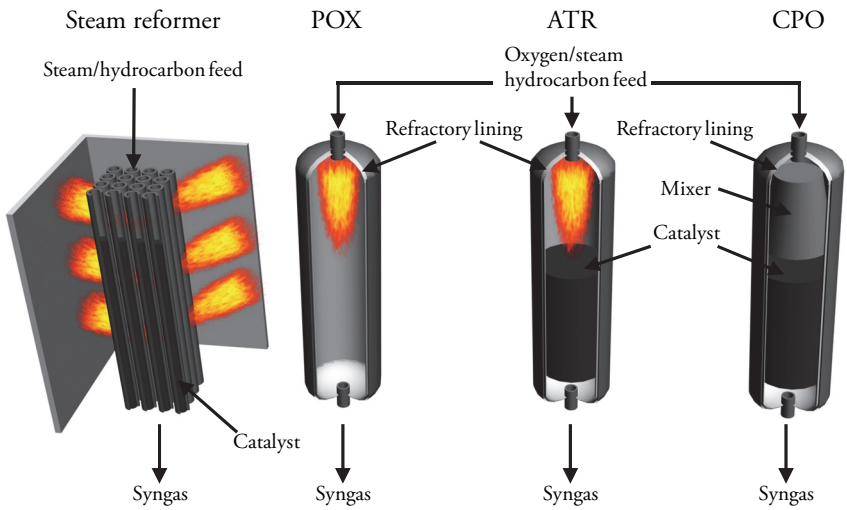

Figure 6: Reactor design for the most common reformer types.

Figure 6 shows that all reformers except CPO have burners to provide the heat necessary for reforming, although some compact ATR designs have eliminated the burner [19]. ATR and the partial oxidation reactors also have a refractory lining on the side of the reactor wall to protect the pressure vessel from the high temperature and harsh environment in the reactor. Because steam reforming requires external heating, no refractory lining can be used as it would reduce the heat transfer through the reactor wall.

2.3.1 Steam reforming

Steam reforming is a catalytic process in which the hydrocarbon feedstock is mixed with steam to produce a synthesis gas with a high H_2:CO ratio. The high H_2:CO ratio is preferred if the end product is hydrogen as it decreases the load in the water-gas shift (WGS) reactor. Steam reformers (SREFs) are externally heated tube reactors that are usually filled with a nickel-based catalyst that operate at 750–850 °C and at pressures of 20–40 bar [17, 20]. Steam to carbon (S/C) ratios in steam reformers typically range from 2:1 to 4:1 depending on feedstock and catalysts. Carbon deposition on the catalyst can become a problem in steam reformers, especially at lower S/C ratios and with feedstocks containing higher hydrocarbons than methane, such as naphtha. Carbon can cause blocking on the surface of the catalyst. The carbon formed can grow whiskers that push the active metal particle from the support [21]. The carbon can also deposit in the catalyst pores, which will eventually disintegrate the catalyst pellets to powder [20]. A lower S/C ratio is economically desirable. Steam reforming catalysts are most often nickel metal dispersed on a support of α-alumina (Al_2O_3) [20], calcium aluminate or magnesium aluminate, and promoted by alkalis such as potassium or activated magnesia [20, 21]. Acid sites on supports such as α-alumina are prone to coking [22, 23]. Alkali promotion decreases coking on the catalyst; one theory is that alkalis neutralise the charge of the acidic sites on the support [24]. However it is well known that alkali promotion decreases the rate of reaction for higher hydrocarbons [25]. Both the higher resistance towards carbon formation and the decreased activity can be an effect of alkali promotion as it increases the steam adsorption on the catalyst surface. Other metals such as cobalt and iron can be used but their activity is lower than nickel. Metals from the platinum group are too expensive even though they are highly active [20].

The major limitation of steam reforming is not catalyst activity but heat transfer and wall temperature. The wall of the reformer tubes needs to be as thin as possible to transfer as much heat as possible from the burners to the catalyst but still be able to handle the reactor pressure at high temperature.

Steam reforming catalysts are very sensitive to sulphur poisoning as sulphur is chemisorbed, forming Ni_3S_2, which has a lower activity than the nickel metal [17,

20]. Sulphur-poisoned catalysts have much lower activity and thus lower conversions, especially for methane. The allowable amount of sulphur in the feed gas varies, but values below 0.2 to 0.5 ppm are cited for commercial applications [20, 24]. Apart from carbon formation and sulphur poisoning, sintering of the nickel metal is a problem caused by temperatures that are too high, carbon formation and sulphur adsorption. Sintering is a process in which active metal sites dispersed on the catalyst surface grow and undergo agglomeration with other metal sites. Two mechanisms have been proposed for this behaviour: migration of metal particles from other active sites or Ostwald ripening (vapour transport or atom migration) [17]. In addition, the catalyst support can also sinter, which reduces the surface area and pore volume. A sintered catalyst has a lower active surface area and is therefore less active.

2.3.2 Autothermal reforming

Unlike steam reforming, autothermal reforming is directly heated by combusting a part of the feedstock to raise the temperature upstream of the catalytic bed. The overall reaction is slightly exothermic. The advantage of autothermal reforming over steam reforming is a higher thermal and chemical efficiency due to the direct heating, and a more favourable H_2:CO ratio for downstream synthesis such as Fischer-Tropsch and methanol. The disadvantage is that pure oxygen is needed if a nitrogen-free syngas is required. Temperatures are higher in autothermal reformers (ATRs) than in SREFs, typically at 900–1150 °C, allowing high reaction rates and thus high throughputs [19]. The higher temperature requires different reactor material. ATR reactors are typically refractory lined to endure the high temperature, high pressure and high partial pressure of hydrogen. ATR reactors can be operated in a wide pressure range of some 1 to 80 bar [19]. The pressures in ATR reactors can be higher than in steam reformers due to the internal heat source and the refractory lining that protects the pressure vessel. ATR catalysts also need to be chemically different from steam reforming catalysts to be able to handle the higher temperatures without sintering. ATR catalysts are supported on magnesia/alumina [26] and have a lower nickel content than steam reforming catalysts.

Due to the higher temperature in ATRs compared to steam reformers, the feed is usually prereformed to reduce the potential soot formation associated with high temperatures and rich fuel mixtures (high carbon to oxygen ratios) containing lower hydrocarbons such as ethylene.

The efficiency and total capital investment (TCI) of the ATR reactor can be further improved by using lower S/C ratios, as seen in Table 4. Operating with lower S/C ratios will increase the risk of carbon formation in prereformers and soot formation in the ATR. S/C ratios of 0.6 have been proven industrially, and < 0.4 in pilot plants [27].

Table 4: Process energy consumption and economics at different S/C ratios for ATR [28].

S/C	0.2	0.6	1.0
Relative investment	0.9	1.0	1.1
Relative energy consumption	0.97	1.00	1.03

At lower S/C ratios, precise burner control is needed to minimise soot formation. Other effective methods for minimising soot formation include small additions of steam to the oxygen, prereforming to remove C_2 (ethane, ethylene and acetylene) and higher hydrocarbons [27].

2.3.3 Catalytic partial oxidation

Catalytic partial oxidation is very similar to ATR as oxygen is injected to increase the temperature in the reactor. The differences are that no burner is used in CPO and that oxygen and fuel are premixed at the reactor inlet. The premixed gas is reacted on the catalyst. Fuel and oxygen consumption are higher for CPO than for ATR, as shown in Table 5. The lower feed temperature of CPO is necessary due to the premixing of feed and oxygen in the reactor inlet. The auto ignition temperature of the mixture will typically be about 250 °C [29]. The lower inlet temperature is the reason for the higher natural gas and oxygen consumption and thus lower efficiency. The higher oxygen demand for CPO compared to ATR is

economically unfavourable, especially when considering that 40 % of the TCI in the front-end is the air separation unit (ASU) [27].

Table 5: Comparison of relative natural gas and oxygen consumption of ATR and CPO when used as front-end in a gas-to-liquid plant. The exit temperature is 1050 °C and pressure 25 bar(a) [27].

Reactor	Feed temperature (°C)	S/C ratio	Relative natural gas consumption	Relative oxygen consumption
ATR	650	0.6	100	100
CPO	200	0.6	109	121
ATR	650	0.3	102	97
CPO	200	0.3	109	114

2.3.4 Homogenous partial oxidation

Homogenous POX operates at temperatures of 1150–1600 °C [19, 20] and pressures in the range 25–80 bar [19]. The high temperature is achieved by oxygen injection. Some systems use a small steam co-feed to reduce soot formation and improve the H_2:CO ratio [19]. Homogenous POX can be considered to be a burner with rich fuel mixtures producing incomplete combustion products. The main advantage of the POX reactor is that it can operate on nearly all kinds of hydrocarbon feedstocks. Another advantage is the non-catalytic design, which is very chemically robust as there is no risk of catalyst poisoning, for example due to sulphur. The disadvantage is a lower efficiency compared to both SREF and ATR due to the higher temperature required. POX reactors usually produce relatively high amounts of soot due to the high reactor temperature and low S/C ratio.

2.4 Unconventional methods of synthesis gas production

In addition to the conventional methods described above, synthesis gas can also be produced by first producing H_2 and then reacting H_2 with CO_2 (see water-gas

shift, p. 49). The CO_2 can either be obtained from a plant releasing CO_2, such as a power plant, or captured from the air. As long as a source of H_2 is available, synthesis gas and thus synthetic fuels and chemicals can be produced while at the same time reducing CO_2 in the atmosphere. However, the energy efficiency of these systems is very low.

The most common carbon-free source of H_2 production is electrolysis, but there are also microorganisms that produce H_2 by fermentation. H_2 production by electrolysis is a very energy-intense process requiring 18 MJ/Nm^3 of H_2 at an electrolysis efficiency of 71 % [30]. The lower heating value (LHV) of H_2 is 10.7 MJ/Nm^3, which equates to an energy efficiency of around 60 % joule to joule, neglecting the exergy of electric and chemical energy.

There are, however, applications that benefit from electrolysis, especially small systems and systems in remote locations that need H_2, even though it is expensive.

2.5 Gas conditioning

Gas conditioning is a general term for removing impurities and adjusting gas to meet the specifications of downstream uses. Depending on the feedstock, the raw gas produced by a gasifier or reformer may need thorough cleaning and conditioning to set it up for downstream synthesis. Different downstream equipment has different requirements regarding the amount of contaminants and, as mentioned previously, the H_2:CO ratio. If no downstream synthesis is to take place, for example in combined heat and power (CHP) plants where a gas engine burns the syngas to create power and heat, the only necessary clean up would be the removal of particles, alkalis and tars. Gas cleaning and conditioning of syngas from any source accounts for almost 60–70 % of the final product cost [31].

2.5.1 Particles, ash and alkali

The gas produced by most gasifiers contains particles. The particles are often formed from the ash (alkalis, inorganic) in the fuel, or they may be soot (organic)

formed due to the high gasification temperature. Fluidising bed gasifiers will also lose some of the bed material to the gas stream as particles due to attrition of the bed material. A cyclone is commonly used to remove particles. A cyclone contains a cylinder (barrel) on top of a cone. Cyclones are simple and cost effective and, as they contain no mechanical or electrical parts, almost maintenance free. Cyclones have designations like 2D2D or 1D3D. The numbers preceding the D's indicate the cyclone length and the barrel length in relation to the cyclone diameter. Thus A 1D3D cyclone has a barrel length equal to the diameter and a cone with a length three times longer than the diameter [32].

The gas inlet is perpendicular to the cyclone barrel, forcing the gases to swirl downwards in a vortex along the cyclone wall. As the diameter decreases in the cone, the velocity of the gas increases and separation of particles and gas is achieved. The particles fall out of the cyclone at the bottom where the gas velocity changes, the gas swirl upwards in the centre vortex of the cyclone and exits at the top, see Figure 7. The particle cut-off size of a cyclone depends on the dimensions of the cyclone and the gas velocity and is usually greater than 5–10 µm [33].

Cyclones are often used as a pre-collector for more sophisticated downstream equipment. Filters and electrostatic precipitators are among the most common commercial high-temperature particle removal systems.

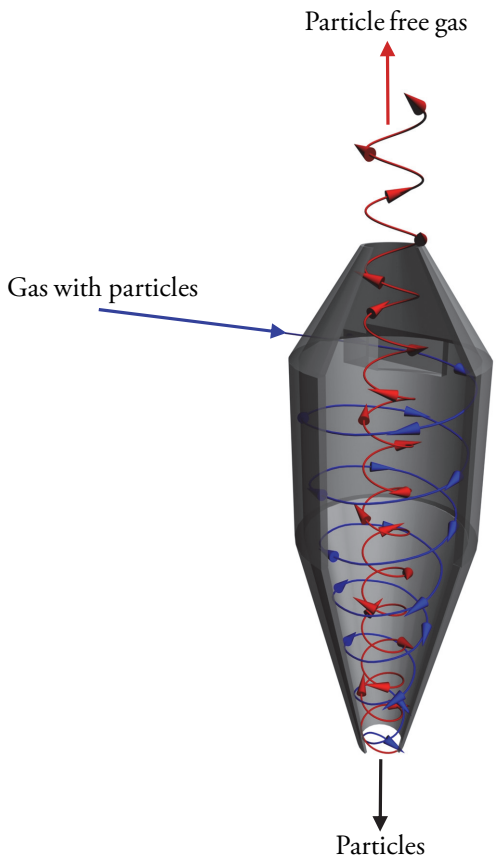

Figure 7: Working principle for cyclones.

The filters are constructed from either metal or ceramic materials and the principle is the same as with any filtration device. The filter cake formed on the filters needs to be removed periodically. Removal of the filter cake can be achieved by pulsing gas in the opposite direction.

The principle for electrostatic precipitator (ESP) gas cleaning is that particles are charged in an electric field between two metal plates. The charged particles are pulled/pushed towards the plate with the opposite charge. When the particles come into contact with the plate, they lose their charge and fall to the bottom of the device where they can be collected, as shown in Figure 8.

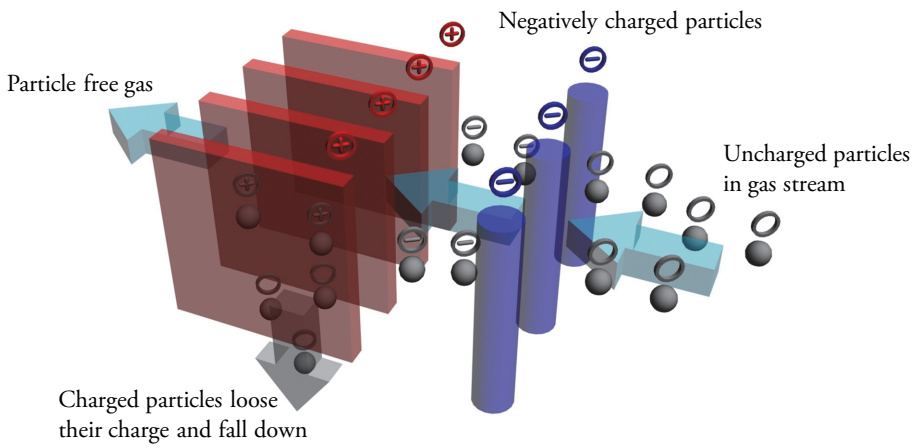

Figure 8: Plate precipitator particle removal.

ESPs can handle very high temperatures of up to 700–800 °C with collection efficiencies up to 99% for particles smaller than 10 nm [34].

An important property related to particle removal is the pressure drop that occurs. It is important to remove as many particles as possible with as little pressure drop as possible.

Table 6 presents the composition of the inorganic part of the ash produced in a biomass gasifier. Entrained flow and especially fluidised bed gasifiers produce a lot of particles and dust that will carry the inorganic particles away with the gas

stream. For fixed bed gasifiers and slagging gasifiers the ashes are collected at the bottom of the gasifier.

Table 6: Ash composition from biomass gasification [6].

Species wt-%	Wood	Agricultural waste (wheat straw, corn stover, rice straw)
Al_2O_3	1–10	0–2
SiO_2	0–2	18–78
MgO	1–17	2–3
CaO	10–60	2–14
K_2O	2–41	10–26
Fe_2O_3	0.5–4	0–2
Na_2O	1–20	2–13
Total ash [35]	0.3–2.1	2–6

Of the elements in Table 6, potassium and sodium are the species that are most likely to volatilize and follow the gas stream [6]. Alkalis in the gas stream can poison downstream catalysts.

2.5.2 Producer gas reforming

The feedstock used in gasification greatly influences the composition of the producer gas. Coal gasification generally produces gases with much lower tar content than peat and woody biomass [36]. As described in 2.2 (p. 10), the different types of gasifiers produce gas with varying hydrocarbon content. Producer gas from a steam-blown gasifier generally contains more CH_4 than that from an air or oxygen-blown gasifier. Entrained flow gasifiers generally produce a gas stream with low amount of hydrocarbons. In order to increase the synthesis gas yield and avoid tar condensation, the tars and hydrocarbons in producer gas need to be reformed or cracked into synthesis gas.

To indicate the amount of energy contained in the methane, lower hydrocarbons (C_{2+}) and tars, the gas composition in Table 2 was recalculated on an energy-basis and is presented in Table 7. The MILENA and FICFB gasifiers were assumed to

have a steam content of 35 % by volume to compare the composition with that of the Värnamo gasifier.

Table 7: Producer gas components lower heating values. Numbers in parentheses are the percentage of the total lower heating value.

Component	Värnamo	MILENA	Güssing FICFB
CO [MJ/Nm^3]	1.5 (21%)	3.9 (31%)	2.2 (26%)
CO_2 [MJ/Nm^3]	0	0	0
H_2 [MJ/Nm^3]	1.3 (17%)	1.2 (10%)	2.9 (35%)
CH_4 [MJ/Nm^3]	2.9 (40%)	4.1 (32%)	2.4 (30%)
H_2O [MJ/Nm^3]	0	0	0
C_2H_4 [MJ/Nm^3]	0.94 (13%)	2.2 (18%)	0.77 (9.3%)
Tars [MJ/Nm^3]	0.70 (9.5%)	1.25 (10%)	0.06 (0.7%)
Total LHV [MJ/Nm^3]	7.4	12.8	8.25

Lower hydrocarbons and methane account for around 50 % of the total lower heating value of the gas for the Värnamo and MILENA gasifier. For the FICFB almost 40 % of the heating value is contained in the methane and lower hydrocarbons. Tars represent almost 10 % of the total energy content in the gas for the Värnamo and MILENA gasifiers. The FICFB uses a bed material with catalytic activity to crack and reform the tars, which could explain the lower concentrations of methane, lower hydrocarbons and tars [37].

Reforming of the hydrocarbons in producer gas is more problematic than reforming of natural gas due to the sulphur content in the gas and the chemical nature of the sulphur, such as organic sulphur.

Industrial reforming catalysts are very sensitive to sulphur, as mentioned in 2.3 (p. 17). As a result, sulphur must be removed before using reforming catalysts on producer gas. Furthermore, not all the sulphur in the gas is present as H_2S, a form that can be removed by adsorbents (see 2.5.3, p. 44); some of the sulphur is present as organic sulphurs such as thiophene (C_4H_4S). Recent studies have indicated that organic sulphur could be even more problematic for Ni-based catalysts than H_2S

[38, 39]. Struis et al. concluded that the larger thiophene molecule increased the number of blocked sites on the Ni-catalyst surface compared to H_2S [38].

Sulphur removal prior to reforming requires cooling the gas after the gasifier. This is typically performed at 400 °C, prior to reforming, followed by heating to reforming temperature (1050 °C for ATR). Heating the gas costs energy that must come from the synthesis gas. For biomass- generated synthesis gas, which has a low heating value to begin with, heating is detrimental to process efficiency. The alternative to catalytic reforming is POX, which also has a great impact on the energy content of the gas. Table 8 shows the effect that cooling prior to reforming has on the energy content of the producer gas, and the difference between ATR and POX operating at 1300 °C. The calculations were performed in Aspen Plus using a Gibbs free energy reactor and the producer gas composition of the MILENA gasifier. The producer gas flow was 10 kg/s, and the reactor outlet temperature was 1050 °C for the ATR and 1300 °C for the POX.

Table 8: Effect of cooling prior to reforming on the lower heating value of producer gas, and comparing ATR to POX.

Component	Producer gas	ATR	ATR with cooling/heating	POX
CO [MW]	41.1	60.1	58.1	58.1
H_2 [MW]	13.0	49.7	46.6	45.0
CH_4 [MW]	43.1	0	0	0
C_2H_4 [MW]	23.5	0	0	0
Total [MW]	121	110	105	103
O_2 demand [kg/s]	–	1.66	1.98	2.08
Chemical Efficiency (LHV) [MW/MW]	–	91%	87%	85%

The cost of cooling the gas prior to reforming to remove sulphur is evident in Table 8 as the efficiency (LHV basis) drops from 91% to 87%. Comparing the cooling and heating with ATR to a POX, there are only small differences in efficiency loss. A non-catalytic POX would be almost as efficient as an ATR under these conditions. Although it would not be feasible to operate a catalytic nickel-

based reformer even after H_2S removal as the organic sulphur is still present [40], the comparison still shows the impact of unnecessary cooling and heating of the syngas. Four percentage points in reduced efficiency at the front-end mean four percentage points less product at the end.

The POX reactor is the only non-catalytic reformer that can convert methane with adequate conversion rates. However, using a POX reactor has a large impact on efficiency due to the higher temperatures necessary (Table 8).

When reacting a fluid at high temperature, a recuperative arrangement is normally used in which a heat exchanger is placed between the inlet and the outlet of the reactor making the reactor autothermal (Figure 9).

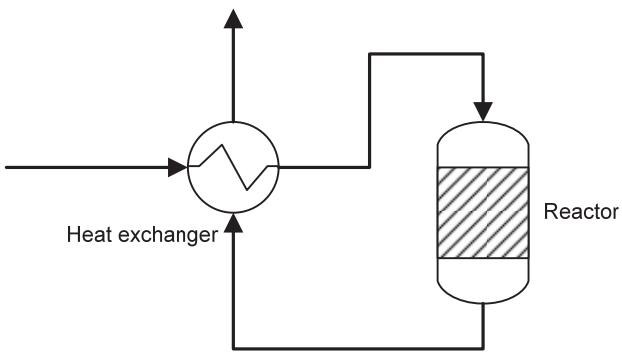

Figure 9: Recuperative reactor arrangement.

The recuperative reactor works well but has some limitations. If the heat of reaction is insufficient to preheat the ingoing fluid, the reaction will stop as the heat exchanger is unable to recover 100 % of the heat in the fluids. More importantly, heat exchangers are unable to operate at reforming temperatures due to material problems. For example, a recuperative ATR is unable to preheat the inlet gases to 1000 °C even though the outlet is around 1050 °C. For the ATR example, 600–700 °C at the inlet is more realistic than 1000 °C. As a result additional energy is required.

2.5.2.1 Reverse-flow reactors

As was shown in Table 8, the impact of reforming on the LHV of the producer gas is noticeable, particularly when using POX. Better heat utilisation of the reformer

is essential for efficiency and the recuperative approach is not practical at POX temperatures. However, reverse-flow reactors are a practical alternative. This chapter describes some of the work on reverse-flow reactors that the author has performed (Papers I, II and III). The work was both experimental and computational.

Reverse-flow reactors were first used for combustion of low calorific gases and have since been extensively studied for other processes such as catalytic reforming of methane [41-54].

The principle of reverse-flow reactors is that a bed of particulates acts as a heat buffer. A hot fluid flows through an initially cold packed bed of particulates, thus heating up the bed while at the same time cooling the fluid. Due to the differences in heat capacity between a solid and a gas or liquid, the bed will heat up more slowly than the gas cools. As a result a thermal front is formed in the bed, and the bed will heat up gradually from the inlet to the outlet, as is seen to the left in Figure 10.

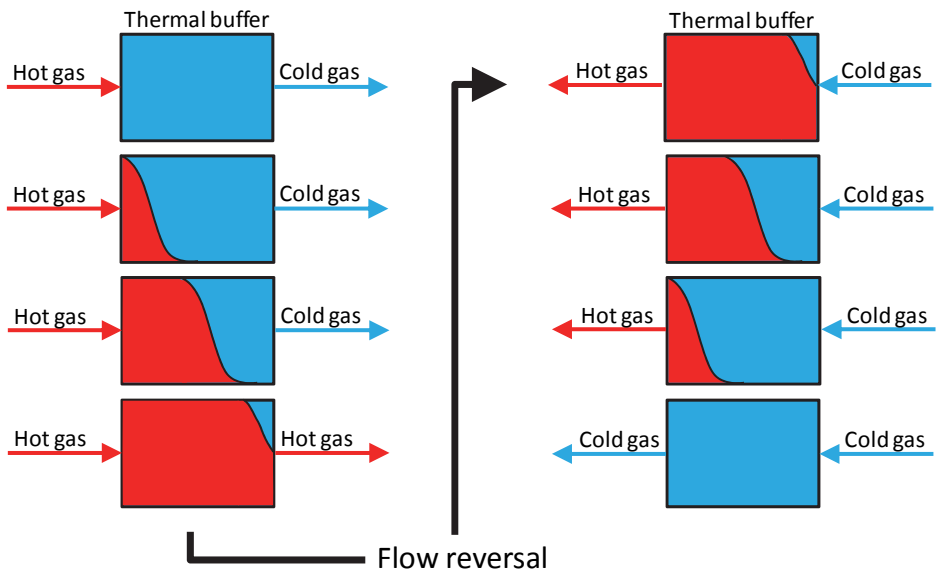

Figure 10: The principle for reverse-flow thermal buffering.

2.5 Gas conditioning

Figure 10 shows how heat is transferred from the hot fluid (gas in the figure) to the bed. When the flow direction is reversed, the stored heat can be used to heat up a cold fluid. This results in a heat exchanger with very high efficiency due to the large internal surface area of the bed. Because of the direct contact of the fluid and solid, the fluid temperature will be almost the same as that of the solid at the outlet.

If two thermal buffers were placed on either end of a reaction zone in which an exothermic reaction was to take place, the thermal buffer in front of the reaction zone would preheat the fluid and the thermal buffer behind the reaction zone would recover the heat, as shown in Figure 11.

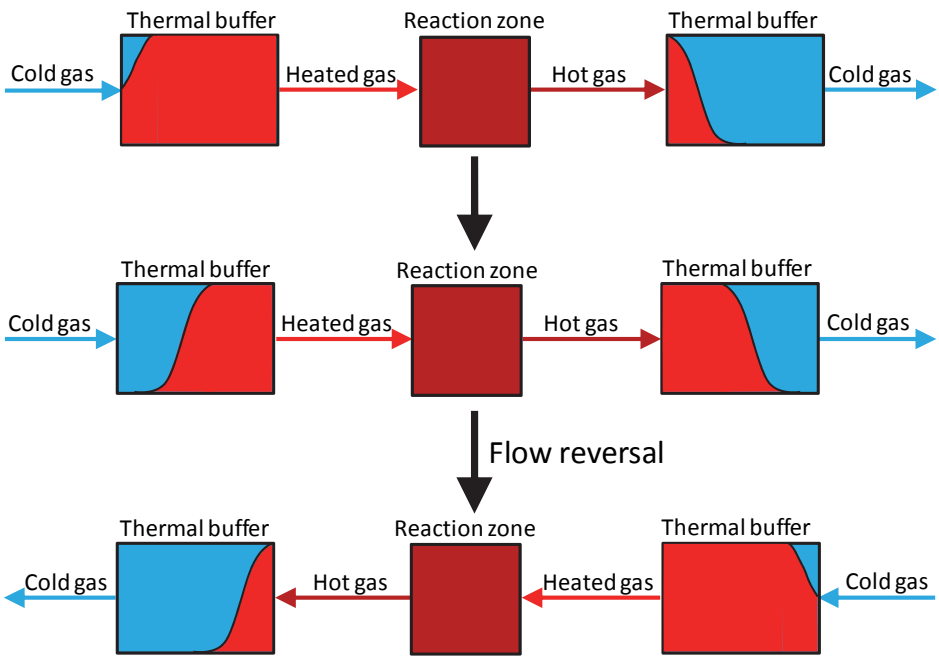

Figure 11: Reverse-flow reactor, two thermal buffers on each side of a reaction zone.

The end result of the periodic flow reversal is a very efficient heat exchange built into the reactor. In order to achieve the flow reversal, a minimum of four 2-way valves are required, as illustrated in Figure 12.

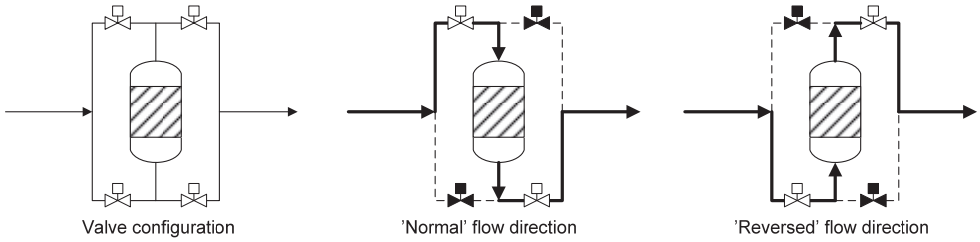

Figure 12: Valve configuration and valve operation for reverse-flow operation.

The valves are operated as is seen in Figure 12 to direct the flow from either the top (middle figure) or the bottom (right figure). It should be noted here that it is important for the valves to have a high on-off rate, otherwise the fluid would by-pass the reactor during flow reversal.

The temperature profile in a reverse-flow reactor with a single heat source, or oxygen inlet (located in the centre) can take the shape shown in Figure 13.

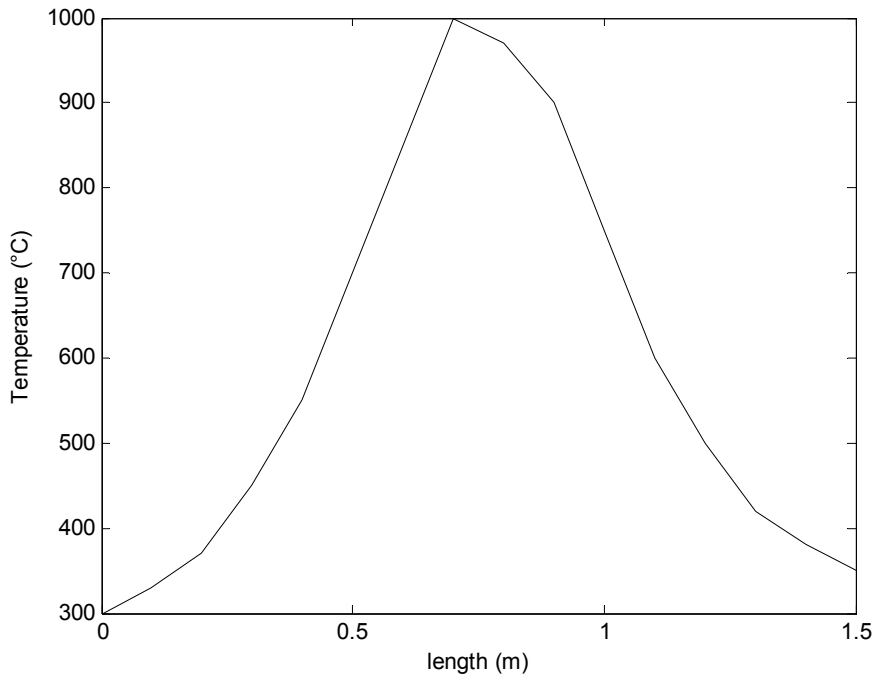

Figure 13: Temperature profile in a reverse-flow reactor with one centred oxygen inlet.

The profile in Figure 13 could be achieved if a combustion reaction were to take place in the middle of the reactor and only one source of oxygen (inlet or injection point) was provided. The direction of flow in Figure 13 is from the left to the right. Using a single oxygen inlet centred in the reactor results in a simple reactor design, but it also means that a large part of the reactor volume is left unused as the temperature is too low. If two oxygen inlets are used instead, the profile might look like the profile in Figure 14. Note that here the inlets are located at one-third and two-thirds of the reactor length.

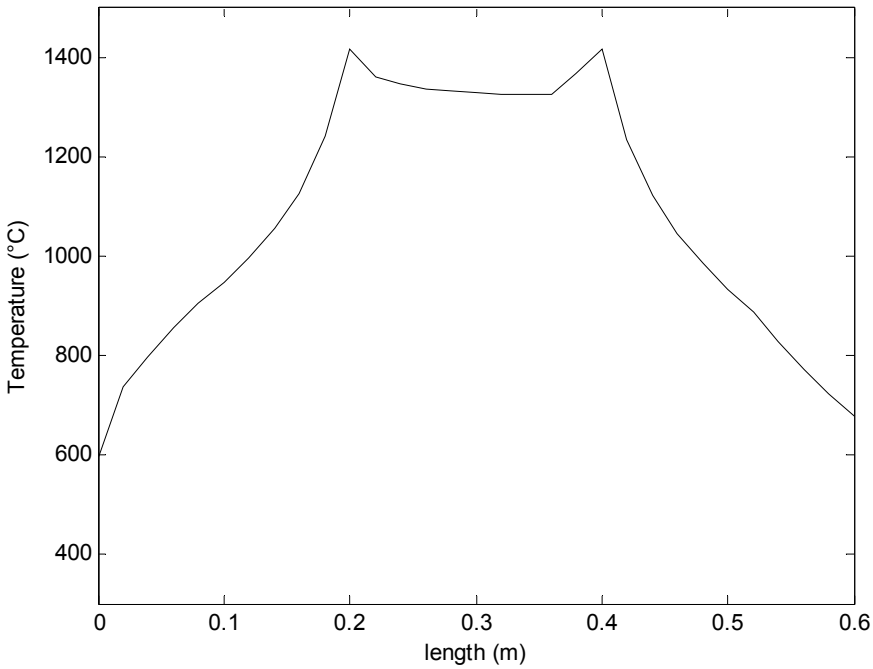

Figure 14: Temperature profile in reverse-flow with two oxygen inlets, adapted from the work in Paper I.

The data in Figure 13 and Figure 14 are not from the same system. More reactor volume is available at a higher temperature for the system in Figure 14 as there are two peaks separated by a valley. The system can be run with only the oxygen inlet closest to the current inlet active, or with both active. When two oxygen inlets are used, two oxidation zones are formed with a reaction zone in between, as seen in Figure 15.

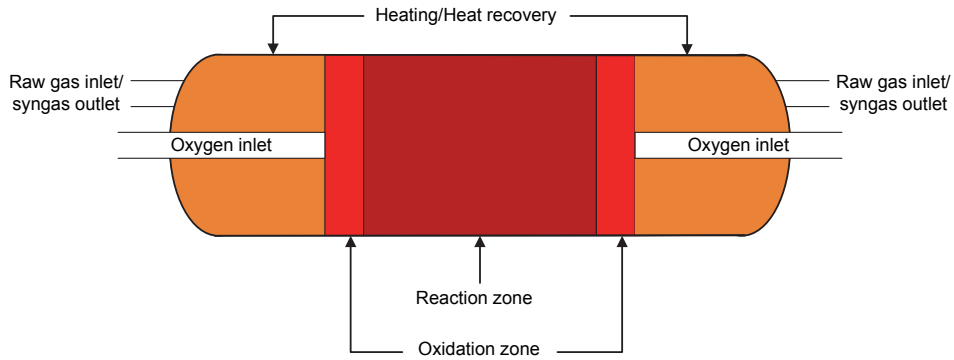

Figure 15: The different zones in a reverse-flow reactor with two oxygen inlets.

In the two oxidation zones in Figure 15 the temperature is increased from around 1200 °C to 1400 °C, as can be seen in Figure 14. The temperature in the reaction zone then drops from 1400 °C to 1300 °C due to the endothermic reforming reactions. The higher temperature in the oxidation zone is necessary in order to achieve acceptable methane conversion. The reaction zone actually includes both oxidation zones as the temperature is sufficient for reforming. If only one oxygen inlet is active, the temperature in the inactive oxidation zone drops as the reforming reactions consume the stored heat. When the direction of flow is reversed, the temperature is increased in the previously inactive oxidation zone, which becomes active.

For a reverse-flow reactor, no heat recuperation is necessary as the gas will be preheated internally, almost to the reaction temperature, in the first part of the reactor. For an ATR operating with an outlet temperature of 1050 °C, the temperature at the flame core of the burner can be over 2000 °C, and the gas entering the top of the catalyst bed has a temperature of 1100–1400 °C [26]. In other words, the ATR needs to provide the energy necessary to heat the gas from an inlet temperature of 600–700 °C to a reaction temperature of 1100–1400 °C, whereas the reverse-flow reformer only needs to increase the temperature from around 1200 °C up to 1400 °C. A catalytic reverse-flow reformer would need even less of a temperature increase, but would suffer from the same poisoning problems as the ATR. The energy required to increase the temperature in the reactor comes

from burning part of the feed. The lower the required temperature increase, the higher the resultant efficiency.

Not much research has been done on reforming hydrocarbons in producer gas using the reverse-flow technique. The focus has been on finding a nickel-based catalyst that can withstand the high sulphur load. Non-catalytic POX reforming of producer gas using the reverse-flow concept is a very energy efficient and chemically robust alternative to catalytic reforming, as was concluded in Paper I. But it is not without its problems.

To begin with, when the direction of flow is reversed, the old inlet becomes the outlet. The raw gas that was in the first part of the reactor (from valve mixing point to oxidation zone) is ejected unreacted. The percentage of unreacted gas that leaves the reactor depends on the flow reversal interval, which in turn depends on the application, reactor dimensions, bed and reactor material and so forth. With the reactor setup in Paper I and a flow reversal interval of 3 min, 1.5 % of the raw gas exits the reactor unreacted over time. With an interval of 6 min, only 0.7 % of the raw gas exits the reactor unreacted.

Secondly, as discussed in Paper I, the reverse-flow reactor as designed in Paper I is not suitable for gases with high concentrations of hydrocarbons such as natural gas. High hydrocarbon concentrations require more energy for reforming per volume of ingoing gas. The heat of reforming must be supplied at the oxidation zone and with higher hydrocarbon concentrations in the gas, higher temperatures are required in the oxidation zone to supply sufficient heat. With sufficiently high hydrocarbon concentrations, the temperatures required would eventually exceed the melting point of most materials. High temperatures are not a problem in flames, but can become a problem in a packed bed due to thermal expansion and local peak temperatures that exceed the melting point of the reactor material. However, there are solutions to this, such as adding more oxygen inlets along the reactor length, as shown in Figure 16.

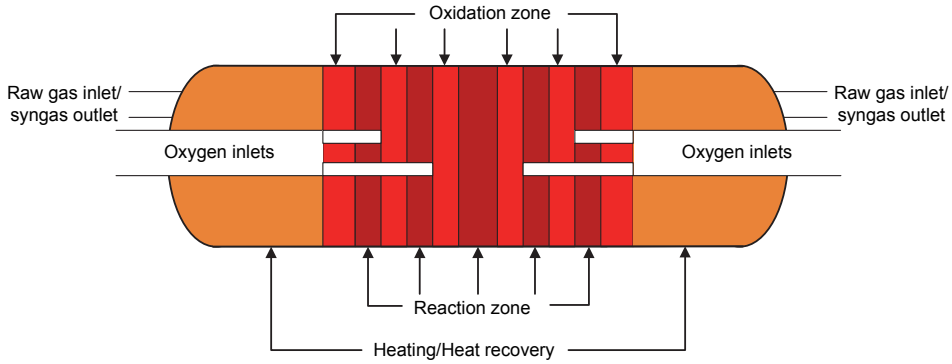

Figure 16: Multiple oxygen inlet configuration in a reverse-flow reactor.

With more oxygen inlets, multiple oxidation/reaction zones are created along the reactor length. The end result is that more oxygen can be added without local overheating of the reactor as the oxygen is distributed more evenly throughout the reactor length. The drawback to this is a much more complicated reactor design. Paper I showed that this is not necessary for biomass-generated producer gas, as the hydrocarbon conversion was almost 99 % with an efficiency of 97 % based on the lower heating value and peak temperatures of 1400 °C.

2.5.2.2 Lower hydrocarbons and methane

Methane is the most stable hydrocarbon found in the producer gas, and thus methane reforming requires higher temperatures than reforming other hydrocarbons [55]. At the same time, methane is the most common hydrocarbon in most producer gases (see Table 7) and can have the highest energy content of all species in the gas. For synthetic natural gas synthesis it is important to keep as much methane as possible in the gas to increase the efficiency of the entire process. (See 3.2.1, p. 65 for more details) For all other syntheses, reforming of methane is crucial for maximum efficiency.

Of the lower hydrocarbons, ethylene is the most troublesome as reforming of ethylene leads to rapid carbon formation on the catalyst surface [56]. Olefins can also accumulate on the surface and polymerise, causing blockage of the catalyst pores. Lastly, pyrolytic carbon formation in the gas phase is a direct result of olefins in the gas stream, which leads to soot formation [56].

Soot formation in packed beds is a big problem in processes such as catalytic reforming. When the catalyst is covered in soot, the soot both blocks the active sites and increases the pressure drop. In Paper II, the formation of soot in producer gas under reforming conditions in a reverse-flow POX was investigated. Soot formation was predicted using computer simulation. Although the model probably over-predicts the formation of soot, it can be concluded that prereforming of the lower hydrocarbons and tars is an absolute necessity when using reverse-flow POX.

2.5.2.3 Tars

The tar components are the most troublesome of all the hydrocarbon species when it comes to cleaning producer gas and have even been referred to as "the Achilles' heel of the [biomass gasification] process" by senior researchers in the field [57]. Tars are formed when the lignocellulosic biomass decomposes into smaller fragments. There is no definite definition of tars, but most agree that they are aromatic compounds with a molecular weight greater than that of benzene [58]. Figure 17 shows a schematic of the formation of tars. It is intended to provide some basic information about the subject, even though the mechanism for tar formation is not well established.

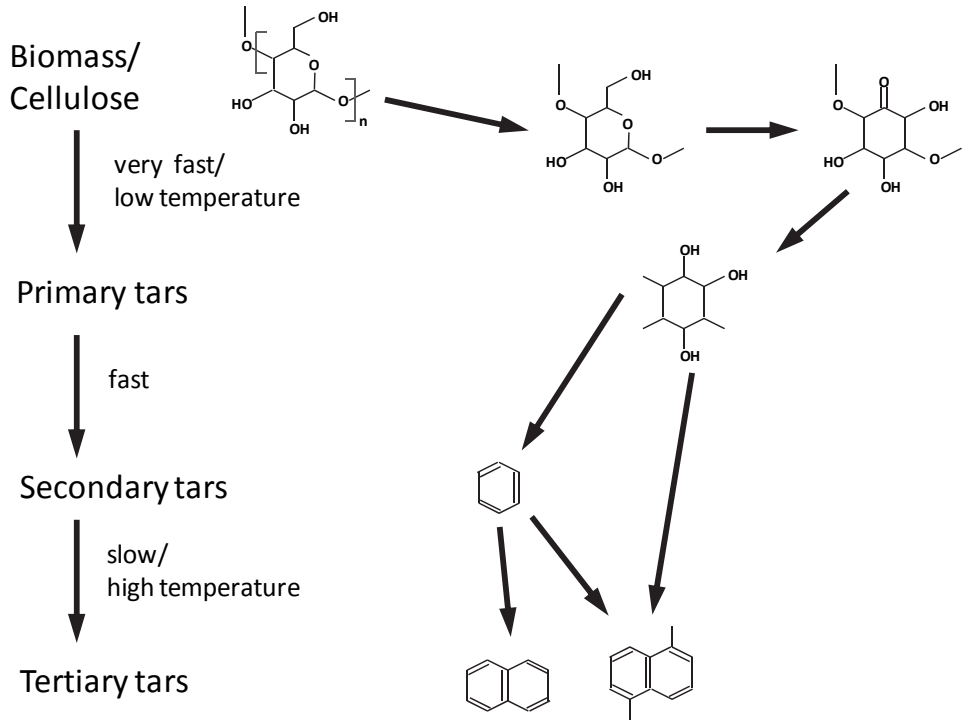

Figure 17: Schematic of the formation of tars. Adapted from work by Devi et al. [59].

As depicted in Figure 17, the biomass is decomposed into cyclic molecules that undergo aromatization to yield benzene. A benzene molecule in turn can react with another benzene molecule to yield naphthalene or with any other hydrocarbon in the gas to yield other tar species. The tars also consist of heterocyclic compounds containing elements such as nitrogen (pyridine) and sulphur (thiophene).

Tars can be classified according to the physical properties of the compounds, as was done by Devi et al. (Table 9).

Table 9: Tar classification as reported by Devi et al. [59].

Tar class	Class name	Property	Representative compound
1	GC-undetectable	Very heavy tars, undetectable on GC.	None
2	Heterocyclic	Tars containing for example elements S, N, O. High water solubility.	Thiophene, pyridine, phenol
3	Light aromatic	Single-ring aromatics, usually do not cause problems upon condensation.	Toluene, xylene, ethylbenzene, styrene
4	Light polyaromatic (PAH)	Two- and three-ring aromatics. Condense at low temperature and at low concentrations.	Indene, naphthalene, methylnaphthalene, anthracene
5	Heavy polyaromatic	Larger than three rings. Condense at high temperature and low concentrations.	Pyrene, perylene, coronene, chrysene

Of the classes presented in Table 9, classes 4 and 5 are the most troublesome because these tars condense due to the decrease in temperature as the gas is cooled after the gasifier, and then stick to surfaces of heat exchangers, tubing and other equipment in contact with the gas.

The problems associated with the reforming of hydrocarbons in biomass-generated producer gas can be summarized as follows:

- The gas contains sufficiently high amounts of H_2S to deactivate traditional Ni-based reforming catalysts
- The gas also contains organic sulphur that is not removed by traditional desulphurisation
- Tars and ethylene produce soot under POX conditions

It is thus clear that reforming of producer gas generated from biomass requires a prereformer and, depending on downstream processes, a secondary reformer.

A prereformer can be used to convert the hydrocarbons in the producer gas, except methane, without the risk of carbon and soot formation [56]. A catalytic prereformer can be operated at 350–550 °C depending on the feedstock. Prereformers operating on naphtha would be operated above 450 °C to avoid formation of gum (carbon deposition and polymerisation of olefins) [56]. As most catalytic prereformers utilise a nickel-based catalyst that is deactivated by sulphur, chlorine and alkalis, these should not be considered for biomass-generated producer gas.

Dolomite $(Ca, Mg)CO_3$ and olivine $(Mg, Fe)_2SiO_4$ are naturally occurring inexpensive minerals with catalytic activity for tar cracking [60]. Olivine is primarily used in fluidised beds due to the high attrition resistance of the mineral [60]. Dolomite has a higher activity than olivine for tar cracking and has received much attention, both as a catalytic active bed material in fluidised beds [61], and also as a reforming catalyst in fixed bed applications [57, 59, 62]. However, tar conversion activity ceases when the partial pressure of CO_2 exceeds the equilibrium pressure of the decomposition of dolomite. Higher temperatures increase the equilibrium pressure to some extent, but as a rule, elevated operating pressures are problematic.

The research reported in Paper III showed excellent results with reverse-flow tar cracking using dolomite as the bed material. This was also reported by Bridgwater et al. [63]. The laboratory setup in Paper III is depicted in Figure 18.

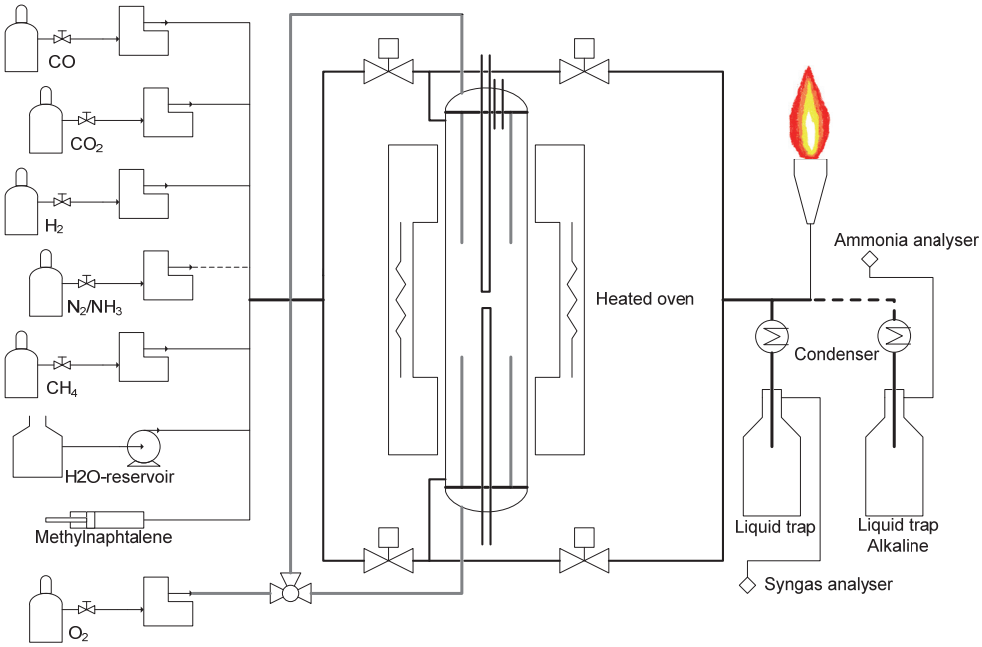

Figure 18: Laboratory setup of the reverse-flow tar cracker.

The reactor was built with a high-temperature steel alloy with enhanced endurance for reducing environments. As no biomass gasifier was available at Lund University, the producer gas was modelled using bottled gas and a model tar compound. The tar compound 1-methylnaphthalene was chosen because naphthalene is the most common tar component in biomass derived producer gas [36, 59]. Naphthalene is a solid at room temperature, whereas 1-methylnaphthalene is a liquid, which makes injection much easier. 1-methylnaphthalene was injected using a syringe pump to deliver a gas with a tar concentration of 15 000 mg/Nm^3 (Table 10).

Table 10: Model synthesis gas composition for the reverse-flow tar cracker in Paper III.

Component	Concentration [vol-%]
CO	25
CO_2	15
H_2	25
H_2O	25–27
CH_4	8–10
1-methylnaphthalene	15 000 [mg/Nm^3]

The results of the tar cracking clearly show that temperatures over 800 °C are required for adequate tar conversion. Naphthalene is the predominant tar specie in the outlet at 700 °C. This gives an indication that the tar destruction mechanism of 1-methylnaphthalene starts with separation of the methyl group from the naphthalene molecule. This is to be expected since the aromatic ring structure is very stable. Total tar conversion was only around 25 %, but 1-methylnaphthalene conversion was over 60 % at a reactor temperature of 700 °C. At 850 °C, conversion of 1-methylnaphthalene was over 97 % with total tar conversion over 90 %. The highest total tar conversion measured was 95 % at the lowest flow rate.

During tar reforming, CH_4, CO and H_2 are formed as the aromatic compounds decompose. The ideal prereformer should only remove tars and lower hydrocarbons, and for methane production (see 3.2.1, p. 65) should increase methane at the outlet. If an increase in methane is impossible, the prereformer should convert as little methane as possible. The reasons for this are that if the downstream synthesis involves methane production, it is important to retain as much of the methane formed during gasification as possible to increase efficiency. Furthermore, methane reforming requires higher temperatures than reforming of other hydrocarbons; the higher temperatures increase the potential for soot formation as previously described.

The results reported in Paper III show that the dolomite used has some methane reforming activity at higher temperatures, as the methane content in the outlet

decreased significantly at 850 °C compared to that with experiments performed at 800 and 700 °C. This methane reforming activity could be an effect of impurities such as iron in the dolomite or from the reactor wall, which had a high nickel content. With a real producer gas from a biomass gasifier, the sulphur in the gas is likely to deactivate those active sites and lower the methane conversion significantly.

2.5.3 Sulphur

As mentioned previously, sulphur is prone to poisoning reforming catalysts. Most downstream synthesis catalysts are also readily deactivated by sulphur poisoning. Table 11 lists the most important synthesis catalysts and the maximum allowable sulphur levels in the synthesis gas for the respective synthesis.

Table 11: Maximum tolerable sulphur levels in synthesis gas for some important synthesis catalysts.

Synthesis	Catalyst	Maximum allowable sulphur levels
Methanol	Cu/ZnO	~ 1 ppm by volume [31, 64]
Fischer-Tropsch	Fe, Co	0.02, 1-2 ppm by volume [65], [31]
Methanation	Ni	A few ppm by volume [66]
Ammonia	Fe	< 1 ppm by volume [67]

Sulphur is present in producer gas in quantities around 20–-250 ppm by volume for woody biomass [6]. Coal-derived producer gas can contain several volume per cent H_2S [65] depending on the feedstock. Low temperature and low steam concentration during gasification yields a gas with higher COS and CS_2 concentrations [6]. Organic sulphur concentrations are generally low and occur predominately as COS and thiophene but also as benzothiophene (C_8H_6S). Cui et al. measured different sulphur species in dry biomass derived producer gas as 93, 1.7 and 2.2 ppm by volume for H_2S, COS and C_4H_4S [40].

The most common sulphur removal technique is adsorption by zinc oxide (ZnO). Zinc oxide reacts with H_2S according to reaction (8)

$$ZnO + H_2S \rightarrow ZnS + H_2O \quad (8)$$

Zinc oxide beds can reduce H_2S in gas streams from a few hundred ppm down to several hundred ppb at 350 °C [40]. COS are also removed from the gas by one order of magnitude (from 1 to 0.1 ppm). C_4H_4S, however, is unaffected by ZnO removal [40]. If organic sulphur is present, prereforming of the gas prior to sulphur removal to convert the organic sulphur into H_2S is necessary in order to remove all sulphur from the gas. Some zinc oxide beds can be regenerated, but they lose some reactivity each time, and can lose as much as 50 % reactivity after 25–50 cycles [68]. A report by van Dijk claims that CS_2 can be removed from syngas by ZnO beds, even though the ZnO used was non-regenerative [69].

Zinc oxide beds are also used as guard beds in large-scale plants upstream of reactors with sulphur-sensitive catalysts. For large-scale operation, wet desulphurisation is more common. Technologies such as Rectisol and Selexol also remove CO_2 from the syngas. In both of the aforementioned processes, cool liquid is used to physically absorb H_2S, COS and CO_2. CO_2 removal is necessary for downstream syntheses to increase the partial pressure of CO and H_2 and to reduce the load on the syngas compressor. Wet desulphurisation also has the benefit of producing a relatively pure H_2S stream for use in a Claus plant to produce elemental sulphur. Elemental sulphur can be further processed into sulphuric acid.

2.5.4 Ammonia

Ammonia concentrations in producer gas vary from gasifier to gasifier and with the feedstock used. Levels ranging from 0.04–1.8 vol-% have been reported [70]. Biomass contains nitrogen as part of its protein content. During gasification almost all of the nitrogen ends up as ammonia [71].

Table 12: Maximum tolerable ammonia levels in synthesis gas for some important synthesis catalysts.

Synthesis	Catalyst	Maximum allowable ammonia levels
Methanol	Cu/ZnO	10 ppm by volume [72]
Fischer-Tropsch	Fe, Co	Fe unaffected Co deactivation at 100 ppb by volume NH_3 + HCN [73]

Ammonia must be removed from the synthesis gas prior to synthesis of the products listed in Table 12. Furthermore, combustion of raw producer gas containing ammonia in a gas turbine or gas engine, as in combined heat and power (CHP) plants, produces flue gases with elevated NO_X levels.

Ammonia is decomposed under reforming conditions over most reforming catalysts including dolomite [74, 75]. All of the ammonia may not be decomposed under the desired reforming conditions, however, as was the case in [75]. Björkman et al. reported that the ammonia conversion decreased from 95 % to almost zero when steam was added to the gas [75].

If the ammonia is left in the gas, it will eventually end up either in an acid scrubber or in water knock-out drums prior to syngas compression. Either way, the ammonia will cause problems as the concentration of ammonia in producer gas can be several per cent. Scrubbing the syngas will not solve the problem with ammonia; it will merely move it to another location and, at the same time, affect the waste water treatment plant.

Other approaches are necessary in order to either convert the remaining ammonia after reforming, or to decrease the load on the waste water treatment plant when producing a gas free from ammonia for CHP plants where no reformers are present.

Ammonia can be selectively oxidised by nitrogen oxides (NO and NO_2) to nitrogen over a suitable catalyst. The reaction is usually performed the other way around for NO_X reduction in power plants where ammonia is injected into the flue

gas before a catalytic bed. The reaction is commonly known as selective catalytic reduction (SCR) of NO_X and the catalyst most often used is either a vanadium oxide on titania with tungsten ($V_2O_5/WO_3/TiO_2$) [76] or an acid zeolite such as H-mordenite [77]. In normal flue gas NO accounts for 90–95 % of the total NO_X. It is normally considered that the SCR reaction follows reaction (9).

$$4NO + 4NH_3 + O_2 \rightarrow 4N_2 + 6H_2O \quad (9)$$

As can be seen in reaction (9), oxygen is present, as is normally the case for flue gases in which oxygen levels can be around 2–10 vol-%. Oxygen is not present in synthesis gas, however, and without oxygen the conversion falls to relatively low values (almost zero without NO_2) [77]. Reactions (10) and (11), on the other hand, do not require any oxygen. Furthermore, reaction (10) has a higher reaction rate than reaction (9) and is called the fast SCR reaction [77].

$$NO + NO_2 + 2NH_3 \rightarrow 2N_2 + 3H_2O \quad (10)$$

$$6NO_2 + 8NH_3 \rightarrow 7N_2 + 12H_2O \quad (11)$$

Several studies have been performed on selective catalytic oxidation of ammonia over an alumina catalyst at a relatively high temperature (400–700 °C) by oxygen injection [78-80]. In these studies and patents, the oxygen level is increased by several volume per cent prior to a catalytic bed, to remove ammonia with a concentration of several thousand ppm. At 2 vol-% O_2 and 2000 ppm NH_3, oxygen is added with a ratio of 10:1. The remaining oxygen is reacted primarily with H_2 but also with CO to give H_2O and CO_2, a process that drains the synthesis gas of energy and increases the temperature unnecessarily.

In Paper IV a new process was proposed to avoid unnecessary oxidation of the energy carriers in the synthesis gas. The process uses injection of NO_2 at almost equimolar ratio (up to 1.25:1) to NH_3 prior to a catalytic bed of commercially available SCR catalysts. The stability of the SCR catalysts in reducing environments with high partial pressures of H_2 and CO is of concern, since the catalysts were developed for use in oxidizing environments with high partial pressures of oxygen. During the experiments in Paper IV the commercial H-

mordenite catalyst did not show any signs of change. The vanadium-based catalyst did turn grey after several hours use but still retained its catalytic activity.

Both catalysts performed excellently. The vanadium-based catalyst reduced the NH_3 level in the gas from 2000 ppm to 25 ppm (99 % conversion) at 325–350 °C and a stoichiometry of 1.25:1 for NO_2:NH_3. The H-mordenite achieved a conversion of 97 % (from 2000 ppm to 50 ppm) at the outlet at a temperature of 400 °C and a stoichiometry of 1.25:1 for NO_2:NH_3, as can be seen in Figure 19.

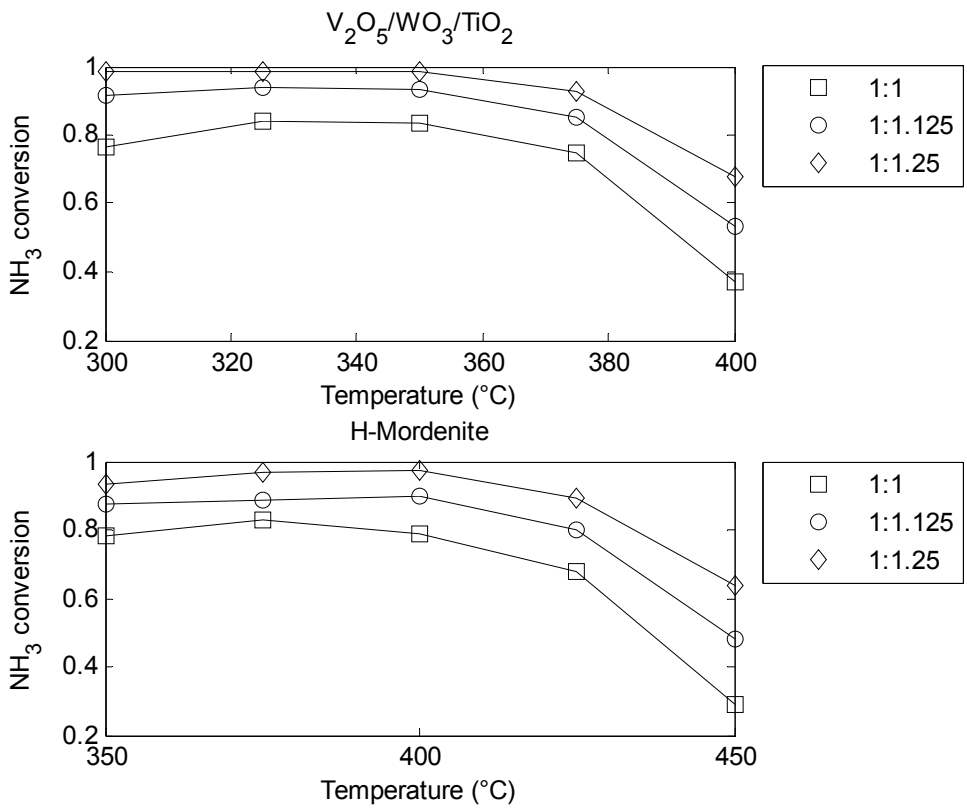

Figure 19: Ammonia conversion for the two tested catalysts at different temperatures and stoichiometry of NH_3:NO_2, adapted from Paper IV.

The conversion of ammonia is high for both catalysts at the higher NO_2 levels, and both catalysts show almost the same behaviour with a maximum at the middle of their temperature range. It should be noted that there is a 50 °C temperature difference between the catalysts. The $V_2O_5/WO_3/TiO_2$ is more active than the H-

mordenite and consequently the H-mordenite requires higher temperatures to reach similar conversion rates.

NO_2 is not an abundant molecule in the atmosphere and must therefore be manufactured before it can be injected into the gas stream in an industrial scale plant. A feasible route for the production of NO_2 is by decomposing nitric acid (HNO_3) either by reaction with a metal or by simply injecting nitric acid directly into the gas stream, which should yield a mixture of NO_2, H_2O and O_2 according to reaction (12).

$$4HNO_3 \rightarrow 4NO_2 + 2H_2O + O_2 \qquad (12)$$

Nitric acid is easier to handle than NO_2 and would be less expensive, being a bulk chemical. In Paper IV NO_2 generated from nitric acid was evaluated and the results were promising with over 75 % conversion of NH_3.

Due to analysis problems the study did not include water in the synthesis gas, which is present in any producer gas. Further studies have shown that there is a small effect of water that lowers the ammonia conversion rate, necessitating higher temperatures. The same catalysts were run on-stream for over 50 hours in the model synthesis gas without loss of activity, which further proves the concept.

2.5.5 Water-gas shift

The gas exiting a gasifier or reformer usually does not have the necessary ratio between H_2 and CO (and CO_2) that is required for downstream synthesis. The water-gas shift reaction (3) is an equilibrium reaction that is slightly exothermic.

$$CO + H_2O \rightleftharpoons CO_2 + H_2 \qquad \Delta H^0_{298} = -41\text{kJ/mol} \qquad (3)$$

The reaction is usually performed in an adiabatic catalytic reactor with different catalysts depending on the gas mixture and target H_2:CO ratio. The three most common commercial catalysts for the water-gas shift (WGS) reaction are Fe/Cr, Co/Mo and Cu/ZnO. Fe/Cr is actually Fe_3O_4, which is the stable iron phase under reaction conditions, promoted by chromium. The catalyst contains some 55 wt-% Fe and 6 wt-% Cr [20]. Copper metal is the active specie in the Cu/ZnO catalyst;

2.5 Gas conditioning

ZnO is added to protect the copper from poisons such as sulphur by reacting with the poisons. ZnO may also act as support for the copper metal. Before reduction, the catalyst contains roughly one third each of CuO, ZnO and Al_2O_3 [20]. Of the three water-gas shift catalysts, Co/Mo is the only one that requires sufficient amounts of sulphur in the gas (see Table 13). The Co/Mo is active in the sulphided state and is reported to contain about 4.5 wt-% CoO and 15 wt-% MoO_3, with the remainder being the support. The catalyst is promoted by alkalis, usually potassium. Furthermore, the Co/Mo catalyst can convert organosulphur compounds into H_2S [20].

Table 13: Commercial water-gas shift catalyst operating temperature range and sulphur properties.

Catalyst	Temperature	Sulphur
Fe/Cr	310–550 °C [20, 81]	Changes to FeS/Fe_2S_3 which has WGS activity although less than Fe
Co/Mo	200–500 °C [20, 82]	Sulphide is the active phase, requires at least 300 ppm in the gas [83]
Cu/ZnO	200–250 °C [20, 81], deactivated by sintering above 300 °C [81]	Permanently deactivated by small amounts of sulphur (and chlorine) ~1 ppm [20, 83]

Of the three commercial WGS catalysts, Cu/ZnO is the only catalyst that is readily deactivated by sulphur. Shifting in sulphur-rich environments is also known as sour shift. This high amount of sulphur is usually only available in syngas from coal gasification. WGS catalysts are usually divided into two groups, high temperature (HT) and low temperature (LT). Fe/Cr is a HT shift catalyst and Cu/ZnO is a LT shift catalyst. Co/Mo can be operated in a wide temperature range if there is sufficient sulphur present in the gas. The Fe/Cr catalyst is deactivated by small amounts (150 ppm) of NH_3 and HCl [84], both of which are present in biomass derived producer gas.

Table 14: Energy consumption when shifting syngas with a H_2:CO ratio of 1:1 at 1 bar.

H_2:CO ratio (starting at 1:1)	2:1	3:1	All hydrogen
Energy consumption (% of LHV)	3	4	8

Shifting a gas from a H_2:CO ratio of 1:1 to 2:1 will consume roughly 3 % of the energy in the gas (based on the lower heating value) as can be seen in Table 14. Going to maximum hydrogen content is necessary when producing pure hydrogen for ammonia synthesis or for refinery use, for example. Due to the equilibrium of the WGS reaction, a low temperature (200–225 °C) is required. Shifting a gas from a H_2:CO ratio of 1:1 to all hydrogen consumes 8 % of the chemical energy in the gas, which is released as heat.

Normally all of the gas is not shifted but instead a portion of the gas stream bypasses the shift reactor, unless the aim is pure hydrogen production. The reason for bypassing the shift reactor is that kinetically controlling the H_2:CO ratio is very difficult. Instead the outlet temperature of the adiabatic reactor is controlled by splitting the gas stream and the portion of gas that goes through the shift reactor almost reaches equilibrium at the outlet. When the gas streams are mixed after the reactor, the target H_2:CO ratio is achieved.

3 Chemical synthesis

After all the gas cleaning and conditioning, the synthesis gas can be used for synthesis. All syntheses involving syngas with hydrocarbons as the end product are highly exothermic.

3.1 Liquid fuels and chemicals

The liquid fuels and chemicals covered in this thesis include Fischer-Tropsch liquids, methanol and synthetic gasoline. Methanol is the feedstock for many important chemicals such as formaldehyde. Its use as a vehicle fuel is not limited to direct use, methanol is also used in transesterification of triglycerides when producing biodiesel. The production of biodiesel produces glycerol as a by-product that can be further processed into fine chemicals or fuels. Furthermore, methanol and isobutylene are used in the production of the octane booster methyl tert-butyl ether (MTBE).

Liquid fuels have some advantages over gaseous fuels, the most important of which is energy density, as shown in Table 15.

Table 15: Energy density for conventional and potential future vehicle fuels.

Fuel	LHV [GJ/Nm^3]	LHV [GJ/m^3] @ application pressure	LHV [MJ/kg]
Gasoline	32.1	32.1	43.4
Diesel	35.5	35.5	42.8
Methanol	15.9	15.9	20.1
Ethanol	21.3	21.3	27.0
Natural gas (100 % CH_4)	0.036	7.1 (200 bar)	47.1
LPG (70% C_3H_8, 30% C_4H_{10})	0.099	25.4 (7 bar)	46.6
Hydrogen	0.011	2.1 (200 bar) 8.6 (800 bar)	120
Dimethyl ether	0.059	21.7 (5 bar)	28.9

Table 15 shows a few important properties of various fuels. The gaseous fuels, starting with natural gas, have a considerably lower energy density per volume (almost 1000 times less for natural gas at atmospheric pressure compared with diesel). The liquefied gases, LPG (liquefied petroleum gas) and dimethyl ether, surpass the energy density of ethanol in their liquefied state. Hydrogen, which is seen by many as the fuel of the future, has the highest energy density per mass, but the lowest energy density per volume, which is an important factor. As fuel is stored in tanks with a finite volume, as much energy as possible should be stored in that volume.

Future gas-storage techniques may improve on these energy densities, but for now it is clear that to obtain the longest range possible the fuel should be stored as a liquid. Both methane and hydrogen can be stored as liquids, but this requires temperatures below –160 °C and is thus not feasible for small vehicles such as those used for personal transportation. Furthermore, due to heat transfer into the storage vessel, both liquefied natural gas (LNG) and liquefied hydrogen release gas when stored. Thus long-term storage is not feasible.

There are several other syntheses that will not be described in detail here that use syngas as feedstock. A few interesting syntheses for fuel production are the mixed alcohols and isosynthesis that are mentioned briefly in 3.1.5 (p. 64).

3.1.1 Fischer-Tropsch liquids

The Fischer-Tropsch (FT) synthesis was developed in the 1920s in Germany and is believed to be a polymerisation or oligomerisation of CO by H_2. The first catalysts were iron-based and required pressures in excess of 100 bar as the catalysts performed poorly at atmospheric pressure. A cobalt-based catalyst promoted by ThO_2 and MgO was developed to operate at more modest pressures [20]. The most common catalysts in use today are either iron- or cobalt-based. The choice of catalyst depends on the desired production distribution. The hydrocarbons produced in FT synthesis are primarily straight-chain and are most suited for diesel (Fischer-Tropsch diesel or FTD) and jet fuels. Some alcohols and aldehydes are also present in the product stream.

The two main reaction pathways are outlined in reactions (13 and 14)

$$CO + 2H_2 \rightarrow —CH_2— + H_2O \quad (13)$$

$$2CO + H_2 \rightarrow —CH_2— + CO_2 \quad (14)$$

Where the $—CH_2—$ represents a single carbon in the hydrocarbon chain. For iron-based catalysts, the WGS reaction takes place which allows CO_2 to be converted into hydrocarbons [85]. From reaction (13 and 14) it is clear that a H_2:CO ratio of 2:1 is ideal for FT synthesis.

The hydrocarbon distribution in FT synthesis is generally considered to follow the Anders-Shulz-Floury (ASF) distribution (15) [86]:

$$W_n = n \cdot (1 - \alpha)^2 \cdot \alpha^{(n-1)} \quad (15)$$

where n is the chain length and α the chain growth probability. The distribution is depicted in Figure 20 as the selectivity to a specific hydrocarbon range as a function of the chain growth probability.

Recent studies have shown that the product distribution does not follow the ASF distribution with newly developed catalysts that are tailored to yield more middle distillates and fewer heavy waxes [87, 88]. Furthermore, it has been shown that the ASF distribution under-predicts the methane formation and over-predicts the formation of C_2-C_3 [89]. The distribution can, however, still be used to some extent for modelling of FT diesel production, as long as heavier hydrocarbon production is restrained.

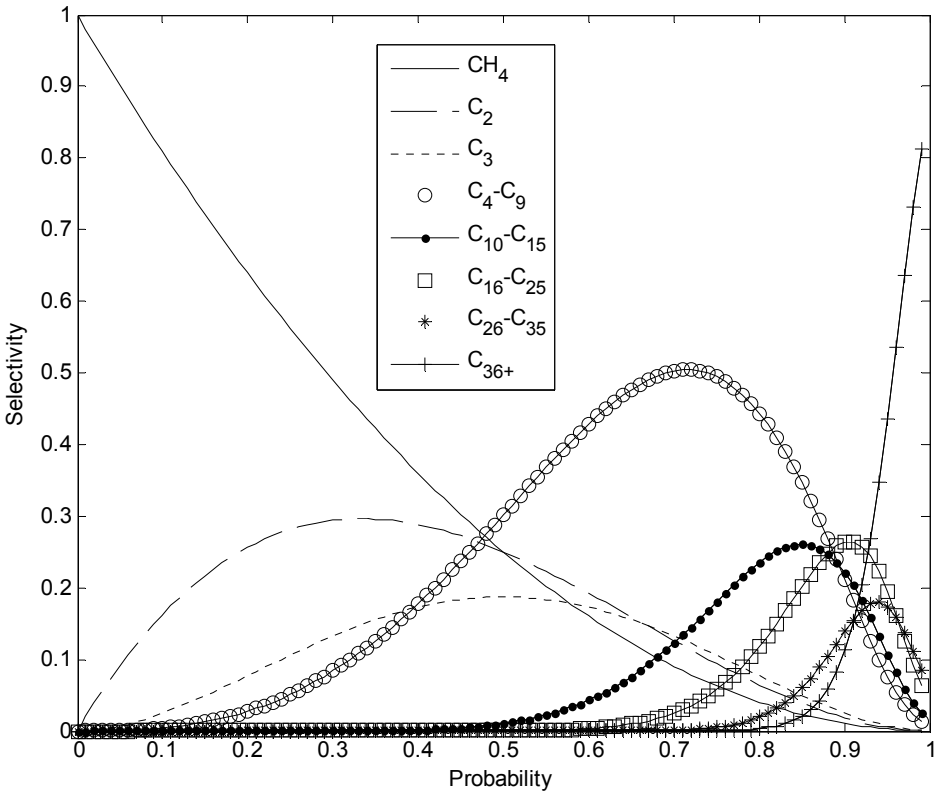

Figure 20: The Anderson-Schulz-Flory distribution.

In Figure 20, C_4–C_9 is typically the gasoline hydrocarbon range and C_{10}–C_{15} the diesel range. The heavier hydrocarbons are unwanted for most fuel applications, although catalytic cracking can increase their fuel yield. For vehicle fuels it is desirable to decrease the amount of hydrocarbons lower than, and to some extent including, butane (C_4), as they are gaseous at normal conditions found in vehicles. Figure 20 shows that when producing hydrocarbons in a certain range, for

example, gasoline (probability ~0.7), a large part of the end product contains hydrocarbons from the other ranges. The end product will always contain a mixture of hydrocarbons with varying molecular weight.

FT synthesis can be divided into high-temperature processes (HTFT) (operating at 300–350 °C) and low-temperature processes (LTFT) (operating at 200–240 °C). Iron catalysts are used at HTFT plants yielding hydrocarbons in the gasoline range and light olefins. The LTFT process uses either iron or cobalt catalysts to produce high molecular weight waxes, which after refining serve as diesel fuel. Operating pressures for the FT synthesis are in the range 20–30 bar [85]. Iron catalysts yield much lower ratios of paraffins to olefins and more oxygenated species such as alcohols and aldehydes than cobalt catalysts [20].

Hydrocarbon production from FT synthesis is not limited to vehicle fuels, as the product contains high amounts of olefins such as ethylene and propylene. These can be further processed into plastic monomers or higher alcohols.

Reactors are either multi-tubular fixed bed or fluidised bed. Fluidised bed reactors have the advantage of higher cooling capacity compared to fixed bed reactors. As the synthesis is highly exothermic, it is necessary to effectively remove the reaction heat to avoid overheating of the catalyst, which would result in premature deactivation. However, if poisons such as sulphur enter the reactor, the catalyst in fluidised bed reactors will need to be completely replaced, whereas in fixed bed reactors the sulphur deactivation occurs gradually from the inlet of the bed and only a part of the bed may need to be replaced.

3.1.2 Methanol

Methanol (MeOH) synthesis involves low temperatures and high pressures as it is a highly exothermic equilibrium-constrained reaction (16)

$$CO + 2H_2 \rightleftharpoons CH_3OH \qquad \Delta H^0_{298} = -91 kJ/mol \qquad (16)$$

The equilibrium for methanol under isothermal conditions is depicted in Figure 21, which shows that a combination of low temperature and high pressure is ideal

for high conversions. In reality the operating temperature is a compromise between catalyst activity (higher temperatures increase the rate of reaction) and thermodynamic limitations. Increasing the pressure favours the thermodynamics, but increased pressure increases both operating and investment cost.

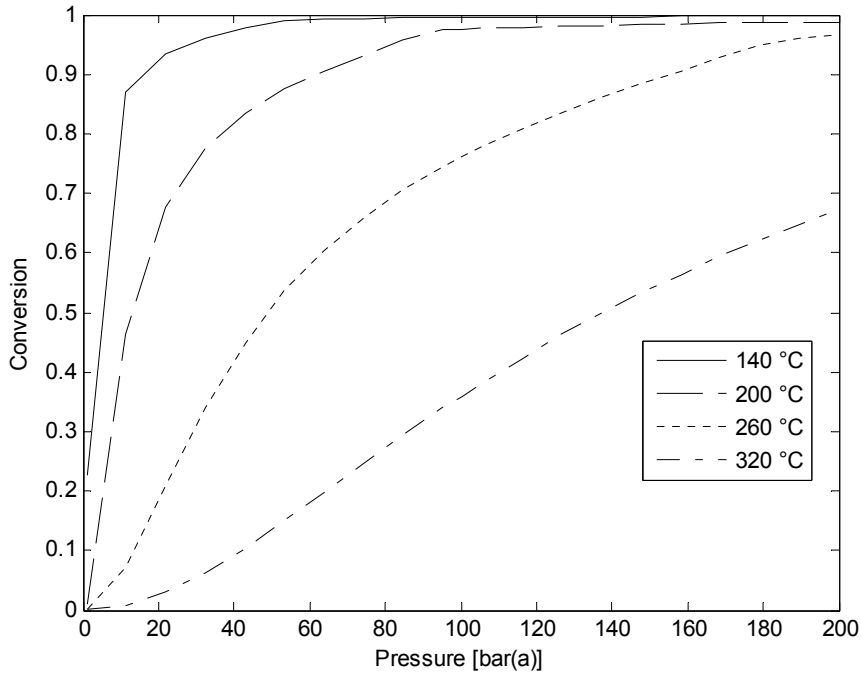

Figure 21: Equilibrium conversion of syngas to methanol ($H_2/CO/CO_2$: 2/1.05/0.01).

The catalyst used in methanol synthesis needs to be highly selective to methanol to minimise the formation of hydrocarbons. The catalyst used in the first commercial plant was ZnO/Cr_2O_3, and needed very high pressures and high temperature. This process is also known as the high-pressure process and is operated at 240–300 bar and 350–400 °C [20].

The low-pressure process uses a different catalyst based on copper and zinc. The catalyst is similar to the WGS catalyst, although different in formulation, and is also readily deactivated by sulphur. The low-pressure process operates at 50–100

bar. The operating temperature dictated by the catalyst is about 240–260 °C. At higher temperatures, catalyst deactivation by sintering becomes a problem.

From reaction (16) one could draw the conclusion that the ideal H_2:CO ratio for methanol synthesis is 2:1. That is not the case, as CO_2 plays a role in the reaction. Klier et al. reported that the ideal ratio between the species is 2/28/70 for CO_2, CO and H_2 respectively [90]. Klier et al. also reported significant CH_4 formation when CO_2 was in excess of 10 vol-% [90]. The H_2:CO/CO_2 ratio for methanol synthesis is often expressed according to equation (17), or module M as it also known [91].

$$\frac{H_2 - CO_2}{CO + CO_2} \qquad (17)$$

The ideal value for module M is 2 (as it is in Figure 21) although industrially it is operated at closer to 2.05 to suppress the formation of by-products [91]. As the catalyst is active for the WGS reaction, when CO_2 is consumed, water is formed.

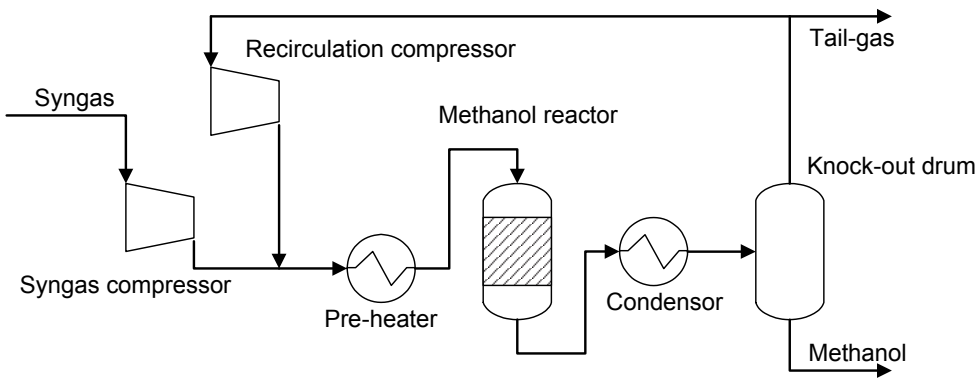

Figure 22: Methanol synthesis loop.

Recirculation of product gases is required to achieve high syngas conversion in methanol synthesis. Figure 22 shows the methanol synthesis loop with compression and product separation. Typical recirculation ratios are in the range of 3:1 to 7:1 of recycle gas to fresh syngas. The methanol product typically contains some 80 % MeOH and 20 % H_2O [20].

3.1.3 Dimethyl ether

Dimethyl ether (DME) is synthesised either directly from synthesis gas or by dehydration of methanol. DME is not a liquid at normal temperature and pressure, but it is covered here as it is connected to both methanol and methanol-to-gasoline synthesis. Moreover, DME used in vehicles would be stored as a liquid.

DME is used primarily as an intermediate in the synthesis of other chemicals such as dimethyl sulphate. DME is also used to replace chlorofluorocarbons (CFCs) as a propellant in aerosol spray cans. DME has also been tested as a replacement for diesel in diesel engines with great success and has shown reduced particle and NO_X emissions [92]. The synthesis of DME from methanol follows reaction (18), which is exothermic.

$$2CH_3OH \rightarrow CH_3OCH_3 + H_2O \qquad \Delta H^0_{298} = -23.4\text{kJ/mol} \qquad (18)$$

The dehydration reaction is performed at 300–340 °C and 10–20 bar [93] over a strong acidic catalyst such as alumina.

Direct DME synthesis involves the catalytic synthesis of methanol and in-situ dehydration to yield DME. Typical reaction conditions for direct synthesis are 240–280 °C and around 50 bar [94]. Reaction (19) describes the overall reaction of direct synthesis, which is a combination of reactions (16) and (18).

$$2CO + 4H_2 \rightarrow CH_3OCH_3 + H_2O \qquad \Delta H^0_{298} = -205\text{kJ/mol} \qquad (19)$$

The advantage of direct synthesis is the circumvention of the methanol equilibrium as methanol is continuously removed by dehydration.

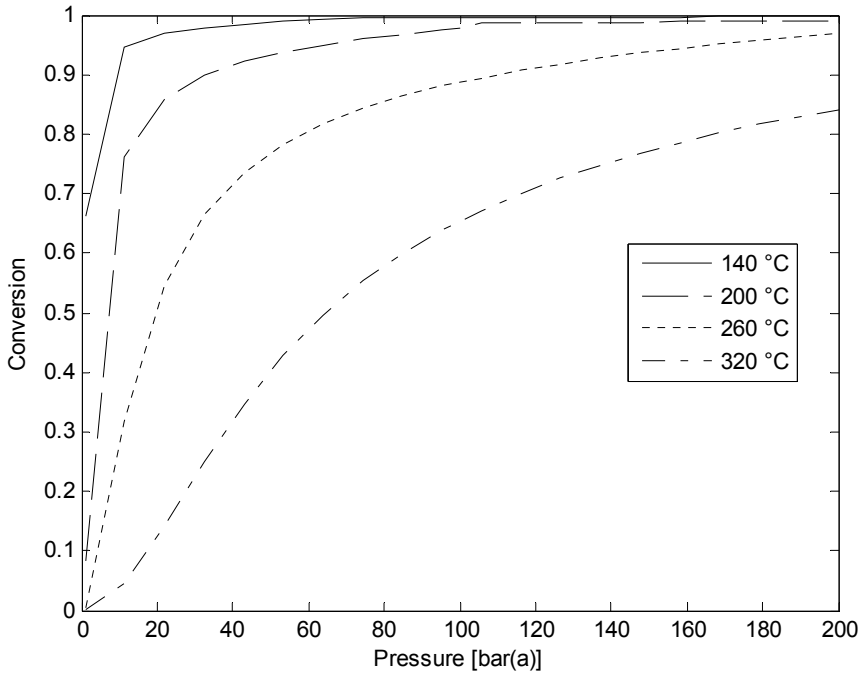

Figure 23: Equilibrium conversion for direct synthesis of DME from syngas (H_2:CO 2:1).

Comparing Figure 21 and Figure 23 shows that the conversion of syngas to DME is higher than that for methanol for any given temperature and pressure. Direct synthesis is not without its problems, however, as using acidic catalysts such as H-ZSM-5 can promote the formation of olefins [95], which are unwanted if the end product is DME. However, this could be a desired property if the end product is olefins.

3.1.4 Methanol-to-gasoline

The methanol-to-gasoline (MTG) process was developed by Mobil in the 1970s as a direct result of soaring oil prices. The first commercial plant was deployed in New Zealand in the mid-1980s. Methanol is first dehydrated to DME at equilibrium concentrations, and then the mixture is fed to the reactor (Figure 24). The reaction conditions are 360–415 °C and 20 bar [20].

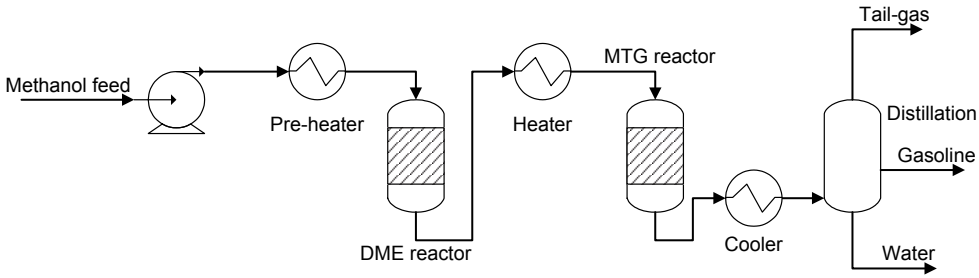

Figure 24: Basic schematic of the MTG process.

The catalyst used in MTG is ZSM-5, which is a zeolite. Zeolites are shape-selective catalysts that contain pores with specific volumes (apertures) that give the zeolites the following properties:

- Selectivity towards reactants

  The aperture of the zeolite permits only smaller molecules to enter the pores and excludes larger molecules, effectively allowing only the smaller molecules to react.
- Selectivity towards products

  Only products with a size smaller than the aperture size may diffuse out of the pores. Larger molecules are converted into either smaller molecules or carbonaceous deposits inside the pores.

As for FT, the products formed during MTG are a mixture of hydrocarbons, as seen in Table 16. The first steps of the reaction are the formation of olefins such as ethylene and propylene. The olefins then undergo oligomerisation to form larger olefins which are further reacted to form aromatics and aliphatics. The overall reaction (20) is exothermic.

$$CH_3OH \rightarrow \text{—}CH_2\text{—} + H_2O \qquad \Delta H^0_{298} = -50\text{kJ/mol} \ [13] \qquad (20)$$

Table 16: Product distribution of MTG [96].

Component	Yield [wt-%]
H_2O	55.20
CO	0.12
MEOH	1.00
DME	1.00
CH_4	0.34
C_2H_6	0.07
C_2H_4	1.60
C_3H_8	1.00
C_3H_6	1.50
i-C_4H_{10}	5.40
C_4H_{10}	0.47
C_4H_8	1.20
C_{5+}	31.10

Table 16 shows the yield from a MTG reactor. The largest part of the product is water, which is to be expected since half the weight of the methanol is oxygen that is removed from the hydrocarbons during reaction. Selectivity towards gasoline (C_{5+} and to some extent C_4) is very good. The lighter olefins can be further alkylated into gasoline.

The ZSM-5 catalyst was specifically developed for the MTG process as it is shape-selective to only allow C_9–C_{10} hydrocarbons (included in C_{5+} in Table 16) to diffuse out of the pores [13, 20]. This selectivity yields hydrocarbons with a good octane rating and boiling range for high-quality gasoline production. However, the use of shape-selective catalysts also causes high carbon deposits in the catalyst pores, as mentioned above. Mobil's process requires regeneration of the catalyst every two weeks to burn off coke [13].

If other zeolites with smaller aperture size are used, such as *erionite*, smaller olefins are formed with little to no C_{6+} [20]. The production of light olefins is wanted in

the methanol-to-olefins (MTO) process where ethylene, propylene and butylenes are desired products.

There are other variants of Mobil's MTG process, including Topsoe's integrated gasoline synthesis process (TIGAS) that uses methanol, DME and MTG synthesis in a single synthesis loop.

3.1.5 Other syntheses

Mixed alcohols or higher alcohol synthesis (HAS) is a synthesis that produces alcohols like methanol, ethanol and propanol. The synthesis is almost a combination of methanol and Fischer-Tropsch syntheses in which modifications are made to minimise the hydrocarbon yield. The catalysts used are modified methanol and Fischer-Tropsch catalysts. MoS_2 is a very interesting catalyst for both Fischer-Tropsch synthesis and mixed alcohols synthesis as it is sulphur tolerant. The catalyst requires at least 50 vppm H_2S in the gas, but concentrations above 100 vppm reduce the reaction rate and the higher alcohol selectivity [97].

The operating conditions for mixed alcohols synthesis are about 300–350 °C and 100–140 bar. Just like methanol and, to some extent, Fischer-Tropsch synthesis, some CO_2 is allowed in the gas (0–7 vol-%) as the catalyst has some WGS activity. The H_2:CO ratio of 1–1.2:1 [97] for mixed alcohols is almost in the range of producer gas H_2:CO ratio, which means that no WGS reactor is needed.

Another interesting synthesis from syngas is isosynthesis. Isosynthesis is the synthesis of branched aliphatic hydrocarbons over a metal oxide catalyst. Of the catalysts with sufficient selectivity, thorium oxide (ThO_2) is the most promising, but others such as zirconia (ZrO_2) may also be used. The operating conditions are severe, requiring high temperature 350–500 °C and very high pressure 100–1000 atm (best results are reported at 300–600 atm) [98]. A temperature of 400–450 °C is optimal as decreased temperature increases the dimethylether production and higher temperatures increase carbon formation. A H_2:CO ratio of 1.2:1 is ideal for isosynthesis as it produces the maximum amount of hydrocarbons [98].

As previously mentioned, isosynthesis yields branched hydrocarbons, the most important of which are isobutylene and isobutane. Polymerisation or alkylation of isobutylene with, for example, n-butylene will yield 2,2,4-trimethylpentane (isooctane), a hydrocarbon with an octane rating of 100 (MON and RON) by definition. In other words, isosynthesis can be used to produce one of the best blending additives to boost low grade gasoline. Synthetic rubber or butyl rubber is also manufactured from isobutylene, which should be more valuable than vehicle fuels.

3.2 Gaseous fuels and chemicals

The major disadvantage of gaseous fuels compared to liquid fuels is the low energy density (see 3.1, p. 53). In addition, the separation of products and contaminants after synthesis is more problematic with a gaseous product. However, there are some specific fuels that are of interest, despite the lower energy density. Furthermore, several important gaseous bulk chemicals are produced from synthesis gas.

3.2.1 Synthetic natural gas

Methane produced from synthesis gas is often referred to as synthetic natural gas or substitute natural gas (SNG). The synthesis of methane from syngas follows the reverse reaction (2) and is termed methanation.

$$CO + 3H_2 \rightleftharpoons CH_4 + H_2O \qquad \Delta H^0_{298} = -206\text{kJ/mol} \qquad (2)$$

This synthesis has been studied since the beginning of the 20th century and was first used in the 1950s to remove low concentrations of CO in gas mixtures containing H_2, primarily for ammonia production.

The catalysts primarily used for methanation are nickel-based. Methanation is highly exothermic. Cooled recycle gas mixed with fresh syngas to control temperature in the reactor is used in Topsoe's TREMP (Topsoe Recycle Energy-

efficient Methanation Process). In TREMP three adiabatic reactors are used with recycling of gas over the first reactor where the temperature increase is the highest, as shown in Figure 25.

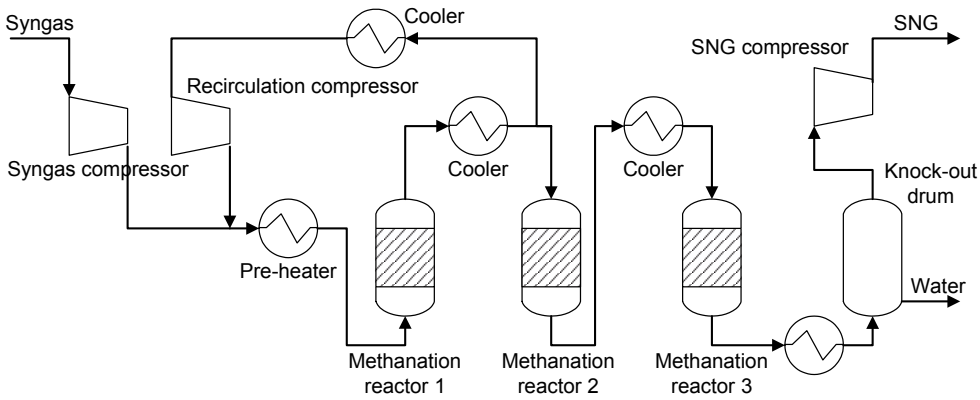

Figure 25: Schematic of TREMP.

The methane will be more or less pure depending on the composition of the syngas. The catalysts have activity for the WGS reaction and some CO_2 is to be expected at the reactor outlet for low H_2:CO ratios. Furthermore, as conversion of CO and H_2 is incomplete, small amounts of both are to be expected when producing SNG.

The advantage of Topsoe's TREMP is that the methanation catalyst is capable of operating at 250–700 °C. The high synthesis temperature allows the generation of high-pressure superheated steam (100 bar/540 °C), which can be used to generate electricity.

The minimum temperature of the process is 200 °C, in part because of catalyst activity but also because volatile nickel carbonyl will be formed at lower temperatures [20].

Methanation reactors can also be operated as fluidised bed reactors, which is favourable for heat removal as the reaction is highly exothermic. Typically fluidisation is not coupled with recirculation of product gas.

Reactor temperatures during methanation are in the range of 250–450 °C [99], except for TREMP, but can be lower in fluidised beds because of the excellent cooling capabilities of the operation, which permit a range of 250–350 °C [99, 100].

Operating pressures for methanation are very flexible, and pressures in the range 10–30 bar are not uncommon [20] as higher pressures are both favourable for the equilibrium and increase throughput at the expense of compression power.

When using methanation for purification, both CO and CO_2 can be effectively removed down to a few ppm [101].

It is difficult to separate the SNG product and contaminants. N_2 in the producer gas must be kept to a minimum, as it is not removed by most gas conditioning techniques upstream of synthesis. A producer gas with 0.8 vol-% N_2 results in a product SNG with over 3 vol-% N_2 after methanation and CO_2 and water removal.

3.2.2 Ammonia

The first inorganic fertilizers used saltpetre ($NaNO_3$) mined in the Atacama Desert in Chile. The use of inorganic fertilizers is one of the reasons that the world population has been able to rise so dramatically during the past century, from 1.6 billion in 1900 to 7 billion 2011. Erisman et al. have estimated that almost half of the current population is alive today only thanks to the use of nitrogen fertilizers [102]. The mining of nitrogen fertilizers was not enough to meet demand, and several attempts at fixating nitrogen from the air were developed, such as the cyanamide and electric arc processes [103]. Both processes were discontinued due to a much more energy efficient process, the Haber-Bosch process. This process was developed by Haber and Bosch in the early 1900s. In the Haber-Bosch process nitrogen from the air is fixed to ammonia according to reaction (21).

$$N_2 + 3H_2 \rightleftharpoons 2NH_3 \qquad \Delta H_{798} = -109\text{kJ/mol} \qquad (21)$$

The reaction has a strong equilibrium which favours low temperatures and high pressures (Figure 26).

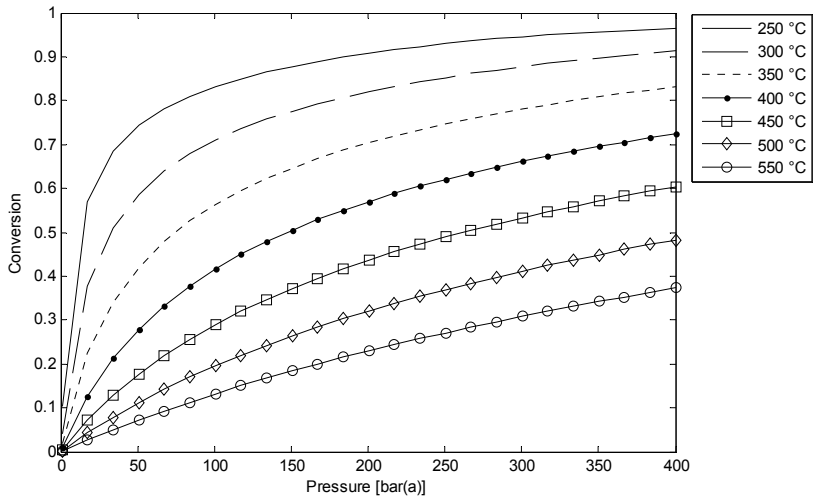

Figure 26: Ammonia equilibrium as a function of pressure and temperature.

The catalyst used is magnetite (Fe_3O_4) promoted by Al_2O_3, K_2O and in some cases CaO and MgO [20]. The catalyst is highly susceptible to all kinds of catalyst poisons such as chlorine and sulphur, but most importantly to carbon oxides and water vapour [20]. Carbon oxides and water are present in large quantities in synthesis gas and must be removed prior to ammonia synthesis. Carbon oxides are typically removed by methanation as CH_4 is inert in the presence of the iron catalyst.

As can be seen in Figure 26, high pressures are an absolute necessity. Industrial plants operate at 150–300 bar and 430–480 °C, even though low temperatures are preferred. The higher temperatures are required to reach acceptable reaction rates [20].

Ammonia synthesis is one of the most important chemical processes in use due solely to its role in food production. However, the production of nitrogen fertilizers (ammonia) is energy intense and accounted for 1 % of the total energy consumption in the world in 2001 [104]. Yet the energy requirement for ammonia

production has steadily declined from over 210 GJ/tonne NH_3 to below 40 GJ/tonne NH_3 today [104].

The production of ammonia requires over half of the total annual world production of hydrogen, or some 28 million tonne [105]. Almost all of the hydrogen produced worldwide comes from fossil feedstocks with natural gas accounting for almost 50 %. In order to produce sustainable and renewable ammonia, renewable and sustainable hydrogen must first be produced.

Most new ammonia plants are large plants located in the Middle East or Asia where there is both cheap energy and a growing demand of fertilizer. For really sustainable production, however, decentralised production is preferable with smaller plants utilising renewable resources. Three alternative processes for renewable ammonia were suggested in Paper V: electrolysis to hydrogen using clean power, reforming of biogas to hydrogen, and lastly, biomass gasification for hydrogen production. All three process use downstream ammonia synthesis.

Paper V concluded that renewable ammonia production with renewable hydrogen is several times more expensive than traditional natural gas- based ammonia. Production from a renewable feedstock is not likely to become cheaper in the future, but green incentives could possibly create a niche market for renewable and fossil-free fertilizers, enabling the establishment of small-scale installations.

4 System studies and integration

Which of the fuels and chemicals described in chapter 3 has the highest production efficiency? Which has the highest production cost? These are among the more important questions that will be answered in this chapter based on studies performed by the author.

There are several benefits to integrating a synthesis plant with another production facility for large-scale production of fuels and/or bulk chemicals. The integration can be minimal, such as sharing only already present feedstock logistics, or it can be a full integration in which both energy and material streams are interconnected. A synthesis plant can also produce several types of fuels and/or chemicals for increased efficiency. Lastly, co-firing of renewable feedstocks with fossil feedstocks can increase the economics of the plant by enabling an increase in scale, making an unprofitable plant profitable. Profitability is essential for the implementation of renewable fuels and chemicals.

4.1 System studies

Paper VI contains a comparison of all vehicle-type fuels covered in chapter 3 and was performed by the author to evaluate which of the fuels had the highest energy efficiency from well-to-wheel (WTW) (biomass as input, vehicle travel distance as output). In addition to the thermochemical fuels, bioethanol produced from woody biomass was considered in the study. A different gasifier was used for SNG production than for the other fuels because SNG efficiency benefits from gasifiers with high methane output.

Table 17: Energy distribution for synthetic fuel plants from wood to product based on Paper VI.

Fuel	SNG	MeOH	MTG	DME	FT	EtOH
Product	66.5%	58.7%	50.6%	53%	45.6%	41.2%
Electricity	3.5%	1.8%	4.7%	3.7%	5.9%	0.1%
District heating	23%	0.36%	1.4%	0%	13%	0%
Losses	7.3%	39.1%	43.2%	43.3%	35.5%	58.7%

The energy distribution of the synthetic fuels plants investigated in Paper VI is shown in Table 17. For SNG plants, 66.5 % of the energy in the biomass is converted into SNG. For FT plants, only 45.6 % of the energy in the biomass feedstock is converted into diesel. From Table 17 it can be seen that some electricity and district heating can be produced along with the fuels.

The WTW results showed a not unexpected advantage for diesel-type fuels (FT and DME) over gasoline types, as shown in Table 18. This is all thanks to the higher efficiency of the diesel engine.

Table 18: Range on one kilogram of dry wood based on Paper VI

Fuel	SNG	MeOH	MTG	DME	FT	EtOH[1]	EtOH[2]
Range (km)	4.89	4.16	3.59	5.71	4.91	2.92	3.81
Fuel cost ($/100 km)	5.09	6.17	7.48	4.68	6.13	8.51	–

[1)] Based on data presented by Gnansounou et al. [106].

[2)] Theoretical maximum production of 455 litres ethanol/dry ton wood

DME is the clear winner in the longest-range contest, thanks to high synthesis and engine efficiency. Bioethanol when used in gasoline engines is the clear loser due to inefficient production and fuel utilisation.

High efficiency is not the only parameter by which the success of biofuels is measured. Production cost is also important, as the product has to compete with fossil energy prices.

The production cost was used to calculate the cost of driving 100 km and is also presented in Table 18. Ethanol is the most expensive fuel in this study, due to the lower efficiency of production and fuel utilisation in the gasoline engine. The range for FT is longer than methanol by 0.75 km, but the cost differs only $0.04. DME is once again the clear winner, but SNG is not far behind. Both of these products are gaseous, and as such not as easy to substitute for conventional fuels. Ethanol is used as a low level blending additive to gasoline and for E85 (85 % ethanol, 15 % gasoline). It is interesting to note that synthetic gasoline (MTG) is both cheaper to produce and has higher energy efficiency than ethanol.

During oil extraction, dissolved light fractions are emitted from the well. This well-head gas is generally flared on-site to reduce methane emissions. Paper VII describes a way to make better use of this energy by synthesising more crude oil. Well-head gas can contain up to 5 vol-% H_2S, necessitating a comprehensive desulphurisation either upstream of the reformer or prior to crude synthesis. To make this well-head gas upgrading system simple, self-sustained and able to handle any gas quality without expensive gas cleaning, pressure swing adsorption (PSA) was used to remove CO_2 and most of the H_2S. A POX reactor was used, as that is the only option given the high sulphur load. Reverse-flow POX was also evaluated to compare the benefits of its higher energy efficiency. Oxygen for both POX reactors was produced by either electrolysis, PSA or a combination of both. The synthetic crude was produced in a FT reactor.

Paper VII also discusses the production costs, which ranged from $71/ bbl when using PSA to $156/bbl for electrolysis. With a fixed input of 100 MW well-head gas, the production of crude ranged from 270 bbl/day to 436 bbl/day for the different cases studied.

4.2 Sub-integration versus full integration

Full integration of a synthesis plant is achieved if it and the other industry depend on each other for operability. A typical example of this is black liquor gasification (BLG) in pulp and paper mills. Black liquor is a residual of the pulping process,

and contains a large percentage of the energy of the wood used as input to the process. A gasifier is used in place of a lime kiln to recover both the pulping chemicals and the energy in the black liquor. A lime kiln uses heat to generate steam, whereas a gasifier produces syngas. The advantage of the BLG concept is that the syngas can be used to synthesise fuels or chemicals or to produce integrated gasification combined cycle (IGCC) power, rather than just steam for power production. The BLG producer gas, however, has higher levels of both sulphur and alkalis and thus requires expensive gas conditioning.

The clear disadvantage of full integration is the requirement that both processes must be reliable. If the gasifier must be stopped, the pulp mill must be stopped as well, and vice versa. Stopping production in a large and complex plant such as a pulp and paper mill is both time-consuming and costly. Furthermore, the potential for fully integrated plants is more limited than for stand-alone plants or sub-integration as there are a limited number of pulp and paper mills.

If the paper and pulp mill handles the pulping chemical recovery and only exchanges heat streams with a gasification plant, an option evaluated in Paper VIII, some synergies can be expected. One possibility is using fuel synthesis tail gas or a part of the raw syngas to replace the fuel oil used to increase the flame temperature in the recovery boiler. In such scenarios gasification plants are located in the vicinity of an existing paper and pulp mill and share the feedstock logistics, which is an added bonus for the gasification plant.

The integration of biomass gasification plants is not limited to pulp and paper mills, although that is a logical scenario as the logistics are already in place. For example, steel plants use coke produced from coal to produce steel from iron ore. During coke production, large quantities of energy-rich gases are formed containing CO, H_2, CH_4, CO_2 and some C_2H_6 with varying composition. The gas is used in the steel plant for heat and power production, but could be used to produce synthetic fuels and chemicals, along with synthesis gas produced in a gasifier.

The methanol discussed in Paper IX was produced in an integrated biomass gasification/steel plant. The gasifier could be coal- or biomass- fired, or a

combination of both. As the logistics for coal are already in place, coal could be a viable option, although biomass would be preferred on a sustainability basis. The energy removed from the steel plant in the form of coke oven gas can be replaced by high-pressure steam generated by the synthesis plant. The use of coke oven gas and biomass-generated synthesis gas is a form of co-firing. Adding a methanol synthesis plant to a steel plant by utilising biomass-generated synthesis gas and coke oven gas can increase plant profit and energy utilisation and reduce CO_2 emissions.

4.3 Co-production

Producing more than one product in the same process is called co-production and can have several benefits. A clear example of this is the production of FT liquids and SNG. FT synthesis produces lighter hydrocarbons in the range C_1–C_4, which is an ideal addition to SNG. SNG with a higher heating value can be produced along with the FT liquids. The yield of C_1–C_4 in the FT process can be controlled by the choice of catalyst and operating conditions. An ideal in the ASF expression (Figure 20) would be around 0.5–0.6 for production of liquids and gases.

Zwart et al. [107] studied the synergies of producing FT diesel and SNG in several co-production configurations. Although overall efficiencies are a little optimistic, there is a clear advantage to co-production. Stand-alone FT synthesis would typically require separation of lighter fractions followed by recirculation upstream of a reformer to increase efficiency. Recirculation requires more energy than once-through configuration because compression power is increased by the higher mass flow, and additional energy is lost due to reforming and synthesis.

The possibility of co-producing fuels and power was also investigated by de Lange [108]. The benefits of this are many. In IGCC implementations a gasifier produces syngas for fuel in a gas turbine. Increasing the gas output of the gasifier and using the extra syngas for synthesis of fuels comes almost without efficiency loss as the synthesis heat can be used to preheat steam for power production or for district

heating. Synthesis reactors could be operated either once-through with most of the producer gas, or in recirculation with a smaller part of the gas.

The synthetic fuels could either be sold or used in the plant for peak-shaving during high loads. A system with a gasifier designed for outputs that covers normal loads could also cover peaks, as long as a sufficient amount of synthetic fuels is produced during off-peak hours. As most syntheses require syngas with little to no CO_2, a CO_2-rich stream is available for carbon capture and storage or sequestration (CCS) operation, thus reducing CO_2 emissions [108]. The drawbacks are increased plant costs because of the expense of conditioning the syngas as compared to cleaning flue gas. The system also becomes more complex with other demands on start up and shutdown.

5 Conclusions

Synthetic fuels and chemicals have the potential to replace crude oil in the future. Coal, natural gas and biomass are potential feedstocks. Using biomass would make the processes renewable and carbon dioxide neutral. The problem is that not enough sustainable biomass is available to replace all the crude oil used in the world. If biomass is used as feedstock, it is crucial to utilise processes with as high efficiency as possible to get as much product as possible out of the limited feedstock. The critical part of the synthesis plant is the gas conditioning.

5.1 Suggested process configuration

Much can be gained by using the reverse-flow reactors described in this thesis, as can be seen in Figure 27 and Figure 28 below.

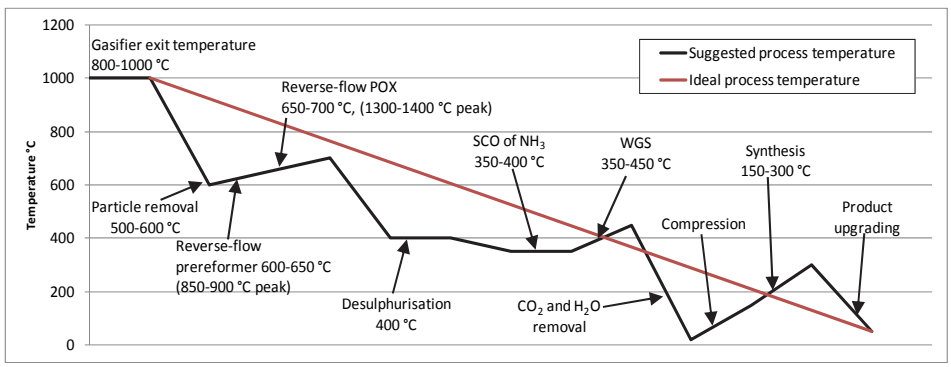

Figure 27: Suggested process design based on unconventional technology presented in this thesis and temperature intervals for gas conditioning and synthesis.

5.1 Suggested process configuration

For ideal heat utilisation, the reactor with the highest exit temperature in the process should be the gasifier. After the gasifier, the temperature should drop to synthesis temperature during gas conditioning and subsequent product upgrading in steps with as little heating as possible along the way. Figure 27 shows how this could be achieved by using the reverse-flow reactors presented in 2.5.2.1 and 2.5.2.3 (p. 30 and 38).

Desulphurisation can be performed at a better temperature range after the reformers by not using nickel-based catalytic reformers. The desulphurisation can be located either before or after NH_3 removal and WGS. Removal of NH_3 is performed before WGS due to the problems with FeCr catalysts and NH_3, as described in 2.5.5 (p. 49). Synthesis of the desired fuel or chemical can be performed after CO_2 removal and water knock-out.

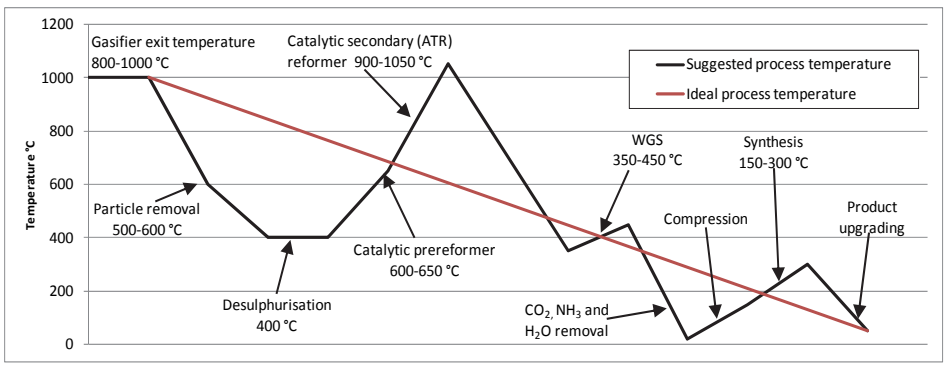

Figure 28: Suggested process design based on conventional technology and temperature intervals for gas conditioning and synthesis.

The process configuration in Figure 28 is based on nickel-based prereforming and nickel-based secondary reforming. As has been mentioned previously, there are problems with this configuration if sulphur is present. Organic sulphur will not be removed in a desulphurisation step, and thus requires prereforming to convert organic sulphur to H_2S. The prereformer can be placed either before or after desulphurisation. If placed before desulphurisation, the catalyst will be deactivated faster. When placed after desulphurisation, the prereformer will act both as a reformer and as a guard bed for the secondary reformer. The temperature of ZnO desulphurisation (approx. 400 °C) is far from the required burner temperature in

an ATR, resulting in a less energy- conserving solution than the reverse-flow POX in Figure 27. A large portion of the energy, but far from all of it, can be recovered in heat-exchangers. Much of the ammonia is converted in the reformers and the remainder is removed with the water and CO_2 after the WGS.

In the author's opinion, the configuration in Figure 27 is more suitable for biomass-generated producer gas than the conventional configuration in Figure 28. Furthermore, the prereformer in the configuration in Figure 28 will eventually be deactivated due to sulphur poisoning.

The findings of Papers I, II and III on reverse-flow reactors are very promising in terms of their energy efficiency and ability to handle the sulphur in producer gas. The work done on catalytic tar cracking in Paper III using dolomite as bed material showed particular potential. Future work should use real producer gases from biomass gasifiers. The same applies to the selective catalytic oxidation of ammonia in producer gas using nitrogen oxides investigated in Paper IV.

5.2 Synthesis conclusions

Of the syntheses covered in chapter 3, FT and MTG are the processes that produce liquid hydrocarbons that most resemble crude oil derived fuels, which are easier to integrate into the existing refinery and fuel distribution infrastructure. However, these are also the processes with almost the lowest energy efficiency (LHV basis). The strength of the hydrocarbon fuels compared to ethanol or methanol is the lower oxygen content and thus the higher energy density. Furthermore, ethanol and methanol in particular are much more corrosive than the hydrocarbons. The well-to-wheel analysis in Paper VI also shows good overall efficiency for FT liquids compared to ethanol and methanol. MTG does not show equally good overall efficiencies. Both of these processes can also be used to synthesise valuable chemicals such as aromatics and plastic monomers.

Methanol is a high octane fuel but is primarily an important bulk chemical and, as such, could be a higher value product than motor fuel. Methanol is produced in large quantities from coal and natural gas, and biomass-based methanol will need

to compete with that. The higher prices of biomass- based methanol means that it needs either incentives or a niche market to be competitive.

When produced from gas produced in a gasifier with high methane content in the producer gas, SNG is the most efficient synthesis, as part of the product exists in the producer gas. The separation of product and contaminants after synthesis is not as easy as it is for liquid chemicals. This is one of the reasons that the nitrogen content in the producer gas should be kept to a minimum. The distribution of SNG is straightforward as long as a gas grid is available, as it is in many places in Europe. Without a gas grid, the distribution becomes much less ideal.

DME has the highest efficiency on a well-to-wheel basis. Ideally the synthesis should be direct from syngas to give a more favourable equilibrium rather than with methanol as an intermediate step.

6 References

1. Baker, E.G., et al., *Characterization and treatment of tars from biomass gasifiers*, 1988.
2. Beenackers, A.A.C.M., *Biomass gasification in moving beds, a review of European technologies.* Renewable Energy, 1999. **16**(1–4): p. 1180-1186.
3. Chatterjee, A., *Sponge Iron Production By Direct Reduction Of Iron Oxide*2010: PHI Learning.
4. Henrich, E. and F. Weirich., *Pressurized Entrained Flow Gasifiers for Biomass* Environmental Engineering Science, 2004. **21**(1): p. 53-64.
5. McKendry, P., *Energy production from biomass (part 3): gasification technologies.* Bioresource Technology, 2002. **83**(1): p. 55-63.
6. Baker, E.G., et al., *Engineering analysis of biomass gasifier product gas cleaning technology*, 1986.
7. Teislev, B., *Harboore – Woodchips updraft gasifier and 1500 kW gas-engines operating at 32% power efficiency in CHP configuration*, 2002: Babcock & Wilcox Volund R&D Centre, Centervej 2, DK-6000 Kolding, Denmark.
8. Meijden, C.M.v.d., *Development of the MILENA gasification technology for the production of Bio-SNG*, 2010: Energy research Centre of the Netherlands.
9. Boerrigter, H. and R. Rauch, *Review of applications of gases from biomass gasification*, 2006: Vienna, University of Technology, Institute of Chemical Engineering.
10. Chrisgas, *Intermediate Report*, 2008.
11. Tremel, A., et al., *Entrained flow gasification of biocoal from hydrothermal carbonization.* Fuel, 2012. **102**(0): p. 396-403.
12. Prins, M.J., K.J. Ptasinski, and F.J.J.G. Janssen, *More efficient biomass gasification via torrefaction.* Energy, 2006. **31**(15): p. 3458-3470.
13. Probstein, R.F. and R.E. Hicks, *Synthetic Fuels*1982.
14. Kıpçak, E. and M. Akgün, *Oxidative gasification of olive mill wastewater as a biomass source in supercritical water: Effects on gasification yield and biofuel composition.* The Journal of Supercritical Fluids, 2012. **69**(0): p. 57-63.

15. Withag, J.A.M., et al., *System model for gasification of biomass model compounds in supercritical water – A thermodynamic analysis.* The Journal of Supercritical Fluids, 2012. **61**(0): p. 157-166.
16. Kruse, A., *Hydrothermal biomass gasification.* The Journal of Supercritical Fluids, 2009. **47**(3): p. 391-399.
17. Sehested, J., *Four challenges for nickel steam-reforming catalysts.* Catalysis Today, 2006. **111**(1–2): p. 103-110.
18. Moulijn, J.A., M. Makkee, and A. van Diepen, *Chemical process technology*2001: John Wiley & Sons.
19. Liu, K., C. Song, and V. Subramani, *Hydrogen and Syngas Production and Purification Technologies*2009: Wiley.
20. Satterfield, C.N., *Heterogeneous Catalysis in Industrial Practice*1991: Krieger Pub.
21. Alstrup, I., et al., *Promotion of steam reforming catalysts*, in *Studies in Surface Science and Catalysis*, D.S.F.F.A.V. A. Parmaliana and A. F, Editors. 1998, Elsevier. p. 5-14.
22. Beltramini, J.N. and R. Datta, *Coke deposition on naphtha reforming catalysts: I. Influence of the hydrocarbon feed.* Reaction Kinetics and Catalysis Letters, 1991. **44**(2): p. 345-352.
23. Froment, G.F. and B. Delmon, *Catalyst Deactivation 1987*1987: Elsevier Science.
24. Rostrup-Nielsen, J.R., *Steam Reforming Catalysts*1975, Copenhagen: Teknisk Forlag A/S.
25. Rostrup-Nielsen, J.R. and L.J. Christiansen, *Internal steam reforming in fuel cells and alkali poisoning.* Applied Catalysis A: General, 1995. **126**(2): p. 381-390.
26. Dybkjaer, I., *Tubular reforming and autothermal reforming of natural gas — an overview of available processes.* Fuel Processing Technology, 1995. **42**(2–3): p. 85-107.
27. Aasberg-Petersen, K., et al., *Recent developments in autothermal reforming and pre-reforming for synthesis gas production in GTL applications.* Fuel Processing Technology, 2003. **83**(1–3): p. 253-261.
28. Dybkjaer, I. and T.S. Christensen, *Syngas for large scale conversion of natural gas to liquid fuels*, in *Studies in Surface Science and Catalysis*, J.J.S. E. Iglesia and T.H. Fleisch, Editors. 2001, Elsevier. p. 435-440.
29. Bao, X. and Y. Xu, *Natural Gas Conversion VII: Proceedings of the 7th Natural Gas Conversion Symposium, June 6-10, 2004, Dalian, China*2004: Elsevier.

30. Kato, T., et al., *Effective utilization of by-product oxygen from electrolysis hydrogen production.* Energy, 2005. **30**(14): p. 2580-2595.
31. Wender, I., *Reactions of synthesis gas.* Fuel Processing Technology, 1996. **48**(3): p. 189-297.
32. Wang, L., *Theoretical study of cyclone design*, in *Texas A&M University*2003, Texas A&M University: Texas A&M University.
33. Kuo, K.-Y. and C.-J. Tsai, *On the Theory of Particle Cutoff Diameter and Collection Efficiency of Cyclones.* Air and Air Quality Research, 2001. **1**(1): p. 47-56.
34. Saxena, S.C., R.F. Henry, and W.F. Podolski, *Particulate removal from high-temperature, high-pressure combustion gases.* Progress in Energy and Combustion Science, 1985. **11**(3): p. 193-251.
35. McKendry, P., *Energy production from biomass (part 1): overview of biomass.* Bioresource Technology, 2002. **83**(1): p. 37-46.
36. Kurkela, E. and P. Ståhlberg, *Air gasification of peat, wood and brown coal in a pressurized fluidized-bed reactor. I. Carbon conversion, gas yields and tar formation.* Fuel Processing Technology, 1992. **31**(1): p. 1-21.
37. Hofbauer, H., et al., *Six years experience with the FICFB-Gasification Process*, in *12th European Conference and Technology Exhibition on Biomass for Energy, Industry and Climate Protection*2002: Amsterdam, The Netherlands.
38. Struis, R.P.W.J., et al., *Sulphur poisoning of Ni catalysts in the SNG production from biomass: A TPO/XPS/XAS study.* Applied Catalysis A: General, 2009. **362**(1–2): p. 121-128.
39. Czekaj, I., et al., *Sulphur poisoning of Ni catalysts used in the SNG production from biomass: Computational studies.* Catalysis Today, 2011. **176**(1): p. 429-432.
40. Cui, H., et al., *Contaminant Estimates and Removal in Product Gas from Biomass Steam Gasification.* Energy & Fuels, 2010. **24**(2): p. 1222-1233.
41. Matros, Y.S. and G.A. Bunimovich, *Control of Volatile Organic Compounds by the Catalytic Reverse Process.* Industrial & Engineering Chemistry Research, 1995. **34**(5): p. 1630-1640.
42. Boreskov, G.K. and Y.S. Matros, *Flow reversal of reaction mixture in a fixed catalyst bed - a way to increase the efficiency of chemical processes.* Applied Catalysis, 1983. **5**(3): p. 337-343.
43. Matros, Y.S., et al., *Is it economically feasible to use heterogeneous catalysts for VOC control in regenerative oxidizers?* Catalysis Today, 1996. **27**(1–2): p. 307-313.

44. Matros, Y.S. and G.A. Bunimovich, *Reverse-Flow Operation in Fixed Bed Catalytic Reactors.* Catalysis Reviews, 1996. **38**(1): p. 1-68.
45. Boreskov, G.K. and Y.U.S. Matros, *Unsteady-State Performance of Heterogeneous Catalytic Reactions.* Catalysis Reviews, 1983. **25**(4): p. 551-590.
46. Neumann, D. and G. Veser, *Catalytic partial oxidation of methane in a high-temperature reverse-flow reactor.* AIChE Journal, 2005. **51**(1): p. 210-223.
47. Mitri, A., et al., *Reverse-flow reactor operation and catalyst deactivation during high-temperature catalytic partial oxidation.* Chemical Engineering Science, 2004. **59**(22–23): p. 5527-5534.
48. Neumann, D., V. Gepert, and G. Veser, *Some Considerations on the Design and Operation of High-Temperature Catalytic Reverse-Flow Reactors.* Industrial & Engineering Chemistry Research, 2004. **43**(16): p. 4657-4667.
49. Neumann, D., M. Kirchhoff, and G. Veser, *Towards an efficient process for small-scale, decentralized conversion of methane to synthesis gas: combined reactor engineering and catalyst synthesis.* Catalysis Today, 2004. **98**(4): p. 565-574.
50. Blanks, R.F., T.S. Wittrig, and D.A. Peterson, *Bidirectional adiabatic synthesis gas generator.* Chemical Engineering Science, 1990. **45**(8): p. 2407-2413.
51. Kaisare, N.S., J.H. Lee, and A.G. Fedorov, *Hydrogen generation in a reverse-flow microreactor: 2. Simulation and analysis.* AIChE Journal, 2005. **51**(8): p. 2265-2272.
52. Kaisare, N.S., J.H. Lee, and A.G. Fedorov, *Operability Analysis and Design of a Reverse-Flow Microreactor for Hydrogen Generation via Methane Partial Oxidation.* Industrial & Engineering Chemistry Research, 2005. **44**(22): p. 8323-8333.
53. Kikas, T., et al., *Hydrogen Production in a Reverse-Flow Autothermal Catalytic Microreactor: From Evidence of Performance Enhancement to Innovative Reactor Design.* Industrial & Engineering Chemistry Research, 2003. **42**(25): p. 6273-6279.
54. Friedle, U. and G. Veser, *A Counter-Current Heat-Exchange Reactor for High Temperature Partial Oxidation Reactions - I. Experiments.* Chemical Engineering Science. **54**(10): p. 1325-1332.
55. Wang, X. and R.J. Gorte, *A study of steam reforming of hydrocarbon fuels on Pd/ceria.* Applied Catalysis A: General, 2002. **224**(1–2): p. 209-218.

56. Rostrup-Nielsen, J.R., T.S. Christensen, and I. Dybkjaer, *Steam reforming of liquid hydrocarbons*, in *Studies in Surface Science and Catalysis*, T.S.R.P. Rao and G.M. Dhar, Editors. 1998, Elsevier. p. 81-95.
57. Rabou, L.P.L.M., et al., *Tar in Biomass Producer Gas, the Energy research Centre of The Netherlands (ECN) Experience: An Enduring Challenge.* Energy & Fuels, 2009. **23**(12): p. 6189-6198.
58. Maniatis, K. and A.A.C.M. Beenackers, *Tar Protocols. IEA Bioenergy Gasification Task.* Biomass and Bioenergy, 2000. **18**(1): p. 1-4.
59. Devi, L., et al., *Catalytic decomposition of biomass tars: use of dolomite and untreated olivine.* Renewable Energy, 2005. **30**(4): p. 565-587.
60. Zwart, R.W.R., *Gas cleaning downstream biomass gasification, Status Report 2009*, 2009: Energy research Centre of the Netherlands (ECN), The Netherlands.
61. de Andrés, J.M., A. Narros, and M.E. Rodríguez, *Behaviour of dolomite, olivine and alumina as primary catalysts in air–steam gasification of sewage sludge.* Fuel, 2011. **90**(2): p. 521-527.
62. Yu, Q.Z., et al., *Effects of Chinese dolomites on tar cracking in gasification of birch.* Fuel, 2009. **88**(10): p. 1922-1926.
63. Bridgwater, A.V. and D.G.B. Boocock, *Developments in thermochemical biomass conversion*1997: Blackie Academic & Professional.
64. Berube, M.N., B. Sung, and M.A. Vannice, *Sulfur poisoning of supported palladium methanol synthesis catalysts.* Applied Catalysis, 1987. **31**(1): p. 133-157.
65. Chaffee, A.L., I. Campbell, and N. Valentine, *Sulfur Poisoning of Fischer-Tropsch Synthesis Catalysts in a Fixed-Bed Reactor.* Applied Catalysis, 1989. **47**(2): p. 253-276.
66. Erekson, E.J. and C.H. Bartholomrw, *Sulfur poisoning of nickel methanation catalysts: II. Effects of H2S concentration, CO and H2O partial pressures and temperature on reactivation rates.* Applied Catalysis, 1983. **5**(3): p. 323-336.
67. Chen, H.-C. and R.B. Anderson, *Studies of a triply promoted ammonia synthesis catalyst with an electron probe microanalyzer.* Journal of Catalysis, 1973. **28**(1): p. 161-173.
68. Jothimurugesan, K., et al., *Advanced Hot-Gas Desulfurization Sorbents*, in *Advanced Coal-Based Power and Environmental Systems '97 Conference*1997: Pittsburgh, Pennsylvania.
69. Dijk, H.v., *Tail gas treatment of sour-SEWGS CO2 product*, 2012: Energy research Centre of the Netherlands.

70. Tunå, P. and J. Brandin, *Selective catalytic oxidation of ammonia by nitrogen oxides in a model synthesis gas.* Fuel, 2013. **105**(0): p. 331-337.
71. Torres, W., S.S. Pansare, and J.G. Goodwin, *Hot Gas Removal of Tars, Ammonia, and Hydrogen Sulfide from Biomass Gasification Gas.* Catalysis Reviews, 2007. **49**(4): p. 407-456.
72. Spath, P.L. and D.C. Dayton, *Preliminary Screening -- Technical and Economic Assessment of Synthesis Gas to Fuels and Chemicals with Emphasis on the Potential for Biomass-Derived Syngas*, in *NREL Technical Report 510-34929: 22 Apr*2004.
73. Lillebø, A.H., et al., *Fischer–Tropsch conversion of biomass-derived synthesis gas to liquid fuels.* Wiley Interdisciplinary Reviews: Energy and Environment, 2013.
74. Tunå, P. and C. Hulteberg, *Reverse-flow catalytic tar cracking of a model biomass derived synthesis gas.* 2013.
75. Björkman, E. and K. Sjöström, *Decomposition of ammonia over dolomite and related compounds.* Energy & Fuels, 1991. **5**(5): p. 753-760.
76. Chen, L., J. Li, and M. Ge, *The poisoning effect of alkali metals doping over nano V2O5–WO3/TiO2 catalysts on selective catalytic reduction of NOx by NH3.* Chemical Engineering Journal, 2011. **170**(2-3): p. 531-537.
77. Brandin, J.G.M., L.A.H. Andersson, and C.U.I. Odenbrand, *Catalytic reduction of nitrogen oxides on mordenite some aspect on the mechanism.* Catalysis Today, 1989. **4**(2): p. 187-203.
78. Leppälahti, J., *Process for Removing Ammonia from Gasification Gas*, S.P. Office, Editor 1996, Valtion Teknillinen Tutkimuskeskus (VTT): Sweden Patent.
79. Nassos, S., et al., *The influence of Ni load and support material on catalysts for the selective catalytic oxidation of ammonia in gasified biomass.* Applied Catalysis B: Environmental, 2007. **74**(1–2): p. 92-102.
80. Nassos, S., et al., *Microemulsion-prepared Ni catalysts supported on cerium-lanthanum oxide for the selective catalytic oxidation of ammonia in gasified biomass.* Applied Catalysis B: Environmental, 2006. **64**(1–2): p. 96-102.
81. Schumacher, N., et al., *Trends in low-temperature water–gas shift reactivity on transition metals.* Journal of Catalysis, 2005. **229**(2): p. 265-275.
82. Lian, Y., et al., *Water gas shift activity of Co-Mo/MgO-Al2O3 catalysts presulfided with ammonium sulfide.* Journal of Natural Gas Chemistry, 2010. **19**(1): p. 61-66.
83. Hulteberg, C., *Sulphur-tolerant catalysts in small-scale hydrogen production, a review.* International Journal of Hydrogen Energy, 2012. **37**(5): p. 3978-3992.

84. Einvall, J., et al., *High temperature water-gas shift step in the production of clean hydrogen rich synthesis gas from gasified biomass.* Biomass and Bioenergy, 2011. **35, Supplement 1**(0): p. S123-S131.
85. Dry, M.E., *The Fischer–Tropsch process: 1950–2000.* Catalysis Today, 2002. **71**(3–4): p. 227-241.
86. Bartholomew, C., *Recent technological developments in Fischer-Tropsch catalysis.* Catalysis Letters, 1990. 7(1-4): p. 303-315.
87. Patzlaff, J., et al., *Studies on product distributions of iron and cobalt catalyzed Fischer–Tropsch synthesis.* Applied Catalysis A: General, 1999. **186**(1–2): p. 109-119.
88. Kuipers, E.W., et al., *Non-ASF Product Distributions Due to Secondary Reactions during Fischer–Tropsch Synthesis.* Journal of Catalysis, 1996. **158**(1): p. 288-300.
89. Puskas, I. and R.S. Hurlbut, *Comments about the causes of deviations from the Anderson–Schulz–Flory distribution of the Fischer–Tropsch reaction products.* Catalysis Today, 2003. **84**(1–2): p. 99-109.
90. Klier, K., et al., *Catalytic synthesis of methanol from COH2: IV. The effects of carbon dioxide.* Journal of Catalysis, 1982. **74**(2): p. 343-360.
91. Holm-Larsen, H., *CO2 reforming for large scale methanol plants—an actual case*, in *Studies in Surface Science and Catalysis*, J.J.S. E. Iglesia and T.H. Fleisch, Editors. 2001, Elsevier. p. 441-446.
92. Arcoumanis, C., et al., *The potential of di-methyl ether (DME) as an alternative fuel for compression-ignition engines: A review.* Fuel, 2008. **87**(7): p. 1014-1030.
93. Ohno, Y., et al., *Slurry phase DME direct synthesis technology -100 tons/day demonstration plant operation and scale up study*, in *Studies in Surface Science and Catalysis*, M.S. Fábio Bellot Noronha and S.-A. Eduardo Falabella, Editors. 2007, Elsevier. p. 403-408.
94. Ogawa, T., et al., *Direct Dimethyl Ether (DME) synthesis from natural gas*, in *Studies in Surface Science and Catalysis*, B. Xinhe and X. Yide, Editors. 2004, Elsevier. p. 379-384.
95. Sofianos, A.C. and M.S. Scurrell, *Conversion of synthesis gas to dimethyl ether over bifunctional catalytic systems.* Industrial & Engineering Chemistry Research, 1991. **30**(11): p. 2372-2378.
96. Liederman, D., et al., *Process Variable Effects in the Conversion of Methanol to Gasoline in a Fluid Bed Reactor.* Industrial & Engineering Chemistry Process Design and Development, 1978. **17**(3): p. 340-346.

97. Phillips, S., et al., *Thermochemical Ethanol via Indirect Gasification and Mixed Alcohol Synthesis of Lignocellulosic Biomass*, 2007: National Renewable Energy Laboratory.
98. Pichler, H. and K.H. Ziesecke, *The Isosynthesis*1950: U.S. Government Printing Office.
99. Seemann, M.C., et al., *The regenerative effect of catalyst fluidization under methanation conditions.* Applied Catalysis A: General, 2006. **313**(1): p. 14-21.
100. Kai, T. and S. Furusaki, *Methanation of carbon dioxide and fluidization quality in a fluid bed reactor—the influence of a decrease in gas volume.* Chemical Engineering Science, 1987. **42**(2): p. 335-339.
101. Bridger George, W. and C. Woodward, *Formulation and Operation of Methanation Catalysts*, in *Methanation of Synthesis Gas*1975, AMERICAN CHEMICAL SOCIETY. p. 71-86.
102. Erisman, J.W., et al., *How a century of ammonia synthesis changed the world.* Nature Geosci, 2008. **1**(10): p. 636-639.
103. Lawrence, S.A., *Amines: Synthesis, Properties and Applications*2004: Cambridge University Press.
104. Ramírez, C.A. and E. Worrell, *Feeding fossil fuels to the soil: An analysis of energy embedded and technological learning in the fertilizer industry.* Resources, Conservation and Recycling, 2006. **46**(1): p. 75-93.
105. Zakkour, P. and G. Cook, *CCS Roadmap for Industry: High-purity CO2 sources*, 2010: Carbon Counts Company (UK) Ltd.
106. Gnansounou, E. and A. Dauriat, *Techno-economic analysis of lignocellulosic ethanol: A review.* Bioresource Technology, 2010. **101**(13): p. 4980-4991.
107. Zwart, R.W.R. and H. Boerrigter, *High Efficiency Co-production of Synthetic Natural Gas (SNG) and Fischer–Tropsch (FT) Transportation Fuels from Biomass.* Energy & Fuels, 2005. **19**(2): p. 591-597.
108. de Lange, T.J., *Co-production of Fuels as an Option for Demkolec?: A Preliminary Review of Opportunities for the Co-production of Liquid Or Gaseous Energy Carriers*2001: Netherlands Energy Research Foundation ECN.

Paper I

Fifth International Conference on Thermal Engineering: Theory and Applications
May 10-14, 2010, Marrakesh, Morocco

Modeling of Reverse-Flow Partial-Oxidation Process for Gasifier-Product Gas Upgrading

Per Tunå [a], Helena Svensson [a], Jan Brandin [a, *]

[a] *Department of Chemical Engineering, Lund University*

Abstract

Biomass gasification and subsequent fuel synthesis is one of the alternatives to producing liquid fuels and chemicals from biomass residues. The gas produced in gasification contains CO, H_2, H_2O, CO_2, light hydrocarbons and tars. Depending on the gasifier type, operating conditions and fuel, the light hydrocarbons can contain as much as 50 % of the total energy contents in the gas. The gas also contains catalyst poisons such as sulfur, in the form of H_2S and COS. This paper presents simulation work of a reverse- flow partial- oxidation reformer that converts the light hydrocarbons to more synthesis gas and at the same time reaches efficiencies approaching conventional catalytical processes. Furthermore, different reactor designs and parameter variations such as pressure, oxidant amount and steam/carbon ratio are investigated. For comparison, natural gas simulations are included which clearly show the benefits of using reverse flow operation with lean gases such as gasifier product gas.

Keywords: Reverse Flow Operation, Partial Oxidation, Gasification

Nomenclature

H	Gas enthalpy, kJ/kg
$\dot{m}$	Gas mass flow, kg/s
$\dot{m}_i$	Mass flow of specie i, kg/s
α	Heat transfer coefficient kJ/m^2 .K
S	Solid Specific Surface area, m^2/m^3
λ	Solid phase heat conductivity, kJ/m.K
$\nu_{i,j}$	Stoichiometric coefficient for specie i in reaction j , kg/s

1. Introduction

Second generation bio-fuels utilize non-food crops for the production of fuels, which means that agriculture waste, forest residue and energy crops become useful for fuel production [1, 2]. One important process for utilization of cellulose rich biomass is gasification. Gasification is a well proven technique for processing of fossil fuels and has been used extensively and has recently been used on biomass feed stocks. During the gasification, the coal containing material is oxidized in contact with air/oxygen and/or steam that convert the solid fuel into a gas and an ash fraction. Gasification is an endothermic reaction and heat has to be supplied, either directly or indirectly.

The produced gas contains as major components CO, CO_2, H_2, H_2O (and N_2 if air is used for the gasification). The composition depends on gasifier type, operating conditions and fuel. However, it may also contain some lower hydrocarbons, C_1-C_3, tars and smaller amounts of contaminates such as H_2S, COS, NH_3, HCN. A large portion of the Lower Heating Value (LHV) of the gas can be bound in the lower hydrocarbons (CH_4 + C_2-C_3), up to 50% depending on gasifier type, feed stock etc., while the tars can contain about 10% of the LHV. If the aim is to produce synthesis gas, these hydrocarbons need to be converted.

Because of the contaminants present in the gas, mainly sulfur, conventional technology, such as steam reforming using traditional catalysts, cannot be used to convert the hydrocarbons to synthesis gas, at least not the methane [3]. Other techniques such as auto-thermal reforming and catalytic partial oxidation, might work, due to higher operating temperature, but have not yet been proven. These techniques all rely on a catalyst, which is highly sensitive to sulfur poisoning, to function effectively. The alternative then is to use a non-catalytic process, for instance partial oxidation. The problems associated with non-catalytic partial oxidation (POX) are mainly related to the high temperature needed for the reactions to occur and the loss of chemical energy in the gas. The temperature is typically 1200-1400°C [4]. In order to address this problem and make the process more energy efficient a regenerative reverse- flow reactor can be utilized.

In a regenerative reverse- flow reactor, heat is transferred between a fluid and a stationary phase. Usually streaming hot gas heats a bed of granular material, while the gas cools down. One of the most important parameters for the thermal buffer is the heat storage capacity and the mass of the solid packing

* Corresponding author. Tel.: +46 46 222 88 82
Fax: +46 46 14 91 56; E-mail: janb@chemeng.lth.se

material. The stored heat in the bed can be utilized by flowing cold gas in the opposite direction, heating the gas and cooling the bed. The reason for using such a device is the thermal efficiency that can be achieved. It is not unusual with up to 95 % efficiency [5]. This is partly due to the large heat transfer area that can be obtained in a bed of granular material, and partly to the high heat transfer coefficients that can be obtained in a packed bed with a proper choice of grain size and gas flow rate.

The forced unsteady-state conditions that occur during reverse flow operation have been shown to have a positive influence on several catalytic processes [5-7]. The main advantages of this reactor operation mode are the absence of a catalyst that can be deactivated, the high thermal efficiency, due to the heat recuperation, and that an optimal temperature profile can be achieved in the reactor, benefiting the reactions [8-11]. Blanks et al [9] demonstrated the concept of CPO, with Ni-catalyst, and POX of natural gas first in laboratory scale with a natural gas flow of 3 Ndm^3/min using air as oxidant. Since then several simulation and laboratory investigations have been performed predominantly on CPO [12-15].

2. Modeling

The regenerative reformer is modeled as a tank-series. The simulations were performed in a C++ program as the performance advantages over scripted programs such as MATLAB are very noticeable. Simulations were reduced a several times with the move to C++ compared to MATLAB. A third party library, Cantera, is utilized to calculate kinetics and thermodynamics. Cantera uses GRI-Mech 3.0 [16] for the kinetics. GRI-Mech 3.0 contains 53 species and 325 reactions and was originally designed to model combustion of natural gas. Initial equilibrium calculations did not reveal any limitations of the model.

2.1. Heat and Mass Balances

The heat and mass balances for the system is described with the following ordinary and partial differential equations:

Energy balance for the gas phase

$$\frac{dH}{dt} = \dot{m}_{in} H_{in} - \dot{m}_{out} H_{out} + \Delta H_{reaction} + \alpha S (T_{solid} - T_{gas}) \quad (1)$$

Energy balance for the solid phase

$$\rho_{solid} C_{p,solid} \frac{\partial T_{solid}}{\partial t} = \lambda \frac{\partial^2 T_{solid}}{\partial z^2} + \alpha S (T_{gas} - T_{solid}) \quad (2)$$

Mass balance for the gas phase

$$\frac{dm_i}{dt} = m_{i,in} - m_{i,out} + \sum_{j=0}^{k} \nu_{i,j} V \quad (3)$$

The solid phase is not modeled as a tank series (2), but by Partial Differential Equations, therefore it needs boundary conditions (4, 5). The Partial Differential Equation (PDE) for the solid heat balance has the following boundary conditions:

$$\left.\frac{\partial T_{solid}}{\partial z}\right|_{z=0} = \frac{1-\varepsilon}{\lambda} \alpha (T_{solid}(0,t) - T_{gas,in}) \quad (4)$$

$$\left.\frac{\partial T_{solid}}{\partial z}\right|_{z=L} = 0 \quad (5)$$

2.2. Pseudo Steady-State

Evaluating the results from simulation of a forced un-steady state system such as the regenerative reactor requires additional programming to determine when pseudo steady-state is achieved. The evaluation algorithms store the temperature profiles in the reactor during the simulation and when sufficient number of cycles shows the same profile over the reactor it evaluates the efficiency and conversion of methane. We allowed a deviation of 5K between the profiles during our simulations. After five almost identical cycles the system was deemed to be in pseudo steady-state and the results could be evaluated.

2.3. Reactor Design

The design of the reformer was originally a straight pipe but the design soon evolved. The need for increased residence times was apparent. The reactor is to be evaluated at the laboratory, but reactor length in excess of one meter was undesired due to laboratory constraints. The result was an increased reactor diameter. But increasing the diameter also increases the mass of the bed material. This had a negative effect as the inlet gas could no longer cool the inlet of the reactor before the next switch and the consequence was that the temperature at the end points of the reactor reached the same temperature and the system failed.

In order to avoid too much heating of the end points the diameter at the ends was reduced by two thirds. This design was further improved by leaving 50 % of the large section hollow for an additional increase in residence time.

The original concept had the oxygen inlet in the centre of the reactor. This has the advantage of only using one inlet, but a clear disadvantage is that only half of the reactor volume can be utilized. Adding oxygen to the inlet gas stream enables the whole volume of the reactor but it heats the inlet at the same time resulting in a system failure due to end point temperature as mentioned above. The ideal solution lies somewhere in between and it was decided to add oxygen at the beginning of the large section and at the end of the large section. Only the oxygen inlet closest to the reactor inlet is in use and when the flow direction switches the active oxygen inlet switches as well.

Fig. 1: Reactor setup with two heat buffers, each with its own oxygen inlet.

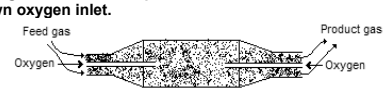

Fig. 2: Reactor setup with a fully packed bed with two independent oxygen inlets.

2.4. Evaluation Criteria

Two different cases were tested to evaluate the capabilities of the regenerative reformer, natural gas and synthesis gas from gasified biomass. Maximum LHV

output of syngas (CO + H_2) from the reformer is wanted and thus efficiency calculations were defined as:

$$\eta = \frac{LHV_{CO+H_2 out}}{LHV_{total\ in}} \quad (6)$$

For natural gas, the enthalpy of the additional steam is added to $LHV_{total\ in.}$ Both the methane conversion and the efficiency in the reactor have to be considered when determining the effect of different parameters. When the steam/carbon-ratio in the gas is too low, the reforming becomes equilibrium constrained and yields too low methane conversion. Since the efficiency calculations include the energy in the steam and because additional steam is needed for the natural gas reforming the efficiency figures for natural gas are overall lower. Since the efficiency calculations exclude the unconverted hydrocarbons, the remaining hydrocarbon in the gas is a loss of efficiency. Therefore it is difficult to compare a methane-rich gas, such as natural gas, to a lean gas such as gasifier producer gas, as the requirements to maximize efficiency are different.

All simulations were run with the properties presented in Table 1.

Table 1: Properties for the reactor during simulations.

Property	Value
Reactor length	0.6 (m)
Reactor diameter (thickest)	0.1 (m)
Diameter ratio (max/min)	3
Inlet gas flow	6 Ndm3/min
Inlet temperature	873 K
Switch-temperature	1000 K
Particle size	1x1 mm spheres

The composition for the natural gas and the gasifier product gas are given in Table 2.

Table 2: Gas composition used in the simulations.

Component	Natural Gas	Gasifier Product Gas
N_2	0.5 %	-
CO_2	0.5 %	27.8 %
C_2H_6	4.5 %	-
C_3H_8	2.5 %	-
CH_4	92 %	8.1 %
CO	-	11.8 %
H_2O	-	37.6 %
C_2H_4	-	3 %
H_2	-	11.7 %

3. Results

Fig. 3 shows the typical profile for gas temperature and component mole fractions for a simulation. The temperature of the solid is the same as the temperature of the gas and is therefore omitted. There are three sections of the reactor, two heat buffers and a reaction zone. Following the inlet from left to right in Fig 3**Fel! Hittar inte referenskälla.**, the inlet gas cools the first heat buffer in the reactor before entering the oxidation zone (first peak) were the temperature is increased. After the oxidation zone the temperature decreases due to the endothermic reactions. The second peak is the oxidation zone for operation in the opposite direction. As the gas exits the reactor and goes through the second heat buffer, it heats the bed which effectively moves the heat from the first heat buffer to the second. When the flow is reversed, the heat is moved back to the first heat buffer and a cycle is completed.

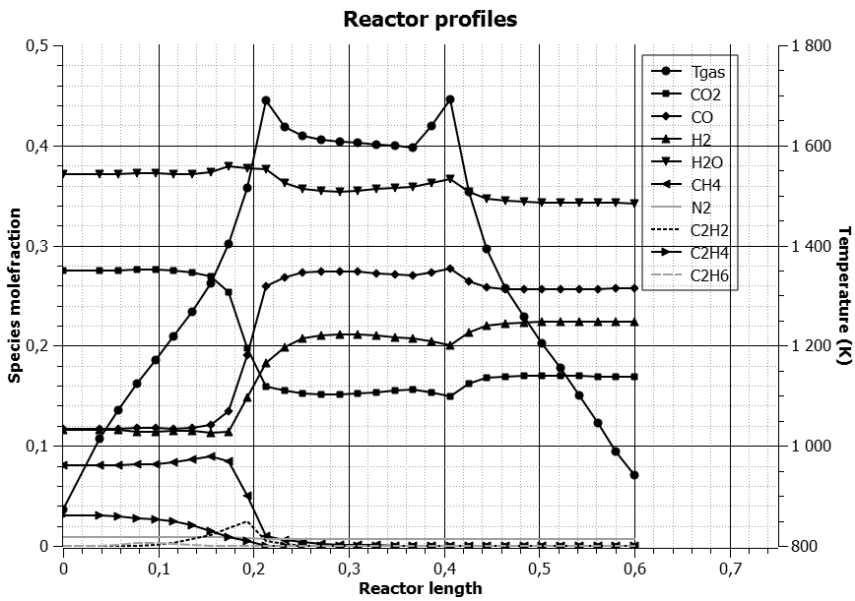

Fig. 3. Typical reactor profile for gasifier product gas.

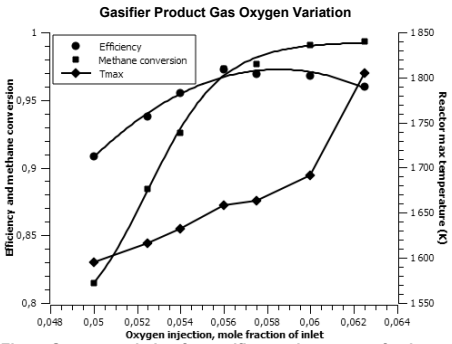

Fig. 4. Oxygen variation for gasifier product gas as feed.

Fig. 4 shows the performance figures for gasifier product gas reforming with varying oxygen inlet amount. There is a clear trend for increased oxygen amount as the methane conversion increases which increases the efficiency. However, there is a point at which further increase of oxygen decreases the efficiency. Adding more oxygen to the gas will oxidize more of the feed gas towards carbon dioxide and water which increases temperature and lowers efficiency.

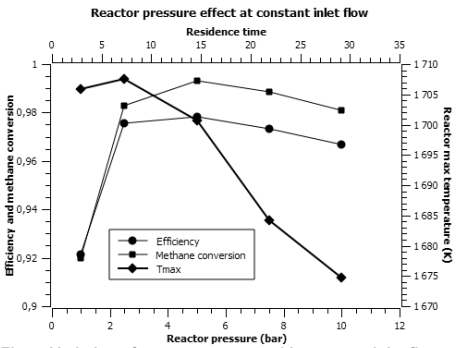

Fig. 5. Variation of reactor pressure with constant inlet flow.

Varying the reactor pressure, while keeping the inlet flow constant, as can be seen in Fig. 5, also varies the residence time (top X-axis in Fig.5 shows the residence time in seconds). The low residence time for atmospheric pressure, results in low conversions of methane and higher temperature as the endothermic reforming reactions are less evident. Increasing the residence time increases the reforming which lowers the reactor temperatures. Lower reactor temperatures decrease the reforming which explains the drop in methane conversion at higher residence times.

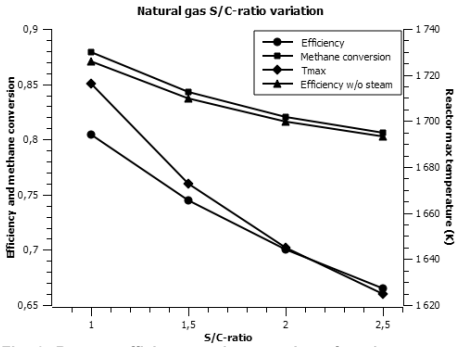

Fig. 6. Reactor efficiency and conversion of methane as a function of steam/natural gas-ratio.

Fig. 6 shows the reactor efficiency and the conversion of methane as a function of the steam/natural gas-ratio. The simulations were run using a constant oxygen/natural gas-ratio and the result is a decrease in the reactor temperature, T_{max}, due to the decrease of energy input, which has a negative effect on the conversion. Increasing the steam/natural gas-ratio is however better for the equilibrium which explains why the conversion is nonlinear as a function of steam/natural gas-ratio. Increasing the steam/natural gas-ratio has a negative effect on the efficiency as more steam is required. The efficiencies, with and without steam, in the figure can be considered to be two extreme points. In an industrial application, the heat in the exit gas can be utilized and the efficiency goes up somewhat for the gas with higher steam ratio.

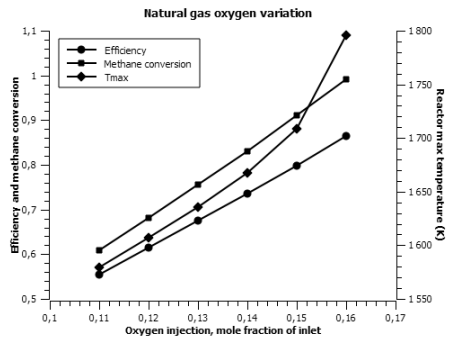

Fig. 7. Methane conversion and reactor efficiency as a function of added oxygen.

Fig 7 shows the conversion of methane and the reactor efficiency as a function of the added oxygen in percent of the total inflow of reactants. There is a clear trend that increasing the oxygen amount increases the temperature and methane conversion, which results in higher reactor efficiencies. But when too much oxygen is added (16 %), the temperature in the oxygen-inlet zone gets too high, over 1723 K, which is considered the maximum temperature for safety reasons.

4. Conclusion

When natural gas is used as feed, additional steam must be added to the inlet in order to achieve an acceptable conversion of methane. The synthesis gas contains a relatively low amount of methane and higher hydrocarbons and a sufficient amount of steam for high methane conversion. It is also necessary to increase the residence time when the concentration of methane increases.

The regenerative reformer seems well suited for reforming of methane in gasifier product gas. The same system is however not equally suited for reforming of natural gas and further research is required.

The two most important parameters for the reforming of methane are residence time and temperature. Both parameters are dependent on a number of other parameters such as the oxygen inlet flow, reactor dimensions, reactor pressure etc.

Cycle times for the gasifier product gas simulations were in the range 5-6 minutes and 7-8 minutes for natural gas. The systems can not, however, be compared with each other as the temperature in the reactors differ. Natural gas reforming requires more energy, in absolute terms, as it contains more methane, which lowers the temperature after the oxidation zone. The temperature falls faster as more methane is present in the gas. The lower temperature requires longer residence times, or higher reactor temperatures. It is however not realistic to increase the temperature too much, and instead several oxidation zones could be used. Higher reactor temperature also consumes more of the chemically bonded energy in the outgoing gas and thus lowers the efficiency.

Acknowledgments

The authors gratefully thank financial support from the European Commission in the framework of the FP7 Integrated Project “GreenSyngas” (Project NO. 213628).

The authors also thank the Swedish Energy Agency, STEM for their financial support.

References

[1] Albertazzi, S., et al., *The technical feasibility of biomass gasification for hydrogen production.* Catalysis Today, 2005. **106**(1-4): p. 297-300.

[2] CHRISGAS, *Clean Hydrogen-rich Synthesis Gas - fuels from biomass*, in *Intermediate Report*. 2008, Swedish Energy Agency: Växjö.

[3] Albertazzi, S., et al., *Effect of fly ash and H2S on a Ni-based catalyst for the upgrading of a biomass-generated gas.* Biomass and Bioenergy, 2008. **32**(4): p. 345-353.

[4] *Kirk-Othmer Encyclopedia of Chemical Technology*. 4th ed. Vol. 13. 1995: John Wiley & Sons, Inc.

[5] Matros, Y.S. and G.A. Bunimovich, *Control of Volatile Organic Compounds by the Catalytic Reverse Process.* Industrial & Engineering Chemistry Research, 1995. **34**(5): p. 1630-40.

[6] Boreskov, G.K. and Y.S. Matros, *Unsteady-state performance of heterogeneous catalytic reactions.* Catalysis Reviews - Science and Engineering, 1983. **25**(4): p. 551-90.

[7] Matros, Y.S., et al., *Is it economically feasible to use heterogeneous catalysts for VOC control in regenerative oxidizers?* Catalysis Today, 1996. **27**(1-2): p. 307-13.

[8] Neumann, D., M. Kirchhoff, and G. Veser, *Towards an efficient process for small-scale, decentralized conversion of methane to synthesis gas: combined reactor engineering and catalyst synthesis.* Catalysis Today, 2004. **98**(4): p. 565-574.

[9] Blanks, R.F., T.S. Wittrig, and D.A. Peterson, *Bidirectional adiabatic synthesis gas generator.* Chemical Engineering Science, 1990. **45**(8): p. 2407-13.

[10] Kaisare, N.S., J.H. Lee, and A.G. Fedorov, *Hydrogen generation in a reverse-flow microreactor: 2. Simulation and analysis.* AIChE Journal, 2005. **51**(8): p. 2265-2272.

[11] Neumann, D., V. Gepert, and G. Veser, *Some Considerations on the Design and Operation of High-Temperature Catalytic Reverse-Flow Reactors.* Industrial & Engineering Chemistry Research, 2004. **43**(16): p. 4657-4667.

[12] Friedle, U. and G. Veser, *A counter-current heat-exchange reactor for high temperature partial oxidation reactions I. Experiments.* Chemical Engineering Science, 1999. **54**(10): p. 1325-1332.

[13] Kikas, T., et al., *Hydrogen Production in a Reverse-Flow Autothermal Catalytic Microreactor: From Evidence of Performance Enhancement to Innovative Reactor Design.* Industrial & Engineering Chemistry Research, 2003. **42**(25): p. 6273-6279.

[14] Mitri, A., et al., *Reverse-flow reactor operation and catalyst deactivation during high-temperature catalytic partial oxidation.* Chemical Engineering Science, 2004. **59**(22-23): p. 5527-5534.

[15] Neumann, D. and G. Veser, *Catalytic partial oxidation of methane in a high-temperature reverse-flow reactor.* AIChE Journal, 2005. **51**(1): p. 210-223.

[16] Gregory P. Smith, D.M.G., Michael Frenklach, Nigel W. Moriarty, Boris Eiteneer, Mikhail Goldenberg, C. Thomas Bowman, Ronald K. Hanson, Soonho Song, William C. Gardiner, Jr., Vitali V. Lissianski, and Zhiwei Qin. Available from: <http://www.me.berkeley.edu/gri_mech/>.

Paper II

Fuel 106 (2013) 271–278

Contents lists available at SciVerse ScienceDirect

Fuel

journal homepage: www.elsevier.com/locate/fuel

Modeling of soot formation during partial oxidation of producer gas

Helena Svensson [a,*], Per Tunå [a], Christian Hulteberg [a], Jan Brandin [b]

[a] Department of Chemical Engineering, Lund University, P.O. Box 124, SE-221 00 Lund, Sweden
[b] Bioenergy Technology, Linnaeus University, SE-351 95 Växjö, Sweden

HIGHLIGHTS

- Modeling of a reverse flow partial oxidation reactor for reforming.
- Study of soot formation for reforming of a gasifier product gas.
- CO and CO_2 content of gas has great influence on soot formation.
- Reduction of tars in incoming gas significantly reduces soot formation.

ARTICLE INFO

Article history:
Received 2 February 2012
Received in revised form 12 October 2012
Accepted 23 October 2012
Available online 12 November 2012

Keywords:
Gasification
Reforming
Partial oxidation
Reverse-flow operation
Synthesis gas

ABSTRACT

Soot formation in a reverse-flow partial-oxidation reactor for reforming of gasifier producer gas has been studied. The process was modeled using a detailed reaction mechanism to describe the kinetics of soot formation. The numerical model was validated against experimental data from the literature and showed good agreement with reported data. Nine cases with different gas compositions were simulated in order to study the effects of water, hydrogen and methane content of the gas. The CO and CO_2 contents, as well as the tar content of the gas, were also varied to study their effects on soot formation. The results showed that the steam and hydrogen content of the inlet gas had less impact on the soot formation than expected, while the methane content greatly influenced the soot formation. Increasing the CO_2 content of the gas reduced the amount of soot formed and gave a higher energy efficiency and methane conversion. In the case of no tar in the incoming gas the soot formation was significantly reduced. It can be concluded that removing the tar in an energy efficient way, prior to the partial oxidation reactor, will greatly reduce the amount of soot formed. Further investigation of tar reduction is needed and experimental research into this process is ongoing.

1. Introduction

The need to replace liquid fuels, such as gasoline and diesel, produced from crude oil resources has given rise to much research in the area of biofuels. Examples of liquid biofuels are ethanol, methanol and bio-diesel produced from different types of biomass using various technologies. Fischer–Tropsch diesel produced from synthesis gas (CO and H_2) derived from renewable resources is a growing area of research [1–4].

Traditionally, the synthesis gas used for the Fischer–Tropsch process was produced via coal gasification. Recently, research has been focused on the production of synthesis gas utilizing gas produced by biomass gasification [4–10]. The gas produced by the gasifier is often referred to as producer gas. This producer gas contains CO, CO_2, H_2 and H_2O, as well as CH_4 and higher hydrocarbons, including some tar compounds. There are also small amounts of contaminants present in the syngas, such as NH_3, H_2S, COS and HCN. The composition of the producer gas and the range and amounts of contaminants is largely dependent on the type of biomass and gasifier used for the production of the producer gas.

In order to upgrade the producer gas to synthesis gas, which can be used e.g. to produce liquid fuels, a reforming process is necessary. Many alternatives are available and have been the subject of much research, such as steam reforming, autothermal reforming, and catalytic partial oxidation. The main problem associated with these techniques is that they rely on catalysts that are highly susceptible to sulfur poisoning [11–14]. Although much research has been devoted to finding suitable catalysts for these techniques no clear alternative has yet emerged. An alternative would be to use a non-catalytic process such as partial oxidation (POX). One drawback associated with POX is the high temperature needed to reform methane. This results in a process with a lower energy efficiency than the catalytic alternatives and a loss of chemically

* Corresponding author. Tel.: +46 46 222 9313; fax: +46 46 14 91 56.
E-mail addresses: helena.svensson@chemeng.lth.se (H. Svensson), per.tuna@chemeng.lth.se (P. Tunå), christian.hulteberg@chemeng.lth.se (C. Hulteberg), jan.brandin@lnu.se (J. Brandin).

0016-2361/$ - see front matter © 2012 Elsevier Ltd. All rights reserved.
http://dx.doi.org/10.1016/j.fuel.2012.10.061

bound energy in the gas. One way of making the process more energy efficient is to use a reverse-flow POX reactor. The reverse-flow reactor consists of a vessel filled with an inert granular material with high thermal capacity, which acts as a heat buffer. As the gas flows through the packed bed, heat produced by the reactions is transferred from the gas to the stationary phase. When the flow direction is reversed the heat stored in the bed is used to heat the incoming cold gas. Eventually, a pseudo-steady-state temperature profile is established with a high temperature in the middle of the reactor and lower temperatures at the inlet and outlet. This concept has been studied previously and has proven highly effective for reforming hydrocarbon fuels [15–17].

The reverse-flow POX reactor has been modeled in previous work, showing potential in dealing with the unique qualities of the producer gas that make it difficult to reform using conventional techniques [18]. However some issues still remain to be resolved. Because of the high temperature required for POX, and the general composition of the producer gas, soot is likely to form during reforming. Furthermore, soot precursors, such as ethylene, acetylene and tars, are present in the producer gas promoting soot formation [19–21]. Since the reverse-flow reactor consists of a packed bed it is vulnerable to blockage if too much soot is formed.

In order to evaluate the ability of the reverse-flow POX reactor to reform producer gas, it is of the utmost importance to establish how much of the incoming carbon is likely to be converted into soot, and explore ways of reducing the formation of soot, while maintaining an energy efficient process and high methane conversion. Because of the inherent difficulties in measuring and analyzing the soot formed in different parts of the reactor, modeling of the process was undertaken as a first step in this investigation. The aim of the investigation was to examine the extent to which soot is likely to form and possible ways of counteracting such formation. The results were evaluated from the viewpoint of synthesis gas energy efficiency and methane conversion, as well as soot reduction.

2. Modeling

The reverse-flow POX reactor is an example of a forced unsteady-state system due to the reversal of flow direction during operation. The system consists of a reactor filled with a granular material with high thermal capacity that acts as a heat buffer. As the gas flows through the packed bed, heat produced by the reactions is transferred from the gas to the stationary phase. When the flow direction is reversed, the heat stored in the bed is used to heat the incoming cold gas. Eventually a pseudo-steady-state temperature profile is established with a high temperature in the middle of the reactor while the inlet and outlet are kept at a lower temperature. A depiction of the modeled system is given in Fig. 1. When the incoming gas flow is introduced in the top of the reactor the reformed gas exits at the bottom. When the flow direction is reversed the reformed gas exits at the top of the reactor. The dimensions of the modeled reverse flow reactor are given in Table 1.

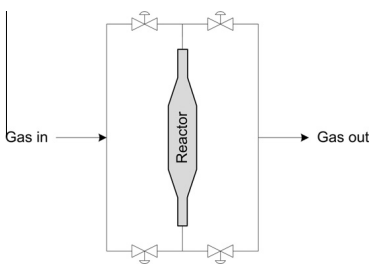

Fig. 1. Modeled reactor system with four valves to reverse the flow direction through the reactor.

In order to model a forced unsteady-state system, such as the reverse-flow reformer, the dynamic behavior needs to be described within the model. However, in order to capture the dynamic behavior the model needs to be very extensive. In order to study the soot formation in the reverse-flow reformer a very extensive reaction mechanism is needed to describe the growth to soot. Because a more detailed reaction mechanism is needed to describe the soot formation the model describing the reverse flow reformer has to be simplified, otherwise the numerical model will be unable to converge and find a solution.

Within the work on the reverse flow reformer conducted at the Department of Chemical Engineering at Lund University, a detailed numerical model of the reverse-flow reactor, designed to accurately describe the dynamic behavior of the reactor, has been developed and previously reported [18]. A brief description of the dynamic model will be given in Section 2.1. A simplified description of the reverse flow reformer has also been developed for the evaluation of soot formation in the reverse flow reformer [22]. This model can be described as a static model of the forced unsteady-state system. The static model is described in brief in Section 2.2.

The static model has been validated against the more extensive dynamic model in previous work, showing that the simplified model gives an accurate description of the reactions taking place during reforming of a producer gas in a reverse-flow POX reactor [22]. A short summary will be presented here. The GRI-mechanism was used within the two models for both simulations. The composition of the gas for these simulations is given in Table 2. The oxygen flow is 6% of the total inlet molar flow and is injected 0.2 m from the gas inlet. The results are presented in Fig. 2. Good agreement between the models can be noted in Fig. 2 and only minor differences between the models could be discerned. It is therefore believed that the static model is able to adequately describe the trends observed in the dynamic model.

2.1. Dynamic model

This model was used to investigate how the reverse flow concept could be applied to reforming a producer gas. The simulations were performed using a C++ program, and a third party library, Cantera, was used to calculate thermodynamics and kinetics. Cantera uses the GRI-Mech 3.0 mechanism for the kinetics [23]. This reaction mechanism was originally designed to model the combustion of natural gas, and has been shown to give results that agree closely with experimental data for reforming processes [6]. However, this mechanism does not include the formation of tars and soot.

The reverse flow reformer is described by a numerical model designed to accurately describe the dynamic behavior of the reactor. The gas phase is modeled as a series of tank reactors. This simplifies the mass balances and the energy balance for the gas phase making the calculations less demanding. The outgoing composition from each reactor is used as the ingoing composition in the following reactor in the reactor series. The solid phase is

Table 1
Dimensions of the modeled reactor.

Property	Value
Reactor length	0.6 (m)
Reactor diameter (thickest)	0.1 (m)
Diameter ratio (max/min)	3

Table 2
Gas composition used for validation of the static model against the dynamic model.

Component	Composition (vol%)
C_2H_4	3.1
CH_4	8.2
CO	11.9
CO_2	27.9
H_2	11.8
H_2O	37.7

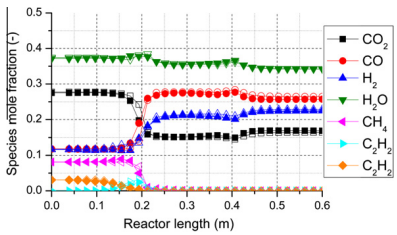

Fig. 2. Comparison of species mole fractions obtained with the detailed and simplified simulation models. Filled symbols represent the dynamic model and empty symbols represent the static model.

modeled with the finite difference method and the partial differential equation describing the solid phase has to be discretised in the space dimension.

For the sake of evaluation, it was necessary to achieve a pseudo-steady-state in the reactor. The time the system is operated in each direction is called the cycle time, and this will vary depending on the conditions in the system. In order to determine when pseudo-steady-state was achieved the temperature profiles of each cycle were evaluated. A deviation of 5 K between the temperature profiles of the cycles was allowed. After five cycles with a temperature difference of 5 K or less the system was considered to be in pseudo-steady-state.

2.2. Static model

For the purpose of studying soot formation the GRI-Mech 3.0 reaction mechanism cannot be used as it does not include higher hydrocarbons and tars. Therefore another reaction mechanism is needed to describe the kinetics in the numerical model. A mechanism that describes conventional gas phase reactions and particle growth was therefore used [24,25]. The mechanism, together with the corresponding thermodynamic and transport property data, is available on-line [26]. This mechanism was developed to describe the formation of polycyclic aromatic hydrocarbons and soot in fuel-rich benzene flames. Because the mechanism that describes soot formation is much larger than the GRI-Mech 3.0 mechanism it was not possible to use it within the dynamic model of the reverse-flow reformer previously described. For this reason, a simplified numerical model was developed for the evaluation of soot formation in the reverse-flow POX reactor [22].

The simplified model can be described as a static model, the principle of which is illustrated in Fig. 3. The model consists of a series of reactors. The reverse-flow reactor is divided into segments and each segment is modeled as a separate reactor. The residence time of each reactor corresponds to the residence time of the reverse-flow reactor segment modeled. The temperature profile over the series of reactors is determined at pseudo-steady-state for each case modeled, using the more extensive dynamic model previously described in Section 2.1. The temperature and pressure in each reactor are kept constant. The composition of the gas leaving each reactor is used as the incoming composition in the following reactor in the series. The oxygen inlet is located 0.2 m from the gas inlet. The solid phase is not included in the model.

2.3. Validation of the static model

Soot formation during the reforming of hydrocarbon fuels has been observed in several experimental studies [5,10,15,16,27]. These mainly concerned the partial oxidation of methane–air mixtures, although ethane and propane have also been studied [15]. The experiments were performed in packed-bed reactors, some operated in reverse-flow mode [15,16]. The formation of higher hydrocarbons was noted in all studies at high equivalence ratios, although the onset of soot formation varied due to differences in the experimental setups. In some cases, the size of the packing material affected soot formation; smaller particles showing less soot formation [5,27]. The bed material itself should be inert and not affect the gas phase reaction. An explanation of a particle-size dependency could be that the void space between the individual particles increases with increasing particle size. When the free distance in the void exceeds the quenching distance for the local gas mixture in question, the gas can be ignited in the void space. This will give rise to a local high temperature in the flame affecting the formation of soot. When the free void distance is less than the quenching distance, the reaction instead proceeds via a homogeneous gas phase reaction.

Soot formation was observed by Valin et al. [10] when reforming a producer-gas-like gas. They investigated the methane conversion of a simulated producer gas during thermal reforming at high temperatures (1273–1773 K) and various residence times. The gas mixture consisted of CO, CO_2, CH_4, H_2 and H_2O. No higher hydrocarbons or tars were included. The experiments were performed in a down-flow isothermal plug-flow reactor, referred to as the PEGASE reactor. The reactor was designed to study the conversion of methane, light hydrocarbons and tars at high temperature. The reactor is heated by Kanthal heating elements and consists of a preheating zone and an isothermal reaction zone. The reacting gas was injected into the reactor and preheated to the desired temperature in the preheating zone before entering the reaction zone. The gas was then cooled to 1173 K and maintained at that temperature until it left the experimental setup [10]. Soot formation was observed during the experiments but not measured quantitatively. However, qualitative comparisons were made regarding the amount of soot formed at various experimental conditions. The results of their study regarding soot formation are summarized in Table 3. A peak in soot formation was observed between 1363 and 1645 K. The hydrogen content of the gas was observed to have considerable influence on the soot formation. More hydrogen in the gas significantly reduced the amount of soot formed. This is in agreement with prior studies reporting that hydrogen represses soot formation due to tar cracking [28,29].

Because of the difficulty in finding experimental data on the reforming of a producer-gas-like gas using a reverse-flow POX reactor it was decided to validate the simplified numerical model, i.e. the static model presented in this work, with the experimental data obtained by Valin et al. for the thermal reforming of producer gas using the PEGASE reactor [10]. The reactor setup described by the numerical model was modified to suit the PEGASE reactor setup, with three reactors representing the preheating zone, the reaction zone and the cooling zone. The main difference between the PEGASE and reverse-flow reactor setups is that the PEGASE reactor is isothermal and is operated unidirectionally.

As a first check of the validity the results for the numerical model was compared to the trends observed by Valin et al. and

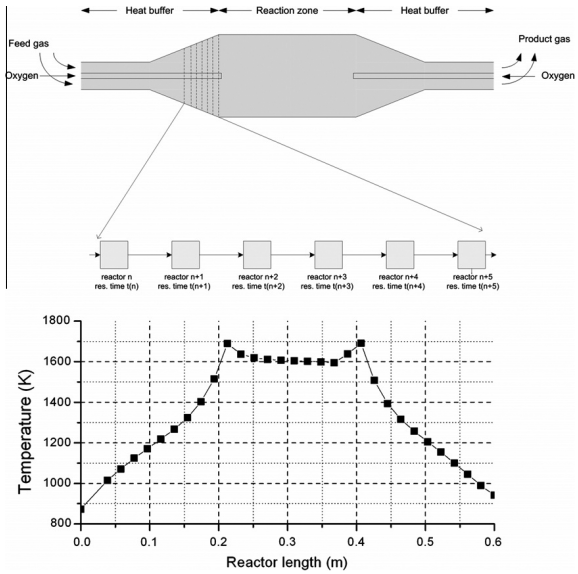

Fig. 3. A schematic description of the series of tanks employed in the model and an example of the temperature profile over the length of the reactor.

Table 3
Soot formation during thermal reforming of bio-syngas according to Valin et al. [10].

	Gas composition (mol%)					Temperature (K)	Residence time (s)	Soot formation
	CO	CO_2	CH_4	H_2	H_2O			
A	19	14	7	16	25	1363–1645	2.1	A peak in soot formation was observed between 1356 and 1645 K.
B	19	14	7	16	25	1783	3.5	Soot formation was relatively low.
C	19	14	7	16	15	1453	2.1	Soot formation was relatively high.
D	19	14	7	32	15	1453	2.1	Soot formation was considerably reduced compared to case C.

summarized in Table 3. The static model showed a peak in soot formation between 1363 and 1645 K with the largest soot formation predicted at 1453 K which corresponds to the observed trend of Valin et al., case A. The predicted soot formation for case B was low and there was a drastic decrease in the predicted soot formation between cases C and D, as was also observed by Valin et al. A simulation of the experimental conditions described by Valin et al. was then conducted and the results obtained with the numerical model were then compared to the experimental data. The results are presented in Fig. 4.

Fig. 4 shows the output gas composition as a function of temperature in the reaction zone. It can be seen that the numerical model shows an overall good correlation with the experimental data. However, at higher temperatures the concentration of CO is underpredicted, and the concentration of H_2O is overpredicted by the numerical model. This may be a consequence of an overprediction of soot formation, in the reaction mechanism used, which results in a loss of carbon. The main reaction controlling the proportions of CO and H_2O is the water gas shift (WGS) equilibrium described below.

$$CO + H_2O \leftrightarrow CO_2 + H_2 \quad (1)$$

If the carbon that is transformed into soot mainly originates from reactions involving CO this concentration would be lowered, shifting the WGS equilibrium to the left. As a result of this, more H_2O would be formed, which would explain the results obtained with the numerical model. The results for the higher hydrocarbons, C_2H_2, C_2H_4 and C_2H_6, are well within the range of those obtained during the experiments, with levels below 0.6% by volume. There does, however, seem to be a slight overprediction of the C_2H_2 in the case of low carbon content in the gas (Fig. 4a) and also in the production of ethane in the high carbon case (Fig. 4b).

It can be concluded from the results obtained with the numerical model that the model will underestimate the CO concentration and overpredict the H_2O concentration at higher temperatures. However, the results for the concentrations of CH_4, CO_2 and H_2 correspond very well with the experimental data over the entire temperature range. The deviations of the model from the experimental data for CO and H_2O occur only at higher temperatures.

In conclusion, the results obtained with the numerical model were found to show good agreement with the experimental data. However, the output of the numerical model should not be interpreted in terms of absolute values but as a basis for the comparison of different operational alternatives.

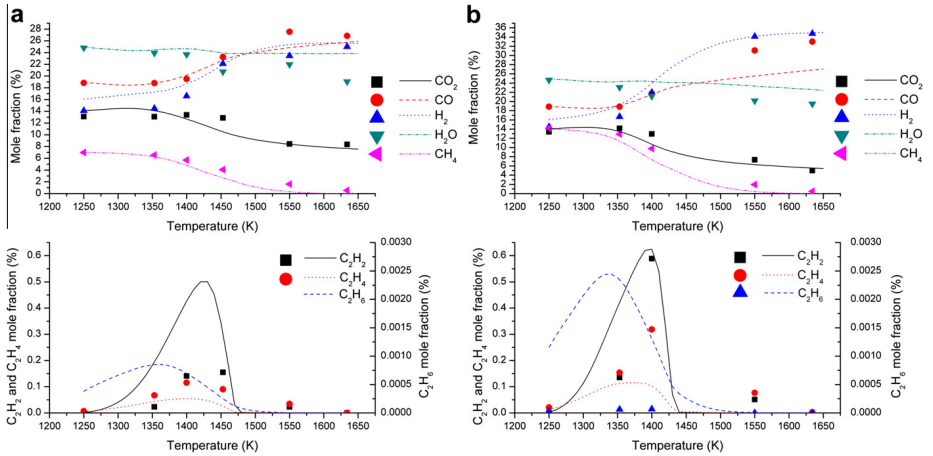

Fig. 4. Concentration profiles in the reactor as a function of temperature with a residence time of 2.1 s. Experimental (symbols) and calculated (lines) values; (a) CH_4: 7 mol% and (b) CH_4: 14 mol% (H_2O: 25 mol%; H_2: 16 mol%; CO: 19 mol%; CO_2: 14 mol% in both cases). Experimental data taken from Valin et al. [10].

3. Simulations

Simulations were performed with varying incoming gas composition in order to determine the extent to which certain species affect soot formation. The results of the simulations were evaluated regarding synthesis gas energy efficiency and methane conversion, as well as soot reduction. As the incoming gas composition was varied the temperature profile over the reactor will also be affected, as well as the amount of oxygen that must be added. Therefore, the temperature profiles for the different cases and the amount of oxygen required in each case were determined prior to the simulations with the dynamic model previously described. All simulations regarding soot formation were performed with the static model described in the modeling section.

One base case was modeled and eight cases with different gas compositions, as summarized in Table 4. The composition of the gas in the base case was chosen to represent a typical composition of a gas leaving a gasifier in terms of CO, CO_2, CH_4, H_2 and H_2O content. The composition from a gasifier depends greatly on the type of gasifier and the operating conditions as well as on which type of biomass is used. In cases 1 and 2 different water contents in the gas were investigated. In case 3 the hydrogen content in the gas was doubled to study the effect of hydrogen on soot formation. As has been observed previously, the hydrogen content has a considerable influence on the amount of soot formed, but it is not known how this will affect the synthesis gas energy efficiency and methane conversion. In cases 4 and 5 the methane content of the gas was studied. The effect of carbon monoxide content in the gas was studied in case 6, and in case 7 the influence of carbon dioxide content on soot formation was investigated. From these simulations it will be possible to deduce which gas component has the greatest influence on soot formation, or whether the total carbon level is more important. In case 8 the effect of tar content was studied. All the naphthalene, the model compound for tar, was assumed to be reformed to ethylene. Both ethylene and naphthalene are known soot precursors but differ in molecular size and structure. In order to determine if it is advantageous to reform the tars present in the producer gas before the reverse flow reformer all the naphthalene was assumed to be reformed to ethylene and the effect of this on the soot formation was determined.

The synthesis gas energy efficiency was calculated according to Eq. 2, where LHV stands for lower heating value.

$$\eta = \mathrm{LHV}_{\mathrm{CO+H2out}} / \mathrm{LHV}_{\mathrm{total\ in}} \quad (2)$$

Table 4
Composition of incoming gas in the modeled cases (mol%) and the amount of oxygen added to the process (mol% of total incoming gas flow).

Component	Base case	1	2	3	4	5	6	7	8
CH_4	7	7	7	7	4	10	7	7	7
C_2H_4	1.5	1.5	1.5	1.5	1.5	1.5	1.5	1.5	4
CO	19	19	19	19	19	19	12	19	19
CO_2	14	14	14	14	14	14	14	24	14
H_2	16	16	16	32	16	16	16	16	16
H_2O	25	15	35	25	25	25	25	25	25
$C_{10}H_8$	0.5	0.5	0.5	0.5	0.5	0.5	0.5	0.5	0
N_2	17	27	7	1	20	14	24	7	15
Added O_2	5	5	5	5	4	5	5	5.5	5.5
Peak temperature (K)	1665	1659	1667	1680	1683	1570	1655	1679	1663
Total carbon (g/m^3)	77	77	77	77	72	82	66	93	77

Table 5
Summary of the results from the cases modeled. Soot formation is given as mass% of the incoming carbon and energy efficiency and methane conversion are given in %.

	Base case	1	2	3	4	5	6	7	8
Soot formation (mass% of incoming carbon)	11.1	11.5	10.7	10.9	10.6	12.2	13.0	8.9	6.6
Synthesis gas energy efficiency	74	73	75	77	75	70	71	76	81
Methane conversion	95	96	95	92	94	97	96	97	94

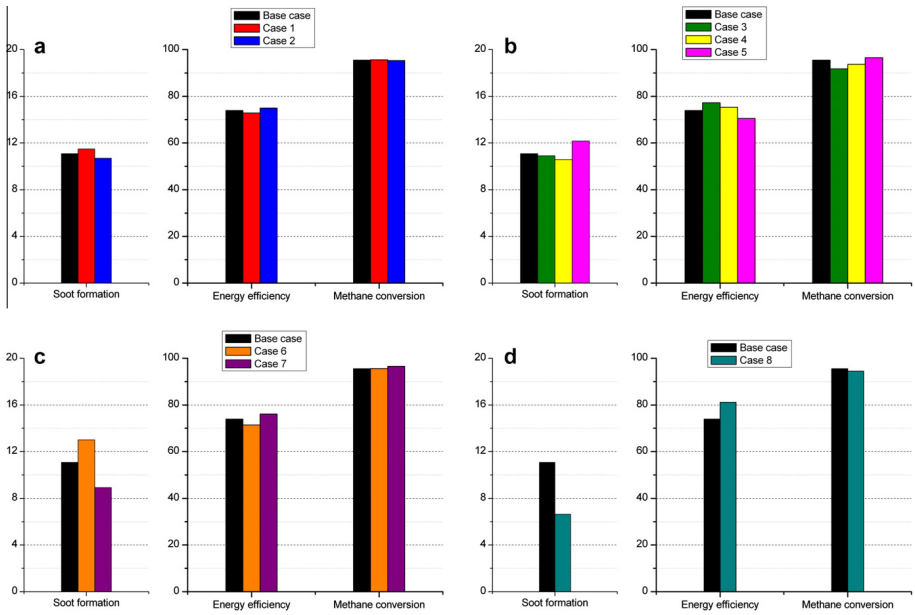

Fig. 5. The results of the cases modeled compared to the base case. Energy efficiency and methane conversion are given in % and the soot formation is given in mass% of the incoming carbon.

The soot formation is reported as the amount of carbon in the soot as a percentage of the incoming total carbon content in the gas. The amount of incoming carbon was not the same in all simulations (Table 4).

4. Results and discussion

The results of the simulations are summarized in Table 5, where the soot formation, synthesis gas energy efficiency and methane conversion are reported. This is also illustrated in Fig. 5. The relatively low synthesis gas energy efficiency is mainly attributed to the, albeit high, but not full, conversion of methane and, of course, to the formation of soot. A substantial amount of energy remains in the unconverted methane. As can be seen in Table 4 the peak temperature differs only slightly between the simulated cases, except for case 5 where the peak temperature is significantly lower due to the high methane content of the gas. Therefore the impact of the peak temperature on the results will probably be negligible, except for case 5.

Not surprisingly, lowering the water content of the gas (case 1) increased the amount of soot formed and increasing the water content of the gas (case 2) showed a slight decrease in soot formation, see Fig. 5a. However, the effect of water content on the soot formation was not as significant as anticipated. It appears that, at the concentrations studied, the water content of the gas has only a minor effect on the amount of soot formed. The synthesis gas energy efficiency and methane conversion for these alternatives were also insignificantly reduced with higher water content (case 2).

Soot formation is reduced, compared with the base case, in case 3 (increased H_2 content) and case 4 (reduced methane content), see Fig. 5b. This is consistent with previous findings that increasing the hydrogen content of the gas reduces soot formation [28,29], and also that methane seems to have a negative effect on soot formation, as in case 5 (increased methane content). However, the increase in hydrogen content in the gas did not affect the soot formation as much as expected but only shows slightly lower soot formation compared to the base case. Since the hydrogen content in the gas was doubled, the effect on soot formation was expected to be higher. Instead the hydrogen content only seems to have a minor effect on the amount of soot formed in the reverse flow reformer. In order to determine the cause of this minor effect further investigations are necessary. For case 5 the soot formation is

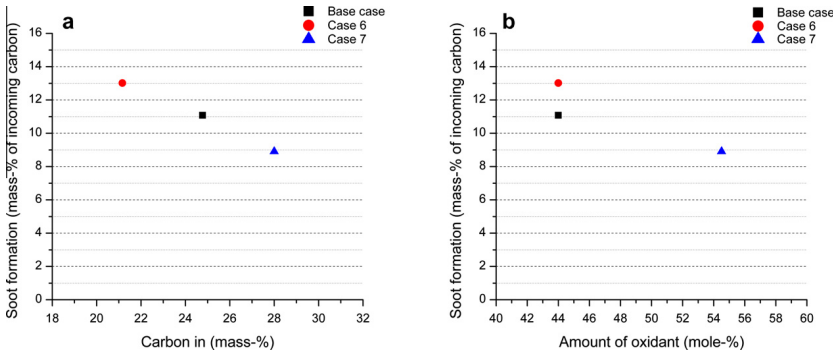

Fig. 6. Soot formation as a function of the amount of carbon (a) and amount of oxidant (b) for each case modeled. The amount of oxidant is the combined amount of O_2, CO_2 and H_2O. Square symbols represent the base case, circles represent case 6 and triangles represent case 7.

increased and the synthesis gas energy efficiency is decreased. This is most likely due to the lower peak temperature for this case (see Table 4). Both synthesis gas energy efficiency and methane conversion are of course greatly affected by varying the methane and hydrogen content of the gas.

In the cases with less CO and more CO_2 in the gas (cases 6 and 7) shown in Fig. 5c, it was found that decreasing the CO content of the gas gave rise to an increase in the amount of soot formed. The opposite was observed when the CO_2 content of the gas was increased, as has been reported previously [22]. This is not surprising since it is well known that CO_2 can act as an oxidizing agent in this type of reaction, donating oxygen and thus forming CO [30,31]. Both the synthesis gas energy efficiency and methane conversion were increased in case 7. Case 6 has the lowest concentration of CO in the outgoing gas and case 7 has the highest. It appears that the concentration of CO in the outgoing gas is somehow correlated to the amount of soot formed. This is believed to be connected to the addition of CO_2 as it will act as an additional oxidation agent (forming CO) and thus increase the oxidation potential of the gas mixture, which will further suppress the soot formation. However, the amount of incoming carbon is not the same in all cases (see Table 4). It may, therefore, be more correct to take this into account when the results are discussed. The amount of incoming carbon is lower in case 6, compared to the base case, and significantly higher for case 7, compared to the base case. If the actual mass of soot formed, i.e. the mass% (given in Table 5) times the total amount of carbon in (given in Table 4), is compared instead, it can be seen that the mass of soot formed is almost the same for case 6 and the base case (8.55 g/m^3 and 8.57 g/m^3 respectively). The mass of soot formed for case 7 is somewhat lower (8.30 g/m^3). The results from these cases were further investigated in Fig. 6. In Fig. 6a it can be seen that the amount of soot formed decreases as the carbon content in the incoming gas increases. In terms of the actual amount of soot formed this is not entirely true as the mass of soot is almost the same for the base case and case 6. In case 7 the mass of soot formed is somewhat lower than that for the base case and case 6. In Fig. 6b it can also be seen that the amount of oxidant (O_2, CO_2 and H_2O) in case 7 is higher than in case 6 and the base case, due to a larger addition of oxygen and a higher CO_2 content (see Table 4). This indicates that the amount of oxidant in each case may be the dominating factor controlling the amount of soot formed. Fig. 6 also shows that the amount of oxidant is not the sole factor affecting soot formation; the kinetics will of course also play an important role in the amount of soot formed.

For case 8, depicted in Fig. 5d, the soot formation was considerably reduced. For this case a slightly higher amount of oxygen was added (see Table 4) which will also influence the results to some extent. However, the higher amount of oxygen added in this case is only part of the explanation and most of the reduction will be due to the fact that no tars are present in the gas. The synthesis gas energy efficiency of the process was greatly improved for case 8, mainly due to the lower amount of energy bounded in the soot formed. The methane conversion was somewhat lower in this case. The results clearly show that the more large soot precursors that are present in the gas, the more soot will be formed. It is therefore of great interest to further study ways of cracking the tars in the producer gas in an energy efficient way before reforming the methane and C_2-hydrocarbons.

5. Conclusions

The aim of this investigation was to examine the extent to which soot is likely to form and possible ways of reducing soot formation. One base case and eight cases with different gas compositions were simulated and studied. The results were evaluated from the viewpoint of synthesis gas energy efficiency and methane conversion, as well as soot reduction. The results showed that neither the steam nor the hydrogen content of the gas affected the soot formation to any high degree, which was unexpected. The methane content of the gas had a greater impact on the amount of soot formed. The amount of soot formed was reduced when more CO_2 was present in the incoming gas, probably due to the increased amount of oxidant present. The synthesis gas energy efficiency and methane conversion were also positively affected by increasing the concentration of CO_2. The best results regarding soot formation were obtained for the case in which no tars were present in the incoming gas.

The reaction mechanism used in the numerical model presented in this work was not developed to describe reforming, but was designed to describe the combustion of benzene in fuel-rich flames. Theoretically, the model should also be valid for reforming, but the deviation from expected behavior may indicate that it does not adequately describe the reactions involved. It would therefore

be of interest to develop a reaction mechanism that describes soot formation in reducing environments such as reforming.

From the results obtained it was concluded that in order to reduce the amount of soot formed in the reverse-flow POX reactor studies should be carried it to further study ways of reducing the amount of tars in the gas in an energy efficient way. Experimental research on this process is under way and will be presented in a later publication.

Acknowledgements

The authors are grateful to the European Commission for financial support within the framework of the FP7 Integrated Project "GreenSyngas" (Project No. 213628). We would also like to thank the Swedish Energy Agency (STEM) and E.ON for their financial support.

References

[1] Hamelinck CN, Faaij APC, den Uil H, Boerrigter H. Production of FT transportation fuels from biomass; technical options, process analysis and optimisation, and development potential. Energy (Amsterdam, Neth.) 2004;29:1743–71.
[2] Buragohain B, Mahanta P, Moholkar VS. Thermodynamic optimization of biomass gasification for decentralized power generation and Fischer–Tropsch synthesis. Energy 2010;35:2557–79 [Oxford, UK].
[3] James OO, Mesubi AM, Ako TC, Maity S. Increasing carbon utilization in Fischer–Tropsch synthesis using H_2-deficient or CO_2-rich syngas feeds. Fuel Process Technol 2010;91:136–44.
[4] Manganaro J, Chen B, Adeosun J, Lakhapatri S, Favetta D, Lawal A, et al. Conversion of residual biomass into liquid transportation fuel: an energy analysis. Energy Fuels 2011;25:2711–20.
[5] Al-Hamamre Z, Vosz S, Trimis D. Hydrogen production by thermal partial oxidation of hydrocarbon fuels in porous media based reformer. Int J Hydrogen Energy 2009;34:827–32.
[6] Dufour A, Valin S, Castelli P, Thiery S, Boissonnet G, Zoulalian A, et al. Mechanisms and kinetics of methane thermal conversion in a syngas. Ind Eng Chem Res 2009;48:6564–72.
[7] Peña MA, Gomez JP, Fierro JLG. New catalytic routes for syngas and hydrogen production. Appl Catal A 1996;144:7–57.
[8] Albertazzi S, Basile F, Brandin J, Einvall J, Hulteberg C, Fornasari G, et al. The technical feasibility of biomass gasification for hydrogen production. Catal Today 2005;106:297–300.
[9] CHRISGAS. Clean hydrogen-rich synthesis gas – fuels from biomass. Intermediate report, Swedish Energy Agency, Växjö; 2008.
[10] Valin S, Cances J, Castelli P, Thiery S, Dufour A, Boissonnet G, et al. Upgrading biomass pyrolysis gas by conversion of methane at high temperature: experiments and modelling. Fuel 2009;88:834–42.
[11] Albertazzi S, Basile F, Barbera D, Benito P, Brandin J, Einvall J, et al. Deactivation of a Ni-based reforming catalyst during the upgrading of the producer gas, from simulated to real conditions. Top Catal 2011;54:746–54.
[12] Albertazzi S, Basile F, Brandin J, Einvall J, Fornasari G, Hulteberg C, et al. Effect of fly ash and H_2S on a Ni-based catalyst for the upgrading of a biomass-generated gas. Biomass Bioenergy 2008;32:345–53.
[13] Christensen TS. Adiabatic prereforming of hydrocarbons – an important step in syngas production. Appl catal A. Gen 1996;138:285–309.
[14] Jens S. Four challenges for nickel steam-reforming catalysts. Catal Today 2006;111:103–10.
[15] Toledo M, Bubnovich V, Saveliev A, Kennedy L. Hydrogen production in ultrarich combustion of hydrocarbon fuels in porous media. Int J Hydrogen Energy 2009;34:1818–27.
[16] Drayton MK, Saveliev AV, Kennedy LA, Fridman AA, Li Y.-E. Syngas production using superadiabatic combustion of ultrarich methane-air mixtures. In: 27th Symp. (Int.) Combust., Proc.; 1998. p. 1361–7.
[17] Weinberg FJ, Bartleet TG, Carleton FB, Rimbotti P, Brophy JH, Manning RP. Partial oxidation of fuel-rich mixtures in a spouted bed combustor. Combust Flame 1988;72:235–9.
[18] Tunå P, Svensson H, Brandin J. Modeling of reverse flow partial oxidation process for gasifier product gas upgrading. In: 5th International conference on thermal energy: theory and applications, Marrakesh, Morocco; 2010.
[19] Kennedy IM. Models of soot formation and oxidation. Prog Energy Combust Sci 1997;23:95–132.
[20] Frenklach M. Reaction mechanism of soot formation in flames. Phys Chem Chem Phys 2002;4:2028–37.
[21] Richter H, Howard JB. Formation of polycyclic aromatic hydrocarbons and their growth to soot – a review of chemical reaction pathways. Prog Energy Combust Sci 2000;26:565–608.
[22] Svensson H, Tunå P, Brandin J. Soot formation in reverse flow reforming of biomass gasification producer gas. In: Proceedings of 18th European biomass conference and exhibition. ETA-florence reneweble energies/WIP-renewable energies, Lyon, France; 2010.
[23] Frenklach M, Bowman T, Smith G, Gardiner B. <http://www.me.berkeley.edu/gri_mech/index.html, in>.
[24] Ergut A, Granata S, Jordan J, Carlson J, Howard JB, Richter H, et al. PAH formation in one-dimensional premixed fuel-rich atmospheric pressure ethylbenzene and ethyl alcohol flames. Combust Flame 2006;144:757–72.
[25] Richter H, Granata S, Green WH, Howard JB. Detailed modeling of PAH and soot formation in a laminar premixed benzene/oxygen/argon low-pressure flame. Proc Combust Inst 2005;30:1397–405.
[26] J.B. Howard, et al. <http://web.mit.edu/anish/www/MITcomb.html>.
[27] Gavrilyuk VV, Dmitrienko YM, Zhdanok SA, Minkina VG, Shabunya SI, Yadrevskaya NL, et al. Conversion of methane to hydrogen under superadiabatic filtration combustion. Theor Found Chem Eng 2001;35:589–96.
[28] van der Hoeven TA, de Lange HC, van Steenhoven AA. Analysis of hydrogen-influence on tar removal by partial oxidation. Fuel 2006;85:1101–10.
[29] Houben MP, de Lange HC, van Steenhoven AA. Tar reduction through partial combustion of fuel gas. Fuel 2005;84:817–24.
[30] Ginsburg JM, Piña J, El Solh T, de Lasa HI. Coke formation over a nickel catalyst under methane dry reforming conditions: thermodynamic and kinetic models. Ind Eng Chem Res 2005;44:4846–54.
[31] Valderrama G, Kiennemann A, Goldwasser MR. Dry reforming of CH_4 over solid solutions of $LaNi_{1-x}Co_xO_3$. Catal Today 2008;133–135:142–8.

Paper III

Regenerative reverse-flow reactor system for cracking of producer gas tars

Authors: Per Tunå, Fredric Bauer, Christian Hulteberg*, Laura Malek

Affiliation: Department of Chemical Engineering, Lund University, P.O. Box 124, SE-221 00 Lund, Sweden

*Corresponding author. E-mail: christian.hulteberg@chemeng.lth.se, tphn: +46-46-2228273

Abstract:

With increasing concern for future energy supply and increasing prices of crude oil, much research focus on fuels and chemicals produced by thermo-chemical conversion of biomass. In the thermo-chemical conversion of biomass, the biomass is first gasified to yield synthesis gas, which is then converted into fuels and/or chemicals. The gas produced in a gasifier contains high amounts of both tars and sulphur. Tars are readily converted over Ni-based catalyst, but Ni-based catalysts are permanently deactivated by the sulphur levels present in biomass derived producer gas. Calcined dolomite is catalytically active for tar cracking reactions. In this paper, calcined dolomite is used as bed material in a reverse-flow reactor for cracking of tars in a model synthesis gas. 1-methylnaphthalene was used as model tar compound at a concentration of 15 000 mg/Nm^3. Total tar conversion was over 95 % for the system under reverse-flow conditions. Furthermore, calcined dolomite is active for the water-gas shift reaction and the H_2:CO ratio of gas exiting the reactor can be controlled which may limit the need for a subsequent shift-reactor.

Keywords: biomass gasification; tars; tar removal; dolomite

1. Introduction

The production of the next generation of bio-fuels is based on utilizing non-food crops, e.g. agricultural waste, forest residues and energy crops [1]. One important process for the efficient utilization of such feedstocks is gasification, a technology originally developed for processing fossil fuels such as coal. In the gasification process, the feedstock is partly oxidized and the solid feedstock is reacted into a gaseous fraction and a solid ash fraction [2–4]. The composition of the gas depends on the type of gasifier, operating conditions and feedstock, but it mainly contains CO, CO_2, H_2, H_2O and N_2, if air is used in the gasifier. Nevertheless, the gas also contains some lower hydrocarbons, tars and trace amounts of contaminants such as NH_3, H_2S and HCN [5]. A significant share – approximately 50 % – of the heating value of the producer gas is available in the lower hydrocarbons and tars, depending on gasifier type and process conditions [6].

The tar compounds formed does however constitute a well-known problem, as these compounds limit the utilization of the gas in many applications. The tars can condense in piping and/or harm downstream materials and equipment. Removal or conversion of these tar compounds is thus a priority to ensure the successful large scale deployment of biomass gasification processes. Yet, there is not one clearly accepted definition of the word tar in the context of biomass gasification, although the definition by Evans and Milne[1] is often used and suits the purposes also of this study [7]. The tar compounds may further be characterized as primary, secondary or tertiary [8]. Primary tar compounds are products derived directly from cellulose, hemi-cellulose or lignin, thus having high oxygen content; secondary tar compounds consist of phenolics and olefins; tertiary tars are either condensed tertiary tars – e.g. poly-aromatics without substituent groups – or alkyl tertiary tars, such as methyl derivatives of poly-aromatics.

Different approaches to tar removal in producer gas from biomass gasifiers have been investigated, physical as well as thermal and catalytic methods to eliminate or separate the tar from the producer gas [9]. Due to the high energy content in the

[1] The definition of Evans and Milne states that "the organics, produced under thermal or partial-oxidation regimes (gasification) of any organic material, are called "tars" and are generally assumed to be largely aromatic"

tars, it is preferable to decompose the tars to other gas compounds rather than to scrub or otherwise physically remove the tars from the gas. Thus catalytic methods for tar conversion and decomposition have been thoroughly studied and reviewed [10–13]. Common Ni-based catalysts perform well in the tar cracking application and are available at relatively low costs, but a major disadvantage is their high sensitivity to sulphur compounds which are inevitably present in producer gas. The use of dolomite and olivine as catalysts for tar cracking has also been investigated, both as active catalyst particles in fluidized bed gasifiers and for downstream treatment [14–17]. As the tar content depends largely on the reaction conditions in the gasifier [18], the optimization of gasifiers to yield a gas with a low tar content has also been investigated thoroughly, and reviewed recently [19, 20].

In a regenerative reverse flow system heat is transferred between the fluid passing through the reactor and the stationary reactor bed, heating the bed and cooling the fluid. The bed acts as a thermal buffer, and when the flow is reversed, this heat is exchanged with the gas entering the reactor from the new direction. Thus two alternating thermal buffer zones are created with an active zone inbetween, as seen in Figure 1. This mode of operation enables a very high thermal efficiency, up to 95% [21]. An in-depth description of reverse-flow reactor systems, suitable applications and important aspects of the operation of such systems was published by Matros & Bunimovich [22]. Reverse flow reactors have traditionally been applied to exothermic processes such as regenerative thermal oxidation and regenerative catalytic oxidation used for VOC abatement, oxidation of SO_2 and partial oxidation of methane for syngas production. The concept has however also been shown to be applicable to endothermic reactions, such as dehydrogenation of ethylbenzene [23].

FIGURE 1

A reverse flow reactor for tar cracking, the first reverse flow process combining an exothermic and an endothermic reaction, has been demonstrated earlier [24]. The reactor was filled with bauxite in the thermal buffer zones and catalytically active

calcined dolomite in the active zone, operated at very high temperatures, about 1 050 °C, which leads to large energy losses and increases the risk for soot formation. The lower hydrocarbons present in producer gas will, at high temperatures, form soot in the presence of oxidizers [25].

The aim of the research presented in this paper has been to demonstrate a regenerative reverse flow reactor for tar reforming, operating at temperatures below 1 000 °C and using a model producer gas with 1-methylnaphthalene (1-MN) as a model compound for tertiary tars. The lower operating temperature ensures that the methane present in the producer gas is not reformed, which is important if the objective of the gasification is to produce synthetic natural gas (SNG). By addition of pure oxygen at temperatures of about 800 °C the tar is converted to syngas components by reforming and partial oxidation. By also retaining the methane content of the gas, a higher efficiency of the complete process (biomass to SNG) can be achieved as a higher share of the total energy content is utilized and methane is not first reformed and thereafter resynthesized.

2. Materials and methods

2.1 Experimental setup

The experimental setup used for the tar reforming experiments is shown in Figure 2. The reactor is vertically oriented and constructed from a Sandvik 253 MA high-temperature steel tube with an outer diameter of 152 mm (6") and a length of 700 mm. Five smaller steel tubes are inserted into the reactor from the top and the bottom, one is used as a thermocouple pocket, welded shut in the reactor centre, and four are used as diffusers for oxygen injection. The oxygen diffusers enter the reactor from a manifold at each end of the reactor. As the reactor is constructed for reverse-flow operation the construction is completely symmetrical. The reactor is filled with Swedish dolomite (from Sala) particles with a size of 1-3 mm. The size of the dolomite particles was chosen to yield a balance between a large surface area and a low pressure drop over the reactor. Further, it is crucial to minimize the void volume to suppress the formation of flames. The dolomite bed, the effective reactor length, is 620 mm. The reactor is insulated with ceramic half shell insulation

modules. The shells covering the middle part of the reactor have integrated heating elements with a capacity of 3 500 W. Additional to the external heating, the reactor bed is heated by combustion of methanol before operation. At sufficient temperature (>200 °C) methanol is injected together with H_2, N_2 and O_2, which heats the reactor bed to the desired operating temperature, at which the methanol flow is exchanged for water.

Process gas inlets are 19 mm (3/4") steel tubes connected to the side of the reactor top and bottom. The flow direction is controlled using four electromagnetic valves. The gas flow is controlled by digital mass flow controllers and the water flow is controlled by a peristaltic pump. 1-MN is injected into the gas stream using a syringe pump. The oxygen flow direction is controlled by an additional three-way valve and is via the manifold distributed to the diffusers which inject the oxygen 240 mm into the reactor bed. Oxygen is injected co-current with the process gas, creating a hot, active zone slightly shifted from the center of the reactor. When the flow direction of process gas and oxygen is reversed, the temperature of the former active zone decreases due to endothermic reforming reactions, heat transfer to the reactor ends and heat losses, whereas a new active zone is formed in which the temperature increases.

FIGURE 2

2.2 Experiments

The reverse flow tar reformer was tested at active zone temperatures of 700, 800 and 850 °C, at flow rates of 0.5, 0.85 and 1.2 Nm^3/h, corresponding to gas hourly space velocities (GHSV) of 45, 75 and 105 h-1 and residence times of 29, 17 and 12 seconds. The reactor, which is rather large for laboratory testing purposes, can most probably be used with higher flow rates. The mass flow controllers limited the testing of the reactor at higher flow rates, as they were not designed to handle larger flows. As seen in Figure 2, the model producer gas was mixed from separate bottles of gas, instead of using a premixed gas. Into this model producer gas the

model tar compound 1-MN was injected, at a ratio of 15,000 mg/Nm^3. The composition of the model producer gas is shown in Table 1.

TABLE 1

2.3 Analysis and characterization

As seen in Figure 2, a share of the gas exiting the reactor system is flared, giving an indication of some of the gas properties; varying flow rates yield a flame with changing flame height and a gas containing hydrocarbons with C-C bonds burn with a yellow flame, whereas a gas with only CO, H_2 and CH_4 is faintly blue, giving an immediate indication of the performance of the tar reformer.2 Thus, operating conditions yielding yellow flames are easily discarded as non-productive.

The gas after tar conversion was sampled and analyzed using a method developed at the Swedish Royal Institute of Technology [26]. 100 ml of the process gas that is to be analyzed is sucked through a matrix of 500 mg aminopropyl bond silica during a period of approximately 60 seconds. The sample is then eluted from the matrix by first adding 100 µl of an internal standard consisting of 2.5 mg/ml tert-butylcyclohexane in dichloromethane (DCM). An additional 2 ml of DCM is then added and the solvent is pressed through the matrix into a glass vial with a flow rate of 1-2 ml/min using nitrogen gas. After elution, the sample is analysed using gas chromatography to identify and quantify the tar compounds in the gas.

The bed particles were analyzed for changes in their BET surface areas measured by the adsorption of nitrogen at liquid nitrogen temperature using a Micromeritics ASAP 2400 instrument after degassing for 16 h at 473 K. Pore volume analysis was performed using the BJH method [27]. The Halsey formula [28] was used to

[2] A movie showing the flare is available as electronic supplementary material.

calculate the thickness of the adsorbed layer (t-value). The desorption-isotherm was used for the analysis; the values are average values of 2 analysis runs were used. The content of the bed particles was analysed using X-ray diffraction (XRD) analysis, performed on a Seifert XRD 3000 TT diffractometer using CuK- radiation and a rotating sample holder. The tube voltage and the current were set to 40 kV and 40 mA, respectively. The instrument was calibrated using a Si standard. Diffractograms were recorded between 5° and 80° 2θ in steps of 0.05° (10 s/step). The elemental composition was analysed from <200 µm fragments from crushed catalyst particles, using energy dispersive x-ray spectroscopy (EDS) in a scanning electron microscope (SEM) operated at 15 kV.

3 Results and Discussion

3.1 Reactor operation

The reactor was operated successfully at temperatures up to approximately 850 °C in the active zone. As the thermocouples are placed along the centre of the reactor tube, it is possible that single hot spots reached higher temperatures than were measured by the thermocouples. A typical temperature profile for the reactor in operation is shown in Figure 3. The active zone is clearly visible between approx. 320 and 420 mm. As described earlier, the oxygen is injected at 420 mm reactor length. The temperature profile thus shows that mixing of oxygen and fuel gas is not instant since the temperature increases for about 50 mm indicating reforming reactions taking place.

FIGURE 3

However, a few problems were experienced which were most probably due to the reactor bed and the diffusion of oxygen and feed gases inside it. When heating the reactor by combustion of methanol, the combustion was incomplete when the reactor was operated at top-to-bottom flow, whereas complete conversion was

reached when the flow direction was reversed. This is most probably the effect of the oxygen diffusers entering from the top being unevenly packed with dolomite particles, creating a larger flow of oxygen in one of the diffusers and thus not reaching an even concentration gradient along the vertical reactor axis. It is possible that with smaller bed particles, it would be easier to pack the reactor bed more evenly and reduce these problems, although this would also increase the pressure drop over the reactor. This is however not believed to have had a major influence on the tar reduction experiments.

3.2 Tar cracking

The regenerative reverse-flow system showed good conversion of 1-MN, up to 78 %, at temperatures as low as 700 °C. At these low temperatures the 1-MN was however not reformed to syngas compounds, but mainly rather to other, lighter tar compounds such as benzene, toluene, xylene, indane, indene, several unidentified species and – predominantly – naphthalene. Apart from these light tar compounds, there are also trace amounts of heavier compounds such as phenanthrene, fluorene, pyrene and other unidentified species. The total tar conversion, i.e. conversion of both 1-MN and its derivatives such as toluene and naphthalene, at 700 °C was no higher than 24 %. Furthermore, at 700 °C more naphthalene than 1-MN was present at the reactor outlet. This is an indication that the initial step in the decomposition of 1-MN is separation of the methyl group from the aromatic rings, which is to be expected as the aromatic ring structure is very stable. With increasing temperature in the active zone of the reactor, the conversion of 1-MN increased slowly, whereas the total tar conversion increased rapidly. The increase in total conversion is almost entirely because of increased naphthalene conversion. At 850 °C, the total tar conversion was as high as 95 %, with a 1-MN conversion of more than 99 % for the lowest flow rate.

FIGURE 4

Several other studies [29–31] have identified naphthalene as being one of the most difficult tar compounds to crack, which is to be expected as the aromatic ring structure is very stable. The tar cracking mechanism is very complex and difficult to map, but the results from this study with fast conversion of 1-MN but high contents of naphthalene left in the gas at the lower temperatures align well with observations by others. Aldén et al showed that most of the tars in the producer gas are easily converted with dolomite at 800 °C but that BTX, naphthalene, biphenyl, phenanthrene and pyrene remain [29]. Coll et al showed that the reactivity of the aromatic compounds decrease with the number of rings in the molecular structure with the exception of naphthalene which is very difficul to convert, i.e. the order of reactivity is benzene > toluene >> anthracene >> pyrene > naphthalene [32]. Garcia and Hüttinger [30] proposed a reaction scheme for the steam gasification of naphthalene which is applicable to naphthalene cracking, in which one of the aromatic rings is broken forming indene, from which styrene, toluene and subsequently benzene are formed. The dolomite is most probably active in forming naphthalene radicals by hydrogen abstraction, i.e. the initiating step in breaking the aromatic ring of the naphthalene, but that the cracking process is inhibited by the hydrogen present in the gas as this will easily react with the naphthalene radical and reform naphthalene [29].

FIGURE 5

3.3 Gas composition and WGS properties

The gas composition used during experiments for feeding the reactor closely resembled a gas produced in an oxygen and/or steam blown fluidized bed gasifier. The exception was that no lower hydrocarbons, such as ethylene, were present in the model gas and the only tar compound present was 1-MN. It has been shown in earlier studies [15, 33] that dolomite catalyzes the water-gas shift reaction. This is noticeable at the lowest temperature and flow rate with up to 45 mol-% H_2 with only 10 mol-% CO measured at the outlet of the reactor. For the highest flow rate, H_2 and CO was equal at 30 mol-%. Measurements were performed on a dry gas. For the lowest temperature and flow rate, the H_2:CO ratio is higher than 4:1, see

Figure 6. If the purpose of the synthesis gas conditioning is downstream synthesis of hydrocarbons, 2:1 (3:1 for synthetic natural gas) is desirable. The higher flow rates gave a H_2:CO ratio of almost 1:1, indicating that the kinetics for water-gas shift is to slow to reach equilibrium. A gain in simplicity could be achieved for the whole gasification train if the desirable H_2:CO ratio could be achieved in the tar cracker without using a downstream water-gas shift reactor.

FIGURE 6

3.4 Catalyst characterization

The fresh dolomite had a BET surface area of 42 m^2/g whereas the used dolomite had an area between 0.36 and 8 m^2/g. The initial surface area is significantly larger than what has been found in the literature [17, 34–36], which is usually in the 0.5-10 m^2/g range. However, the BET surface area and the pore volume clearly shows how the catalyst is sintered as it gets procedurally hotter in the reactor bed from the producer gas inlet to the oxygen inlet and the surface areas are well in-line with what has previously been reported in the literature at these conditions [34–36].

The catalyst samples in Table 2, with the exception of the fresh catalyst, were taken from different positions along the reactor length, from the inlet to the middle. Table 2. Composition and BET surface area of the fresh and used dolomite.

TABLE 2

The catalyst composition was determined with EDS in a SEM. Figures 7 and 8 show SEM images of the dolomite surface and the EDS spectrum from the marked area in the SEM image, showing the content of Ca, Mg, O, C, Si, and Al in the dolomite. The literature reports a growing particle size with increasing

temperature, something that has been indicated also in this investigation, but more images and samples would have to be taken to statistically confirm this [35].

FIGURE 7

FIGURE 8

The EDS analysis reported in Figures 7 and 8 show different results compared to the XRD analysis, hence there is a difference between the bulk and the surface composition. The XRD analysis confirmed the presence of both calcined and uncalcined dolomite (oxide form) in the reactor centre, from before one oxygen inlet, throughout the reactor to after the second oxygen inlet. The XRD analysis revealed the presence of $CaMg(CO_3)_2$ as well as CaO and MgO. However the dolomite analysed in Figures 7 and 8 is clearly calcined and contains more magnesium than calcium at the analysed surface and this surface-concentration is well in-line with other literature findings [35]. The increased Mg concentration on the surface of the dolomite grains is interesting as it has been speculated that the surface oxygen atoms are responsible for hydrogen abstraction (Alden). This speculation has been founded on an analogy with methane reforming over MgO and the higher the Mg surface concentration the more likely this is to represent the true mechanism of the tar decomposition.

4. Conclusions

A novel system comprising a regenerative reverse-flow reactor with a dolomite bed for reforming of tars in producer gas from biomass gasification has been developed. The system was tested using a model producer gas and a single model tar compound, 1-methylnaphthalene, resulting in a total tar conversion of up to 95 %. The high thermal efficiency of the system promises a highly efficient process step

for integration in a gasification process train. The water-gas shift activity was apparent at the lower flow rates and temperature as the H_2:CO ratio was over 4:1. At higher temperatures, the ratio was closer to 1:1. If the cracker could be operated to yield a gas with a 2:1 ratio between H_2 and CO, no water gas shift reactor would be necessary for downstream methanol or Fischer-Tropsch synthesis. The catalyst characterization showed that not all of the bed in the reactor centre was calcined and that the bed contained several phases of both carbonated and oxidised calcium and magnesium. The surface area of the catalyst decreases by almost 100 times and not much surface area remains on the active catalyst.

Future work should be performed on producer gas from a real gasifier. There are many important compounds present in producer gas that were not present in this study, for practical and safety reasons, such as benzene, ethylene and ammonia, which could have a significant impact on downstream process equipment. Other aspects to investigate are the effects of reactor bed particle size, higher flow rates and improved diffusion of oxygen in the reactor.

5. Acknowledgements

The research was funded by the Swedish energy Agency through the Swedish Gas Technology Centre and the Danish Gas Technology Centre, in cooperation with the industrial partners ABB Corporate Research, Alufluor AB, E.ON Gasification Development AB, E.ON Sverige AB, Göteborg Energi AB, Statoil ASA, Stockholm Gas AB, Tekniska Verken i Linköping AB, ÅForsk and Öresundskraft AB.

6. References

1. Albertazzi S, Basile F, Brandin J, et al. (2005) The technical feasibility of biomass gasification for hydrogen production. Catalsis Today 106:297–300. doi: 10.1016/j.cattod.2005.07.160

2. Kumar A, Jones DD, Hanna MA (2009) Thermochemical Biomass Gasification: A Review of the Current Status of the Technology. Energies 2:556–581. doi: 10.3390/en20300556

3. Damartzis T, Zabaniotou A (2011) Thermochemical conversion of biomass to second generation biofuels through integrated process design—A review. Renewable Sustainable Energy Rev 15:366–378. doi: 10.1016/j.rser.2010.08.003

4. Kirubakaran V, Sivaramakrishnan V, Nalini R, et al. (2009) A review on gasification of biomass. Renewable Sustainable Energy Rev 13:179–186. doi: 10.1016/j.rser.2007.07.001

5. Xu C, Donald J, Byambajav E, Ohtsuka Y (2010) Recent advances in catalysts for hot-gas removal of tar and NH3 from biomass gasification. Fuel 89:1784–1795. doi: 10.1016/j.fuel.2010.02.014

6. Tunå P, Svensson H, Brandin J (2010) Modeling of Reverse Flow Partial Oxidation Process for Gasifier Product Gas Upgrading. Fifth International Conference on Thermal Engineering: Theory and Applications, Marrakesh.

7. Evans RJ, Milne TA (1997) Chemistry of Tar Formation and Maturation. In: Bridgwater A, Boocock D (eds) Developments in Thermochemical Biomass Conversion, vol 2. Blackie Academic & Professional, London, pp 803–816

8. Milne TA, Abatzoglou N, Evans RJ (1998) Biomass gasifier“ tars”: Their nature, formation, and conversion NREL/TP-570-25357. doi: 10.2172/3726

9. Anis S, Zainal ZA (2011) Tar reduction in biomass producer gas via mechanical, catalytic and thermal methods: A review. Renewable Sustainable Energy Rev 15:2355–2377. doi: 10.1016/j.rser.2011.02.018

10. Abu El-Rub Z, Bramer EA, Brem G (2004) Review of Catalysts for Tar Elimination in Biomass Gasification Processes. Ind Eng Chem Res 43:6911–6919. doi: 10.1021/ie0498403

11. Zhang R, Brown RC, Suby A, Cummer K (2004) Catalytic destruction of tar in biomass derived producer gas. Energy Convers Manage 45:995–1014. doi: 10.1016/j.enconman.2003.08.016

12. Yung MM, Jablonski WS, Magrini-Bair KA (2009) Review of Catalytic Conditioning of Biomass-Derived Syngas. Energy Fuels 23:1874–1887. doi: 10.1021/ef800830n

13. Dayton D (2002) A Review of the Literature on Catalytic Biomass Tar Destruction Milestone Completion Report. NREL/TP-510-32815. National Renewable Energy Laboratory, Golden.

14. Olivares A, Aznar MP, Caballero MA, et al. (1997) Biomass Gasification: Produced Gas Upgrading by In-Bed Use of Dolomite. Ind Eng Chem Res 36:5220–5226. doi: 10.1021/ie9703797

15. Orío A, Corella J, Narváez I (1997) Performance of Different Dolomites on Hot Raw Gas Cleaning from Biomass Gasification with Air. Ind Eng Chem Res 36:3800–3808. doi: 10.1021/ie960810c

16. Delgado J, Aznar MP, Corella J (1996) Calcined Dolomite, Magnesite, and Calcite for Cleaning Hot Gas from a Fluidized Bed Biomass Gasifier with Steam: Life and Usefulness. Ind Eng Chem Res 35:3637–3643. doi: 10.1021/ie950714w

17. Simell PA, Hepola JO, Krause AOI (1997) Effects of gasification gas components on tar and ammonia decomposition over hot gas cleanup catalysts. Fuel 76:1117–1127. doi: 10.1016/S0016-2361(97)00109-9

18. Li C, Suzuki K (2009) Tar property, analysis, reforming mechanism and model for biomass gasification—An overview. Renewable Sustainable Energy Rev 13:594–604. doi: 10.1016/j.rser.2008.01.009

19. Han J, Kim H (2008) The reduction and control technology of tar during biomass gasification/pyrolysis: An overview. Renewable Sustainable Energy Rev 12:397–416. doi: 10.1016/j.rser.2006.07.015

20. Devi L, Ptasinski KJ, Janssen FJJG (2003) A review of the primary measures for tar elimination in biomass gasification processes. Biomass Bioenergy 24:125–140. doi: 10.1016/S0961-9534(02)00102-2

21. Matros YS, Bunimovich GA (1995) Control of Volatile Organic Compounds by the Catalytic Reverse Process. Ind Eng Chem Res 34:1630–1640. doi: 10.1021/ie00044a016

22. Matros YS, Bunimovich GA (1996) Reverse-Flow Operation in Fixed Bed Catalytic Reactors. Catal Rev 38:1–68. doi: 10.1080/01614949608006453

23. Haynes TN, Georgakis C, Caram HS (1992) The application of reverse flow reactors to endothermic reactions. Chem Eng Sci 47:2927–2932. doi: 10.1016/0009-2509(92)87153-H

24. Van de Beld L, Wagenaar BM, Prins W (1997) Cleaning of hot producer gas in a catalytic adiabatic packed bed reactor with periodic flow reversal. In: Bridgwater AV, Boocock DGB (eds) Developments in Thermochemical Biomass Conversion, vol 2. Blackie Academic & Professional, London, pp 907–920

25. Svensson H, Tunå P, Hulteberg C, Brandin J (2012) Modeling of soot formation during partial oxidation of producer gas. Fuel 106:271-278. doi: 10.1016/j.fuel.2012.10.061

26. Myrén C, Hörnell C, Björnbom E, Sjöström K (2002) Catalytic tar decomposition of biomass pyrolysis gas with a combination of dolomite and silica. Biomass Bioenergy 23:217–227. doi: 10.1016/S0961-9534(02)00049-1

27. Barrett EP, Joyner LG, Halenda PP (1951) The Determination of Pore Volume and Area Distributions in Porous Substances. I. Computations from Nitrogen Isotherms. J Am Chem Soc 73:373–380. doi: 10.1021/ja01145a126

28. Halsey G (1948) Physical Adsorption on Non-Uniform Surfaces. J Chem Phys 16:931. doi: 10.1063/1.1746689

29. Aldén H, Björkman E, Carlsson M, Waldheim L (1994) Catalytic cracking of naphthalene on dolomite. In: Bridgwater AV (ed) Advances in Thermochemical Biomass Conversion, vol 1. Blackie Academic & Professional, London, pp 216–232

30. Garcia XA, Hüttinger KJ (1989) Steam gasification of naphthalene as a model reaction of homogeneous gas/gas reactions during coal gasification. Fuel 68:1300–1310. doi: 10.1016/0016-2361(89)90246-9

31. Devi L, Ptasinski KJ, Janssen FJJG (2005) Pretreated olivine as tar removal catalyst for biomass gasifiers: investigation using naphthalene as model biomass tar. Fuel Processing Technology 86:707–730. doi: 10.1016/j.fuproc.2004.07.001

32. Coll R, Salvadó J, Farriol X, Montané D (2001) Steam reforming model compounds of biomass gasification tars: conversion at different operating conditions and tendency towards coke formation. Fuel Process Technol 74:19–31. doi: 10.1016/S0378-3820(01)00214-4

33. Pérez P, Aznar PM, Caballero MA, et al. (1997) Hot Gas Cleaning and Upgrading with a Calcined Dolomite Located Downstream a Biomass Fluidized

Bed Gasifier Operating with Steam–Oxygen Mixtures. Energy Fuels 11:1194–1203. doi: 10.1021/ef970046m

34. Boucif F, Marouf-Khelifa K, Batonneau-Gener I, et al. (2010) Preparation, characterisation of thermally treated Algerian dolomite powders and application to azo-dye adsorption. Powder Technol 201:277–282. doi: 10.1016/j.powtec.2010.04.013

35. Sasaki K, Qiu X, Hosomomi Y, et al. (2013) Effect of natural dolomite calcination temperature on sorption of borate onto calcined products. Microporous Mesoporous Mater 171:1–8. doi: 10.1016/j.micromeso.2012.12.029

36. Ávila I, Crnkovic PM, Milioli FE, Luo KH (2012) Investigation of the pore blockage of a Brazilian dolomite during the sulfation reaction. Appl Surf Sci 258:3532–3539. doi: 10.1016/j.apsusc.2011.11.108

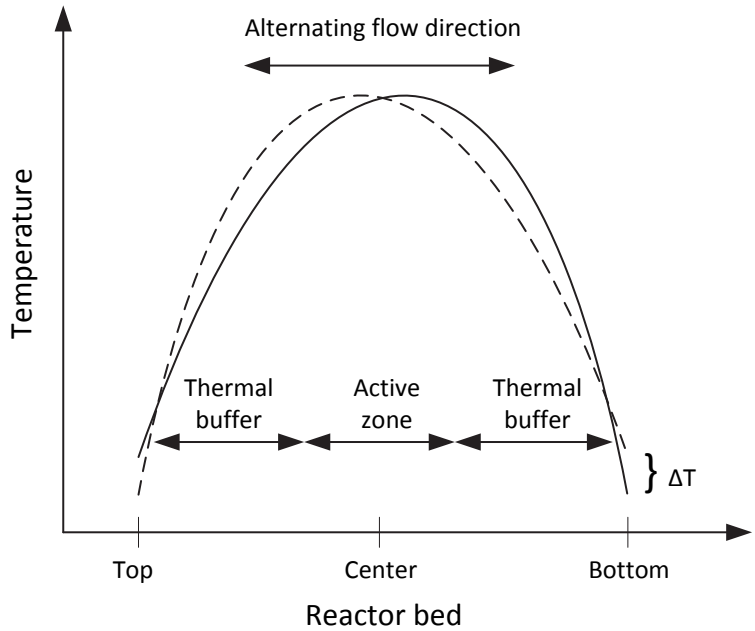

Fig 1 Alternating temperature profile with two thermal buffer zones and an active zone in a regenerative reverse flow reactor.

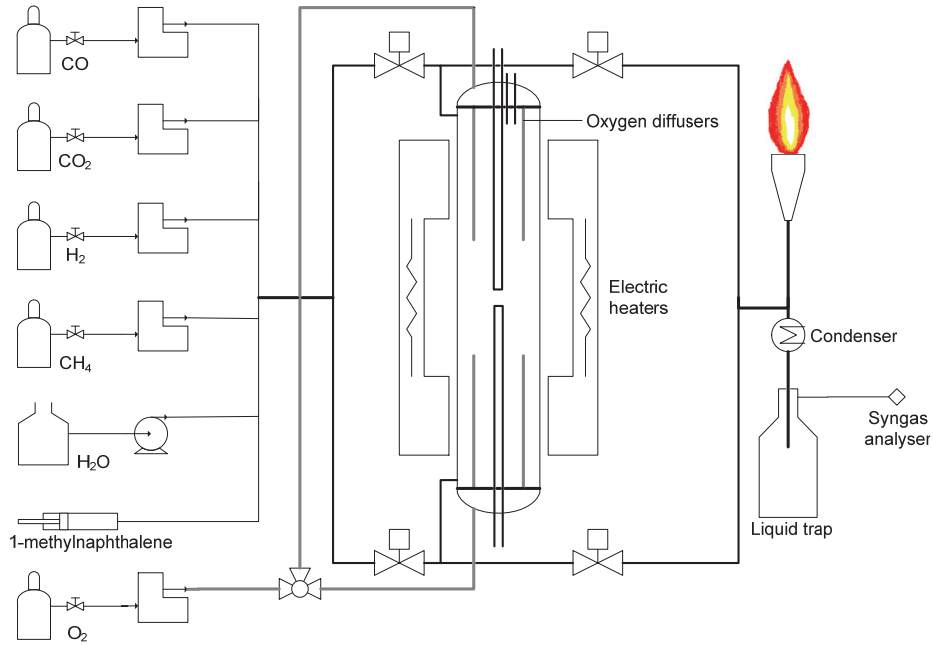

Fig 2 The experimental setup.

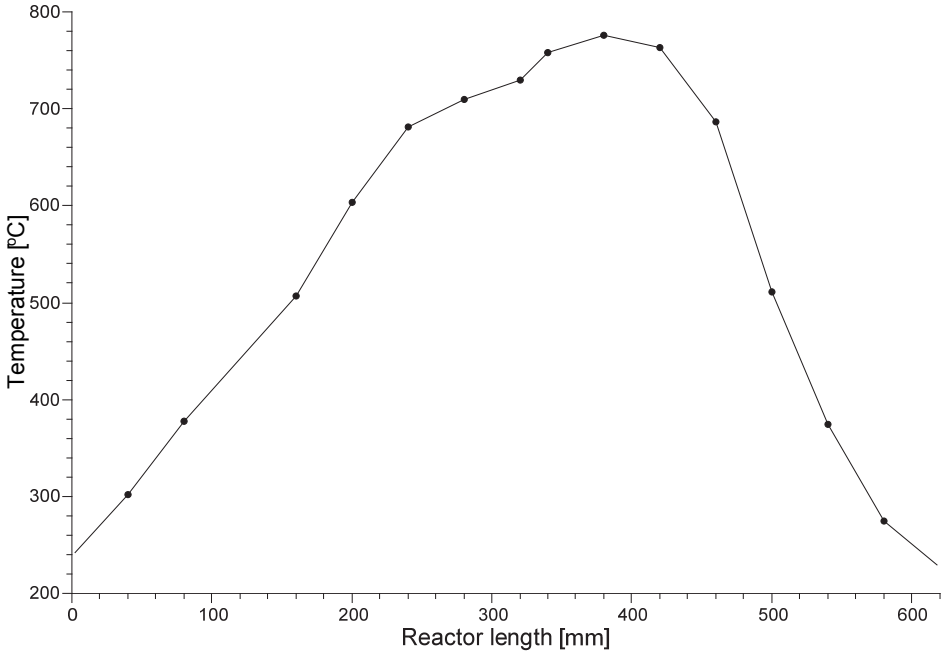

Fig 3 Typical temperature profile of the reactor.

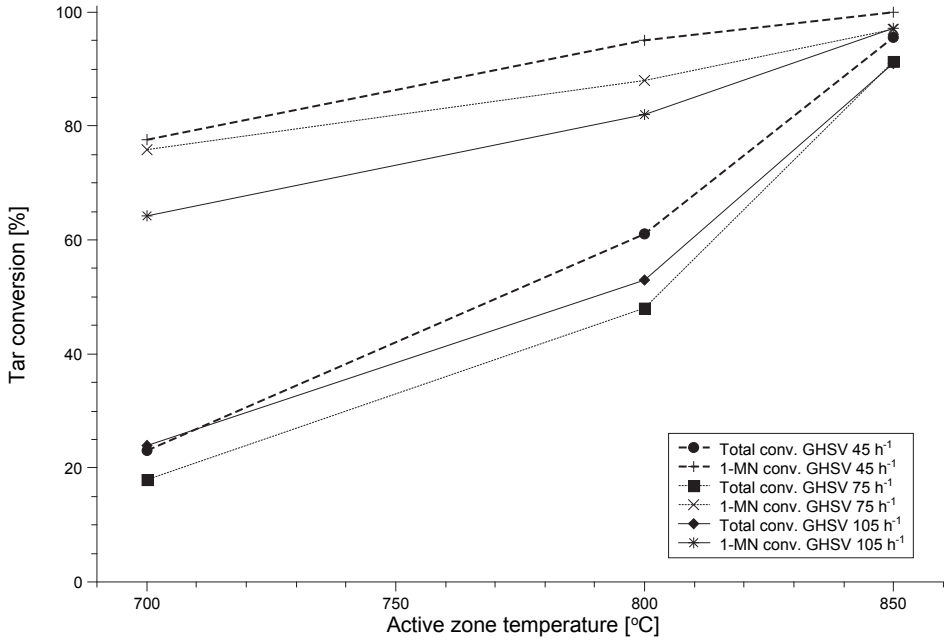

Fig 4 Total tar conversion and conversion of 1-MN at tested temperatures and flow rates.

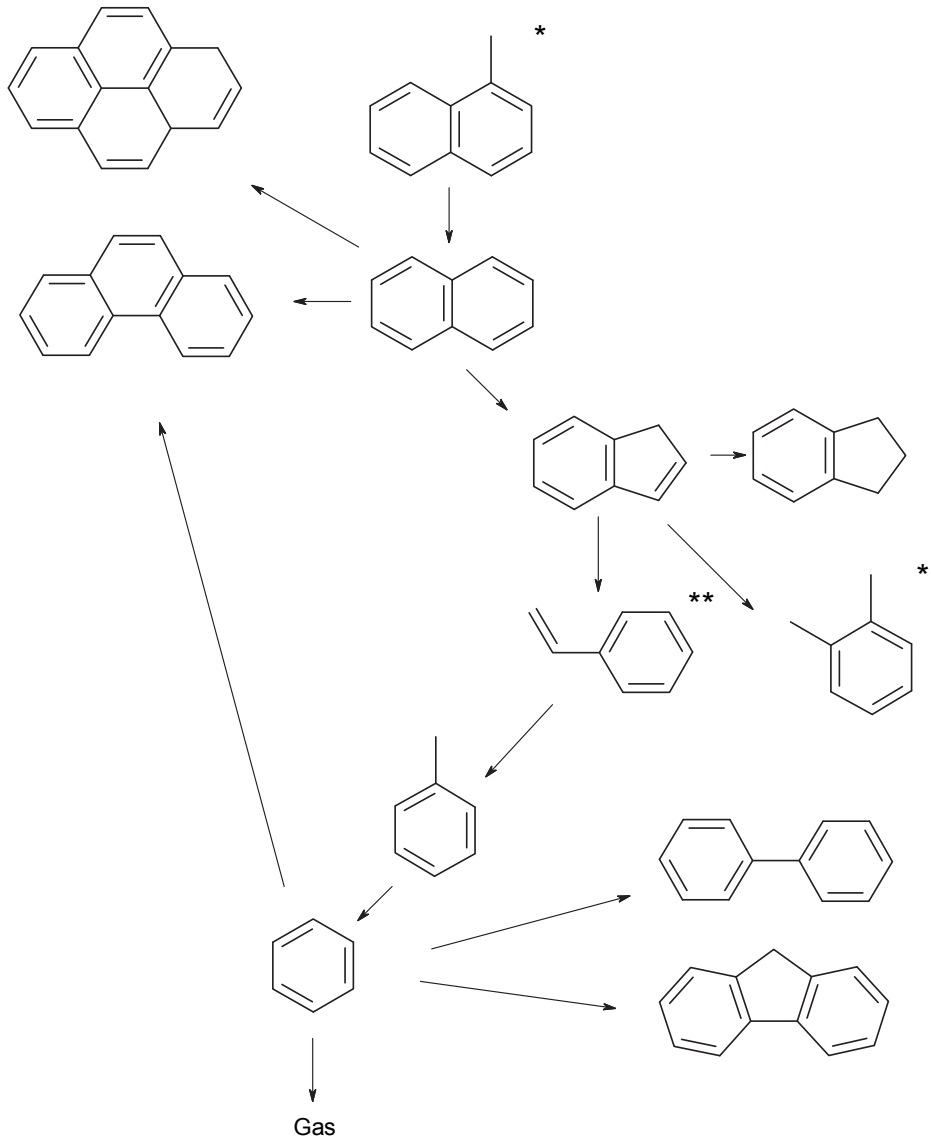

Fig 5 Reaction scheme for the conversion of naphthalene to the species identified in the gas from the reverse flow reactor, adapted from [30]. 1-MN and xylene (*) were not included in the original figure, whereas the important intermediate styrene (**) could not be identified although it most likely exists in the gas, probably due to detection and identification difficulties.

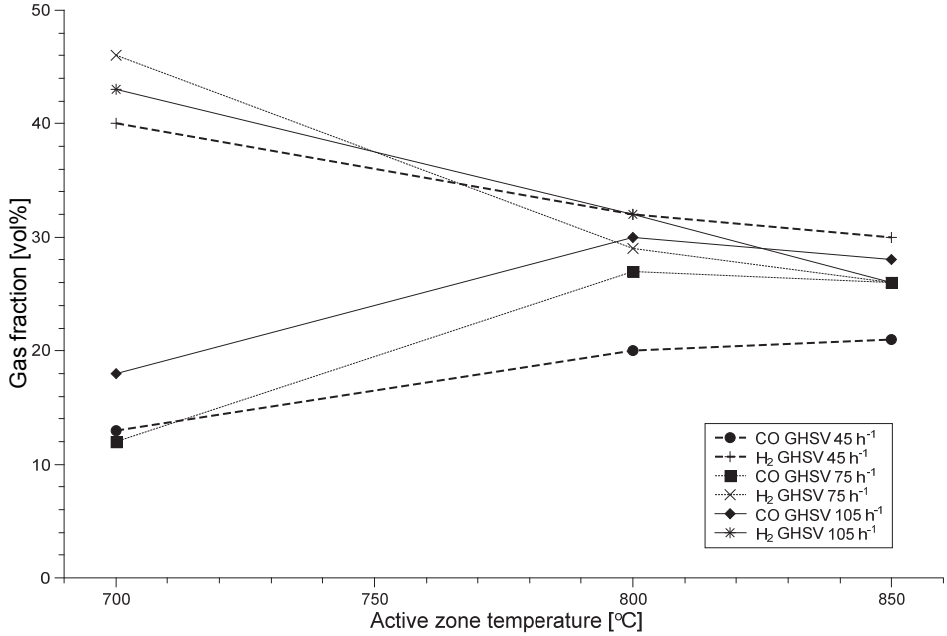

Fig 6 Fraction of CO and H2 in the gas after tar reforming.

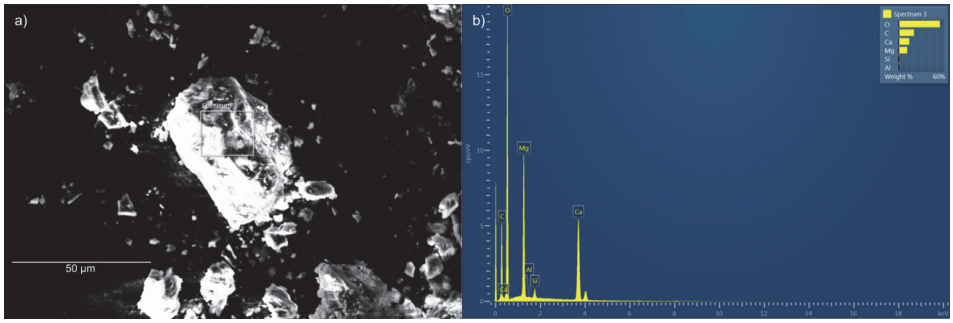

Fig 7 Fresh dolomite sample, a) showing a SEM image of the sample and b) showing the EDS spectrum of a selected area of the sample.

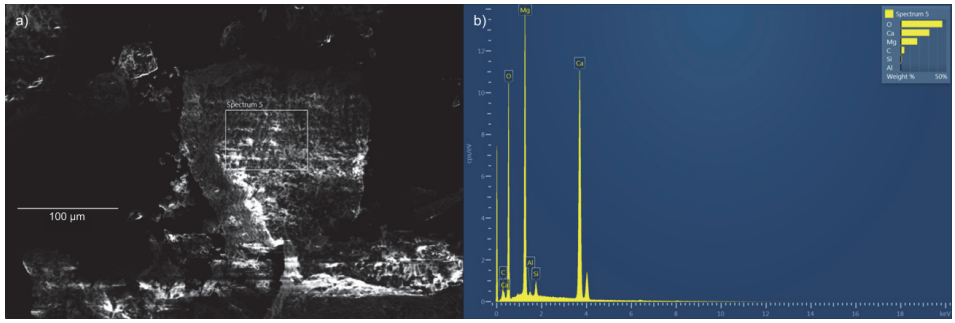

Fig 8 Dolomite sample from the reactor centre, a) showing a SEM image of the sample and b) showing the EDS spectrum of a selected area of the sample.

Table 1. Composition of the model producer gas.

Component	Volumetric fraction
CO	25 %
CO2	15 %
H2	25 %
CH4	10 %
H2O	25 %
1-Methylnaphtalene	15 000 mg/Nm3

Table 2. Results from the BET surface area measurements of the dolomite.

Catalyst sample	BET surface area [m2/g]	BJH Cumulative desorption area of pores [m2/g]	BJH Cumulative desorption volume of pores [cm3/g]
Fresh	42.0	48.4	0.20
Producer gas inlet	8.0	10.5	0.070
Between inlet and oxygen 1	1.9	2.1	0.0057
Between inlet and oxygen 2	0.94	0.9	0.0018
Oxygen inlet	0.31	0.29	0.0020
Middle	0.36	0.113	0.00020

Paper IV

Fuel 105 (2013) 331–337

Contents lists available at SciVerse ScienceDirect

Fuel

journal homepage: www.elsevier.com/locate/fuel

Selective catalytic oxidation of ammonia by nitrogen oxides in a model synthesis gas

Per Tunå [a,*], Jan Brandin [b]

[a] Department of Chemical Engineering Lund University, Getingevägen 60, SE-22100 Lund, Sweden
[b] Departament of Bioenergy Technology, Linnaeus University, 351 95 Växjö, Sweden

HIGHLIGHTS

- Gas phase removal of ammonia from synthesis gas is evaluated.
- Selective oxidation of ammonia in synthesis gas is possible with addition of NO_X.
- $V_2O_5/WO_3/TiO_2$ and H-morenite SCR catalyst perform well in reducing environments.
- On-site generation of the necessary NO_X is possible by nitric acid decomposition.

ARTICLE INFO

Article history:
Received 13 February 2012
Received in revised form 13 August 2012
Accepted 14 August 2012
Available online 1 September 2012

Keywords:
SCR
Synthesis gas
$V_2O_5/WO_3/TiO_2$
H-mordenite
Ammonia removal

ABSTRACT

Synthesis gas generated by the gasification of nitrogen-containing hydrocarbons will contain ammonia. This is a catalyst poison and elevated levels of nitrogen oxides (NO_X) will be produced if the synthesis gas is combusted. This paper presents a study of the selective oxidation of ammonia in reducing environments. The concept is the same as in traditional selective catalytic reduction, where NO_X are removed from flue gas by reaction with injected ammonia over a catalyst. Here, a new concept for the removal of ammonia is demonstrated by reaction with injected NO_X over a catalyst. The experiments were carried out in a model synthesis gas consisting of CO, CO_2, H_2, N_2 and NH_3/NO_X. The performance of two catalysts, $V_2O_5/WO_3/TiO_2$ and H-mordenite, were evaluated. On-site generation of NO_X by nitric acid decomposition was also investigated and tested. The results show good conversion of ammonia under the conditions studied for both catalysts, and with on-site generated NO_X.

1. Introduction

Synthesis gas, generated by natural gas reforming, or by gasification of heavy oils or other carbon-containing feedstocks, is one of the most important intermediates in the chemical industry, and has been used for a long time for the production of essential bulk chemicals such as ammonia and methanol, as well as fuels. In the gasification process, the hydrocarbons in the feedstock (natural gas, coal, organic waste, woody biomass, etc.) are converted into a mixture of gases, consisting mainly of carbon monoxide (CO), carbon dioxide (CO_2), hydrogen (H_2), water (H_2O), methane (CH_4), lower hydrocarbons (C_{2-3}) and tars. If air is used as the oxidant, the gas will also contain large amounts of nitrogen (N_2). Depending on the origin and composition of the feedstock, and the process conditions, the gas produced will contain varying amounts of contaminants, such as sulphur, predominantly as hydrogen sulphide (H_2S), ammonia (NH_3), alkali and chloride such as potassium chloride (KCl), and hydrogen cyanide (HCN). If the feedstock used, for instance coal or biomass, contains high amounts of nitrogen, the gas produced will contain high levels of ammonia [1–4]. In the case of biomass gasification for the production of energy gas, for instance, for use in Combined Heat and Power Plants (CHP), or for the production of synthesis gas, the ammonia levels in the producer gas typically range from 0.04 to 1.8 vol.% [2,4,5].

This ammonia must be removed from the produced synthesis gas before usage, since it could poison the catalysts in the subsequent synthesis steps or form NO_X when combusted. Ammonia is very water soluble and can easily be removed with a water scrubber or a flue gas condenser. This has two drawbacks, the gas must be cooled down, which can increase operating costs and the ammonia is not eliminated as it ends up in the process water and must be handled by other processes.

Ammonia in the synthesis gas could be decomposed, to H_2 and N_2, over a reforming catalyst (usually Ni-based) at high temperature (~1073 K), a process called ammonia cracking. However, the conversion of ammonia is, as is hydrocarbon reforming, restrained because of sulphur poisoning [6].

* Corresponding author.
E-mail address: per.tuna@chemeng.lth.se (P. Tunå).

0016-2361/$ - see front matter © 2012 Elsevier Ltd. All rights reserved.
http://dx.doi.org/10.1016/j.fuel.2012.08.025

The removal of ammonia from air or any other oxygen containing gas can be accomplished with selective catalytic oxidation (SCO) over a suitable catalyst. The ammonia is then oxidised to N_2 and H_2O. Much research have been published in this area, for instance [7,8]. But due to the low oxygen content in synthesis gas, this has little to no relevance as a comparison.

A few publications on SCO have been performed under reducing conditions by injection of oxygen. In some of them [9,10] the concentration of CO and H_2 is very low, compared to a real synthesis gas produced in a gasifier. In others [11–16], it is not clear if the process studied really is SCO or ammonia cracking driven by the temperature increase, caused by CO and H_2 combustion in the catalytic bed due to the oxygen injection.

Selective catalytic reduction (SCR) is an industrial process for the removal of nitrogen oxides from combustion flue gases, by injection of nearly equimolar amounts of ammonia into the flue gas [17,18]. The ammonia can be injected into the hot flue gas either as ammonia or as a urea solution [19].

Since the NO_X in normal combustion flue gases consists of 90–95% nitrogen monoxide (NO), and the rest being nitrogen dioxide (NO_2), it is normally considered that the reaction over a solid catalyst, for instance $V_2O_5/WO_3/TiO_2$ [20] or an acidic zeolite [21], proceeds according to the following reaction:

$$4NO + 4NH_3 + O_2 \rightarrow 4N_2 + 6H_2O \quad (1)$$

Oxygen (O_2) participates in reaction (1), and in combustion flue gases the oxygen level is normally 2–10 vol.%. Without oxygen, the rate of reaction, or conversion, falls to relatively low values [22].

Reactions (2) and (3), do not require any oxygen. Reaction (2) has a much higher reaction rate than reaction (1) and is thus called the fast SCR reaction [22].

$$NO + NO_2 + 2NH_3 \rightarrow 2N_2 + 3H_2O \quad (2)$$

$$6NO_2 + 8NH_3 \rightarrow 7N_2 + 12H_2O \quad (3)$$

As mentioned above, the proportion of NO_2 in the NO_X content in flue gas is normally low and the effects of the fast SCR reaction are usually undetectable. In some diesel automotive SCR applications a part of the NO content in the flue gas is catalytically oxidised to NO_2 [22] to improve low-temperature SCR performance and improve the oxidation of soot in the particulate filter [19].

If the opposite reaction is considered, i.e. the removal, inverse SCR or selective catalytic oxidation (SCO), of ammonia in a gas stream by injection of NO_X over a suitable catalyst. It should be straightforward as long as the gas contains oxygen.

Attempts to remove ammonia from producer gas have previously been made on an industrial scale by applying the inversed SCR technique. Valtion Teknillinen Tutkimuskeskus (VTT) was granted a patent in 1996 for the removal of ammonia in a gasification process by co-injection of NO and O_2 into hot synthesis gas [23]. This ammonia removal is also SCO or ammonia cracking as it was performed at 673–973 K over a γ-alumina catalyst and the oxygen level in the gas was increased to 2 vol.% before the catalyst bed. In their patent, VTT claims that the process can be used to reduce NO_X emissions to the environment after combusting the producer gas, for instance in a gas turbine for power production.

This paper describes the application of the fast SCR reaction (3) in a model producer gas without the addition of oxygen. If NO_2 is injected into the producer gas, the ammonia can be selectively oxidised according to reaction (3). However, NO_2 is not stable in this environment. It is well known that NO_X is reduced by CO and H_2, for instance CO is oxidised to CO_2 and NO_X is reduced to N_2 by three-way catalysts in automotive applications [24]. Before the introduction of NH_3–SCR, hydrogen was used industrially to reduce NO_X over precious-metal catalysts at low temperature. This has recently received increasing attention [25,26]. Without a catalyst, the rate of these reactions is comparatively slow, at least at temperatures up to 600–700 K in the SCR temperature range.

2. Materials and methods

Fig. 1 shows a schematic illustration of the experimental set-up. The gases are supplied from gas bottles using mass-flow controllers. The CO, CO_2, H_2, and a mixture of 0.5 vol.% ammonia in N_2, are mixed and injected in the top of the reactor. The NO_2 is injected separately inside the reactor, approximately 50 mm above the catalyst. The NO_2 is either supplied from a gas bottle as a mixture of 1.0 vol.% NO_2 in N_2 by a mass-flow controller or from the NO_X generator described below.

The reactor consists of a glass tube, 6.35 mm in diameter with a bulb in the middle containing the catalytic bed. A thermocouple (1 mm in diameter) and a steel tube (1.6 mm) for NO_2 injection were inserted into the reactor inlet as shown in Fig. 2.

The glass reactor is placed in an oven and heated to the desired reaction temperature. The temperature in the different experiments was measured just above the bed, using the thermocouple in Fig. 2.

Ammonia was measured using a Bacharach AGMSZ ammonia gas monitor. The AGMSZ uses infrared light to measure the ammonia content in a gas in the range 2.5×10^{-3} to 1 vol.%. This instrument operates at room temperature and to avoid the condensation of water, which would interfere with the measurements, it was necessary to keep the moisture content in the gas below saturation pressure at room temperature during the experiment. The ammonia analyser uses a purging mechanism to reset the base value. A solenoid valve used to switch the inlet to fresh air rather than the measurement inlet. Purging is controlled by the analyser and typically occurs in 5–10-min intervals, depending on the ammonia concentration. The switching of the valve causes a temporary pressure build-up in the reactor. The effect of the purging can be seen in Fig. 8 as a small "bumps" in the ammonia signal. The disturbance in the signal is easily identified in the signal.

2.1. The catalysts

The experiments were performed on two different catalysts: $V_2O_5/WO_3/TiO_2$ and H-mordenite. The H-mordenite used was manufactured by Zeolysts with a Si/Al ratio of 21. The vanadium based catalyst was a commercial catalyst that contains $V_2O_5/WO_3/TiO_2$ but the exact composition is not known and permission to analyse the catalyst was not granted. The catalysts were chosen as example of the two types of SCR catalysts used industrially today, but also because of the differences in chemical composition, structures and difference in operating temperature. Because of this, it is possible they have different resistance to the reducing environment.

For SCR, the $V_2O_5/WO_3/TiO_2$ is usually operated in the temperature range 573–673 K and the H-mordenite above 623 K. Due to the higher activity of the vanadium based catalyst compared to the H-mordenite [27], different space velocities were used for each catalyst. The catalyst particle size was 0.16–0.18 mm.

All materials were analysed to detect any significant changes in their BET and Langmuir surface area before and after use, by measuring the adsorption of nitrogen at liquid nitrogen temperature with a Micromeritics ASAP 2400 instrument after degassing for 16 h at 623 K. Pore volume analysis was performed using the BJH method [28]. The desorption isotherm was used for the analysis and the results are presented in Table 1.

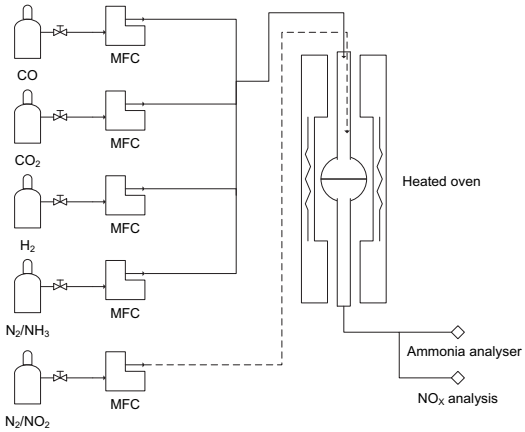

Fig. 1. Experimental set-up used for selective ammonia oxidation. In experiments employing only NO_X, the N_2/NH_3 is replaced by pure N_2.

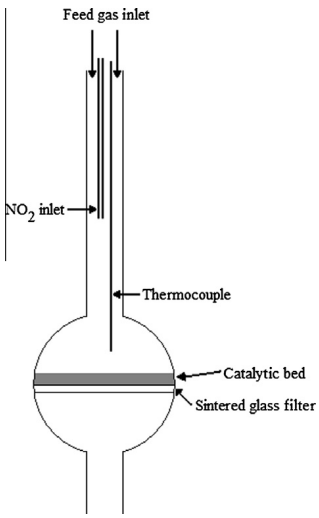

Fig. 2. Enlargement of the reactor inlet and catalytic bed.

2.2. NO_X reduction in model synthesis gas

In order to investigate whether nitrogen oxides were reduced over the catalysts, experiments were run without ammonia in the gas. The gas composition used is presented in Table 2 and is representative of the gas obtained after an air-blown gasifier, with the exception of water. Water/steam is normally a major component in synthesis gas, but due to the limitations the Bacharach AGMSZ ammonia gas monitor, water was excluded. Since the gas is explosive when mixed with air, a normal chemiluminescence NO_X meter could not be used, and the nitrogen oxide level was measured as a total NO_X level using two different Dräger short-term tubes ($2–100 \times 10^{-4}$ and 0.01–0.5 vol.% NO_X) [29]. These tubes are for total NO_X and do not indicate the ratio of NO_2/NO_X.

NO_X was measured at the reactor outlet when the reactor was empty, and when it was filled with each of the catalysts, $V_2O_5/WO_3/TiO_2$ or H-mordenite. At lower concentrations the accuracy for the 0.01–0.5 vol.% NO_X Dräger tubes was insufficient. The gas was sampled and diluted 20:1 and the lower range $2–100 \times 10^{-4}$ - vol.% Dräger tubes was used to give a more accurate reading. No NH_3 was present in the NO_X-only experiments and pure N_2 was used instead of the N_2/NH_3 mix.

Table 1
Results of the BET analysis for the catalysts used.

	Fresh $V_2O_5/WO_3/TiO_2$	Used $V_2O_5/WO_3/TiO_2$	Fresh H-mordenite	Used H-mordenite
BET surface area ($m^2\,g^{-1}$)	69	69	410	390
Langmuir surface area ($m^2\,g^{-1}$)	95	96	540	530
Desorption surface area of pores ($m^2\,g^{-1}$)	82	80	110	120
Micropore area ($m^2\,g^{-1}$)	5	7	320	300
Desorption volume of pores ($cm^3\,g^{-1}$)	0.26	0.26	0.30	0.30
Micropore volume ($cm^3\,g^{-1}$)	0.0016	0.0024	0.15	0.14
Average pore diameter (nm)	13	13	11	10

2.3. Ammonia oxidation in reducing environments

The effect of water in ordinary SCR is limited [19], but the lack of water in the gas will affect the equilibrium in some reactions

Table 2
Gas composition.

Component	Composition (vol.%)
N_2 or (N_2/NH_3)	65
CO_2	11
CO	13
H_2	11
NO_X	0.2
NH_3	0.2

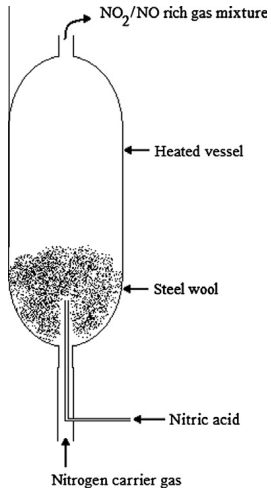

Fig. 3. The laboratory NO_X generator used to produce NO_2.

such as the Boudouard reaction (4) since the formed carbon will not be consumed by steam according to reaction (5).

$$2CO \leftrightarrow C + CO_2 \quad (4)$$

$$H_2O + C \leftrightarrow CO + H_2 \quad (5)$$

At the higher temperatures there was a lower ammonia start concentration which could indicate dissociation of ammonia according to the following reaction:

$$2NH_3 \rightarrow N_2 + H_2 \quad (6)$$

The NO_2 is injected as a mixture of NO_2 in N_2 containing 1 vol.% NO_2. The gas flow was 1.6 Ndm^3/min for the model synthesis gas and N_2/NO_2 contributed an additional 0.4–0.5 Ndm^3/min depending on stoichiometry between NH_3 and NO_2. The gas hourly space velocity for the $V_2O_5/WO_3/TiO_2$ catalysts was 210,000 h^{-1} and for the H-mordenite 75,000 h^{-1}.

2.4. NO_2 generation

In a full-scale plant, the NO_2 required for ammonia oxidation should be created on-site. A suggestion of a feasible process for this is the decomposition of nitric acid according to the following reaction:

$$4HNO_3 \rightarrow 4NO_2 + 2H_2O + O_2 \quad (7)$$

Nitric acid can also be reacted with copper or iron to form nitrogen oxides according to the following reactions [30]:

$$Fe + 4H^+ + NO_3^- \rightarrow Fe^{3+} + NO + 2H_2O \quad (8)$$

$$Fe + 6H^+ + 3NO_3^- \rightarrow Fe^{3+} + 3NO_2 + 3H_2O \quad (9)$$

It is commonly known that concentrated nitric acid yields high NO_2/NO_X ratios and that the reactions occur fast when heated. A small NO_X generator was constructed to test the feasibility of ammonia oxidation using NO_X generated on-site. The generator is illustrated in Fig. 3.

The NO_X generator consists of a stainless steel vessel, which is heated electrically. The temperature of the vessel was 503 K during the experiments. Nitric acid (65 wt.%) was injected into the vessel at a rate of 40 mm^3/min. If the assumption of 100% conversion from HNO_3 to NO_2 where true, it would roughly correspond to a stoichiometry of 1:2 for NH_3:NO_2. The NO_X generated by the NO_X generator was strongly coloured yellow to brown, indicating the presence of NO_2.

3. Results

3.1. NO_X reduction in the model synthesis gas

The results of NO_X reduction in synthesis gas without ammonia present are shown in Fig. 4. The reading error of the Dräger tubes was estimated to ±10% of the value. The error bars are given in Fig. 4.

As can be seen in Fig. 4, the homogenous gas phase reduction (empty reactor) of NO_2 to N_2 is slower than with a catalyst. The measurements show the total NO_X, the NO_2/NO_X ratio is not known. H-mordenite is more effective at reducing NO_X at temperatures above 573 K than the $V_2O_5/WO_3/TiO_2$ catalyst. At temperatures above 623 K, carbon deposits were formed on the thermocouple and on the catalyst surface. This was only observed when there was no NH_3 in the gas. The Boudouard reaction (4) is an equilibrium reaction that is dependent on temperature. The lack of water in the gas leads to the production of carbon, since the carbon formed is not consumed by the steam normally present in producer gas.

3.2. The SCR reaction in the model synthesis gas with bottled NO_2

Fig. 5 shows the result from a typical experiment using NO_2 from a gas bottle. The N_2/NO_2 was added to the stream when the ammonia concentration was just below 0.2 vol.%.

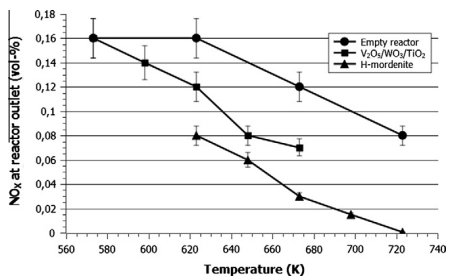

Fig. 4. NO_X levels with the empty reactor (●) and the two catalysts $V_2O_5/WO_3/TiO_2$ (■) and H-mordenite (▲) with an inlet NO_2 level of 0.2 vol.%.

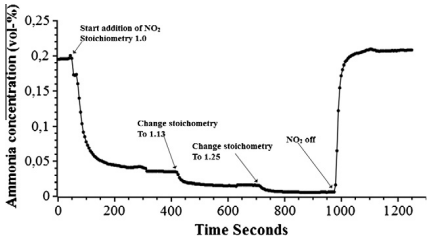

Fig. 5. Ammonia concentration at the outlet using the $V_2O_5/WO_3/TiO_2$ catalyst and bottled gas at 598 K.

Table 3
Calculated conversions of ammonia (molar ratio 1:1) with margins of error.

Temperature (K)	Conversion (%)	Margin of error (%)
573	76.2	0.1
598	83.6	0.2
623	83.1	0.1
648	77.5	0.1
673	54.3	0.4

When the injection of NO_2 starts, the ammonia concentration falls to a value of about 0.034 vol.%. The NH_3:NO_2 stoichiometry was increased to 1:1.125 and the outlet concentration falls to 0.015 vol.%. The final stoichiometry of 1:1.25 gives a gas with only 0.005 vol.% ammonia at the reactor outlet. The N_2/NO_2 injection is then turned off and the ammonia concentration increases to a value similar to the initial concentration.

When the IR-instrument stabilized on a plateau, there was very little variation in the ammonia signal. Approximately 15 measurements were collected for each plateau and the mean value and the margins of error at 95% confidence interval was calculated, with the free software Statcato [31], for each point. The maximum margin of error in the inlet molar ratio was 12×10^{-4} vol.% (2000×10^{-4} vol.% inlet) and 4×10^{-4} vol.% (961×10^{-4} vol.% out) in the outlet molar ratio for all points with the vanadium catalyst.

The conversion (Conv) of ammonia was calculated in the ordinary way as:

$$\mathrm{Conv} = (C_{in} - C_{out})/C_{in} \quad (10)$$

However, since the concentrations, or molar ratios, have margins of error, also the conversion will have a margin of error. This was calculated for each point with the error propagation formula [32]:

$$E_f = |df(x,y)/dx| * E_x + |df(x,y)/dy| * E_y \quad (11)$$

Here, E_f is the error of margin of the conversion, $|df(x, y)/dx|$ the partial differential of the conversion with respect to x (inlet molar ratio, if y is outlet molar ratio) and E_x the margin of error in parameter x. In this way the conversion and margin of error was calculated for the conversion, in Table 3 the results are shown for the run with equimolar ratio (1:1) of NH_3 and NO_X.

The maximum margin of error in the conversation at NH_3:NO_X 1:1 is less than 0.5% (54.3% conversion at 673 K). The margins of errors for the molar ratios of 1:1.125 and 1:1.25 for both vanadium and the mordenite catalyst are very similar.

Fig. 6 shows the conversion of NH_3 for the $V_2O_5/WO_3/TiO_2$ catalyst using bottled gas at different temperatures.

As can be seen in Fig. 6, conversion over the $V_2O_5/WO_3/TiO_2$ catalyst is high up to 623 K after which it starts to decline. The total

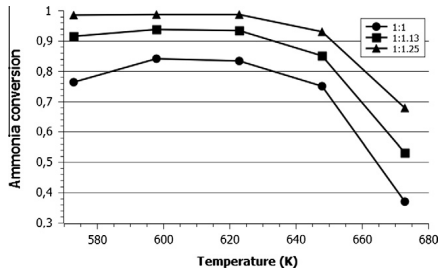

Fig. 6. Conversion of ammonia at different temperatures for three NH_3:NO_2 stoichiometries 1:1 (●), 1:1.125 (■) and 1:1.25 (▲) with the $V_2O_5/WO_3/TiO_2$ catalyst.

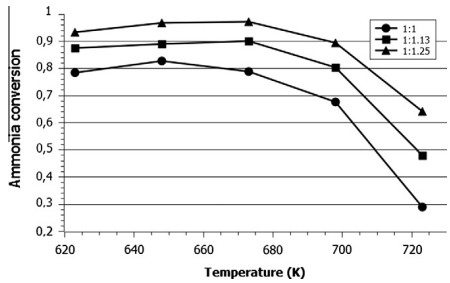

Fig. 7. Conversion of ammonia at different temperatures for three NH_3:NO_2 stoichiometries 1:1 (●), 1:1.125 (■) and 1:1.25 (▲) with the H-mordenite catalyst.

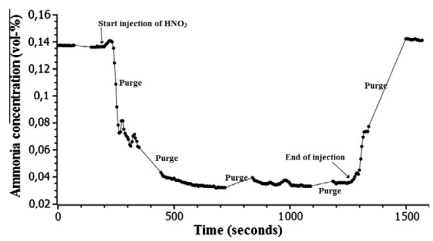

Fig. 8. Ammonia oxidation using NO_X generated from nitric acid.

amount of NO_X at the reactor outlet was measured at 623 K, and found to be to roughly 0.005 vol.% at a stoichiometry of 1:1, 0.005–0.01 vol.% at 1:1.125 and slightly above 0.01 vol.% at 1:1.25.

Fig. 7 shows the NH_3 conversion for the H-mordenite catalyst at different temperatures using bottled gas.

It can be seen by comparing Figs. 6 and 7 that the activity for H-mordenite is lower than the $V_2O_5/WO_3/TiO_2$ catalyst. The operating temperature of the H-mordenite catalyst is higher than for the $V_2O_5/WO_3/TiO_2$ catalyst and shows a peak in conversion at 673 K for the two higher stoichiometries. For the 1:1 stoichiometry the peak is at 648 K. NO_X was measured at the reactor outlet and

found to be approximately 0.001 vol.% at a stoichiometry of 1:1, 0.002 vol.% at 1:1.125 and 0.009 vol.% at a stoichiometry of 1:1.25 at a reactor temperature of 673 K.

3.3. Experiments with generated NO_X

The results of the ammonia oxidation experiment using NO_X generated from nitric acid are presented in Fig. 8. The experiment was run at 598 K using the $V_2O_5/WO_3/TiO_2$ catalyst.

Conversion using NO_X generated from nitric acid is somewhat lower than using the bottled gas at the same temperature as can be seen when comparing Figs. 8 and 5. The analyser purges discussed above are indicated in the figure.

4. Discussion

In this study it has been demonstrated that the concept of using NO_X to remove ammonia from synthesis gas produced from gasification is viable. Previous studies has shown that it is possible to remove ammonia from synthesis gas over a catalyst by injecting O_2, either alone or with NO, thus increasing the oxygen levels to a few vol.%. The increased oxygen level put those systems close to traditional SCR in terms of composition as it enables reaction (1). What has been shown here is a route that does not include O_2 which makes it a more efficient process, as less oxidation of the energy carriers (H_2 and CO) in the syngas occurs.

Hot gas ammonia removal is especially interesting for IGCC plants and plants using catalysts that are sensitive to ammonia such as those employed in methanol synthesis [33], FeCr water gas shift catalysts [34] and others, that may also be affected by ammonia. Apart from preventing catalyst poisoning, this method also has the benefit of not depositing all the ammonia in the scrubber liquid. If a catalytic converter is used for the conversion of tars and lower hydrocarbons, some of the ammonia will also be converted. Like hydrocarbon reforming, ammonia cracking over Ni-based catalysts is, sensitive to sulphur poisoning [35].

The fast SCR reaction must be much faster than the reduction of NO_X by H_2 and CO, in the gas phase and on the catalyst surface. A sufficient amount of the injected NO_X should survive in the gas long enough to react with the ammonia on the catalyst surface, without being converted into N_2. The NO/NO_X-ratio in the surviving portion should not exceed 50 vol.% to ensure that the reaction follows the fast SCR path.

Injecting an excess amount of NO_X into the gas to compensate for possible homogeneous or heterogeneous NO_X side-reduction by H_2 or CO prior the fast SCR step will not be a problem. An excess of NO_X in the gas also ensures a high degree of conversion of the adsorbed ammonia on the catalytic surface. If the residence time of the surplus NO_X in the hot gas is sufficiently long, it will be reduced to N_2.

However, it was not proven explicitly in this work that the ammonia was converted directly into nitrogen, since only total NO_X was measured. The only alternative product would be nitrous oxide (N_2O). Reducing conditions were used, with high concentrations of hydrogen and carbon monoxide, and several catalysts, for instance iron exchanged and natural zeolites, are known to either decompose or reduce N_2O with ammonia [36].

The reduction efficiency was lower using the NO_X generator than when using NO_2 from a gas bottle. The flow of NO_X from the generator was not as stable as that from the bottle, which was controlled by a mass flow controller, and there is thus a greater uncertainty in the amount injected. The gas provided by the generator will also contain some NO, and when the NO_X reaches the catalyst, the NO_2/NO_X ratio may be less favourable than in the case of pure NO_2. Another difference is that the NO_X provided by the generator also contains water. It was ensured that the amount was below the dew point at room temperature to avoid condensation in the sample lines and the ammonia analyser.

The lack, or the small amount, of water in the model gas used in these experiments is the main difference compared with a real synthesis gas, others being contaminants such as H_2S. The SCR reaction is not very dependent on the amount of water in the gas, and the activity and selectivity change only slightly [37]. However, the low water content had other effects, for example the deposition of elemental carbon on the metallic thermocouple and on the catalyst surface by the Boudouard reaction. This was, however, only observed when there was no ammonia in the system, indicating that the metal surface was blocked by ammonia preventing the formation of solid carbon.

The fresh vanadium catalyst was yellow in colour and became grey after use. There was little or no change in the BET surface area between the fresh and used vanadium-based catalyst, as can be seen from Table 1. The used H-mordenite catalyst showed a slightly smaller BET surface area (3.5%) and Langmuir surface area (2.8%) than the fresh. The conversion of ammonia was high for both SCR catalysts although they differ both chemically and structurally.

The model synthesis gas used here had high nitrogen content, resembling that produced by air-blown gasifiers. This also reduces the partial pressure of hydrogen. Higher partial pressures of hydrogen could increase the NO_2 reduction, necessitating higher stoichiometries between NO_X and NH_3.

5. Conclusions

Ammonia removal over traditional SCR catalysts in reducing environments by NO_2 injection has been shown to be a working concept using a model synthesis gas and two different kinds of catalysts and has several benefits compared to the traditional SCO using oxygen as oxidising agent. The lower amount of NO_2 required compared to oxygen is the most significant benefit as it reduces the oxidation of hydrogen that occurs with the addition of oxygen.

As NO_2 is only injected at stoichiometric amounts up to 1:1.25, or 0.05 vol.% above the ammonia level, only small amounts of hydrogen/carbon monoxide will be consumed by the homogeneous reduction of the remaining NO_X.

Injecting NO_2 into the gas will consume some hydrogen as NO_2 is reduced to NO, but the SCR reaction is very selective and the side reactions consume only marginal amounts of hydrogen. The selective oxidation of ammonia in a reducing environment such as a synthesis gas is not trivial, and care must be taken to limit the oxidation of hydrogen and carbon monoxide to preserve as much of the energy in the gas as possible.

The problem of generating the NO_2 must be addressed before large-scale oxidation of ammonia in synthesis gas can be undertaken. The experimental results show that NO_X generated in the lab was able to oxidise a considerable portion of the ammonia in the gas. The generated NO_X could contain some NO, as indicated by the higher amount of NO_X in the outgoing gas compared with the case using bottled N_2/NO_2.

It is well known that some SCR catalysts in oxidising environment, particularly catalysts using TiO_2 as support, are resistant towards or even promoted by, sulphur dioxide, SO_2, in the gas. Nevertheless, the catalysts are not necessarily resistant to hydrogen sulphide in reducing atmospheres.

Future work will include long-term testing of the catalysts in reducing environments to determine their stability and performance. The influence of water will also be investigated as will the effect of hydrogen sulphide.

In conclusion, the SCO system presented in this paper has been shown to be suitable for removing ammonia from a model synthesis gas, representing a gas produced from biomass, coal or other

hydrocarbon-containing feedstocks, except for the impurities found in those systems.

Acknowledgements

The authors gratefully thank financial support from the European Commission in the framework of the FP7 Integrated Project "GreenSyngas" (Project No. 213628). The authors also thank the Swedish Energy Agency (STEM), E.ON Sweden, Statoil, Göteborg Energi and Swedish Gas Center (SGC) for their financial support.

References

[1] Jukka L. Formation and behaviour of nitrogen compounds in an IGCC process. Bioresour Technol 1993;46(1–2):65–70.
[2] Sethuraman S, Huynh CV, Kong S-C. Producer gas composition and NO_x emissions from a pilot-scale biomass gasification and combustion system using feedstock with controlled nitrogen content. Energy Fuels 2011;25(2):813–22.
[3] Kurkela E, Staåhlberg P. Air gasification of peat, wood and brown coal in a pressurized fluidized-bed reactor. II. Formation of nitrogen compounds. Fuel Process Technol 1992;31(1):23–32.
[4] Ohtsuka Y et al. Recent progress in Japan on hot gas cleanup of hydrogen chloride, hydrogen sulfide and ammonia in coal-derived fuel gas. Powder Technol 2009;190(3):340–7.
[5] Zhou J et al. Release of fuel-bound nitrogen during biomass gasification. Ind Eng Chem Res 2000;39(3):626–34.
[6] Hepola J, Simell P. Sulphur poisoning of nickel-based hot gas cleaning catalysts in synthetic gasification gas: I. Effect of different process parameters. Appl Catal B 1997;14(3–4):287–303.
[7] Liang C et al. The role of copper species on Cu/γ-Al2O3 catalysts for NH_3–SCO reaction. Appl Surf Sci 2012;258(8):3738–43.
[8] Brandin JGM. Method and device for processing gases containing nitrogen. In: Office SP, editor. Sweden: Katator AB; 1996.
[9] Nassos S et al. The influence of Ni load and support material on catalysts for the selective catalytic oxidation of ammonia in gasified biomass. Appl Catal B 2007;74(1–2):92–102.
[10] Nassos S et al. Microemulsion-prepared Ni catalysts supported on cerium–lanthanum oxide for the selective catalytic oxidation of ammonia in gasified biomass. Appl Catal B 2006;64(1–2):96–102.
[11] Chang-Mao H. Characterization and performance of Pt–Pd–Rh cordierite monolith catalyst for selectivity catalytic oxidation of ammonia. J Hazard Mater 2010;180(1–3):561–5.
[12] de Boer M et al. Selective oxidation of ammonia to nitrogen over SiO_2-supported MoO_3 catalysts. Catal Today 1993;17(1–2):189–200.
[13] Duan K et al. Rare earth oxide modified Cu–Mn compounds supported on TiO_2 catalysts for low temperature selective catalytic oxidation of ammonia and in lean oxygen. Journal of rare earths 2010;28(Suppl. 1(0)):338–42.
[14] Song S, Jiang S. Selective catalytic oxidation of ammonia to nitrogen over CuO/CNTs: the promoting effect of the defects of CNTs on the catalytic activity and selectivity. Appl Catal B 2012;117–118:346–50.
[15] Xu C et al. Recent advances in catalysts for hot-gas removal of tar and NH_3 from biomass gasification. Fuel 2010;89(8):1784–95.
[16] Leppälahti J, Kilpinen P, Hupa M. Selective catalytic oxidation of NH_3 in gasification gas. 3. Experiments at elevated pressure. Energy Fuels 1998;12(4):758–66.
[17] Skalska K, Miller JS, Ledakowicz S. Trends in NO_x abatement: a review. Sci Total Environ 2010;408(19):3976–89.
[18] Busca G et al. Chemical and mechanistic aspects of the selective catalytic reduction of NO_x by ammonia over oxide catalysts: a review. Appl Catal B 1998;18(1–2):1–36.
[19] Gabrielsson PLT. Urea–SCR in automotive applications. Top Catal 2004;28(1):177–84.
[20] Chen L, Li J, Ge M. The poisoning effect of alkali metals doping over nano V_2O_5–WO_3/TiO_2 catalysts on selective catalytic reduction of NO_x by NH_3. Chem Eng J 2011;170(2–3):531–7.
[21] Ramachandran B et al. Testing zeolite SCR catalysts under protocol conditions for NO_x abatement from stationary emission sources. Catal Today 2000;55(3):281–90.
[22] Brandin JGM, Andersson LAH, Odenbrand CUI. Catalytic reduction of nitrogen oxides on mordenite some aspect on the mechanism. Catal Today 1989;4(2):187–203.
[23] Leppälahti J. Process for removing ammonia from gasification gas. In: Office SP, editor. Sweden Patent: Valtion Teknillinen Tutkimuskeskus (VTT); 1996.
[24] Olympiou GG, Efstathiou AM. Industrial NO_x control via H_2–SCR on a novel supported-Pt nanocatalyst. Chem Eng J 2011;170(2–3):424–32.
[25] Macleod N, Lambert RM. Lean NO_x reduction with CO + H_2 mixtures over Pt/Al_2O_3 and Pd/Al_2O_3 catalysts. Appl Catal B 2002;35(4):269–79.
[26] Yang S et al. An investigation of the surface intermediates of H_2–SCR of NO_x over Pt/H–FER. Appl Catal B 2011;107(3–4):380–5.
[27] Brandin JGM, Hulteberg CP, Odenbrand CUI. High-temperature and high-concentration SCR of NO with NH_3: application in a CCS process for removal of carbon dioxide. Chem Eng J 2012;191:218–27.
[28] Barrett EP, Joyner LG, Halenda PP. The determination of pore volume and area distributions in porous substances. I. Computations from nitrogen isotherms. J Am Chem Soc 1951;73(1):373–80.
[29] Dräger; 2012. <http://www.draeger.com/>.
[30] Karlsson HT et al. Control of NO_x in steel pickling. Environ Prog 1984;3(1):40–3.
[31] Statco; 2012. <http://www.statcato.com/statcato>.
[32] Pohl P. Grundkurs i numeriska metoder (Swedish). Stockholm (Sweden): Liber Stockholm AB; 2005.
[33] Spath PL, Dayton DC. Preliminary screening – technical and economic assessment of synthesis gas to fuels and chemicals with emphasis on the potential for biomass-derived syngas. NREL Technical Report 510-34929, 22 April 2004.
[34] Hepola J, Simell P. Sulfur poisoning of nickel-based hot gas cleaning catalysts in synthetic gasification gas. In: Bartholomew CH, Fuentes GA, editors. Studies in surface science and catalysis. Elsevier; 1997. p. 471–8.
[35] Torres W, Pansare SS, Goodwin JG. Hot gas removal of tars, ammonia, and hydrogen sulfide from biomass gasification gas. Catal Rev 2007;49(4):407–56.
[36] Ozawa Y, Tochihara Y. Catalytic decomposition of ammonia in simulated coal-derived gas over supported nickel catalysts. Catal Today 2011;164(1):528–32.
[37] Darvell LI et al. An investigation of alumina-supported catalysts for the selective catalytic oxidation of ammonia in biomass gasification. Catal Today 2003;81(4):681–92.

Paper V

Techno-Economic Assessment of Non-Fossil Ammonia Production

Authors: Per Tunå[a,*], Christian Hulteberg[a], Serina Ahlgren[b]

a) Department of Chemical Engineering, Faculty of Engineering, Lund University
b) Dep of Energy and Technology, Swedish University of Agricultural Sciences
* Corresponding author. Email: per.tuna@chemeng.lth.se, Phone (+46) 46 222 88 82, Fax (+46) 46 14 91 56

Keywords: Ammonia production; non-fossil based; exergy evaluation; production cost

1 Introduction

Nitrogen fertilisers are used in agriculture to obtain higher yields of agricultural crops. Large-scale use of synthetic nitrogen fertilisers began after Second World War and it is estimated that about one third of the protein in humanity's diet depends on mineral nitrogen fertiliser (Smil, 2004). The use of nitrogen fertilisers is also predicted to increase in the future due to population growth, increased consumption of meat and increased use of biofuels (Erisman et al., 2008; Smeets & Faaij, 2005).

Nitrogen gas accounts for 78% of the volume of our atmosphere, however converting it into a form that is useful for agriculture costs energy. At present, the production of nitrogen fertiliser accounts for 1.2% of global primary energy demand ((IFA), 2009b). All commercially produced nitrogen fertilisers (e.g. urea and ammonium nitrate) use ammonia as raw material. Anhydrous ammonia can also be injected straight into soils, a method extensively used in the US. Around 79 % of the globally produced ammonia is used to produce different types of nitrogen fertilizers, 3% is directly used as fertilizers, and 10% of the ammonia is used in

other sectors. Ammonia is produced in the Haber-Bosch process, according to the overall reaction (1).

$$N_2 + 3H_2 \leftrightarrow 2\ NH_3 \qquad (1)$$

While nitrogen is supplied from ambient air, it is the production of the hydrogen that requires the majority of the energy input. Production of the required hydrogen is most commonly based on reforming of natural gas, but gasification of coal and heavy oil also occurs. In the long run, this is not a sustainable solution for production, as fossil fuels are a finite energy source.

The energy requirement for ammonia production has dramatically decreased over time from about 55 GJ/metric tonne of ammonia produced in the 1950s to 35 GJ/tonne in the 1970s, while nowadays the best plants using natural gas as feedstock need only 28 GJ/tonne (Smil, 2004). There are however large variations: in China coal is commonly used and the estimated average energy use is 59 GJ/metric tonne of ammonia (Kahrl et al., 2010). According to the International Fertilizer Industry Association about 67% of global ammonia production is based on natural gas, 27% on coal while fuel oil and naphtha account for 5% ((IFA), 2009b). Since a number of old plants are still in operation, the global average energy requirement was in 2008 around 37 GJ/ tonne ammonia (ranging from 27-58 GJ/tonne NH3) ((IFA), 2009a).

On a global scale, the production of nitrogen fertilisers is calculated to represent about 1% of anthropogenic greenhouse gas (GHG) emissions ((IFA), 2009b). On a product level, the production of nitrogen fertilisers can have a large impact, e.g. when calculating the carbon footprint of food and biofuel. For example in a recent study (Börjesson & Tufvesson, 2011), nitrogen fertilisers were found to represent between 3-26% of the total GHG emissions from wheat based ethanol production. For rapeseed biodiesel, the nitrogen fertiliser production represented up to 29% of the GHG emissions.

However, the hydrogen needed for ammonia production in the Haber-Bosch synthesis can also be produced from renewable resources. This opens up possibilities for a more sustainable production of food, feed, fibres and fuels. The

concept of renewable based fertiliser production was already considered as an option during the oil crisis in the 1970s and 1980s, as a way of reducing the dependency on fossil oil; techno-economic studies were e.g. carried out on electrolysis-based ammonia production (Dubey, 1978; Grundt & Christiansen, 1982), and a plant for producing ammonia from peat was erected in Finland (Koljonen & Sodervall, 1991). At present, ammonia production based on renewables is becoming interesting again, as a means to both reduce fossil fuel dependency and to reduce GHG emissions. In Minnesota, USA, a plant is currently being commissioned that will produce 1 tonne per day ammonia in a Haber-Bosch synthesis reactor, the hydrogen needed for the synthesis is derived from wind-powered electrolysis (Dispatch, 2012). Further, several life cycle assessment studies have been carried out in Sweden (Ahlgren et al., 2008; Ahlgren et al., 2012; Ahlgren et al., 2010).

There are several parameters that are of interest to quantify with respect to production of ammonia from non-fossil sources. For example the potential amount of ammonia that can be produced from different systems, the investment and production costs, the energy requirement and greenhouse gas emissions. Some of these have been treated in the previous studies mentioned, but there is a need for more research especially concerning the costs. Furthermore, water consumption and wastewater production have not previously been investigated.

The aim of this study was to perform a techno-economic study of a number of promising ammonia production systems based on renewable energy. Different technologies and scales of production were investigated. The studied technologies for hydrogen generation followed by subsequent ammonia synthesis were:

1. Electrolysis of water using renewable electricity
2. Steam reforming of biogas from anaerobic digestion
3. Biomass gasification

The heat and mass balances as well as production costs were calculated for each scenario. Monte Carlo simulations have been used for assessing the sensitivity of the production costs. The results are expected to be useful for further research and could also serve as basis for planning for future production facilities.

2 Materials and methods

2.1 Modelling of the technical systems

The different cases were evaluated by flow sheeting calculations from raw material to product. The models for fuel synthesis were performed in AspenTech's Aspen Plus 7.3.2 and the gasifier was modelled as an energy/material balance. As the raw material differs, different processing equipments are required. Electrolysis requires almost no processing equipment upstream of the ammonia synthesis. Gasification of woody biomass requires a gasifier, particle and contaminants removal. Furthermore, biogas and gasification requires reformers, water-gas shift reactors, CO_2 capture equipment and a methanation reactor to process the gas before the ammonia synthesis; overview process flow diagrams for the technologies are depicted in Figure 1a-c.

Please insert figure 1a here

Please insert figure 1b here

Please insert figure 1c here

The electrolysis was modelled in Aspen Plus as a yield reactor coupled with a calculator block to calculate the necessary electric power draw. As pure hydrogen is produced in the electrolyser, no downstream purification is necessary only the addition of nitrogen. A PSA was modelled as a separator block to provide enriched nitrogen (95% pure). The excess oxygen was reduced to water by hydrogen in a catalytic burner. The water in the hydrogen/nitrogen stream was removed prior to ammonia synthesis.

A steam reformer (SR) is usually used before an auto thermal reformer or secondary reformer (ATR) when producing hydrogen for ammonia synthesis (Satterfield, 1996). The ATR is either oxygen enriched or air-blown to provide the nitrogen necessary to reach a H_2:N_2 ratio of 3:1 prior to synthesis. The reformers were modelled as Gibbs free energy reactors. The steam reformer is externally

heated by burning part of the feed. The burner was modelled as a combustion reactor in Aspen Plus, setup to provide the energy required in the steam reformer. Temperature in the steam reformer was set to 800 °C and with a pressure drop of one bar. The same pressure drop was assumed for the ATR. The ATR was fed with air through a compressor and with sufficient quantity to reach an outlet temperature of 1050 °C. The air compressor was modelled as a multistage compressor with four stages with intercooling to 70 °C and an isentropic efficiency of 0.72.

After reforming, the gas contains H_2, CO, CO_2, N_2 and H_2O. CO and CO_2 are poisons for the ammonia catalyst and CO contains energy that can be used to convert H_2O to H_2 in the water-gas shift reaction (2).

$$CO + H_2O \leftrightarrow CO_2 + H_2 \qquad (2)$$

The water-gas shift reaction is an equilibrium reaction that is pushed towards H2 at low temperature. In order to achieve maximum H2 content in the gas, two water-gas shift reactors are required, a high temperature and a low temperature. The reactors were modeled in Aspen Plus as equilibrium reactors operating adiabatically with outlet temperatures of 450 and 220 °C respectively (Satterfield, 1996).

After the second water-gas shift reactor, the gas contains only trace amounts of CO and most of the carbon in the gas is available as CO_2. 97 % of the CO_2 is removed in a PSA modeled in Aspen as a separator block. As both CO and CO_2 are poisons for the ammonia catalyst, both components needs to be removed. Removal of carbon oxides is achieved by methanation (reactions 3 and 4) in a methanation reactor (Jennings, 1991).

$$3H_2 + CO \leftrightarrow CH_4 + H_2O \qquad (3)$$

$$4H_2 + CO_2 \leftrightarrow CH_4 + 2H_2O \qquad (4)$$

The methanation reactor was modelled as an adiabatic equilibrium reactor operating with an inlet temperature of 200 °C. Complete removal of carbon oxides are achieved while consuming about 6 % of the H_2 in the gas.

Compression of the H_2/N_2 mixture was performed in a multistage compressor with 70 °C intercooling between each step and an isentropic efficiency of 0.72. Recirculation compression was performed in a single stage compressor with an isentropic efficiency of 0.72.

Ammonia synthesis was modelled as three adiabatic reactors with recirculation. Pressure drop was set to 3 bar and inlet temperature was set to 427 °C for each reactor. Usable excess heat, for use in a for example a district heating grid, was set to be available at levels down to 70 °C (Jennings, 1991).

Gasification was not modelled in Aspen Plus, instead the material and energy balance for the Carbona/Andritz gasifier was used. The inlet stream in the gasifier model flow sheet was the producer gas from the gasifier minus particulates. The producer gas composition is listed in Table 1.

Please insert table 1 here

A total of five different scenarios were evaluated: 1 and 3 MW electric power input for electrolysis, 5 and 10 MW biogas and 50 MW biomass input to the gasifier. For the smaller scale of the studied systems, a steam cycle for internal electricity production would be too costly. Therefore, electricity needed for compression and utilities, for the gasifier and biogas routes, were assumed to be purchased externally.

2.2 Energy assessment

When using mixed energy carriers, first law of thermodynamics efficiency calculations are helpful but not necessarily an appropriate indicator of the "best" system as it do not take into account the exergy of the various energy sources. The electricity equivalents method is therefore used in this paper to represent the overall exergy of the system and they are calculated using power generation efficiencies

(Larson et al., 2006), using the best available technology to the knowledge of the author's, see Table 2. This allows for a comparison on an equal basis for all systems. To exemplify, the energy input needed for producing one tonne of ammonia would be calculated by determining the amount of electricity equivalents that are fed to the system, in the form of biomass, biogas and electricity and thus yield a comparable number based on the exergy content.

Please insert table 2 here

2.3 Economic assessment

The investment-cost assessment has been performed by using factor methods from various sources. The heat and mass balances determined from the Aspen simulations have been used to do detail-dimensioning of the process equipment. To the total bare-module cost, 18% contingency and 30% auxiliary has been added giving the overall investment cost; the estimate is believed to be within ±30%. Thereafter the cost-of-production of the ammonia is determined. In Table 3 some key parameters for the financial modeling are listed; for more information on detail-dimensioning please view (Hulteberg, 2007; Hulteberg & Karlsson, 2009).

Please insert table 3 here

The production cost is determined and analysed using Monte Carlo simulations. The simulations constitute 10,000 cases and have been performed using a Beta-PERT distribution function which has a density function (Vose, 2008):

$$f(x) = \left[\frac{x^{v-1}(1-x)^{w-1}}{B(v,w)}\right] \; 0 \le x \le 1 \; ; 0 \text{ otherwise}$$

Where B(v,w) is the beta function:

$$B(v,w) \equiv \int_0^1 t^{v-1}(1-t)^{w-1}dt$$

And the distribution function:

$$F(x) = \frac{B_x(v,w)}{B(v,w)}\ 0 \le x \le 1; 0\ \text{otherwise}$$

Where Bx(v,w) is the incomplete beta function :

$$B(v,w) \equiv \int_0^x t^{v-1}(1-t)^{w-1}dt$$

Typically, sampling from the beta distrubution required minimum and maximum values and two shape parameters (v,w) and a scale parameter which is set to 4 giving. The mean μ is calculated as:

$$\mu = \frac{\left(x_{min} + x_{max} + \lambda * x_{most\ likely}\right)}{(\lambda + 2)}$$

and used to calculate the v and w shape parameters:

$$v = \frac{(\mu - x_{min})\left(2 * x_{most\ likely} - x_{min} - x_{max}\right)}{\left(x_{most\ likely} - \mu\right)(x_{max} - x_{min})}$$

$$w = \frac{v(x_{max} - \mu)}{(\mu - x_{min})}$$

A number of initial values were chosen and these were used as most likely in the Beta-PERT distribution. For each case examined, the minimum production cost, the maximum production cost, the mean production cost and the production cost distribution is determined. The maximum, minimum and most likely values are listed in Table 4.

Please insert table 4 here

3 Results

3.1 Heat and mass balances

The simulation results for energy and water consumption for the different ammonia systems are summarized in Table 5.

Please insert table 5 here

All systems require electric power for compression and auxiliaries. Biomass gasification requires more energy input than the other and the reason is the costly pre-treatment requirement of biomass gasification and the oxygen production. Oxygen production and compression are the most energy intense parts of the gasification system, 4 MW of electric power was required for oxygen production and 3.5 MW for compression.

Biogas as an energy source is a promising alternative to the natural gas used for conventional ammonia synthesis. The simulations results points to a lower electric power demand per tonne than the other two alternatives. The biogas system uses only air for the reformers but still required some 1.0 MW of electric power for compression at the 10 MW scale.

Please insert table 6 here

When using electric power as energy source, roughly 2,000 metric tonnes can be produced by the 3 MW electric input as can be seen in Table 6 at an input of about 43 GJel equ./tonne. At the same time, some 0.46 MW of heat is available for district heating. For the 10 MW electric input case almost 6,800 metric tonnes of ammonia can be produced per year at an input of about 43 GJel equ./tonne and making 1.52 MW of district heat available. The 3 MW electric input scales more or less linearly with the 10 MW input. There is no water knock-out for electrolysis and as a result no wastewater is produced. The water consumption for electrolysis ammonia is roughly 2 tonnes of water per tonne ammonia produced.

At 10 MW (5.8 MWel equ) biogas input, the system requires 1 MW of electric power which totals 6.8 MWel equ.. The overall production of ammonia in this case is 7,480 tonnes per year at 26 GJel equ../tonne; this scale, 3.0 MW heat is available for district heating. The water consumption for the biogas system is higher than the other two systems at 2.8 tonnes water per tonne ammonia produced. Wastewater production from the biogas systems are roughly 2 tonnes per produced tonne of ammonia. The 5 MW biogas input system requires 0.5 MW of electric power giving a total of 3.4 MWel equ. input and produces 3,750 tonnes of ammonia at 26 GJel equ../tonne.

The last studied case is the 50 MW input biomass gasification plant. When comparing the production volume and the energy requirements for the gasification route with those for biogas and electrolysis, it is clear that the gasification requires more energy per produced tonne ammonia than the other technologies (58 GJ compared to 42 GJ per tonne ammonia). However when comparing the energy consumption on an electricity-equivalent basis the biomass gasifier show quite low numbers: 31 GJ/tonne. The water consumption for the gasification plant was lower than for the biogas plant at 2.1 tonne water per produced tonne ammonia. The 50 MW gasification plant produces 14.6 MW of heat that could be utilised for district heating. Wastewater production for the gasification plant was the same as for biogas at 2 tonnes of wastewater per tonne of produced ammonia.

3.2 Economic evaluation

Based on the heat and mass balances presented above, a detailed design of the process equipment may be performed. This has been done for all five cases and results in an overall grass-root investment cost; the results from the analysis are reported in Table 7. With respect to the overall investment cost, the biomass gasification plant is the one with the highest overall investment cost with M$117. However, when looking at the relative investment cost per produced tonne per annum it ranks as number 3 out of the selected cases. The highest investment cost equipment (installed) is the syngas compressor (k$22,632), CO2 separation (k$14,066) and dryer (k$10,101). The biogas-based ammonia synthesis show the lowest relative investment costs with k$3.7 per produced tonne per annum in the 5

MW case and k$3.1 per produced tonne per annum in the 10 MW case. The overall investment is dominated by the CO2 separation (21% and 20% in the 5 MW and 10 MW cases) and the syngas compressor (17% and 22% in the 5 MW and 10 MW cases). The investment cost of the electrolyser systems are dominated by the electrolysers and syngas compressors (23% and 23% in the 3 MW case and 26% and 22% in the 10 MW case). This clearly shows that there is an economy-of-scale effect in the syngas compressor (and the rest of the process equipment for that matter) which is not mirrored in the electrolysis investment.

Please insert table 7 here

Looking at the production costs, there is quite a large span in the production costs between the various technologies. The lowest production cost is found for the biomass gasification case with a mean value of $970/tonne. In this case the variance between the lowest and highest cases is $666/tonne, which is the lowest variance of the cases investigated. In the case of biogas-based production, despite the relatively low investment cost, the ammonia production cost becomes quite high due to the high biogas cost. The mean production cost is $1,671/tonne in the 5 MW case and $1,594/tonne in the 10 MW case. This also shows that there is little influence of the cost-of-production with the increase in scale, which is due to the high percentage of operating cost for the biogas cases (81% and 77% for 5 MW and 10 MW respectively); the high operating cost also indicate that if feedstock production comes down in price, significantly lower costs may be achieved in ammonia synthesis. The same is true in the electrolysis case, where about 30-40% is fixed costs. However, the production cost is even higher in this case compared to the biogas case with averages of $1,725/tonne and $1,640/tonne for 3 MW and 10 MW respectively. The variance in the production cost over the 10,000 Monte Carlo simulations is also larger in the cases using electrolysis compared to the biogas cases; the variances are summarised in Figure 2 for all the cases.

Please insert figure 2 here

4 Discussion

Since natural gas at present is the dominating feedstock, the ammonia price is related to the natural gas price which in turn is also related to the oil price (Pettersen et al., 2010). Abram and Forster (Abram & Forster, 2005) suggest that feedstock makes up around 90% of ammonia production costs. However, it can also be argued that variations in grain prices also influence the nitrogen prices (as previously mentioned, 79% of globally produced ammonia is used for fertilizer production); the higher the crop value is, the more willing the farmer is to pay for the fertilizer. According to the fertilizer producer Yara (2012), approximately 50% of the variations in the urea price can be explained by grain price fluctuations. The driver for grain prices is in turn dependent on many factors e.g. global income growth, biofuels mandates, high petroleum prices, droughts, declining storage reserves (Wright, 2012). This makes any predictions on the future evolvement on ammonia and nitrogen fertilizer prices very challenging.

The US market price for ammonia was on average $ 976 per metric tonne ammonia in January 2013 (Agriculture, 2013), equivalent to $ 1,185 per metric tonne pure nitrogen. In 2008 the ammonia prices peaked and then went down, but have during the last years steadily been rising and are now at around the same level as 2008 (Fertecon, 2013). This means that in the studied scenarios, only the gasification case has a mean production cost in the same vicinity as natural gas based ammonia. It can however be expected that in the future natural gas will be more expensive, which could make nitrogen based on renewables more competitive. Another aspect that should be mentioned is the fact that the costs reported above are free on board Gulf Coast and does not include transport. A more localized production may tolerate a slightly higher cost-of-production due to lower transport costs as well as security of supply aspects. However the future competiveness of ammonia from non-fossil sources is also dependent on the development of food prices; as previously mentioned higher grain prices gives larger willingness to pay for inputs in agriculture.

Looking at the energy input required for producing one tonne of ammonia there are significant differences between the technologies. When only comparing on energy input basis, the electrolysis paths and the biogas pathways have about the same energy input (42 GJ/tonne ammonia). However when changing the basis of comparison to electricity equivalents, better reflecting the exergy use, the numbers differ significantly (42 GJel equ. to 26 GJel equ. per tonne of ammonia). The highest energy consumption is when using biomass gasification, most likely because a more difficult conversion of the solid feedstock, with 58 GJ/tonne or 31 GJel equ.. per tonne of ammonia. The energy consumption in the investigated cases is higher than the industrial average (37 GJ or 21 GJel equ. per tonne of ammonia) both with respect to the energy and exergy use and much higher than the current best-available-technology (28 GJ or 16 GJel equ. per tonne of ammonia). This is most likely due both to the chosen method of production and economy-of-scale effects.

There are significant differences in the above investigated technologies and these are clearly reflected in the varying demand of fresh water, wastewater, energy input and suitable scale of production. An individual assessment will have to be performed from case to case when considering which technology to choose based on the water supply, energy situation, ability to get rid of wastewater etc. to end up with the best solution for each case. An argument for the production of ammonia and nitrogen fertilizers is the potential to reduce fossil energy use and greenhouse gas emissions from agriculture. In a study by Ahlgren et al. (Ahlgren et al., 2012) the production of nitrogen fertilizers from biomass via electrolysis and gasification was studied in a life cycle assessment. The results showed that using this bio-based nitrogen in e.g. rape seed production could lower the emissions from cultivation with up to 46%. This could further have implications for the GHG balance of biodiesel in which the cultivation emissions often constitute a major part. As of today there are no governmental incentives for producing renewable fertilizers, however there may be a spill-over effect from the production of biofuels. As the requirements for CO_2 emission reduction are increasing for qualifying as a biofuel, the ability to pay a premium for a low-emitting fertilizer will increase.

In many countries, ammonia is not used directly as a fertilizer. Instead ammonia is converted to ammonium nitrates or urea and applied to the fields as a solid

granulate. This means that the production costs calculated in this paper is not directly comparable to fertilizer prices in these regions. It is however interesting to note that the price trend for ammonium nitrate and urea seems to follow the ammonia price. One geography where such granulate is used as a fertilizer is Sweden, where prices in January 2013 was around $ 2,000 per metric tonne nitrogen, in the form of ammonium nitrate (ATL, 2013) (to be compared to $1,185 for ammonia). As the granulate price is higher than the ammonia price, an interesting continuation of this paper would be to study the cost of conversion of ammonia to ammonium nitrate or urea. Another interesting continuation would be to look into the infrastructure in Sweden, to see if it would be possible to introduce anhydrous ammonia, or ammonia dissolved in water (ammonia hydroxide). This would save costs for further conversions of the ammonia and also save emissions of nitrous oxides that are formed during ammonium nitrate production. In the neighbouring country Denmark, it is more common to use anhydrous ammonia or nitrogen solutions, approximately representing 3 and 10% of the total nitrogen fertilizer use in 2010 (2013b).

To give a reference point, around 170,000 tonnes of fossil-based nitrogen in straight and compound fertilisers are used every year in Swedish agriculture, and the arable land is 2.6 Mha (Wahlstedt, 2012). The average application of nitrogen is 65 kg N/ha, but the amount of nitrogen varies greatly between fields and crops. During the cropping season 2010/11 the average application to winter wheat was 149 kg N/ha. In the studied scenarios between 2,030 and 28,700 tonne ammonia was assumed to be produced per year. This is enough nitrogen to replace some 1% to 17% of the ammonia used in Sweden or fertilize between 11,000 and 158,600 hectares of winter wheat depending on choice of technology. When assessing the risk of constructing a plant for ammonia production however, the relatively high absolute investment cost in the gasification case may be prohibiting for investment. In that case, the more modular electrolyser-based production comes across as more attractive, despite the higher production cost. This is however a consideration that has to be done on a case to case basis and an individual risk assessment should be the basis of the investment case.

5 Conclusions

Based on the investigation presented above, it can be concluded that production of ammonia from non-fossil sources is possible but not competitive with fossil-based production with respect to cost, perhaps with the exemption of biomass gasification. This can be explained by economy-of-scale effects as well as the lower feedstock cost. There are also significant differences in the exergy use for producing one tonne of ammonia depending on what method is chosen, with biogas-based production showing the lowest values and electrolysis the highest; both values are however higher than the current industrial average. There is however other benefits to non-fossil based production of ammonia, such as security of supply and lower transportation costs. Which technology to choose out of the investigated three will have to be decided upon a case-to-case basis, weighting risk and reward for each case given the local conditions.

6 References

2013a. Bureau of Labor Statisticst, Vol. 2013.

2013b. International Fertilizer Industry Association Statistics Database.

2012. Yara Fertilizer Industry Handbook, (Ed.) Yara, pp. 91.

(IFA), I.F.I.A. 2009a. Energy Efficiency and CO2 Emissions in Ammonia Production

2008-2009 Summary Report.

(IFA), I.F.I.A. 2009b. FERTILIZERS AND CLIMATE CHANGE

Enhancing Agricultural Productivity and Reducing Emissions.

Abram, A., Forster, D.L. 2005. A primer on ammonia, nitrogen fertilizers, and natural gas markets. AEDE-RP-0053-05.

Agriculture, U.S.D.o. 2013. Agricultural Marketing Service. Market News

Ahlgren, S., Baky, A., Bernesson, S., Nordberg, Å., Norén, O., Hansson, P.-A. 2008. Ammonium nitrate fertiliser production based on biomass – Environmental effects from a life cycle perspective. *Bioresource Technology*, **99**(17), 8034-8041.

Ahlgren, S., Baky, A., Bernesson, S., Nordberg, Å., Norén, O., Hansson, P.-A. 2012. Consequential Life Cycle Assessment of Nitrogen Fertilisers Based on Biomass – a Swedish perspective. *Insciences Journal, Climate Change*, **2**(4), 80-101.

Ahlgren, S., Bernesson, S., Nordberg, Å., Hansson, P.-A. 2010. Nitrogen fertiliser production based on biogas – Energy input, environmental impact and land use. *Bioresource Technology*, **101**(18), 7181-7184.

ATL. 2013.

Berglund, P., Bohman, M., Svensson, M., Benjaminsson, J. 2012. Teknisk och ekonomisk utvärdering av lantbruksbaserad fordonsgasproduktion. Swedich Gas Technical Centre.

Börjesson, P., Tufvesson, L.M. 2011. Agricultural crop-based biofuels – resource efficiency and environmental performance including direct land use changes. *Journal of Cleaner Production*, **19**(2–3), 108-120.

Dispatch, B. 2012. Ag & Energy Expo explores producing fertilizer from wind, Brainerd Dispatch. Brainerd Dispatch.

Dubey, M. 1978. Technical and economic feasibility of making fertilizer from wind energy, water, and air. in: Sun, Mankind's future source of energy. *International Solar Energy Society Congress*, January, 1978, New Delhi, India. pp. 1812-1821.

Erisman, J.W., Sutton, M.A., Galloway, J., Klimont, Z., Winiwarter, W. 2008. How a century of ammonia synthesis changed the world. *Nature Geosci*, **1**(10), 636-639.

Fertecon. 2013. Ammonia Report, weekly review of the ammonia market.

Grundt, T., Christiansen, K. 1982. Hydrogen by water electrolysis as basis for small scale ammonia production. A comparison with hydrocarbon based technologies. *International Journal of Hydrogen Energy*, **7**(3), 247-257.

Hulteberg, P.C. 2007. Hydrogen, an Energy Carrier of the Future. in: *Chemical Engineering*, Vol. Ph.D., Lund University. Lund.

Hulteberg, P.C., Karlsson, H.T. 2009. A study of combined biomass gasification and electrolysis for hydrogen production. *International Journal of Hydrogen Energy*, **34**(2), 772-782.

Jennings, J.R. 1991. *Catalytic Ammonia Synthesis: Fundamentals and Practice*. Plenum Press.

Kahrl, F., Li, Y., Su, Y., Tennigkeit, T., Wilkes, A., Xu, J. 2010. Greenhouse gas emissions from nitrogen fertilizer use in China. *Environmental Science & Policy*, **13**(8), 688-694.

Koljonen, J., Sodervall, T. 1991. Synthesis gas from peat; A Finnish peat ammonia venture. *Journal Name: Energy Sources (New York); (USA); Journal Volume: 13:1*, Medium: X; Size: Pages: 95-103.

Larson, E.D., Consonni, S., Katofsky, R.E., Iisa, K., Fredrick Jr., W.J. 2006. A Cost-Benefit Assessment of Gasification-Based Biorefining in the Kraft Pulp and Paper Industry. Princeton Environmental Institute. DE-FC26-04NT42260.

Lundgren, J., Ekbom, T., Hulteberg, P.C., Larsson, M., Grip, C.-E., Nilsson, L., Tunå, P. 2013. Methanol production from steel-work off-gases and biomass based synthesis gas. *Applied Energy*, **Accepted for publication DOI:10.1016/j.apenergy.2013.03.010**.

Pettersen, I., Hval, J.N., Vasaasen, A., Alnes, P.K. 2010. Globalt marked med nasjonale særpreg – Utredning om konkurransen i de nordiske mineralgjødselmarkeder. NILF-rapport 2010-1.

Satterfield, C.N. 1996. *Heterogeneous Catalysis in Industrial Practice*. *Second ed*. Krieger Publishing Company, Malabar.

Seider, W.D., Seader, J.D., Lewin, D.R. 1999. *Process design principles: synthesis, analysis, and evaluation*. Wiley.

Smeets, E., Faaij, A. 2005. Future Demand for Fertilizers from Bioenergy Crop Production. *73rd IFA Annual Conference*, 6-8 June 2005, Kuala Lumpur, Malaysia.

Smil, V. 2004. *Enriching the Earth: Fritz Haber, Carl Bosch, and the Transformation of World Food Production*. Mit Press.

Tunå, P., Hulteberg, C., Hansson, J., Åsblad, A., Andersson, E. 2012. Synergies from combined pulp&paper and fuel production. *Biomass and Bioenergy*, **40**(0), 174-180.

Urban, W., Lohmann, H., Girod, K. 2009. Technologien und Kosten der Biogasaufbereitung und Einspeisung in das Erdgasnetz. Fraunhofer-Institut für Umwelt-, Sicherheits- und Energietechnik UMSICHT.

Wahlstedt, G. 2012. Sales of fertilisers for agricultural and horticultural purposes in 2010/11. Final statistics.

Vose, D. 2008. *Risk Analysis: A Quantitative Guide*. John Wiley & Sons.

Wright, B.D. 2012. International Grain Reserves And Other Instruments to Address Volatility in Grain Markets. *World Bank Research Observer*, **27**(2), 222-260.

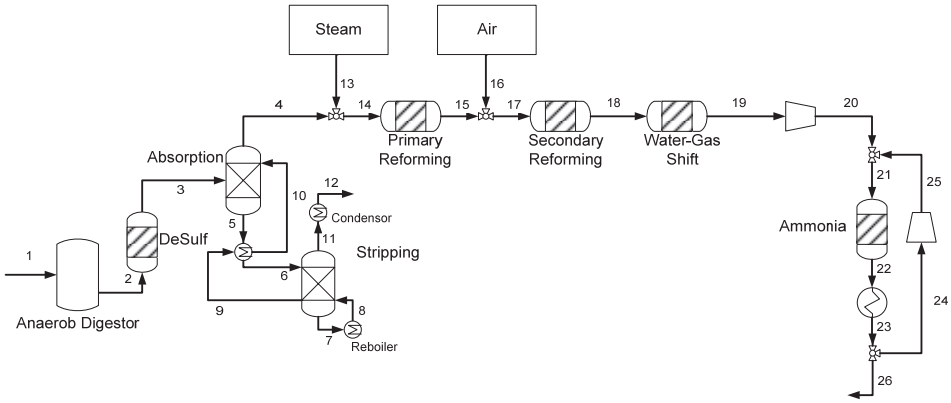

Figure 1a. Biogas-based ammonia production.

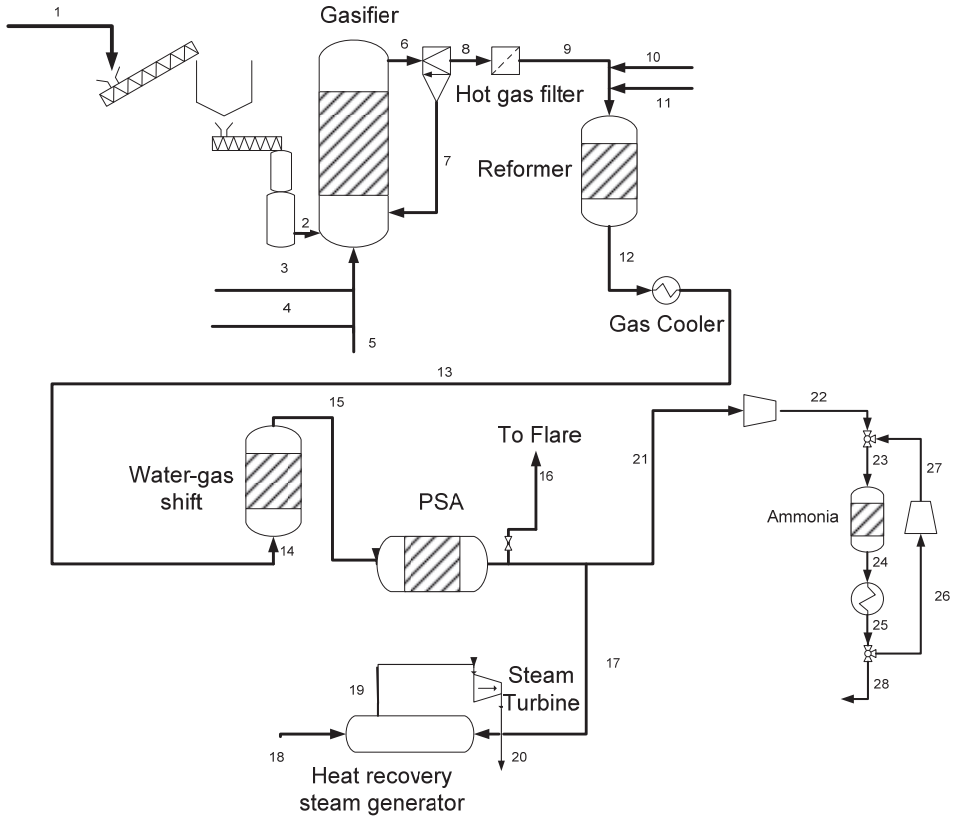

Figure 1b. Biomass gasification-based ammonia production.

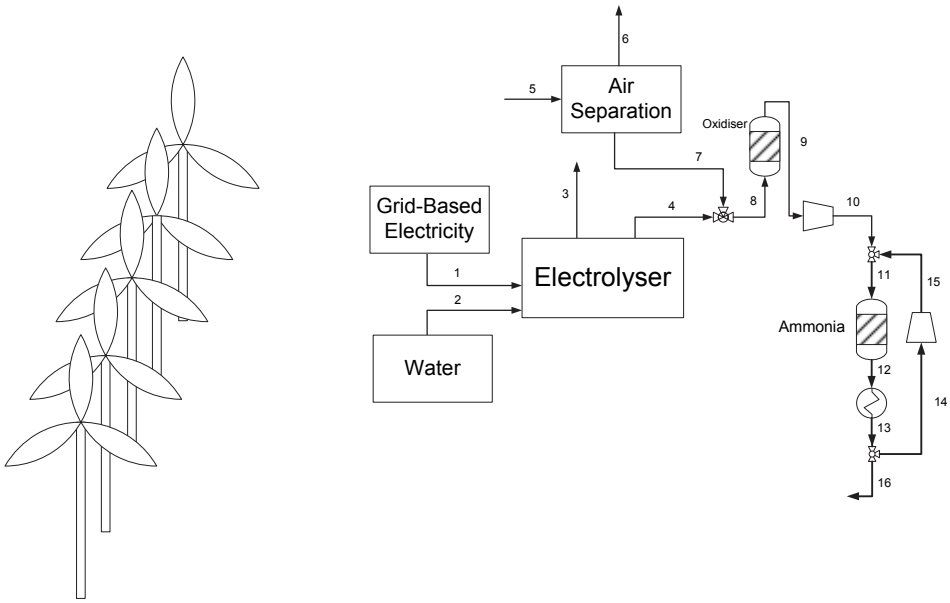

Figure 1c. Electrolyser-based ammonia production from renewable electricity, e.g. wind power.

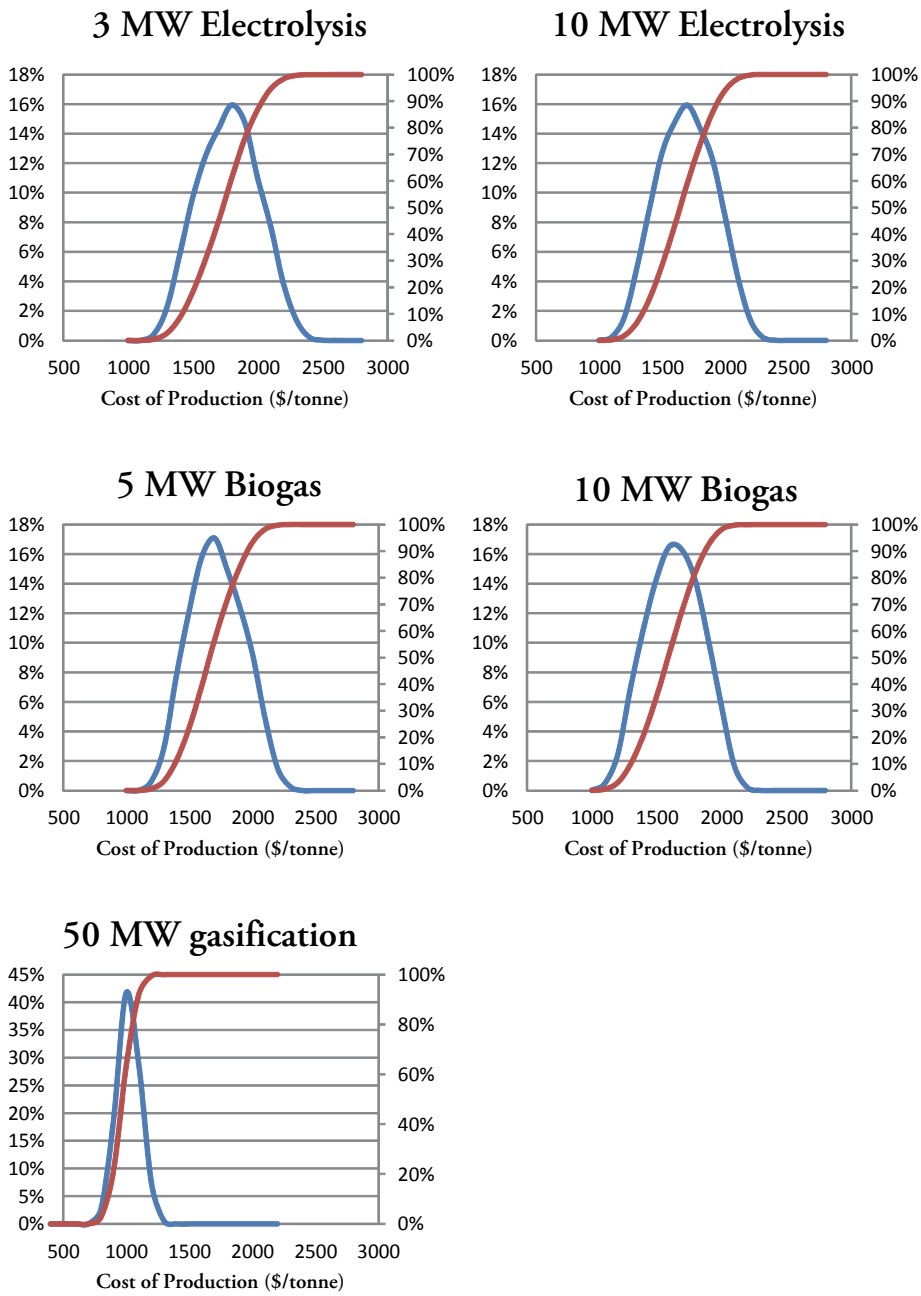

Figure 2. The production cost distribution for the investigated cases, the blue lines indicate the distribution of results from the Monte Carlo simulation, the red lines show the accumulative values

Table 1: Gasifier producer gas composition (Lundgren et al., 2013).

Component	Composition [vol-%]
CO	27.3
H_2	28.8
CO_2	16.9
O_2	0.0
H_2O	22.7
CH_4	3.8
N_2	0.0
Ar	0.0
C_2H_2	0.0
C_2H_4	1.1
C_2H_6	0.0
C_3H_6	0.0
C_6H_6	0.2
C_7H_8	0.0
H_2S [vppm]	150
NH_3 [vppm]	2,000
Tars [mg/Nm^3]	500

Table 2 Assumptions for financial modelling.

Parameter	Value	Reference
Annual time-on-stream	8,000 h	-
Economic plant life	15 years	-
Investment cost electrolyser	$577/ kWh	(Hulteberg & Karlsson, 2009)
Electricity consumption per kWh/(Nm^3 H_2/h) in electrolyser	4.25	(Hulteberg & Karlsson, 2009)
Contingency	18%	(Hulteberg & Karlsson, 2009)
Auxilliary	30%	(Hulteberg & Karlsson, 2009)
Vessel material	Stainless steel	-
CEPCI 2011	585.7	-

Table 3 Input values for the Monte Carlo simulations, converted to 2011 prices using producer price index for chemical and allied products (2013a).

Cost	Minimum	Most Likely	Maximum	Reference
Biomass ($/MWh)	33.9	67.8	101.7	(Hulteberg & Karlsson, 2009)
Electricity ($/MWh)	40.1	80.1	120.2	(Hulteberg & Karlsson, 2009)
Biogas ($/MWh)	50.8	101.7	152.5	(Berglund et al., 2012; Urban et al., 2009)
Water ($/tonne)	1	2	3	(Seider et al., 1999)
Wastewater ($/tonne)	10	20	30	Estimated from (Seider et al., 1999)
Investment cost	-30%	Grass-root cost	+30%	(Hulteberg, 2007; Hulteberg & Karlsson, 2009)
Interest rate (%)	5	8	12	-

Table 4: Energy and water inputs for the studied cases.

Case	Chemical energy input	Electric input	Water consumption
3 MW Electrolysis	-	3 MW	4,030 tonne/yr
10 MW Electrolysis	-	10 MW	13,400 tonne/yr
5 (2.9 el eqv) MW Biogas	5 MW	0.5 MW	10,500 tonne/yr
10 (5.8 el eqv) MW Biogas	10 MW	1.0 MW	20,900 tonne/yr
50 (23 el eqv) MW Biomass	50 MW	7.8 MW	60,400 tonne/yr

Table 5: NH_3 production, district heating and wastewater for the studied cases.

Case	NH_3 production	District heat	Wastewater	Net energy input	Net energy input
3 MW Electrolysis	2,030 tonne/yr	0.46 MW	-	42.6 GJ	42.6 GJel equ.
10 MW Electrolysis	6,760 tonne/yr	1.52 MW	-	42.6 GJ	42.6 GJel equ.
5 (2.9 el eqv) MW Biogas	3,730 tonne/yr	1.5 MW	7,500 tonne/yr	42.3 GJ	26.1 GJel equ.
10 (5.8 el eqv) MW Biogas	7,480 tonne/yr	3.0 MW	14,900 tonne/yr	42.2 GJ	26.1 GJel equ.
50 (23 el eqv) MW Biomass	28,700 tonne/yr	14.6 MW	58,700 tonne/yr	58.0 GJ	31.1 GJel equ.

Table 6 Results from the financial analysis, investment cost given as calculated grass root cost.

Case	Investment cost (k$)	Relative investment cost (k$/(tonne NH_3/y)	Distribution operating cost/fixed cost	Mean production cost ($/tonne)	Max production cost ($/tonne)	Min production cost ($/tonne)
3 MW Electrolysis	10,182	5.0	60%/40 %	1,725	2,392	1,078
10 MW Electrolysis	29,034	4.3	68%/32 %	1,640	2,328	1,015
5 (2.9 el eqv) MW Biogas	13,860	3.7	77%/23 %	1,671	2,297	1,087
10 (5.8 el eqv) MW Biogas	22,923	3.1	81%/19 %	1,594	2,199	1,028
50 (23 el eqv) MW Biomass	117,311	4.1	50%/50 %	970	1,342	676

Paper VI

Woody biomass-based transportation fuels – A comparative techno-economic study

Per Tunå*, Christian Hulteberg[1]

[1]Department of chemical engineering, Lund University, Box 124, 221 00 Lund, Sweden

*Corresponding author, per.tuna@chemeng.lth.se ; +46462868882

Keywords: Biomass gasification; Methanol; Fischer-Tropsch; Methanol-to-gasoline; Dimethyl ether; Synthetic natural gas

Abstract

Production of synthetic vehicle fuels from biomass is a hot topic. There are several alternative fuels to consider when evaluating properties such as cost of production and energy efficiency to both product and final use in a road vehicle. Thermochemical conversion via gasification and downstream synthesis of fuels as well as biochemical conversion of woody biomass to ethanol is considered in this paper. The vehicle fuels considered in this paper include methanol, ethanol, synthetic natural gas, Fischer-Tropsch diesel, dimethyl ether and synthetic gasoline from the methanol-to-gasoline process. The aim of the study is to evaluate all the different fuels on the same basis. The production cost of the various fuels is estimated as well as the overall investment cost. Well-to-wheel energy efficiency calculations were performed to evaluate how far a vehicle can travel on the fuel produced from a specific amount of feedstock. The production cost of the fuel as a function of distance travelled is also presented. Of the fuels considered in this study, dimethyl ether manages the highest efficiency from feedstock to travelled distance and manages to do so at the lowest cost. Ethanol produced from woody biomass is the most inefficient and expensive fuel, when considering the whole chain from feedstock to road use, in this study due to low yields in fuel production. Total investment cost for ethanol is considerably lower at MM$ 281 compared to the thermochemical fuels that ranges from MM$ 580 to MM$ 760. The

production costs of the various fuels range from \$74.8/MWh for synthetic natural gas to 132.1 \$/MWh for Fischer-Tropsch diesel. The production cost translates to a travel cost ranging from \$4.68/100km for dimethyl ether to \$8.51/100km for ethanol.

1 Introduction

The era of cheap crude is behind us, and at the same time, the need for transportation is increasing. There is also a growing demand for fossil-free and sustainable vehicle fuels to mitigate the increased carbon dioxide levels in the atmosphere. The first generation bio fuels, ethanol and bio-diesel from oil containing crops, are also heavily debated as the primary feedstock for those fuels are food crops. The second generation bio fuels are fuels that utilize other feedstocks such as woody biomass, sewage sludge and municipal waste. There are primarily two routes for conversion of the feedstock into a usable fuel - thermo-chemical and biological conversion. For biological conversion, the feedstock must contain cellulose and/or hemicelluloses. If the target product is ethanol, the cellulose-rich feedstock is pre-treated and hydrolysed into a solution with a high glucose content that is fermented into ethanol. If the desired product is methane the feedstock is anaerobically digested into a methane rich gas known as biogas which contains around 60 % methane (CH_4) and 40 % carbon dioxide (CO_2). The biogas needs to be upgraded by removing the CO_2 in order to meet specifications of energy density and CO_2 levels. Biogas is not considered in this study as woody biomass is not the typical feedstock for biogas. The thermo-chemical conversion utilizes gasification to produce an energy-rich gas containing carbon monoxide (CO) and hydrogen (H_2). Gas mixtures containing CO and H_2 are commonly known as synthesis gas or syngas as it is used to produce fuels and chemicals through chemical synthesis. The gas produced in a gasifier (producer gas) contains, in addition to CO and H_2, CO_2, CH_4 and lower hydrocarbons (C_{2+}), tars and other contaminants. The gas needs a thorough cleaning and conditioning before it can be used in chemical synthesis to produce synthetic fuels.

It is advantageous for synthetic fuels to be as similar to the conventional fuels as possible to ease the transformation towards the synthetic fuels. First of all, low blending of the synthetic fuels is possible if the fuels have similar in chemical

properties. Secondly, the whole infrastructure for the fuel handling such as filling stations, storage etc. is already in place. A totally different fuel from what is traditionally used, such as hydrogen, would require a completely new fuel infrastructure which would likely be expensive to implement.

This paper covers the production of renewable vehicle fuels from woody biomass. The fuels produced by thermo-chemical conversion are synthetic natural gas (SNG), methanol (MeOH), dimethyl ether (DME), Fischer-Tropsch diesel (FT) and methanol-to-gasoline (MTG). Flow sheeting calculations are performed in Aspen Plus to solve the material and energy balances. For comparison of thermo-chemical conversion and biological conversion, expected production of lignocellulosic ethanol plants is used.

The literature on the subject of system studies on synthetic vehicle fuels consists of a large quantity of papers. The comparison between the different studies is not always straightforward as the respective authors chose to emphasize different aspects of the purpose of their study. Some papers contain detailed economic assessments while others focus on CO_2 abatement and energy efficiency. Furthermore, some papers include district heating as a means to decrease fuel production cost. District heating is not available in most regions of the world and is therefore not considered in this study. For comparison with the purpose of this work, only papers including techno economic evaluation not utilising district heating revenues will be considered. Among these is an investigation on woody biomass to gasoline (MTG) via gasification and downstream synthesis by Phillips et al [1] that established a gasoline production price of \$57/MWh (\$0.52/L gasoline) and a total plant investment cost of \$ 199.6 MM. Trippe et al estimated the MTG production cost using a direct DME synthesis to \$160/MWh (\$1.47/L gasoline). The total plant investment cost was estimated to \$270-280MM depending on plant configuration [2].

Furthermore, the study on SNG production by Gassner et al resulted in a SNG production price of \$80-125/MWh for a plant size of 150 MWth and above [3]. Energy efficiency for the process were similar to those presented by Juraščík et al [4] at around 55-70 % thermal. Among the studies on biomass-to-Fischer Tropsch liquids, the report by Boerrigter [5] found that the production cost for a 400

MWth input plant would be roughly $75/MWh ($1.2/L diesel). Boerrigter considered an entrained flow gasifier which has, among others, higher investment costs than other gasifier types. Thermodynamic efficiency was reported to 55% from wood to FT diesel [5]. Hamelinck et al calculated the production cost of FT-diesel for a 400 MWth (HHV) to $60/MWh ($0.9/L diesel) [6]. In a similar study by Tijmensen el al the production price of FT diesel ranged from $50-110/MWh ($0.75-1.75/L diesel) for a plant investment cost ranging from $281-338 MM [7]. Furthermore, Trippe et al estimated the production cost of FT diesel to $170/MWh ($1.7/L diesel).For methanol Leduc et al reported production cost of $140/MWh ($0.85/L methanol) [8]. In a report by Altener the production cost of methanol was estimated to $63/MWh ($0.28/L methanol). Total plant investment cost was estimated to $417MM [9].In a paper by Huisman et al the production cost of DME was estimated to $100/MWh, only slightly more expensive than the estimated methanol production cost of $95/MWh. Total capital investment was reported to $310 MM [10].

2 Method

The gasifer chosen for the liquid fuels and DME is a Carbona/Andritz type gasifier. For SNG production, a gasifier with higher methane content in the producer gas is desirable. The MILENA type gasifier is a pressurized allothermal gasifier with high methane and lower hydrocarbons in the producer gas. Unfortunately, it also produces high levels of benzene and tars. The OLGA oil-scrubber is used downstream of the gasifier to produce a gas with low tar content. The OLGA does not remove benzene and lower hydrocarbons and a pre-reformer is still necessary to convert the hydrocarbons except methane into synthesis gas and methane. In Table 1 is presented the composition of the producer gases used as input to the Aspen Plus model. The outlet pressure of the Carbona/Andritz gasifier is 10 bar(a) and the pressure after the OLGA gas cleaning is 6 bar(a).

Please insert table 1 here

The Carbona type gasifier requires both pre-reforming of the tars and lower hydrocarbons and methane reforming to maximize the output of synthetic fuels.

The process configuration can be seen in Figure 1 for all thermo chemical fuels in this study.

Please insert figure 1 here

The unit operations depicted in Figure 1 is used during simulations and a more descriptive schematic over the methanol/DME/MTG processes are depicted in Figure 3-5. Operating parameters for the unit operations are summarised in Table 2.

Please insert table 2 here

2.1 Detailed model description

2.1.1 Fischer-Tropsch

The Fischer-Tropsch reactor was modelled as an isothermal plug reactor with varying length. The reaction kinetics was modelled as power law reactions following the Anderson-Schulz-Flory distribution (1) with -value chosen (= 0.85) to yield as much diesel fuels (C_{10}-C_{15}) as possible, see Figure 2.

$$Wn = n \cdot (1 -)^2 \cdot (n\text{-}1) \qquad (1)$$

Please insert figure 2 here

The hydrocarbons that are heavier than diesel fuels would be a good feedstock for a cracker to produce more vehicle fuels. The length of the reactor is varied to achieve a once-through conversion of 80 % of the ingoing CO. The hydrocarbons produced in the reactor contain alkanes and alkenes from methane to C_{20}. The separation of useful fuels and tail-gases is around C_6, with the most part of the C_6 ending up in the tail-gas and most of the C_7 in the diesel fuel. A part of the tail-gas is burnt to produce heat and power for the plant. The remaining tail-gas is recirculated to the reformer.

2.1.2 Methanol synthesis

Methanol synthesis recycle ratio was 5:1 [17, 18]. The product stream is condensed and methanol and water is removed. The gas is recycled to the inlet of the reactor except a small part that is removed as tail gas, see Figure 3. Methanol and water are distilled to yield 99.9 % pure methanol [11].

Please insert figure 3 here

2.1.3 Dimethylether

Methanol is the feedstock for DME and MTG and both processes utilize the methanol synthesis described above as input. The product is cooled and methanol, DME and water are separated in a two-step distillation. Methanol is recycled back to the reactor inlet, see Figure 4. The purge stream contains methanol, DME, water and trace amounts of H_2, CO etc. The purge stream is burnt to produce heat and power.

Please insert figure 4 here

2.1.4 Methanol-to-gasoline

The methanol-to-gasoline uses a stream containing both DME and methanol as feedstock. The MTG product distribution is presented in Table 3. The C_{5+} and butanes are considered gasoline fuels and are separated from the gaseous components and water. The gaseous components constitute the tail gas for the MTG process as is seen in Figure 5.

Please insert figure 5 here

The model of the MTG synthesis is simplified but should still be valid as it yields a product distribution resembling that of a real process.

Please insert table 3 here

2.1.5 Synthetic natural gas

SNG synthesis is carried out according Topsøe's TREMP where three adiabatic equilibrium reactors are used in series [20]. TREMP uses recirculation of syngas over the first reactor is used to control temperature. In the model, the recirculation of gas over the first reactor was set to have 700 °C at the outlet. The gas is cooled before it is recirculated or fed to the two remaining reactors, see Figure 6. The gas is cooled between the last two reactors. Pressure drop for the methanation reactors are 0.2, 0.05 and 0.05 bar respectively.

Please insert figure 6 here

The SNG needs to be compressed to 200 bar before it is usable as a vehicle fuel. Furthermore, the produced SNG may require additional propane to meet a target energy density. The H_2 and N_2 content of the SNG are a higher than for most natural gas available worldwide. The hydrogen content is the more troublesome of the two as it affects the combustion properties of the gas. It has been show in studies that the addition of H_2 to natural gas mixtures burn more cleanly than plain natural gas [21]. The N_2 content can, if need be, be compensated for by addition of propane.

2.2 Lignocellulosic ethanol

Extensive research on lignocellulosic bioethanol production has been done over the past decades and it is still a hot topic. There are a few different process configurations available, some more mature than others. No flow sheet calculations on the bioethanol production were performed in this work, instead typical production figures are used as a comparison with the thermo chemical fuels. Reported ethanol production ranges from 170 litres/dry ton [22] to almost 350 litres/dry ton [23], it all depends on the amount of available celluloses and hemicelluloses in the feedstock. Typically around 300-325 litres/dry ton are reasonable with current proven technologies. Theoretical maximum ethanol production for a typical softwood containing 43-45% cellulose, 20-23 % hemicellulose and 28 % lignin is 410 litres/dry ton if only the C_6 sugars are utilized and 455 litres/dry ton if all carbohydrates are used [24]. For ease of comparison the above presented production numbers are recalculated to MW ethanol/MW biomass based on the lower heating value. For 170 litres/dry ton, 20.8 MW

ethanol/100 MW biomass is produced, and 349 litres / dry ton equals 42.8 MW ethanol/100 MW biomass. The theoretical maximum ethanol production of 455 litres/dry ton equals 55.7 MW ethanol/100 MW biomass. For comparison with the synthetic fuels, 349 litres/dry ton and the theoretic 455 litres/dry ton are used. For transportation fuels only the lower heating value makes sense for comparison as no personal vehicles have the means to utilize the condense heat in the exhaust gases.

2.3 Production cost estimates

The investment-cost assessment has been performed by using factor methods from various sources [6, 25]; the chemical engineering plant cost index has been used to update the costs to 2011. The heat and mass balances determined from the Aspen simulations have been used to do detail-dimensioning of the process equipment. To the total bare-module cost, 18% contingency and 30% auxiliary cost has been added giving the overall investment cost; the estimate is believed to be accurate within ±30% sources [25]. Thereafter the cost-of-production of the different fuels is determined. In table 4 some key parameters for the financial modeling are listed, for more information on detail-dimensioning please view [26, 27]. The assumptions on the cost-of-goods are also included in table 4 and are identical to the ones used in [22] for biomass and electricity.

Please insert table 4 here

3 Results

The outputs of the models are output of the desired product (lower heating value), electric power, heat and losses. Table 5 summarizes the outputs for the different fuels in percent of the biomass input (lower heating value).

Please insert table 5 here

a) Energy balance for ethanol production with poplar as feedstock with yield of 349 liters/dry ton [23].

As can be seen in Table 5, SNG is the product with the highest efficiency, from biomass to product, having over 66 % efficiency to the desired fuel (MJ/MJ based on the lower heating value). SNG-production also surpluses both heat and power. The total efficiency for the SNG-production is around 92 %. Methanol is not as efficient as SNG, but still manages almost 59 % efficiency. There is some electricity surplus but almost no excess heat is available. The models have been designed to favour export of electricity over heat, by utilising condensing turbines. The biggest difference between the SNG and the methanol synthesis is that SNG operates at higher temperature and lower pressures. This is favourable as higher temperatures allow generation of steam with higher pressure and a lower synthesis pressure requires less electricity for syngas compression. Total efficiency of the methanol plant was above 60 %. Production cost for the SNG is estimated to $74.8/MWh ($73.7/MWh including sales of electricity). The SNG production cost is well within the same range as estimated by Gassner et al [3].The production cost for methanol is a little higher at $87.5/MWh ($86.8/MWh including sales of electricity). Compared with the estimations in the literature ($63/MWh Altener [9] and $140/MWh by Leduc et al [8]) this compares well and is in the lower range of the cited estimates.

MTG uses methanol from the methanol synthesis and manages a product efficiency of almost 51 %. MTG production has no heat export but can export almost 5 % of the input energy as electricity. The electricity production comes from burning of the tail gas. The total efficiency of the MTG-synthesis is almost 54 %. Production cost for the gasoline is estimated to $109.7/MWh ($107.9/MWh including sales of electricity). The production cost for the synthetic gasoline is considerably more expensive than the estimates by Phillips et al ($57/MWh) [1]. MTG would not be cheaper to produce than methanol and based on the production costs of methanol cited in the literature, the estimates by Phillips et al seems rather optimistic. The production cost cited by Trippe et al are almost 50 % higher at $160/MWh [2].

DME is similar to MTG but yielding more fuel and less electricity for export. 53 % of the energy in the biomass remains in the product for the DME synthesis. Total efficiency is a little higher than the MTG synthesis at 56 %. The DME fuel

is estimated to have a production cost of $100.8/MWh ($99.4/MWh including sales of electricity). The production cost of DME is the same as estimated by Huisman et al [10].

Fischer-Tropsch synthesis produces hydrocarbons from CH4 to C20+ but not all of it can be used as a vehicle fuel. The product separation of hydrocarbons around C6 results in an efficiency of almost 36 % to diesel. The lighter fraction accounts for almost 26 % of the total biomass input. With recirculation of a part of the tail-gas, 45 % efficiency to diesel is achieved, at the cost of total efficiency. The total efficiency of 64 % for the FT-plant is higher than methanol and its derivates MTG and DME. Production cost for the FT diesel is estimated to $132.1/MWh ($129.5/MWh including sales of electricity) which is in the same range as cited in the literature ($60-170/MWh).

The production of ethanol by fermentation is a process that is unable to match the thermo-chemical conversion routes in terms of energy efficiency. The major reason for that is due to the fact that not all of the biomass is available for sugar production, a part of the feedstock being lignin; this gives a resulting production cost of $128.7/MWh based on the data presented above. Furthermore the fermented solutions contain around 4 % [w/w] of ethanol, which needs energy intense distillation.

The production and total investment costs for the plants are summarised in Table 6.

Please insert table 6 here

The SNG plant has the highest efficiency of the different plants to their desired product, but how far can a medium-sized car drive on the fuel produced from one kilogram of dry wood (18 MJ/kg [31]).

The chosen car is a Mercedes Benz B-class being available with diesel, gasoline and natural gas engines. Listed in Table 7 is the typical consumption of the vehicle, both in quantity of the fuel and the energy consumption.

Please insert table 7 here

The higher efficiency, and thus lower consumption, of diesel is evident from the consumption numbers listed in Table 7. As can be seen in Table 8 the range that a vehicle can travel on one kilogram of dry wood varies from around 2.9 to 5.7 kilometres.

Please insert table 8 here

a) Range with the theoretical maximum ethanol production of 455 litres/dry ton.

DME has the longest range of the fuels, which is a result of the use of the fuel in diesel engines and the relatively high efficiency of the synthesis. Of the thermo-chemical fuels, FT diesels have the lowest synthesis efficiency but still get good range, all thanks to the higher efficiency of diesel engines over Otto-engines. Ethanol produced by fermentation is far behind the thermo-chemical synthetic fuels and the reason comes both from the energy consumption in converting the wood to fuel and the lower efficiency of the Otto-engine. The theoretical maximum production of ethanol manages about 3.8 km/dry kg wood.

4 Discussion and Conclusions

In this study the production of fuels from woody biomass have been evaluated using models developed in Aspen Plus. The fuels considered are five different vehicle compatible fuels produced by thermo-chemical conversion and ethanol produced by biological conversion. All fuels have been compared on an energy-basis based on the lower heating value. The models of the different synthesises have been built to produce as much fuel as possible rather than to have the highest overall efficiency.

Of the fuels produced, SNG has the highest efficiency from biomass to fuel. SNG production also has the highest energy efficiency when including electric power and district heating export. The composition of the produced SNG may not meet specific standards in individual countries and further upgrading may be necessary.

Methanol and its derivates DME and MTG have efficiencies in the 50-60 % range, with methanol getting an efficiency of almost 59 % from biomass to fuel, MTG and DME ended up at 51 % and 53 % respectively. The high synthesis pressure of the methanol synthesis requires much energy for compression which is the reason for the low electrical output of the methanol. DME and MTG plants had a higher electrical output than methanol due to the burning of more tail-gas. The price of the MTG is in parity with the study of Phillips et al that had a much cheaper raw feedstock and plant investment cost [1].

Of the studied synthesises, Fischer-Tropsch is the least selective, producing hydrocarbons from methane up to C_{20+} following a specific distribution of products. A large part of the produced hydrocarbons are out of the diesel range. The fraction that is heavier than diesel fuels can be cracked at a refinery to yield more diesel fuels. A part of the lighter fraction is recirculated to increase fuel production and the remaining part is burnt to produce steam for power production. The lighter fraction could also, partly, be used as a gasoline fuel thus increasing the output of fuel from the synthesis without recirculating as much gas.

Ethanol produced by fermentation is unable to match the thermo-chemical conversion when comparing the efficiency to fuel which is explained by the amount of sugars available after biomass pre-treatment. The ethanol produced from lignocellulosic ethanol seldom reaches higher than 4 % [wt/wt] which requires much energy for distillation. The energy intense distillation is one of the reasons for the overall low output for the ethanol plant.

Of the fuels produced two are gaseous and four are liquid fuels at room temperature. There are some practical advantages to using liquid fuels in vehicles. The storage of gaseous fuels is bulkier requiring heavy vessels usually made of steel, although there are composite versions available. The filling of the vehicles also requires different equipment. For ease of handling a liquid fuel may be preferred.

The range of the vehicle in Table 8 is based on the assumed consumption of the respective fuel. DME is the fuel that gets the furthest of the fuel due to its use in diesel engines. There are also possibilities of using low blends of, for example, ethanol on diesel fuels that would increase the range of the ethanol fuel because of the higher efficiency of the diesel engine [32]. Low blending of alcohols in diesel and gasoline fuels affect, among others, engine durability, safety, engine performance and emissions. SNG may also be co-fired in diesel engines increasing the range of the SNG. Using traditional gasoline fuels in diesel engines is out of the scope of this study.

As presented above, there is a significant production cost difference between the different fuels. This has to do with the overall process yield as well as the use of consumables in the individual processes. The lowest production cost per MWh is noted for SNG and methanol which are the two compounds that are best defined from a chemical perspective; also DME is well defined but as a derivative of methanol it's not strange that it's priced higher. The two fuels where a distribution of products is produced, MTG and FT, also show higher production costs than in the other cases. When extending the comparison to also include the use in a vehicle, the type of engine that may be used adds another dimension of complexity. In this comparison the DME falls out as the lowest cost transport alternative as it may be used in a diesel engine; indeed even though DME is 34.8% more expensive than SNG it is still 8.7% less expensive per 100 km. It is therefore important to assess not only the production cost of the commodity that is to be produced from biomass, but also the end-use of this commodity to include the overall system efficiency avoiding system sub-optimisation.

5 References

[1] S.D. Phillips, J.K. Tarud, M.J. Biddy, A. Dutta, Gasoline from Woody Biomass via Thermochemical Gasification, Methanol Synthesis, and Methanol-to-Gasoline Technologies: A Technoeconomic Analysis, Industrial & Engineering Chemistry Research, 50 (2011) 11463-11770.

[2] F. Trippe, M. Fröhling, F. Schultmann, R. Stahl, E. Henrich, A. Dalai, Comprehensive techno-economic assessment of dimethyl ether (DME) synthesis and Fischer–Tropsch synthesis as alternative process steps within biomass-to-liquid production, Fuel Processing Technology, 106 (2013) 577-586.

[3] M. Gassner, F. Maréchal, Thermo-economic process model for thermochemical production of Synthetic Natural Gas (SNG) from lignocellulosic biomass, Biomass and Bioenergy, 33 (2009) 1587-1604.
[4] M. Juraščík, A. Sues, K.J. Ptasinski, Exergy analysis of synthetic natural gas production method from biomass, Energy, 35 (2010) 880-888.
[5] H. Boerrigter, Economy of Biomass-to-Liquids (BTL) plants -An engineering assessment, in, Energy research Centre of the Netherlands (ECN), 2006.
[6] C.N. Hamelinck, A.P.C. Faaij, H. den Uil, H. Boerrigter, Production of FT transportation fuels from biomass; technical options, process analysis and optimisation, and development potential, Energy, 29 (2004) 1743-1771.
[7] M.J.A. Tijmensen, A.P.C. Faaij, C.N. Hamelinck, M.R.M. van Hardeveld, Exploration of the possibilities for production of Fischer Tropsch liquids and power via biomass gasification, Biomass and Bioenergy, 23 (2002) 129-152.
[8] S. Leduc, E. Schmid, M. Obersteiner, K. Riahi, Methanol production by gasification using a geographically explicit model, Biomass and Bioenergy, 33 (2009) 745-751.
[9] ALTENER, FEASIBILITY PHASE PROJECT FOR BIOMASS-DERIVED ALCOHOLS FOR AUTOMOTIVE AND INDUSTRIAL USES, in, 1997.
[10] G.H. Huisman, G.L.M.A. Van Rens, H. De Lathouder, R.L. Cornelissen, Cost estimation of biomass-to-fuel plants producing methanol, dimethylether or hydrogen, Biomass and Bioenergy, 35, Supplement 1 (2011) S155-S166.
[11] J. Lundgren, T. Ekbom, C. Hulteberg, M. Larsson, C.-E. Grip, L. Nilsson, P. Tunå, Methanol production from steel-work off-gases and biomass based synthesis gas, Applied Energy, In press (2013).
[12] H. Svensson, P. Tunå, C. Hulteberg, Carbon dioxide removal in indirect gasification, in, Malmö, 2013.
[13] P. Tunå, C. Hulteberg, J. Hansson, A. Åsblad, E. Andersson, Synergies from combined pulp&paper and fuel production, Biomass and Bioenergy, 40 (2012) 174-180.
[14] R.L. Bannister, R.A. Newby, W.C. Yang, Final Report on the Development of a Hydrogen-Fueled Combustion Turbine Cycle for Power Generation, Journal of Engineering for Gas Turbines and Power, 121 (1999) 38-45.
[15] O. Bolland, H.K. Kvamsdal, J.C. Boden, A Thermodynamic Comparison of the Oxy-Fuel Power Cycles Water-Cycle, Gratz-Cycle and Matiant-Cycle, in: International Conference of Power Generation and Sustainable Development, Liège, Belgium, 2001.
[16] S. Aoki, K. Uematsu, K. Suenaga, H. Mori, H., H. Sugishita, A Study of Hydrogen Combustion Turbines, in: International Gas Turbines & Aeroengines Congress & Exhibition, Stockholm, Sweden, 1998.

[17] C.N. Satterfield, Heterogeneous Catalysis in Industrial Practice, Krieger Publishing Company, 1991.
[18] G. Ertl, Handbook of Heterogeneous Catalysis, Wiley-VCH-Verlag, 2008.
[19] D. Liederman, S.M. Jacob, S.E. Voltz, J.J. Wise, Process Variable Effects in the Conversion of Methanol to Gasoline in a Fluid Bed Reactor, Industrial & Engineering Chemistry Process Design and Development, 17 (1978) 340-346.
[20] J. Kopyscinski, T.J. Schildhauer, S.M.A. Biollaz, Production of synthetic natural gas (SNG) from coal and dry biomass – A technology review from 1950 to 2009, Fuel, 89 (2010) 1763-1783.
[21] A. Mariani, B. Morrone, A. Unich, A Review of Hydrogen-Natural Gas Blend Fuels in Internal Combustion Engines, Fossil Fuel and the Environment, (2012).
[22] J.Y. Zhu, W. Zhu, P. Obryan, B. Dien, S. Tian, R. Gleisner, X.J. Pan, Ethanol production from SPORL-pretreated lodgepole pine: preliminary evaluation of mass balance and process energy efficiency, Appl Microbiol Biotechnol, 86 (2010) 1355-1365.
[23] E. Gnansounou, A. Dauriat, Techno-economic analysis of lignocellulosic ethanol: A review, Bioresource Technology, 101 (2010) 4980-4991.
[24] M. Galbe, G. Zacchi, A review of the production of ethanol from softwood, Appl Microbiol Biotechnol, 59 (2002) 618-628.
[25] G.D. Ulrich, P.T. Vasudevan, Chemical Engineering: Process Design and Economics : a Practical Guide, Process Pub., 2004.
[26] P.C. Hulteberg, H.T. Karlsson, A study of combined biomass gasification and electrolysis for hydrogen production, International Journal of Hydrogen Energy, 34 (2009) 772-782.
[27] P.C. Hulteberg, Hydrogen, an Energy Carrier of the Future, in: Chemical Engineering, Lund University, Lund, 2007.
[28] G.D. Ulrich, Chemical Engineering Process Design and Economics: A Practical Guide, Process Publishing, 2004.
[29] W.D. Seider, J.D. Seader, D.R. Lewin, Process design principles: synthesis, analysis, and evaluation, Wiley, 1999.
[30] A. Aden, M. Ruth, K. Ibsen, J. Jechura, K. Neeves, J. Sheehan, B. Wallace, Lignocellulosic Biomass to Ethanol Process Design and Economics Utilizing Co-Current Dilute Acid Prehydrolysis and Enzymatic Hydrolysis for Corn Stover, in, Seattle, Washington, 2002.
[31] Pressurized Oxidative Recovery of Energy from Biomass, Final Technical Report, in.
[32] A.C. Hansen, Q. Zhang, P.W.L. Lyne, Ethanol–diesel fuel blends — a review, Bioresource Technology, 96 (2005) 277-285.

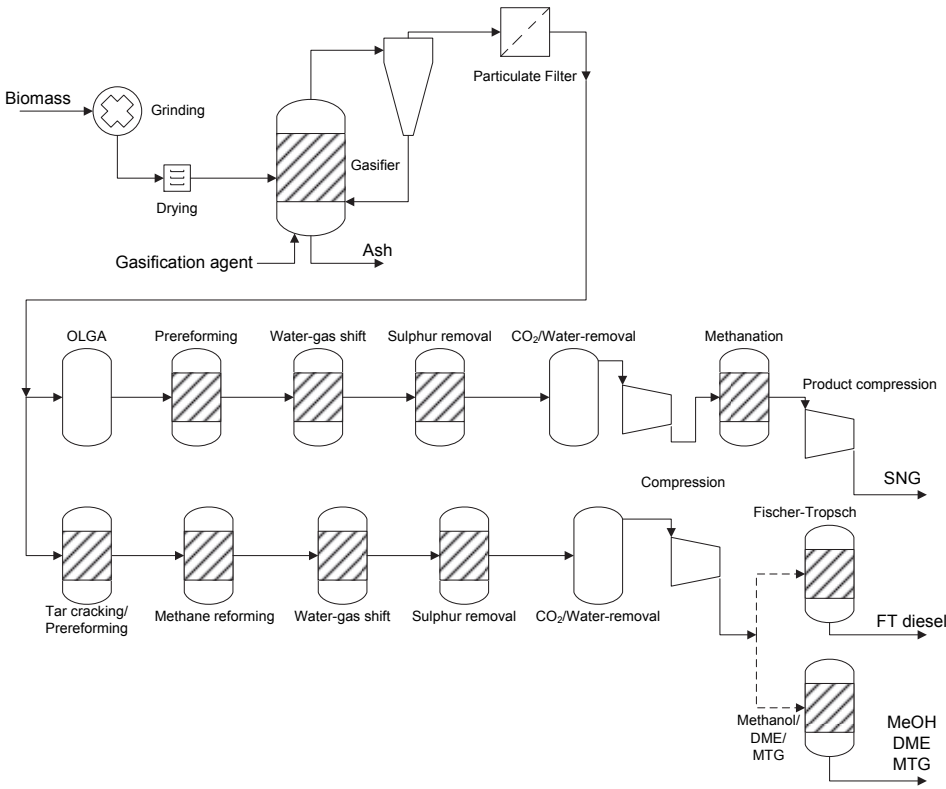

Figure 1. Gasification and downstream processes for synthesising vehicle fuels.

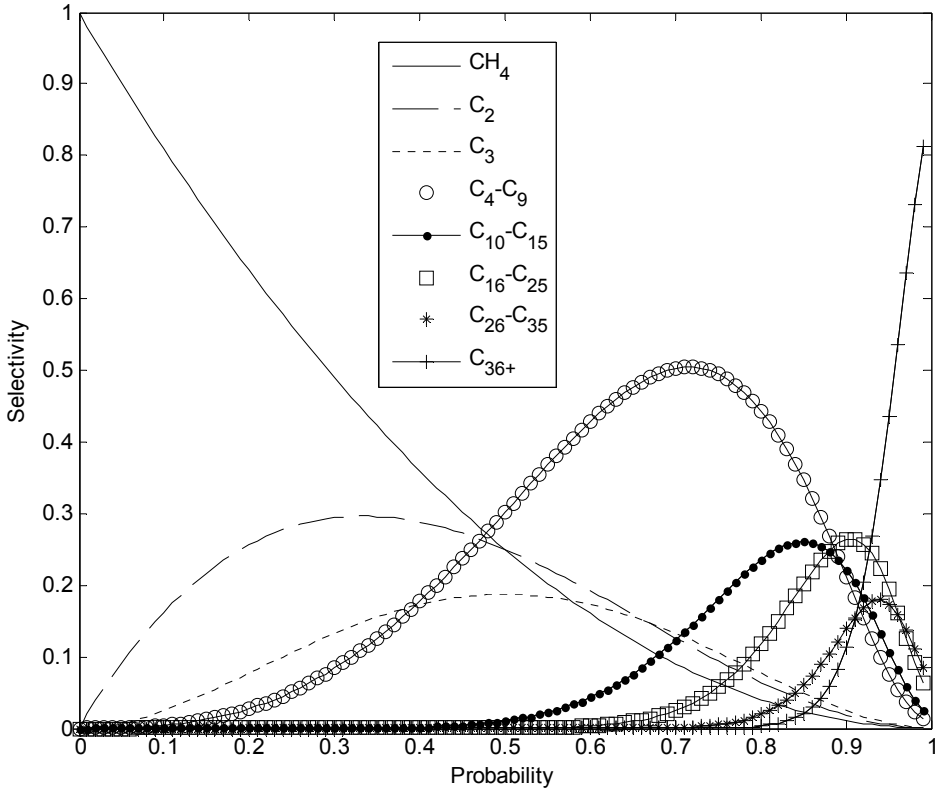

Figure 2. Anderson-Shulz-Flory distribution of selectivity against probability (α-number).

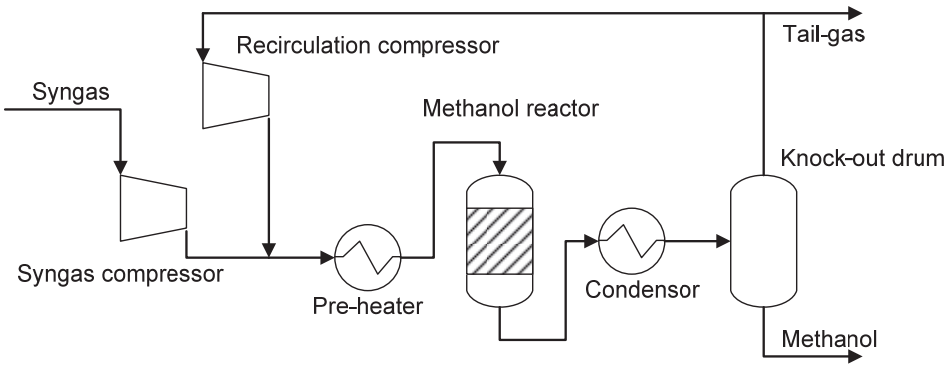

Figure 3. Methanol synthesis loop, recirculation ratio is set to 5:1.

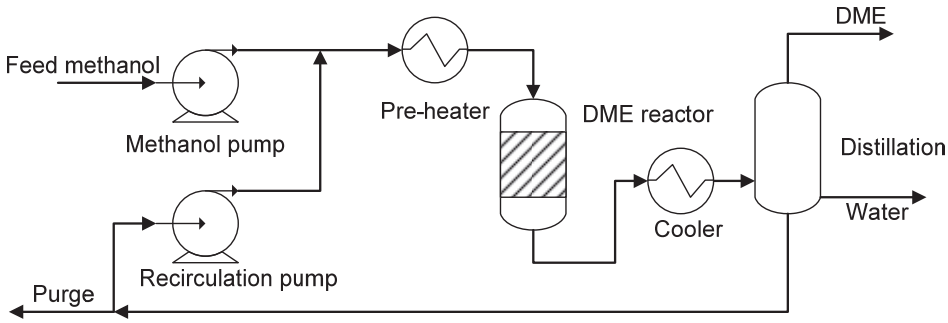

Figure 4. Schematic of the DME synthesis loop.

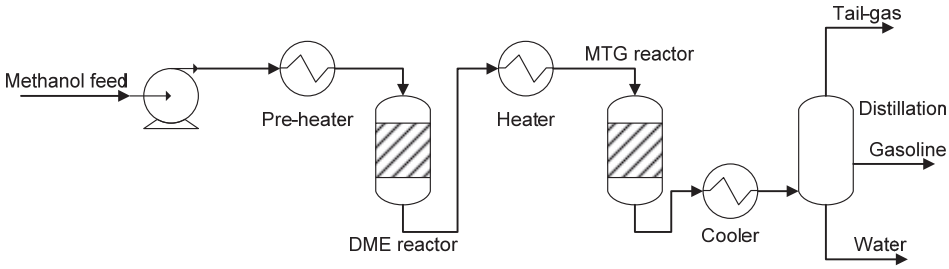

Figure 5. Schematic of the simplified MTG-synthesis.

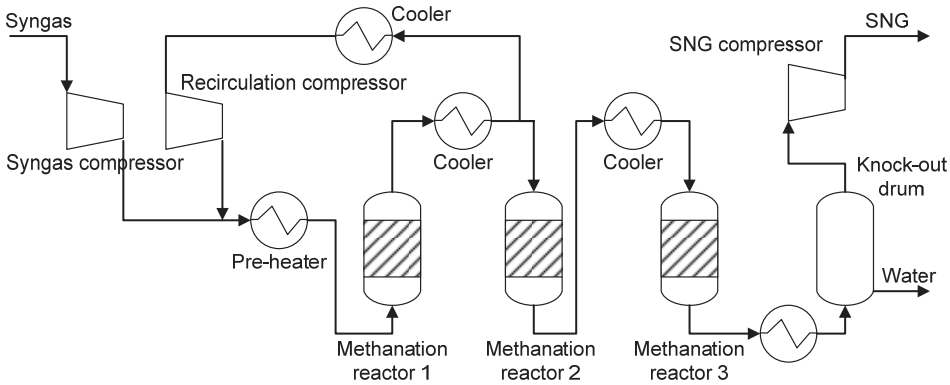

Figure 6. Schematic of TREMP SNG-synthesis.

Table 1: Gasifier producer gas composition [11, 12].

Component	MILENA [vol-%]	MILENA + OLGA [vol-%]	Carbona/Andritz [vol-%]
CO	21.4	21.6	27.3
H_2	16.8	16.9	28.8
CO_2	9.9	10.0	16.9
O_2	0.0	0.0	0.0
H2O	37.6	37.6	22.7
CH_4	8.8	8.9	3.8
N_2	0.8	0.8	0.0
Ar	0.0	0.0	0.0
C_2H_2	0.2	0.2	0.0
C_2H_4	2.9	2.9	1.1
C_2H_6	0.2	0.2	0.0
C_3H_6	0.0	0.0	0.0
C_6H_6	0.7	0.5	0.2
C_7H_8	0.1	0.0	0.0
H_2S [vppm]	150	150	150
NH_3 [vppm]	2000	2000	2000
Tars [mg/Nm^3]	20000	<40	500

Table 2. The operating parameters for the various unit operations in the flow sheet.

Unit operation	Temperature Inlet/Outlet [°C]	Pressure Inlet/Outlet [bar(a)]	Aspen Model
Prereforming (SNG)	400/650	6/5	Gibbs free energy
Prereforming	600/750	10/9	Gibbs free energy
Methane reformer	750/1200	9/8	Gibbs free energy
Water-gas shift (SNG)	350/500	5/4.7	Equilibrium
Water-gas shift	350/520	8/7.7	Equilibrium
CO_2/water removal (SNG)	70/30	4.7/4.7	Separation block/flash
CO_2/water removal	70/30	7.5/7.5	Separation block/flash
Compression (0.72 isentropic efficiency used for all cases)	70 (5 stages with intercooling)		Multistage compressor
Methanation (3 reactors)	300/700 300/530 300/380	30/30 30/30 30/30	Equilibrium
Methanol	125/260	100/92	Equilibrium
DME	300/300	20/18	Equilibrium
Methanol-to-gasoline	350/350	23/19	Yield reactor
Fischer-Tropsch [13]	250/250	27	Plug-flow reactor with power law reactions
Steam for power generation	70/500	90/90	Steam generated down to 150 °C
Turbine isentropic efficiency 0.9 [14-16]	500/39	90/0.07	Compressor/Turbine
District heating	-	-	Interval 150-70 °C

Table 3. Component mass distribution in MTG-reactor [19].

Component	Yield [wt-%]
H_2O	55.20%
CO	0.12%
MEOH	1.00%
DME	1.00%
CH_4	0.34%
C_2H_6	0.07%
C_2H_4	1.60%
C_3H_8	1.00%
C_3H_6	1.50%
i-C_4H_{10}	5.40%
C_4H_{10}	0.47%
C_4H_8	1.20%
C_{5+}	31.10%

Table 4 financial parameters used for modeling.

Parameter	Value	Reference
Annual time-on-stream	8,000 h	-
Economic plant life	20 years	-
Discount rate	10%	
Contingency	18%	[24]
Auxiliary	30%	[24]
Vessel material	Stainless steel except reactors which are in nickel alloy steel	-
CEPCI 2011	585.7	-
Feedstock	$123/dry tonne	[18]
Electricity	$0.02/kWh	[18]
Water	$0.24/tonne	[25]
Wastewater	$20/tonne	[25]

Table 5. Summary of the outputs for the different fuel processes.

	SNG	MeOH	MTG	DME	FT	EtOH [a]
Product	66.5%	58.7%	50.6%	53%	45.6%	41.2%
Electricity	3.5%	1.8%	4.7%	3.7%	5.9%	0.1%
District heating	23%	0.36%	1.4%	0%	13%	0%
Losses	7.3%	39.1%	43.2%	43.3%	35.5%	58.7%
Water usage [kg/s]	0.38	3.4	3.4	3.4	3.8	39.4 [24]
Waste water [kg/s]	7.2	16.8	23.3	19.7	24.8	21.1 [24]

Table 6. Production and total investment cost for the different plants.

Fuel	SNG	MeOH	MTG	DME	FT	EtOH [19]
Production cost [$/MWh]	74.8	87.5	109.7	100.8	132.1	128.7
Total investment cost [MM$]	580	580	650	610	760	281

Table 7. Mercedes Benz B-class fuel consumption when driving on different fuels.

Fuel	Fuel consumption [/100km]	Energy consumption [MJ/100km]	Fuel used in engine
Gasoline	7.3 litres	254	MTG, EtOH, MeOH
Diesel	4.33 litres	167	FT, DME
Natural gas	4.9 kg	245	SNG

Table 8. Vehicle range on one kilogram of dry wood for the different synthetic fuels.

Fuel	SNG	MeOH	MTG	DME	FT	EtOH	EtOH [a]
Range (km)	4.89	4.16	3.59	5.71	4.91	2.92	3.81
Fuel cost ($/100 km)	5.09	6.17	7.73	4.68	6.13	8.51	-

Paper VII

Journal of Natural Gas Science and Engineering 13 (2013) 1–6

Contents lists available at SciVerse ScienceDirect

Journal of Natural Gas Science and Engineering

journal homepage: www.elsevier.com/locate/jngse

A new process for well-head gas upgrading

Per Tunå, Christian Hulteberg*

Lund University, Faculty of Engineering, Department of Chemical Engineering, Box 124, 22100 Lund, Sweden

ARTICLE INFO

Article history:
Received 12 February 2013
Received in revised form
27 February 2013
Accepted 1 March 2013
Available online

Keywords:
Stranded gas
Well-head gas
Upgrading

ABSTRACT

As oil-prices and environmental concerns are increasing, it is of interest to better use the well-head gas. This light fraction co-produced with petroleum is generally flared and in this paper a method for upgrading and returning the co-product to the petroleum stream is suggested. The method is based on a conversion of the gas to synthesis gas and upgrading this synthesis gas into liquid hydrocarbons. But as the placement of such systems would be remote, the design has been performed using the following criteria. First of all the system has to be robust in design and secondly it has to be self-sustaining in that no additional feedstocks or chemicals are required for its operation and thirdly, the product should be crude oil compatible.

In the paper, the system has been outlined, the major unit operations designed and heat and mass balances have been determined. Six cases have been compared, differing in reforming and oxygen generation technology. The comparison has been made on both a technical and production economic premises. In each case the investment cost has been determined and from this, and the calculated produced hydrocarbons, a production cost per barrel has been determined.

The production of hydrocarbons well-head gas is a viable route and the production cost for the hydrocarbons vary between $71 and $156 a barrel, with the lower cost being quite attractive with the crude prices of recent years (around $100 a barrel). The production cost is however heavily influenced by the investment cost and the fact that the stranded natural gas is considered free. The production of an alternative, upgraded fuel would be a possibility; this however warrants additional investment in both production equipment and infrastructure.

1. Introduction

With increasing oil price and environmental concern, there is a driving force to better utilize the well-head gas in a more appropriate way. Well-head gas is the light, gaseous fraction of the crude oil which is released when extracting the oil from under ground; additional gas dissolved in the crude will be separated at the refinery, but that particular fraction is outside the scope of this study. The exploration of oil is, with several exemptions, performed in remote location. This circumstance will further challenge the upgrading of this particular feedstock to something useful. Being remote, a site-operator would be reluctant to bring in additional utilities or products for the upgrading and equally reluctant to arrange a separate distribution chain for transporting a second product from the site. Therefore, the method suggested in this paper has been designed from the following premises. First of all the system has to be robust in design to be able to handle the remote locations in which it has to be able to operate. Secondly, it has been designed to be self-sustaining in that no additional feedstocks or chemicals are required for its operation and thirdly, the product should be crude oil compatible. The suggested process is depicted in Fig. 1.

As can be viewed in Fig. 1, the gas extracted with the crude oil is sent to a processing unit for upgrading. This unit produces synthetic crude, heat and electricity via conversion of the gas to syngas and Fischer–Tropsch (FT) synthesis. The electricity and heat may be used locally and/or exported to the electrical grid, while the hydrocarbon waxes are mixed with the crude oil and moved from the site.

In this paper, the proposed system, based on two different types of syngas and oxygen generators, will be described and modelled using flow sheeting software. The model results will be used for assessing the system efficiency, as well as performing parametric studies for certain parameters. The heat and mass balance will also be used for assessing the investment and production cost of such a process.

* Corresponding author. Tel.: +46 46 2228273; fax: +46 46 2224526.
E-mail address: Christian.Hulteberg@chemeng.lth.se (C. Hulteberg).

1875-5100/$ – see front matter © 2013 Elsevier B.V. All rights reserved.
http://dx.doi.org/10.1016/j.jngse.2013.03.003

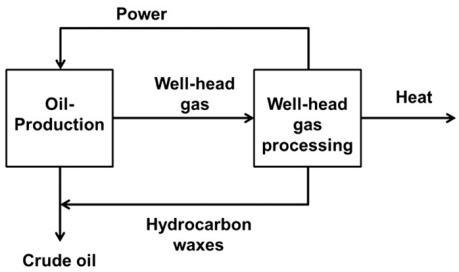

Fig. 1. An outline of the interactions of the suggested system.

2. Method

2.1. System description

As mentioned in the Introduction, the system design has been based on the assumption of a robust design and therefore only existing unit operations have been utilized. Fig. 2 shows a simplified process flow diagram of the system where some of the heat integration has been omitted for clarity. The system workhorse is a non-catalytic partial oxidation (POX) reactor operating at 1 MPa in which the well-head gas (stream 1) is converted to synthesis gas (stream 2) at 1573 K. The temperature is created by partial oxidation using oxygen or oxygen-enriched air (stream 7) and to increase the syngas production and lower the coke-formation potential, steam is added to the reactor (stream 6); the partial oxidation reactor will be described in more detail after the process description. The syngas is cooled and water condensed (stream 3) where after the water is separated (stream 4) and together with make-up water (stream 5) recycled to the POX reactor; the water stream is stripped to remove most of the sulphur before sending it back to the reactor.

After the water separation step, in which much of the sulphur is removed, the CO and H_2 are separated using a pressure swing adsorption (PSA) unit (stream 10). In the PSA, an additional tail-gas stream is created containing CO_2, H_2S as well as some CO and H_2 (stream 20). The syngas (stream 10) is sent to a gas clean-up unit in which the sulphur is removed using an adsorbent that may be regenerated (Sánchez et al., 2004). An active coal bed is used for removing other catalyst poisons; the system design is made to manage with one change of carbon per year. The now clean gas (stream 11) is sent to a compressor, which increases the pressure to 20 MPa before the gas is heated and sent to the FT reactor (stream 13). The effluent from the FT reactor is cooled and separated in a flash vessel where the heavy, liquid stream may be mixed into a crude oil stream (stream 15). The system utilises no recycle over the FT reactor, to simplify the system and make sure it is self-sustaining.

If air is used instead of oxygen, increased compression energy is required. Furthermore, the loss of light fraction in the FT product stream is greater when nitrogen is present. However, some nitrogen may be accepted. The oxidant used in the process (stream 7) is internally generated using either an electrolyser splitting water into hydrogen (stream 8) and oxygen a PSA producing 90% oxygen and 10% nitrogen, or a combination of electrolysis and air. For the combination of electrolysis and air, all the power produced, after syngas compression etc., is directed to the electrolyser to produce as much oxygen as possible. It is however not sufficient for reforming and balance in oxygen-demand is made up by compressed air. The hydrogen stream (when the system utilises electrolysis) is mixed with the light fraction from the post FT hydrocarbon separation (stream 16) and the syngas PSA off-gas (stream 20). This mixed stream (stream 17) is mixed with air (stream 18) and utilised for electricity generation in a combined cycle.

Two different non-catalytic reformers have been evaluated. The decision to use non-catalytic reformers was made to make the system as robust as possible for varying composition of the well-head gas. The most important component is sulphur as H_2S, as elevated levels will poison the catalysts normally used (usually nickel-based) for reforming. The traditional non-catalytic methane reformers are partial oxidation (POX) reactors that operate at a relatively high temperature (1473–1273 K). This is several hundred degrees above catalytic reformers which makes POX reactors less efficient as more energy is required for heating.

Regenerative reactors have been used extensively for the removal of volatile organic compounds (VOC) from air streams

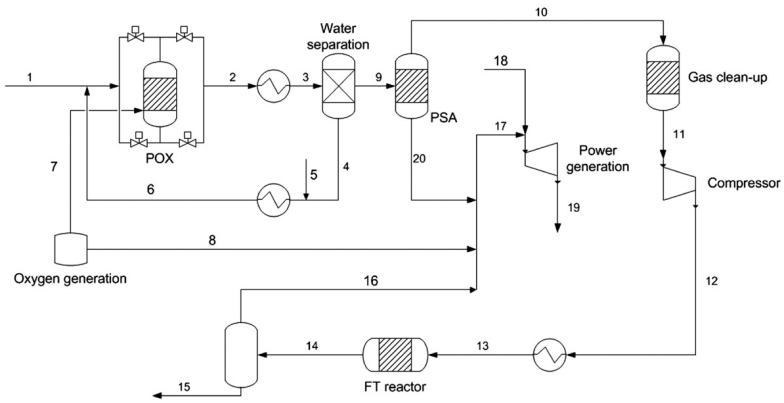

Fig. 2. Simplified process flow diagram.

(Boreskov and Matros, 1983; Matros et al., 1996; Neumann et al., 2004). Regenerative reactors operate as alternating flow direction reactors, meaning they never reach a steady state. By using a packed bed of granular material that acts as a heat buffer, the heat in the outgoing gases can be used to effectively heat up the ingoing gas when the flow direction is changed. In Fig. 3 the principal for the heat exchange is described. In the top figure a hot gas enters the cold heat buffer, thus cooling down the gas and, at the same time, heating up the buffer. As the hot gas flows through the buffer, it becomes gradually hotter as can be seen by the temperature profiles in the figure. When the thermal wave has reached the outlet of the buffer, flow direction is reversed and cold gas is flowed in the opposite direction. The cold gas is heated as it flows through the buffer and the buffer is consequently cooled down.

The regenerative reformer, or autothermal partial oxidation (APOX), has two of these thermal storages on each side of an oxidation/reaction zone. The incoming gas is heated by the buffer as it enters the oxidation zone. As the gas flows out, it is cooled down by the other buffer. When the gas flows, it pushes the heat from one side of the reactor to the other side and the gas always exits the reactor hotter than the inlet. By reversing the flow direction, the heat is pushed back into the reactor, keeping the heat in the center of the reactor where the temperature should be the highest.

The combination of the chemical robustness of POX and the high efficiencies of the reverse-flow operation enables the APOX to have efficiencies approaching catalytic reformers and at the same time be able to process gases rich in sulphur and other contaminants without prior cleaning.

2.2. Modelling

The modelling was performed using AspenTech's Aspen Plus® *2006.5* (2010) with NRTL (non-random two liquid) as the default property model, used for all unit operations except for the hydrocarbon separation. In the hydrocarbon separation case, the Peng–Robinson with Wong–Sandler mixing rule equation-of-state model was used instead; the physical property models were chosen based on Carlson (1996). In all cases, well-head gas with an equal amount of energy (100 MW) has been assumed to enter the system, 12.1 MMscfd, 11.1 MMscfd and 9.3 MMscfd for the gas compositions listed in Table 1. The electrolyser was modelled as a computation block, requiring 4.2 kWh per Nm^3/h of hydrogen

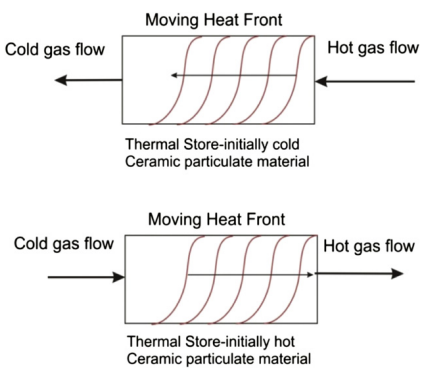

Fig. 3. Principal of regenerative autothermal partial oxidation reactor.

Table 1
Gas compositions used in the simulations (2012).

Gas component	Gas 1	Gas 2	Gas 3
CH_4	0.7	0.7	0.94
CO_2	0.08	0.08	0.02
N_2	0.05	0.02	0.01
H_2S	0.05	0.02	0
C_2H_6	0.07	0.1	0.02
C_3H_8	0.03	0.05	0.01
C_4H_{10}	0.02	0.03	0

produced (Kato et al., 2005; Saxe and Alvfors, 2007). The stream entering the water knock-out system is cooled to 275 K and close to 100% of the CO and 70% of the H_2 is recovered in the syngas pressure swing adsorber (Zhou et al., 2002); 100% of the nitrogen remains in the syngas Three gas compositions have been chosen for the simulation and they are summarised in Table 1 (2012).

The three gas compositions represent different conditions depending on where in the world the gas is available. The first gas has a high content of lower hydrocarbons, sulphur, nitrogen, carbon dioxide and a relatively low content of methane. The second gas composition contains less sulphur and nitrogen than the first composition, but more lower hydrocarbons. Finally the third gas composition is a gas with high methane content and small amounts of nitrogen, carbon dioxide and lower hydrocarbons.

Prior to synthesis, the gas is compressed using a multi-stage compressor with cooling to 343 K between stages and an isentropic efficiency of 0.72. The once-through Fischer–Tropsch synthesis is modelled using an Anderson–Schulz Flory distribution (Puskas and Hurlbut, 2003). The overall reaction can be summarised using the following model-reactions, where CH_2 represent a part of a hydrocarbon chain being lengthened:

$$CO + 2H_2 \rightarrow CH_2 + H_2O \quad (1)$$

$$2CO + H_2 \rightarrow CH_2 + CO_2 \quad (2)$$

The α-value in the Anderson–Schulz Flory distribution was set to 0.8, to result in longer chains and more wax and to decrease the formation of methane and lower hydrocarbons; the process is operated at 20 MPa. The separation of the product is modelled using a flash separation model at 275 K. The electricity generation is modelled as a combined cycle gas and steam turbine with an electrical efficiency of 35%. The process has been heat integrated to a reasonable degree and the required electricity for the electrolysis is produced on-site; for the cases that are short on electricity, some of the natural gas input is burnt to produce more electricity.

2.3. Economic assessment

To get a rough estimate on the investment cost for the proposed unit, literature data on similar systems have been used. The data from (Hamelinck et al., 2004) is originally derived for biomass gasification, but will be used also in this context as there are much similarities system-wise. Only the investment cost has been assessed here, as it is common practice to either flare or vent the well-head gas it is considered to be zero cost; in calculating the APOX investment cost, it has been assumed to be 50% higher than the POX investment cost. The depreciation has been set to 15 years with an 8% interest rate and 15% will be added in contingency. In all cases, the cost-of-production per barrel has been assessed using 8000 operating hours annually. The economic assessment is performed for APOX and POX for gas 1, a steam-to-carbon ratio of 2 and using both oxygen PSA and electrolyser (assuming zero net

electricity import). In addition, the cost of the electrolyser has been set to 600 €/kW (Hulteberg and Karlsson, 2009). The chemical engineering plant cost index has been used to update the investment costs to the 2011 cost level.

3. Results

3.1. Simulation

The model described in detail above has been used to quantify the system behaviour and the influence of several parameters on the system performance. The first parameter to be varied is the gas composition. The gas compositions in Table 1 were entered into the system at a fixed steam-to-carbon ratio of 2 in the partial oxidation reactor. The results of these simulations are depicted in Fig. 4.

Starting with oxygen generated from electrolysis it can be derived from Fig. 4 that about 21% of the energy fed to the system is recovered as useful hydrocarbon product when using the APOX reactor, with gas composition 1 and 2 showing similar result and gas composition 3 showing slightly lower yields of hydrocarbon product. No electricity can be exported when utilising electrolysis for oxygen generation. Comparing this case to the POX case, it is obvious that a lower production of hydrocarbons is at hand. The output of the unit is only 13 MW which is significantly lower than for the APOX. The POX requires more oxygen and as a result more natural gas needs to be burnt to produce electricity for electrolysis.

If a PSA is used to produce a gas with 90% oxygen and 10% nitrogen to use as oxidiser, the results changes significantly. The electricity cost associated with electrolysis is circumvented and a net power production is possible. There is also much less difference between the POX and APOX in the hydrocarbon production, reaching about 25–26 MW and 27–29 MW respectively. In addition, there is about 8–9 MW of electricity available for export in the POX PSA case and 13 MW in the APOX PSA case, making the latter the case of the highest overall efficiency (above 40% on an MW basis).

The last case studied, combined electrolysis and air, there is zero export of electricity. But the hydrocarbon production is much higher than for electrolysis only. The efficiency to hydrocarbon for the POX almost doubles from 13 to 25 MW. For APOX a similar trend is seen, even though the increase is smaller, going from about 21 to 29 MW. Another important parameter in the operation of the system is the steam-to-carbon ratio, the effects of varying this is depicted in Fig. 5.

As can be viewed in Fig. 5, there is a negative effect on hydrocarbon production when increasing the steam-to-carbon ratio. The output of hydrocarbon waxes decrease by some 10% when changing the steam-to-carbon ratio from 2 to 3. This is due to an increased production of hydrogen, more than necessary for the production of Fischer–Tropsch waxes. The increased H_2 production is the result of the water–gas shift reaction in the reformer, yielding more H_2

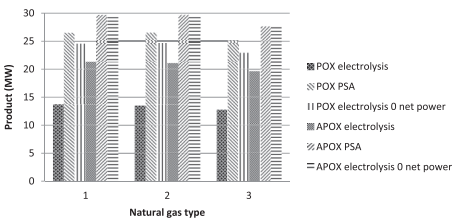

Fig. 4. Output from the model with respect to produced hydrocarbon wax and electricity for all cases and for different natural gas composition.

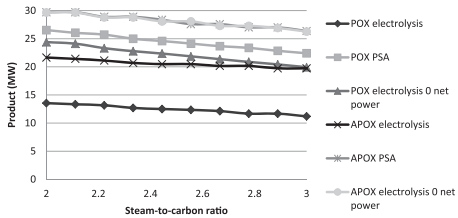

Fig. 5. Output from the model with respect to produced hydrocarbon wax and electricity as a function of steam-to-carbon ratio for the studied cases.

with more steam present. The H_2/CO ratio for the higher steam-to-carbon ratios was above 2 and closer to 2.5. Increasing the steam-to-carbon ratio has positive effect on electricity production as is evident for the PSA cases that have surplus electricity. As the hydrocarbon production goes down, due to increased H_2 and decreased CO contents in the gas, more energy is available for electricity production. Fig. 6 shows the variation of the oxygen content in the stream from the PSA.

As Fig. 6 shows, increasing the oxygen content in the oxygen stream from that in air (20%) to 100% purity has a positive effect on both systems. The gain is greater for the POX, as it requires more oxygen, increasing the hydrocarbon yield from 270 bbl/day (18 MW) to almost 406 bbl/day (27 MW). For the APOX the increase in hydrocarbon production is from 376 bbl/day (25 MW) to 436 bbl/day (29 MW). The increase in hydrocarbon production is a result of less inert in the syngas which results in lower losses during separation. The stream is compressed from 0.13 MPa to the system pressure of 1 MPa and a higher oxygen purity results in a decreased compression work as the stream contains less mass. The POX system is self-sustaining on electricity with an oxygen purity of about 25% but every increase in purity increases the hydrocarbon production as well as the electricity surplus. The APOX is always producing more electricity than is required and increasing oxygen purity has about the same effect on the hydrocarbon production as on the available electricity export.

3.2. Economic evaluation

In the following section the results from the economic evaluation will be reported. Four cases have been assessed with respect to economic performance and they are the cases without any electricity import requirement: APOX PSA, POX PSA, APOX with zero

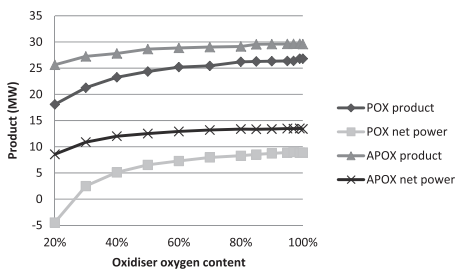

Fig. 6. Product output and electricity surplus for the POX and APOX when using a PSA with a product containing varying oxygen purity.

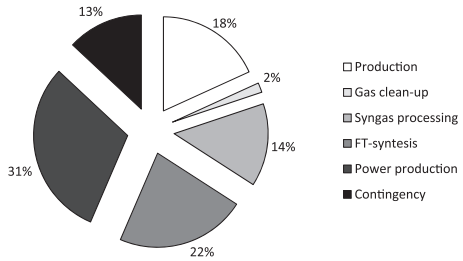

Fig. 7. The investment-cost distribution in the POX PSA case.

external electricity to electrolysers and POX with zero external electricity to electrolysers. The overall investment cost of the systems vary from 197 million € in the POX PSA case to 251 million € in the APOX with zero external cost to electrolyser case. The investment costs in the POX PSA case have been broken down in Fig. 7

The cases with the use of electrolysers (with zero external electricity) in general show higher production costs than the ones without electrolysers. First of all, the electrolyser is a quite costly unit operation. Secondly, since the electricity generated is not enough for producing pure oxygen, the amount of product produced from the natural gas entering the system is lower as the nitrogen balance causes product losses to the combustion. Interestingly, the lower the oxygen content of the oxidant stream the higher the oxygen requirement in the POX/APOX. The system thus have a negative feedback, it is however not that severe, Fig. 6.

When comparing the costs of the different systems, the most relevant production metric is the cost per barrel-of-oil-equivalent produced. Using 15 years and 8% interest rate as the depreciation conditions, the production cost of the various alternatives can be calculated as per Fig. 8.

Again it is clear that the cases where oxygen production using PSA is utilised, a significantly lower production cost is achieved. In the PSA cases, both show similar costs of production ($71 a barrel (bbl)) and with the precision of these calculations, these cases cannot be separated. It is however clear that the APOX electrolyser ($112 a bbl) and POX electrolyser ($156 a bbl), both with zero external electricity addition, are significantly higher in production cost. This despite the relatively low difference in investment cost (12% difference between highest and lowest); however the amount of product varies significantly between the cases. The cases with PSA also have electricity readily available for export (should it be possible from a remote location), with the APOX PSA case being able to export 60% more electricity than the POX PSA case. Taking the electricity export into account using half of the industrial average price of the 27 member states of the European Union (47 €/MWh (2012)), the production costs drop to $60 a bbl in the POX PSA case and $58 a bbl in the APOX PSA case (from the original $71 a bbl). Since the production cost scales linearly with the sales price of electricity the production cost at a given electricity price may be derived using the above information. There is thus a significant impact in the possible sale of electricity, but it does not differ that much between the cases.

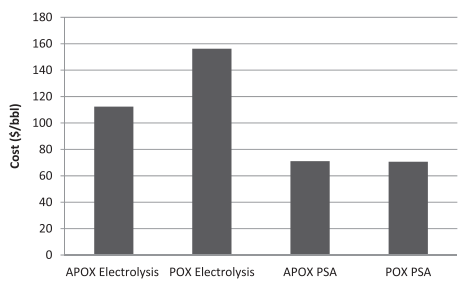

Fig. 8. The production cost of the various alternatives.

4. Discussion and conclusions

The production of hydrocarbons from stranded natural gas is a viable route to utilise the well-head gas that is usually flared. The production cost for the hydrocarbons vary between $71 and $156 a bbl, with the lower cost being quite attractive with the crude prices of recent years (around $100 a bbl). The production cost is however heavily influenced by the investment cost and the fact that the stranded natural gas is considered free. Another factor that influence the cost-of-production is the potential sale of electricity, which further reduce the best options by about $10 a bbl. With respect to production efficiency, the systems perform quite differently and range from 12 to 30% in hydrocarbon efficiency (on a heat basis) and the best system from an efficiency point of view (APOX PSA) has above 40% in overall efficiency.

The system has been designed to be as robust as possible, able to handle varying gas composition and with as few unit operations as possible. A non-catalytic reformer allows conversion of natural gas with several per cent of sulphur present. The composition of the syngas after the reformer has a favourable ratio of H_2:CO at almost 2:1 meaning that no water–gas shift reactor is necessary. A water–gas shift reactor could operate with the levels of sulphur available (Hinrichsen et al., 2008) and that may be the route to choose as the natural gas composition could vary over time. The water–gas shift reactor would then be able to keep the H_2:CO somewhat constant even though the ratio is changing after the reformer.

The chosen plant size is relatively small and that is reflected in the production cost. A larger plant benefits by economy-of-scale with a lower relative capital cost and thus a lower production cost. The determining factor for the plant size is how much well-head gas that is available. For the studied cases with a PSA, electricity can be exported if there is a need for it in the vicinity. That is not a guarantee, with oil wells being in remote locations with, if any, limited infrastructure. The electricity surplus could be used to support the oil production at the wells to reduce the need for alternative electricity generation. If electricity is produced from natural gas, that gas can be directed to the plant to produce more hydrocarbons and still produce sufficient electricity.

Electrolysis is a costly alternative for oxygen production and if the hydrogen produced cannot be utilised in a more valuable way than in electricity production, it is too costly. The case that utilise electrolysis coupled with compressed air is almost as good as using a PSA, depending on the system studied. This may be the most attractive route if there is a need for the hydrogen produced in the electrolyser. One such need would be in the upgrading of the produced waxes to transport fuel (de Klerk, 2011). The production of an alternative, upgraded fuel would however warrant additional investment in both production equipment and infrastructure.

Acknowledgements

The financial support of the Swedish Gas Centre, Statoil, Göteborg energi and E.On are greatly acknowledged.

References

Aspen Plus – AspenTech, 2010. http://www.aspentech.com/core/aspen-plus.aspx (25.02.10).

Boreskov, G.K., Matros, Y.S., 1983. Flow reversal of reaction mixture in a fixed catalyst bed – a way to increase the efficiency of chemical processes. Appl. Catal. 5 (3), 337–343.

Carlson, E.C., 1996. Don't gamble with physical properties for simulations. Chem. Eng. Prog. 10, 35–46.

de Klerk, A., 2011. Refining Technology Selection, Fischer–Tropsch Refining. Wiley-VCH Verlag GmbH & Co. KGaA. pp. 301–334.

Eurostat, 2012. http://epp.eurostat.ec.europa.eu/portal/page/portal/eurostat/home (11.07.12).

Hamelinck, C.N., Faaij, A.P.C., den Uil, H., Boerrigter, H., 2004. Production of FT transportation fuels from biomass; technical options, process analysis and optimisation, and development potential. Energy 29, 1743–1771.

Hinrichsen, K.-O., Kochloefl, K., Muhler, M., 2008. Water Gas Shift and COS Removal, Handbook of Heterogeneous Catalysis. Wiley-VCH Verlag GmbH & Co. KGaA.

Hulteberg, P.C., Karlsson, H.T., 2009. A study of combined biomass gasification and electrolysis for hydrogen production. Int. J. Hydrogen Energy 34 (2), 772–782.

Kato, T., Kubota, M., Kobayashi, N., Suzuoki, Y., 2005. Effective utilization of by-product oxygen from electrolysis hydrogen production. Energy 30, 2580–2595.

Matros, Y.S., Bunimovich, G.A., Patterson, S.E., Meyer, S.F., 1996. Is it economically feasible to use heterogeneous catalysts for VOC control in regenerative oxidizers? Catal. Today 27 (1–2), 307–313.

Naturalgas.org, 2012. http://www.naturalgas.org/overview/background.asp (09.07.12).

Neumann, D., Kirchhoff, M., Veser, G., 2004. Towards an efficient process for small-scale, decentralized conversion of methane to synthesis gas: combined reactor engineering and catalyst synthesis. Catal. Today 98 (4), 565–574.

Puskas, I., Hurlbut, R.S., 2003. Comments about the causes of deviations from the Anderson–Schulz–Flory distribution of the Fischer–Tropsch reaction products. Catal. Today 84 (1–2), 99–109.

Sánchez, J.M., Ruiz, E., Otero, J., 2004. Selective removal of hydrogen sulfide from gaseous streams using a zinc-based sorbent. Ind. Eng. Chem. Res. 44 (2), 241–249.

Saxe, M., Alvfors, P., 2007. Advantages of integration with industry for electrolytic hydrogen production. Energy 32, 42–50.

Zhou, L., Lu, C.Z., Bian, S.J., Zhou, Y.P., 2002. Pure hydrogen from the dry gas of refineries via a novel pressure swing adsorption process. Ind. Eng. Chem. Res. 41, 5290–5297.

Paper VIII

BIOMASS AND BIOENERGY 40 (2012) 174–180

Available online at www.sciencedirect.com

SciVerse ScienceDirect

http://www.elsevier.com/locate/biombioe

Synergies from combined pulp&paper and fuel production

Per Tunå [a], *Christian Hulteberg* [a,*], *Jens Hansson* [b], *Anders Åsblad* [c], *Eva Andersson* [c]

[a] *Department of Chemical Engineering, Faculty of Engineering, Lund University, Box 124, 22100 Lund, Sweden*
[b] *Nordlight AB, Limhamn, Sweden*
[c] *CIT Industriell Energi AB, Göteborg, Sweden*

ARTICLE INFO

Article history:
Received 13 February 2011
Received in revised form
20 February 2012
Accepted 22 February 2012
Available online 10 March 2012

Keywords:
Fuel synthesis
Paper
Pulp
Gasification
Biomass
Integration

ABSTRACT

In this paper, the prospect of integrating a combined paper&pulp mill with fuel production via biomass gasification was investigated. In the study, three different types of gasifiers (circulating fluidised bed, entrained flow and indirect gasification) and three fuel processes (dimethyl ether, methanol and Fischer-Tropsch wax synthesis) were investigated using computer simulations. The paper reports differences from the stand-alone cases and the integrated cases, using the electricity equivalence efficiency as a measure.

Only 6 out of the 18 integrated cases studied displayed a positive result from integration and no obvious fuel selection that stand out as the most beneficial one, however the synthesis of dimethyl ether is, in combination with all gasifiers assessed a rather good choice, with an change in efficiency from integration ranging from −1% to 4%.

Dimethyl ether is not the best choice if the electrical equivalence is to be maximised however. In this case the combination of circulating fluidised bed gasification and methanol synthesis should be pursued. The production of Fischer-Tropsch wax should according to the chosen measure not be produced; however there is an added value in the production of a non-oxygenated fuel which has not been taken into account in this particular study.

All cases leads to a reduction of 0.4–0.9 kg CO_2 per kg of dry biomass used in the process for fuel synthesis and the possibility to export bark is a more significant factor in this respect than which type of fuel is synthesised.

1. Introduction

There is an unprecedented drive for the production of fuels from renewable resources in the world today due to the current interests and tax incentives put in place by various governments following e.g. EU recommendations [1]. The suggested production methods include both thermo-chemical and bio-chemical pathways; in this study only thermo-chemical pathways are considered. This type of biofuels produced are usually designated advanced or second generation biofuels and claim benefits within several major regulations within the US and EU. There have been numerous studies performed on the feasibility of the production of fuels from biomass through gasification [2,3]. In most cases these have been considered as stand-alone units, without the benefits of process integration; an exception is black liquor gasification studied in both scientifically and experimentally [4].

It is however believed that integration with existing biorefineries, in the form of paper and pulp production units, may yield benefits; at least in some process configurations. Combined paper and pulp mills are characterized in that they

* *Corresponding author*. Tel.: +46 733 969420.
E-mail address: Christian.Hulteberg@chemeng.lth.se (C. Hulteberg).
0961-9534/$ – see front matter © 2012 Elsevier Ltd. All rights reserved.
doi:10.1016/j.biombioe.2012.02.020

are net energy importing, or at a minimum energy neutral, due to the heat required for the drying of paper. These integration effects may, aside from logistics benefits, be found in the exchange of heat, utilities and possibly byproducts. In the EU funded project RENEW [5], several gasification technologies were compared with respect to the production of liquid fuels and the case of black liquor gasification came out looking strong. The question is if this is due to actual technology benefits or due to the tight process integration for that process.

The here performed modeling-based study addresses the issue of integration of fuel production via thermo-chemical conversion of biomass with pulp and paper production. It compares a number of different gasification technologies, ranging from indirectly heated and entrained flow to fluidized bed gasifiers, in combination with synthesis of methanol, di-methyl ether and Fischer Tropsch diesel. A simplified process schematic is depicted in Fig. 1.

2. Simulation

The integration model constitutes a pulp and paper mill and a gasification unit followed by one of the fuel synthesis processes, be it methanol, di-methyl ether or Fischer-Tropsch wax/fuels. The choice of scale was determined by the size of the gasifier relative to the pulp and paper mill. With this in mind 200 MW (thermal) feed of biomass with 50% water content by weight was chosen. It is also a scale which does not impose too much on the logistic situation of a mill of this size and that fits the currently available state-of-the-art biomass gasifiers; as single or parallel reactor trains.

The pulp and paper mill modeling was performed using Balas [6] and the gasification and fuel synthesis model using Aspen Plus® [7], both applications support import/export of data via Microsoft Excel and this was used for data transfer between the models, Fig. 2.

The pulp and paper mill used in the calculations is an integrated mill producing fine paper [8]. The data is from a model of a modern, energy efficient chemical pulp mill. The mill size is equal to larger pulp mills in Sweden and the model is based on the model mill used in the Eco-cyclic pulp mill project KAM, completed in 2001 [9,10]. Both soft and hardwood pulp is produced at the pulp mill. The fine paper furnish consists of 19% bleached softwood, 56% bleached hardwood pulp and 25% filler.

The daily production of paper is 3000 tonne (moisture content of paper is 7%, normally designated T_{93}) and, with estimated 355 production days, the annual production is 1 065 000 tonne. Pulp production is done in campaigns and can be 2000 tonne (air dried tonne, 10% water content by weight) per day of softwood or 2500 tonne per day of hardwood.

Integrated pulp and paper mills usually have a steam demand that exceeds the steam production from internal fuels, and would benefit from integration with a facility with surplus steam, such as the gasification unit. Since the chosen pulp and paper mill is quite energy efficient it does not have to import fuel for steam production but uses internal biomass to generate heat for the process (consumes approximately 65% of the average Swedish mill [9]). In this case, integration could make it possible to generate byproducts for sale instead. This means that the results of the integration are conservative, and for a less energy efficient pulp and paper mill the integration would result in more energy savings.

The pulp and paper mill uses only internal fuels (black liquor and bark) for steam production. Steam is used in the process and for electricity generation, but the electricity production does not cover the mill's demand. Gasified bark is assumed to be used as a fuel in the lime kiln. Bark is also used as a fuel in a separate power boiler since not enough process

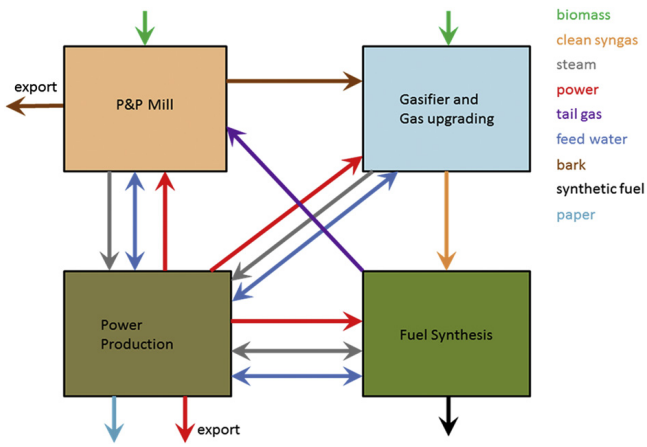

Fig. 1 – Simplified process layout for the integrated system, the bark can be either gasified or sold depending on the ability to handle bark as a gasification feedstock.

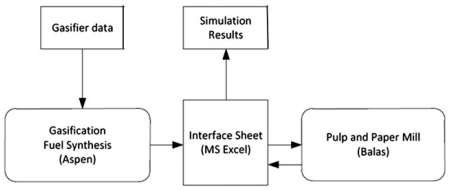

Fig. 2 – Simulation interface.

steam is generated in the recovery boiler. In the modelled pulp and paper mill there is still some bark surplus. Data for the integrated pulp and paper mill is given in Table 1.

The models for fuel synthesis were performed in Aspen-Tech's *Aspen Plus® 2006.5* and the gasifier was modelled as an energy/material balance, with the input data shown in Table 2 [11]. The actual gasifier was not modelled in itself, instead the models used the exit composition of demonstration-scale gasifiers as the starting point of the model. The synthesis models include; three different types of gasifiers (circulating fluidized bed (CFB), entrained-flow gasifier (EF) and indirectly heated fluidized bed gasifier (ID)) sulphur removal, reforming (for CFB and ID), water-gas shift, fuel synthesis (methanol (MeOH), Fischer-Tropsch diesel (FT) or di-methyl ether (DME)), and product upgrading and heat recovery. Oxygen consumed is assumed to be synthesised on-site through cryogenic separation and the energy consumed is included in the calculations.

For the reforming, additional oxygen is consumed and the sulphur removal is achieved with a zinc oxide bed reactor [12]. The gas exits the gasifiers with a H_2/CO ratio ranging from 0.4 to 1.8 depending on the gasification technology utilised. The H_2/CO-ratio for synthesis modelled in this study is set to 2, which thus requires a water-gas shift reactor operating at 603–723 K depending on the H_2/CO-ratio of the ingoing gas.

Table 1 – Key figures for the integrated pulp and paper mill.

	Unit	Softwood	Hardwood
Wood input (incl bark) dry weight	kg s^{-1}	51.4	60.5
Wood input (incl bark) LHV	MW	875	1029
Bark input	MW	76	139
Pulp output	tonne day^{-1}	2000	2500
Black liquor output	MW	465	475
Fresh water in	tonne h^{-1}	3313	3160
Power use	MW	115	119
Power generated	MW	102	98
Steam levels HP	MPa	8.1	8.1
MP2	MPa	2.6	2.6
MP	MPa	1.1	1.1
LP	MPa	0.45	0.45
Steam use MP	tonne h^{-1}	91	110
Steam use LP	tonne h^{-1}	381	411
Paper production (t_{93})	tonne day^{-1}	3000	

Table 2 – Model input data [11].

		CFB	EF	ID
Gas Output Properties				
CO	volume fraction percent	13.7	45.6	17.3
CO_2	volume fraction percent	22.3	5.77	12.3
H_2	volume fraction percent	24.9	19.7	29.4
H_2O	volume fraction percent	27.1	28.7	32.2
CH_4	volume fraction percent	11.8	0	8.7
C_2H_4	volume fraction percent	0	0	0
C_2H_6	volume fraction percent	0	0	0
C_3H_8	volume fraction percent	0	0	0
N_2	volume fraction percent	0.1	0.1	0.1
Temperature	K	1123	1573	1123
Pressure	MPa	1	0.7	0.1
Gasifier Output Mass Flow	kg s^{-1}	17.5	18.1	15.2
Quench Temperature	K	983	983	983
Oxygen Feed	kg s^{-1}	2.22	5.85	0
Steam into Gasifier	kg s^{-1}	5.66	0	3.81
Biomass Input	MW	200	200	200

The reactor is controlled by inlet temperature, amount of bypass and steam injection (when necessary). Prior to synthesis, the gas is compressed using a multi-stage compressor with inter-cooling to 343 K and an isentropic efficiency of 0.72.

All synthesis reactions are highly exothermic and steam is generated from the released energy. Fischer-Tropsch synthesis is modelled with the Anderson-Schulz Flory distribution [13]. The overall reaction can be summarised with the following pseudo-reactions where CH_2 symbolizes a part of the hydrocarbon chain:

$$CO + 2H_2 \rightarrow CH_2 + H_2O \quad (1)$$

$$2CO + H_2 \rightarrow CH_2 + CO_2 \quad (2)$$

The α-value, i.e. the distribution of the chain-length for the hydrocarbons formed, in the Anderson-Schulz Flory distribution was set to 0.85 to produce longer chains and more wax and to reduce the formation of methane and lower hydrocarbons; the process is operated at 20 MPa. The separation of the product is modelled as a flash separation at 293 K. The point-of-separation between liquid and vapour fraction lies between C_6 and C_7 with the majority of the C_6 and shorter chain-length hydrocarbons in the vapour phase, along with un-reacted synthesis gas and carbon dioxide, and the majority of the C_7 and higher hydrocarbons in the liquid-phase.

Methanol synthesis from synthesis gas is equilibrium constrained. The reactions (3 and 4) are carried out over a water-gas shift active catalyst, typically copper, zinc oxides and chromium [14]. The synthesis requires a certain amount of carbon dioxide. The model uses an equilibrium reactor at 10 MPa with 0.8 MPa of pressure drop. The inlet temperature is regulated to keep the exit temperature at 533 K.

$$CO + 2H_2 \rightarrow CH_3OH \quad (3)$$

Table 3 – The simulated cases.

Name	Gasifier	Product	Integrated/ Stand a lone	Bark use	Steam system
1 CFB_MeOH_SA	CFB	Methanol	Stand Alone	N/A	Power Gen
2 CFB_DME_SA	CFB	DME	Stand Alone	N/A	Power Gen
3 CFB_FT_SA	CFB	FT Fuels	Stand Alone	N/A	Power Gen
4 CFB_MeOH	CFB	Methanol	Integrated	Gasified	To P & P Mill
5 CFB_DME	CFB	DME	Integrated	Gasified	To P & P Mill
6 CFB_FT	CFB	FT Fuels	Integrated	Gasified	To P & P Mill
7 CFB_MeOH_B	CFB	Methanol	Integrated	Exported	To P & P Mill
8 CFB_DME_B	CFB	DME	Integrated	Exported	To P & P Mill
9 CFB_FT_B	CFB	FT Fuels	Integrated	Exported	To P & P Mill
10 ID_MeOH_SA	Indirect	Methanol	Stand Alone	N/A	Power Gen
11 ID_DME_SA	Indirect	DME	Stand Alone	N/A	Power Gen
12 ID_FT_SA	Indirect	FT Fuels	Stand Alone	N/A	Power Gen
13 ID_MeOH	Indirect	Methanol	Integrated	Gasified	To P & P Mill
14 ID_DME	Indirect	DME	Integrated	Gasified	To P & P Mill
15 ID_FT	Indirect	FT Fuels	Integrated	Gasified	To P & P Mill
16 ID_MeOH_B	Indirect	Methanol	Integrated	Exported	To P & P Mill
17 ID_DME_B	Indirect	DME	Integrated	Exported	To P & P Mill
18 ID_FT_B	Indirect	FT Fuels	Integrated	Exported	To P & P Mill
19 EF_MeOH_SA	Entrained Flow	Methanol	Stand Alone	N/A	Power Gen
20 EF_DME_SA	Entrained Flow	DME	Stand Alone	N/A	Power Gen
21 EF_FT_SA	Entrained Flow	FT Fuels	Stand Alone	N/A	Power Gen
22 EF_MeOH	Entrained Flow	Methanol	Integrated	Gasified	To P & P Mill
23 EF_DME	Entrained Flow	DME	Integrated	Gasified	To P & P Mill
24 EF_FT	Entrained Flow	FT Fuels	Integrated	Gasified	To P & P Mill
25 EF_MeOH_B	Entrained Flow	Methanol	Integrated	Exported	To P & P Mill
26 EF_DME_B	Entrained Flow	DME	Integrated	Exported	To P & P Mill
27 EF_FT_B	Entrained Flow	FT Fuels	Integrated	Exported	To P & P Mill
28 P & P SA	–	–	Stand Alone	Exported	–

$$CO_2 + 2H_2 \rightarrow CH_3OH + CO \quad (4)$$

The equilibrium conversion is to low and a high recirculation-ratio is necessary for a sufficient overall conversion, typically around 5 [15]. The methanol distillation is modelled at 0.34 MPa using a molar reflux-ratio of 1.5 over 60 trays [15]. The model uses a partial-vapour condenser and a kettle reboiler. The reboiler duty was set to achieve 97% methanol recovery. The product stream contains a weight fraction of 0.90 of methanol with the remainder mostly carbon dioxide.

DME, is synthesized in an adiabatic reactor at 573–673 K [15] and 10 MPa.

$$2CH_3OH \rightarrow CH_3OCH_3 + H_2O \quad (5)$$

The DME synthesis is an addition to the methanol synthesis and uses methanol from the methanol distillation column. The reactor is modelled as an equilibrium reactor with 0.8 MPa pressure drop. The inlet temperature is regulated to 300 °C which allows the reactor outlet to reach over 400 °C. DME is separated from methanol and water by distillation at 1.1 MPa with a molar reflux-ratio of 20 and 40 trays [15,16].

The un-reacted synthesis gas and a part of the product that is not recovered in the separation are burnt. The gas, tail gas, has a low to moderate heating value, consisting mainly of carbon dioxide. Steam is generated as the gas is combusted and the remaining heat is used for drying of the biomass.

When the gasifier is integrated with the pulp and paper plant, there are several options for exchange of material. In the pulp and paper mill base case, bark is gasified and the product gas is used in the lime kiln. When the pulp and paper mill is integrated with the fuel production unit, the gasified bark can be replaced with tail gas from the fuel production process. The tail gas has to reach a combustion temperature of at least 1500 °C to be able to drive the process in the lime kiln where $CaCO_3$ is calcined to CaO [17]. One of the benefits of the integrated plant is the use of the energy containing tail gas. The tail gas could replace fossil oil if supplied in sufficient quantity and quality, assuming that fossil oil is used for heating purposes in the investigated paper and pulp mills. The tail-gas composition can be modified to reach the necessary temperature at the cost of less fuel produced. Bark is used in a biofuel boiler for steam production if the recovery boiler cannot supply enough steam for the process. Surplus bark can either be used as raw

Table 4 – Key conversion factors used in CO_2 emission calculations.

Component	Replaces	CO_2 g MJ^{-1}	Reference
Methanol	Gasoline	72.5	[18]
DME	Diesel	73.9	[18]
FT Wax	Diesel	73.9	[18]
Bark	Natural Gas	56.9	[19]
Hot Water	District Heating (Sweden)	25	[20]
Power	Power mix for Sweden	4.7	[18]
Biomass	–	2.2	[21]

Table 5 – The integration cases with positive of negative effects higher than 1%.

Name	Gasifier	Product	Integrated/Stand alone	Bark use	Steam system
4 CFB_MeOH	CFB	Methanol	Integrated	Gasified	To P & P Mill
7 CFB_MeOH_B	CFB	Methanol	Integrated	Exported	To P & P Mill
5 CFB_DME	CFB	DME	Integrated	Gasified	To P & P Mill
8 CFB_DME_B	CFB	DME	Integrated	Exported	To P & P Mill
6 CFB_FT	CFB	FT Fuels	Integrated	Gasified	To P & P Mill
13 ID_MeOH	Indirect	Methanol	Integrated	Gasified	To P & P Mill
16 ID_MeOH_B	Indirect	Methanol	Integrated	Exported	To P & P Mill
14 ID_DME	Indirect	DME	Integrated	Gasified	To P & P Mill
17 ID_DME_B	Indirect	DME	Integrated	Exported	To P & P Mill
15 ID_FT	Indirect	FT Fuels	Integrated	Gasified	To P & P Mill
22 EF_MeOH	Entrained Flow	Methanol	Integrated	Gasified	To P & P Mill
25 EF_MeOH_B	Entrained Flow	Methanol	Integrated	Exported	To P & P Mill
24 EF_FT	Entrained Flow	FT Fuels	Integrated	Gasified	To P & P Mill
27 EF_FT_B	Entrained Flow	FT Fuels	Integrated	Exported	To P & P Mill

material in the gasification unit or sold as biofuel. In Table 3, the different simulation cases have been compiled.

In Table 4 the emissions from each energy source is presented as CO_2 g MJ^{-1}. Figures for the fossil-based vehicle fuels and natural gas are the emissions at the exhaust pipe, not including emissions during production and refining. The power mix for Sweden is calculated as the weighted average CO_2 emission for all electricity production in Sweden.

3. Results

Using mixed energy carriers in efficiency calculations are helpful, but not necessarily an appropriate indicator of the "best" system. The electricity equivalents method is therefore used in this paper to represent the overall exergy of the system and they are calculated using power generation efficiencies, using the best technology to the knowledge of the author's, as described in Appendix A. The resulting overall efficiency of the system, on electricity equivalents basis, is designated η_{el} eqiv below [18].

As depicted in Fig. 1, an integrated system is created out of two stand-alone processes. This creates the need of comparing the difference in use and production of components instead of setting up a complete balance. For every integrated case simulated, the changes in material, utility and product streams compared to the base case of a stand-alone pulp and paper mill are calculated and an incremental figure is acquired. To reduce the number of cases, only the cases where significant impact, more than ±1% on an exergy basis, compared to the base case will be reported; Table 5 show the down-selected simulation cases.

In Fig. 3 the electricity equivalent efficiencies are shown for the cases with significant changes. Lower quality heats are in this case of lower value and this show up in the total; no economical evaluation for the comparability of the different energy carriers has been performed in this study, only the electricity generation potential has been evaluated.

As can be viewed in the figure, the use of CFB gasification in combination with MeOH synthesis yields the highest equivalent efficiencies and in the configurations in which export of bark is possible, it has a significant contributing factor to the overall electricity equivalent efficiency. It is also clear that there is no category of fuels, or indeed gasifiers that stand out as a clear winner. The entire system has to be investigated and validated for a particular situation before choosing technology. To relate the integrated and stand-alone gasifier/fuel process to each other, the efficiencies are compared to the stand-alone cases as shown in Fig. 4. The deviation is calculated by dividing the electricity equivalent efficiency for the non-stand-alone case with the electricity equivalent efficiency for the stand-alone case.

As depicted, there are only a few cases actually leading to a significant benefit in the integration of the two processes,

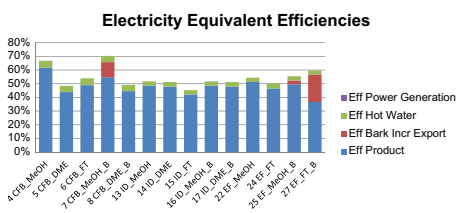

Fig. 3 – Electricity equivalent efficiencies for the chosen cases.

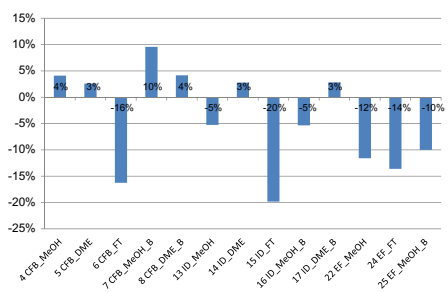

Fig. 4 – The bars show the deviation of the integrated systems from their stand-alone equivalents.

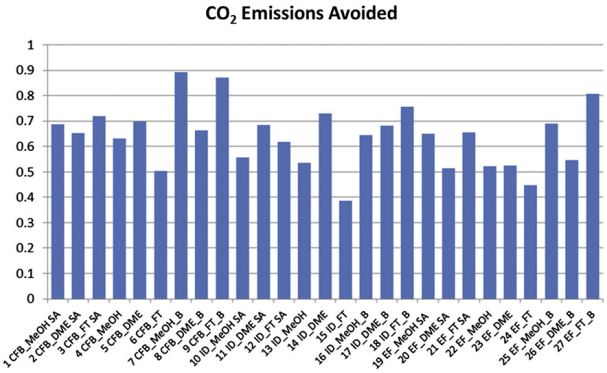

Fig. 5 – Calculated reduction of CO_2 emissions by the use of the respective simulation case in kg CO_2 per kg of biomass.

gasification and paper and pulp production. Using a CFB gasifier and producing methanol, with and without bark export, is a good alternative with savings in the 4–7% range. It is also, from an efficiency standpoint, a good idea to integrate the production of DME with the use of either a CFB or ID gasifier, both if bark is or is not exported. The reason for this high performance of the integrated systems with MeOH and DME is the need for low-quality heat in the distillation of the MeOH. Another interesting finding from the study is that out of the 18 integrated cases, only 6 of them yielded a significant benefit. Some of the cases even showed a lower efficiency when integrated than the systems independent from each other. Worst in this respect was the production of FT with ID, CFB and EF gasification respectively.

A brief inventory of the net CO2 emissions avoided by the use of each simulation cases was done. In this, key conversion factors (as shown in Table 4) were utilised as well as the annual incremental production/consumption of the components. The results are displayed in Fig. 5.

All of the studied cases lead to a reduction of CO_2 of 0.4–0.9 kg CO_2 per kg of dry biomass, where the cases allowing for bark export peak the chart. One of the factors which were not taken into account in the CO_2 calculations were the savings in transports for bark which is used onsite, instead of exported from the site. The possibility to export bark is more significant than which type of fuel is produced and the second most important factor in the reduction seems to be the use of a CFB gasifier; also synthesising DME seems to lower the emissions of CO_2 to a higher degree than the other fuels.

4. Conclusions

After performing this study, it can be concluded that there is not one given answer to the possibilities and advantages with integrating paper and pulp production with thermo-chemical conversion of biomass to vehicle fuels. In some instances there are advantages with the integration, but this is definitely not the case in all instances. Indeed only 6 out of the 18 integrated cases studied displayed a positive result from integration, when using electrical equivalence efficiency as the metric of comparison; however they boil down to three cases with and without bark export. In addition, 5 cases showed no significant added benefit of integration and 7 cases displayed a negative behaviour as a function of integration. There is no obvious case that stand out as the most beneficial in the calculations, however the synthesis of DME is in all cases assessed a rather good choice; with a change in efficiency from integration ranging from −1% to 4%; this may be attributed to the need of low-quality heat needed in the distillation of methanol.

DME is not the best choice if the electrical equivalence is to be maximised however. In this case the combination of CFB and methanol synthesis should be pursued, if possible with the export of bark increasing the increase from 4% to 10%. The production of FT should according to the chosen measure not be produced; however there is an added value in the production of a non-oxygenated fuel which has not been taken into account in this particular study. The synthesis of DME or MeOH comes out differently depending on the availability of heat for the distillation, which explains why some MeOH cases are better and some worse than their DME counterpart.

The gasifier that has the lowest overall performance is the entrained flow. This may be explained by the loss of sensible heat in the outgoing gas stream due to quenching with water. It is advisible that for considering an entrained flow gasifier to quench the heat with additional coal or biomass addition instead of water. However, this will result in different operational challenges that will have to be addressed.

It can also be concluded from the study that when assessing the CO_2 emissions, there is a correlation between the electrical equivalence number and the reduction in CO_2 emissions compared to the stand-alone case. This is however not linear since the different fuels produced replace different fossil energy carriers. By choosing a case in which there is a net gain in the electrical equivalence efficiency there may also be a significant savings in the amount of CO_2 emitted to the atmosphere. There is however a significant saving in CO_2

emissions when the export of bark is possible, a factor with larger impact than the choice of fuel to be synthesised and the type of gasifier used. Please keep in mind that the estimates in this paper are conservative since the used paper and pulp mill is quite efficient compared to existing mills today.

Acknowledgements

The Swedish energy agency (Swedish energy agency) is acknowledged for its financial support under project number P32217-1.

Appendix A

Table A1 – The power generation efficiencies used to calculate electricity equivalent.

Energy carrier	Power generation efficiency	Reference
Biomass	46.2%	Efficiency in IGCC Plant [22]
Bark	46.2%	Efficiency in IGCC Plant [22]
Hot water	10%	Use of Opcon Powerbox [23]
Methanol	55.9%	[24]
DME	55.9%	[24]
Fischer-Tropsch Wax	55.9%	[24]

REFERENCES

[1] Directive 2009/28/EC. On the promotion of the use of energy from renewable sources and amending and subsequently repealing Directives 2001/77/EC and 2003/30/EC.2009.04.23. Official J Eur Union 2009;L140:16.
[2] Tijmensen MJA, Faaij APC, Hamelinck CN, van Hardeveld MRM. Exploration of the possibilities for production of Fischer Tropsch liquids and power via biomass gasification. Biomass Bioenerg 2002;23(2):129–52.
[3] Boerrigter H, Zwart RWR. High efficient co-production of Fischer-Tropsch (FT) transportation fuels and Substitute Natural Gas (SNG) from biomass. Petten: Energy Research Centre of the Netherlands; 2004. 64 pp. ECN-C–;04–001.
[4] Pettersson K, Harvey S. CO_2 emission balances for different black liquor gasification biorefinery concepts for production of electricity or second-generation liquid biofuels. Energy 2010;35(2):1101–6.
[5] Jungbluth N, Frischknecht R, Emmenegger MF, Steiner R, Tuschchmid M. Life cycle assessment of BTL-fuel production: inventory analysis. Uster: ESU-services Ltd; 2007. 110 pp. SES6-CT-2003-502705 D 5.2.7.
[6] Balas process simulation software [Internet] [cited: 2010 Feb 25] http://balas.vtt.fi/.
[7] Aspen plus – AspenTech [Internet] [cited: 2010 Feb 25] http://www.aspentech.com/core/aspen-plus.aspx.
[8] Delin L, Berglin N, Eriksson T, Andersson R, Samuelsson Å, Lundström A, et al. Integrated fine paper mill. Stockholm: STFI; 2005. FRAM Report No. 10.
[9] Andersson E, Harvey S, Berntsson T. Energy efficient upgrading of biofuel integrated with a pulp mill. Energy 2006; 31(10–11):1384–94.
[10] Jönsson J, Algehed J. Pathways to a sustainable European pulp and paper industry: trade-offs between different technologies and system solutions for kraft pulp mills. Chem Eng Trans 2009;18:917–22.
[11] Tunå P. Substitute natural gas from biomass gasification. Malmoe: Swedish Gas Centre; 2008. 65 pp. SGC-R-17-SE.
[12] Hulteberg PC, Karlsson HT. A study of combined biomass gasification and electrolysis for hydrogen production. Int J Hydrogen Energ 2009;34(2):772–82.
[13] Puskas I, Hurlbut RS. Comments about the causes of deviations from the Anderson-Schulz-Flory distribution of the Fischer-Tropsch reaction products. Catal Today 2003; 84(1–2):99–109.
[14] Chen JS. The production of methanol and hydrogen fuel from municipal solid waste. Princeton: Center for Energy and Environmental Studies; March 1995. 247 p. PU/CEES Report No. 289.
[15] Marion CP inventor; Texaco Development Corporation, assignee. Production of Methanol. US patent 3920717. March 24th 1973.
[16] Ohno Y, Yagi H, Inoue N, Okuyama K, Aoki S. Slurry phase DME direct synthesis technology -100 tons/day demonstration plant operation and scale up study. In: Noronha FB, Schmal M, Soura-Aguiar EF, editors. Studies in Surface Science and Catalysis, vol. 167. Elsevier; 2007. p. 403–8. 0167–2991.
[17] Wadsborn R, Berglin N, Richards T. Konvertering av mesaugnar från olje- till biobränsleeldning: drifterfarenheter och modellering. Stockholm: Värmeforsk Service AB; December 2007. 48 pp. Värmeforskrapport 1040.
[18] Larson ED, Consonni S, Katofsky RE, Iisa K, Fredrick Jr WJ. A cost-benefit assessment of gasification-based biorefining in the kraft pulp and paper industry. Princeton: Princeton Environmental Institute; 2006. 152 pp. DE-FC26-04NT42260.
[19] Swedish EPA (Naturvårdsverket) [Internet]. Emission factors and thermal values energy. [cited: 2010 Feb 20] http://www.naturvardsverket.se.
[20] Informationsblad naturgas [Internet] [cited: 2010 Feb 25] http://www.swedegas.se/pub/436/informationsblad%20naturgas.pdf.
[21] Räkna ut dina CO2-utsläpp [Internet] [cited: 2010 Feb 25] http://www.klimatbalans.se/raknaut.html.
[22] Stahl K. The Värnamo demonstration plant. Trelleborg: Berling Skogs; 2001. 133 pp.
[23] Opcon powerbox – emission free electric power. Opcon AB. [Internet] [cited: 2010 Feb 23] www.opcon.se.
[24] Basu A, Gradassi M, Sills R. Use of DME as a gas turbine fuel. New Orleans: ASME Turbo-Expo; 2001. ASME paper no. 2001-GT-0003.

Paper IX

ARTICLE IN PRESS

Applied Energy xxx (2013) xxx–xxx

Contents lists available at SciVerse ScienceDirect

Applied Energy

journal homepage: www.elsevier.com/locate/apenergy

Methanol production from steel-work off-gases and biomass based synthesis gas

J. Lundgren [a,*], T. Ekbom [b], C. Hulteberg [c,d], M. Larsson [e], C.-E. Grip [a], L. Nilsson [f], P. Tunå [d]

[a] Luleå University of Technology, Division of Energy Science, 971 84 Luleå, Sweden
[b] Grontmij AB, Energy and Power, Stockholm, 47303, 100 74, Sweden
[c] Nordlight AB, Limhamn, 30084, 200 61, Sweden
[d] Lund University, Chemical Engineering, 221 00 Lund, Sweden
[e] Swerea MEFOS AB, Division Process Metalurgy, 971 25 Luleå, 812, Sweden
[f] SSAB EMEA, 971 88 Luleå, Sweden

HIGHLIGHTS

- The integration of a methanol synthesis process in steel plants increases the gas utilization efficiency.
- Methanol produced by off-gases from steelmaking combined with biomass show competitive production costs versus petrol.
- The integration of a methanol synthesis process in steel plants may reduce the specific CO_2-emissions of the plant.

ARTICLE INFO

Article history:
Received 26 September 2012
Received in revised form 28 February 2013
Accepted 6 March 2013
Available online xxxx

Keywords:
Methanol production
Steel work off-gases
Biomass gasification
Steel plant

ABSTRACT

Off-gases generated during steelmaking are to a large extent used as fuels in process units within the plant. The surplus gases are commonly supplied to a plant for combined heat and power production. The main objective of this study has been to techno-economically investigate the feasibility of an innovative way of producing methanol from these off-gases, thereby upgrading the economic value of the gases. Cases analyzed have included both off-gases only and mixes with synthesis gas, based on 300 MW_{th} of biomass. The SSAB steel plant in the town of Luleå, Sweden has been used as a basis. The studied biomass gasification technology is based on a fluidized-bed gasification technology, where the production capacity is determined from case to case coupled to the heat production required to satisfy the local district heating demand. Critical factors are the integration of the gases with availability to the synthesis unit, to balance the steam system of the biorefinery and to meet the district heat demand of Luleå. The annual production potential of methanol, the overall energy efficiency, the methanol production cost and the environmental effect have been assessed for each case. Depending on case, in the range of 102,000–287,000 ton of methanol can be produced per year at production costs in the range of 0.80–1.1 EUR per liter petrol equivalent at assumed conditions. The overall energy efficiency of the plant increases in all the cases, up to nearly 14%-units on an annual average, due to a more effective utilization of the off-gases. The main conclusion is that integrating methanol production in a steel plant can be made economically feasible and may result in environmental benefits as well as energy efficiency improvements.

1. Introduction

An integrated steel plant normally consists of various process units, such as coking Plant (CP), Blast Furnace (BF), Basic Oxygen Furnace (BOF), secondary metallurgy, continuous casting, and rolling mill. Most plants also have some auxiliary units on site, for instance, lime kiln, oxygen plant and sinter plant. Process gases are generated from the process units of CP, BF and BOF i.e. Coke Oven Gas (COG), Blast Furnace Gas (BFG) and Basic Oxygen Furnace Gas (BOFG). Typical chemical compositions of the gases are shown in Table 1.

The gases are generally used as fuel in different process units within the plant. It is also quite common to supply the excess to a power plant or combined heat and power plant at the site to utilize the process gases for production of power, process steam and/or heat, which are used internally within the plant and sometimes also for external users in the community. Thus, the energy system for an integrated steel plant is large and complex.

* Corresponding author. Tel.: +46 920 491307.
E-mail address: joakim@ltu.se (J. Lundgren).

0306-2619/$ - see front matter © 2013 Elsevier Ltd. All rights reserved.
http://dx.doi.org/10.1016/j.apenergy.2013.03.010

Nomenclature

Abbreviations

ASU	air separation unit
BF	Blast Furnace
BFG	Blast Furnace Gas
BIOG	biomass based synthesis gas
BOF	Basic Oxygen Furnace
BOFG	Basic Oxygen Furnace Gas
BP	back pressure
CAPEX	capital expenditures
CEPCI	chemical engineering plant cost index
CHP	combined heat and power
COG	Coke Oven Gas
CP	coking plant
DH	district heating
HM	hot metal
HP	high pressure
LHV	lower heating value
LP	low pressure
MeOH	methanol
MILP	mixed integer linear programming
PCI	pulverized coal injection
PI	process integration
V_{syngas}	synthesis gas volume after conditioning
WACC	Weighted Annual Cost of Capital
q_{flared}	flared energy in COG, BFG and BOFG

The process gases have different availabilities and energy densities. The COG has a high heating value (typical LHV 17–18 MJ/N m^3) and is also rich in hydrogen (~60 vol%). The BOFG has a heating value in the range of 6–8 MJ/N m^3 and is rich in carbon monoxide (~60 vol%). It is of great interest to find ways to utilize the excess gases for the production of higher value products, e.g. automotive fuels and/or chemicals instead of production of heat and power. Commercial technology to produce methanol from COG already exists and is of particular progress in China. In 2009, China had a production capacity of approximately 27 Mton of methanol per year, of which COG to methanol accounted for 15% [1].

There is also a possibility to introduce biomass based synthesis gas to blend with the off-gases. This is of particular interest in Scandinavia, which has numerous steel industries and abundant resources of biomass. Li et al. have recently studied the co-utilization of natural gas and biomass for methanol production with beneficial results [2]. Ghanbari et al. have investigated a future integrated steelmaking plant with a polygeneration system to produce methanol as valuable byproduct in addition to heat and electricity. The objective was to minimize the cost of steel production under different boundary conditions, technologies and auxiliary fuels (oil, natural gas and pyrolyzed biomass) [3]. Studies regarding use of steel-work off-gases blended with biomass based synthesis gas can to the authors' best knowledge not be found. Preliminary and more general investigations regarding involvement of biomass in COG based methanol production has however previously been published by authors of this paper [4].

The main objective of this work has been to describe and techno-economically analyze different cases of methanol production from steel-work off gases (COG and BOFG) and biomass based synthesis gas.

Four different methanol production schemes with the following feedstocks have been analyzed:

- Case A: the excess COG and 40% of the available BOFG
- Case B: the excess COG mixed with synthesis gas based on 300 MW_{th} biomass
- Case C: the excess COG, BOFG and synthesis gas based on 300 MW_{th} biomass
- Case D: hydrogen (extracted from the COG via pressure swing absorption) mixed with synthesis gas based on 300 MW_{th} biomass.

Table 1
Composition of the steel-work off gases (vol% dry basis).

Compound	COG	BFG	BOFG
H_2	66	3	4
CO	6	20	58
CH_4	21	0	0
C_2H_6	3	0	0
CO_2	2	24	20
N_2	3	53	18
LHV(MJ/N m^3)	17.5	2.85	7.6

For each case, the annual methanol production potential and efficiency, the overall gas utilization efficiency, the methanol production cost and the environmental effect have been assessed.

2. Materials and methods

An overall process integration model of a steel plant has been used to study the integration of a 300 MW_{th} biomass gasifier, syngas conditioning and a methanol synthesis unit into the plant in order to evaluate the effects on the total energy system. The most important modeling constraints are that the process steam balance and the production of district heating are maintained.

The modeling approach has been an iterative process between the overall process integration model and the detailed process models of the biomass gasification unit, the syngas conditioning and methanol synthesis.

2.1. The process integration model

The model is based on mathematical programming, i.e. Mixed Integer Linear Programming (MILP) and a commercial solver CPLEX has been used. The model structure is represented as a network of nodes and branches, which represent process units and energy/material flows, respectively. The different nodes are connected depending on the input and output to/from each process unit. Each node contains linear equations to express the energy and mass balance required in the process unit. Thus an entire energy system is created.

The current model is based on a previous model version designed for the SSAB EMEA plant [5]. The model core is an overall mass- and energy balance for the production chain and separate sub-balances for the main processes which makes it possible to perform a total analysis for the steel plant and to assess the effect of a change in the operation practice for the different processes. In this work, the modeling system has been extended to include a methanol synthesis unit utilizing the excess of off-gases in some cases combined with synthesis gas produced via biomass gasification.

The process integration model provides the possibility to evaluate the different integration possibilities and the effect on the total energy system. Different technical options to increase or decrease the gas generation have been included in the overall optimization

Please cite this article in press as: Lundgren J et al. Methanol production from steel-work off-gases and biomass based synthesis gas. Appl Energy (2013), http://dx.doi.org/10.1016/j.apenergy.2013.03.010

model. Possibilities to increase the available COG through e.g. increased oxygen utilization in the BF hot stoves [6] and alternative prioritization of the generated COG have been assessed. The effect of changing the BF operation practice through changes in the operation practice e.g. PCI injection rate has also been considered. The objective used in the optimization is minimized flaring and maximized methanol production described according to the objective function:

$$\min z = a\sum q_{\text{flared}} - bV_{\text{syngas}} \quad (1)$$

where q_{flared} is the flared gas energy in BF gas, BOF gas and COG gas. V_{syngas} is the corresponding syngas volume to the methanol synthesis after blending and gas conditioning. The available gas volume varies between the different cases due to the integration effects between the methanol production and power plant and possible gas prioritization within the steel plant.

The possible integration points between the existing power plant and the methanol production unit is through HP steam surplus, district heat production and tail gas from the methanol synthesis. The HP steam is assumed to be able to be integrated directly into the existing steam cycle. The maximum fuel to the boiler is set at 320 MW but the actual amount is limited by the steam cycle. The total district heat production from the system is 753 GW h. The power plant produces heat and electricity in back-pressure and condensing modes. If the back-pressure load is insufficient further condensing-mode electricity production is possible. The electricity generation is limited to 96 MW (both back-pressure and condensing mode operation).

The district heat is supplied either through the power plant back-pressure operation or from the methanol production system. A decreased heat demand from the back-pressure operation limits the recovered process gases at the power plant, resulting in increased flaring.

2.2. The biomass gasifier model

The model is based on pressurized, oxygen-blown bubbling fluidized-bed gasification technology, 300 MW_{th}. The benefits include fuel flexibility and high cold gas efficiency. The drawbacks are need for tar and methane reforming. Therefore, a reformer has been included and raw gas cleaning with hot gas cyclone and filter and water scrubber. Also the gas is cooled from about 900 °C producing high pressure steam. The product is a reformed gas which is cooled and cleaned from most alkali, ammonia, chlorides, metals, tars and particles. The model is based on budget quotations from suppliers which have been integrated also for the steam diagram to complete the material and energy balances, as further described in [7].

2.3. Modeling gas cleaning and conditioning

After gasification, the gas is purified and conditioned. Initially, the temperature of the gas is lowered to 400 °C to allow for filtration. After filtration the tar content of the gas is removed and any methane in the gas is reacted in a reforming step with oxygen addition [8]. In cases B and C, the COG and COG with BOFG is mixed into the biomass-generated gas upstream of the reforming step. The gases are cooled and the high-quality heat is used for steam generation. Thereafter the gases are controlled to the desired set-point in producing methanol, a CO:H_2-ratio slightly above 2, using a water–gas shift reactor. This shift is operated as a high-temperature water–gas shift reactor. To control the ratio, the gases are split and one stream is passed through the reactor, shifting it to equilibrium whilst the other stream is bypassed [9]. The residual heat is used for steam and district heat generation upon cooling for a Rectisol® CO_2 removal.

The Aspen Plus model consists of the most important unit operations. The reformer is modeled as an adiabatic reactor that minimizes the Gibbs free energy. The conversion of methane and lower hydrocarbons is high under the simulated conditions. Following the reformer is a water gas shift reactor. This reactor is modeled as an adiabatic equilibrium reactor. After the shift reactor, the gas is cooled down and CO_2 is removed in a Rectisol process. A multistage compressor with 70 °C intercooling is used to compress the synthesis gas to 100 bar prior to the methanol synthesis reactor. The recycle ratio is set to 4:1. A second compressor is used for the recycled gas. The methanol reactor is modeled as an adiabatic equilibrium reactor. Heaters/coolers are used wherever necessary.

The methanol synthesis is traditionally performed in a packed-bed catalytic reactor operating at elevated pressure. The catalyst used is most commonly based on copper and aluminum oxides [10]. Due to equilibrium reasons, unreacted feedstock is looped for economic reasons. For the purpose of this simulation, the reaction has been performed at 100 bar pressure and the recycle is set to 3, with a reactor pressure drop of 8 bar. The reactor operates adiabatically with a temperature increase of 210 °C. After passing through the reactor, the gas stream is cooled to condense the formed methanol and the non-condensable gas is recycled; part of the recycle is bled off to avoid accumulation of inerts. The condensed methanol is further purified via distillation in two columns, where it is further separated from water and other trace impurities. In addition to methanol production, high-pressure steam (86 bar 300 °C), low-pressure steam 15 bar 200 °C) and district heating are also produced.

2.4. Economic analysis

The economic analysis is based on certain key parameters resulting in a final valuation of the competitiveness of methanol production for the selected plant size. All processes are commercially available at full scale except for biomass gasification which adds some uncertainty. Adding to the production cost is the distribution cost for a correct comparison with fossil fuels and alternative fuels.

As a basis for these calculations certain financial parameters have been specified together with prices of raw material and products, see Tables 2 and 3. The plant produces steam, tail gas and heat which are all sold at assumed market prices for the companies in Luleå.

The investment cost (CAPEX) has been assessed based on conducted studies, third party supplier budget quotations and in-house database information, which have been updated to the first quarter of 2012 and scaled to the studied plant sizes using generally accepted factors. Increases in material prices and engineering costs have been included in the calculations by means of indexation, using generally accepted indices (CEPCI).

Table 2
Assumed financial parameters.

Factor	Value	References
Exchange rate, SEK/USD	6.847	[11]
Exchange rate, SEK/EUR	8.929	[11]
Interest rate	6.0%	Assumption
Equity part of CAPEX	40%	Assumption
Loan part of CAPEX	60%	Assumption
Equity return	10%	Assumption
Weighted Annual Cost of Capital (WACC)	7.60%	Assumption
Project lifetime	20 years	Assumption
Yearly hours of production, methanol	8000	Assumption
Yearly hours of production, heat	5500	Assumption

Please cite this article in press as: Lundgren J et al. Methanol production from steel-work off-gases and biomass based synthesis gas. Appl Energy (2013), http://dx.doi.org/10.1016/j.apenergy.2013.03.010

Table 3
Costs and prices of raw materials and products.

Factor	Value	References
Biofuel, wood chips	22.4 EUR/MW h	[12]
Electricity, purchase price	62.7 EUR/MW h	[13]
COG, purchase cost	22.4 EUR/MW h	Assumption
Tail gas, selling price	22.4 EUR/MW h	Assumption
Steam, selling price	30.8 EUR/MW h	Assumption
Heat, selling price	16.8 EUR/MW h	[14]

2.5. Case descriptions

The SSAB EMEA steel plant in the town of Luleå in Sweden has been used as case basis. The steel plant is based on the BF/BOF route and an annual steel production level of 2.1 Mton of steel slabs has been chosen. The Blast Furnace (BF) is operated with 100% iron-ore pellets, and is equipped with pulverized coal injection (PCI), normally around 150 kg/t HM (tonne hot metal). The CP produces the majority of the coke used in the BF. There are two Basic Oxygen Furnaces (BOFs converters) in the system, operated with hot metal from the BF and a small amount of scrap. The crude steel is further treated in the alloying processes, CASOB and the RH-vacuum degasser. The steelmaking is followed by two continuous casters. The slabs are transported 850 km south by train to the rolling mill located in the town of Borlänge. The steel work gases are used internally as primary fuel; the CP is under-fired with pure COG, and the hot stoves for the BF are fired with a mixture of BFG and COG. The COG is also used as fuel in various burners at the steel plant as well as for primary fuel in a steam boiler and in a lime furnace. Since the rolling mill is located at another geographical location, a surplus of process gases arises. The surplus is therefore used as primary fuel in a combined heat and power plant (CHP), producing steam, heat and electricity. The produced power is used within the steel plant system and the heat covers a main part of the annual heat demand of the community. Drying gas from the power plant is also delivered to a nearby wood-pellet plant. There are large seasonal variations of the district heat load for the municipality. The heat load capacity has a peak of 220 MW_{th} during winter and a low of just 20 MW_{th} during summer.

For each case, the gas utilization efficiency has been calculated. When using mixed energy carriers, efficiency calculations are helpful but not necessarily an appropriate indicator of the "best" system. The electricity equivalents method is therefore used in this paper to represent the overall exergy of the system. It is calculated using power generation efficiencies [15], using the best available technology to the knowledge of the author's, see Table 4. To exemplify, the methanol efficiency would be calculated by first determining the amount of electricity equivalents that are fed to the system, in the form of biomass, steel-plant gases and electricity. Thereafter the electricity equivalence number of the methanol is determined and, to yield the efficiency, it is divided with the feed number.

The most critical factors are the integration of the gases with availability to the synthesis unit, to balance the steam system of the biorefinery and to meet the district heat demand of the city. The four evaluated cases are described below.

Table 4
Electricity equivalence number for various energy carriers in the system.

Energy carrier	Power generation efficiency (%)	References
Biomass, COG and BOFG	46.2	[16]
Hot water	10.0	[17]
Methanol	55.9	[16]

2.5.1. Case A – COG and BOFG

In Case A, the excess COG (656 GW h) and 40% of the BOFG (191 GW h), totally 847 GW h of gas per year is used for methanol production. Energy and material flows are illustrated in Fig. 1. Additional COG is made available by introduction of oxygen enrichment of the hot stoves firing liberating COG, further reprioritization among the COG users. The CHP is operated on the excess of the steel plant gases BFG and BOFG. The steam and heat generated from the MeOH synthesis is integrated with the CHP. The CHP supplies district heat to the community of 753 GW h annually (sold district heating in the year 2006).

2.5.2. Case B – COG mixed with biomass synthesis gas

In this case, synthesis gas based on 300 MW_{th} biomass is mixed with COG as shown in Fig. 2. The considered biomass gasification technology is based on a fluidized bed gasifier unit, where the production capacity is determined by the heat production required to satisfy the local district heating demand. The CHP is operated on the excess of BFG and BOFG. The steam and heat generated from the MeOH synthesis and the gasifier is supplied to the existing CHP cycle.

2.5.3. Case C – COG, BOFG and biomass based synthesis gas

In Case C, also the BOFG is utilized for the methanol production, see Fig. 3. The same amount of COG is utilized as in the Cases A and B. Additional BOFG of 492 GW h is introduced to the MeOH synthesis together with the biomass based synthesis gas. The CHP is fueled by the BFG. In this operational mode the CHP is operated close to the lower limit of heat value of fuel gas.

2.5.4. Case D – extraction of the hydrogen

In this case, the hydrogen is separated from the COG and then mixed with the biomass synthesis gas as shown in Fig. 4. Hydrogen is separated from the COG by pressurized swing absorption technique. The separated H_2 corresponds to 207 GW h. The resulting tail gas is fired in the CHP plant together with BFG and BOFG.

3. Results

Fig. 5 shows the annual production capacities and the methanol efficiencies for the different cases.

Case A results in the smallest production capacity (102,000 ton) but the highest methanol efficiency (70% calculated on an electricity equivalence basis). In Case B, the potential production increases significantly (236,000 ton) but results in a lower efficiency, close to 56%. In Case C, the methanol production increases to 287,000 ton per year with a slightly higher efficiency than in Case B (57%). In Case D, 195,000 ton of methanol per year are produced, but with the lowest efficiency, only 43%. As shown in Table 5, the different cases have different outputs of the other energy carriers. When relating them to the produced methanol amount, the differences in steam production are low, and the only major outlier is the district heat production in Case A, which is unusually low. This is also mirrored in the high methanol efficiency.

3.1. Total site analysis

Table 6 shows the resulting gas balance for the system including gas utilization at the CHP and in the methanol production.

In Case A, the total amount of fuel gases to the CHP plant decreases from 2281 GW h to 2128 GW h. The energy in the fuel gases is however still enough to maintain the DH production. The total flaring of process gases decreases to 131 GW h. The decreased flaring and change in utilization of the fuel gas influences the total energy efficiency of the CHP and the combined efficiency based on

Please cite this article in press as: Lundgren J et al. Methanol production from steel-work off-gases and biomass based synthesis gas. Appl Energy (2013), http://dx.doi.org/10.1016/j.apenergy.2013.03.010

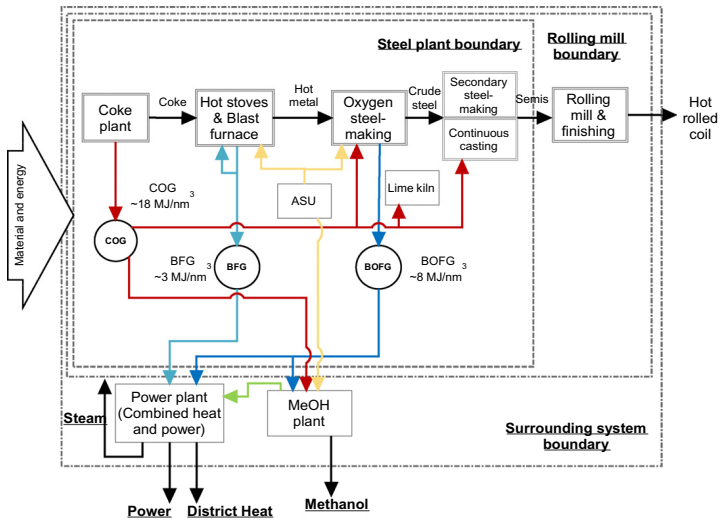

Fig. 1. System configuration in Case A.

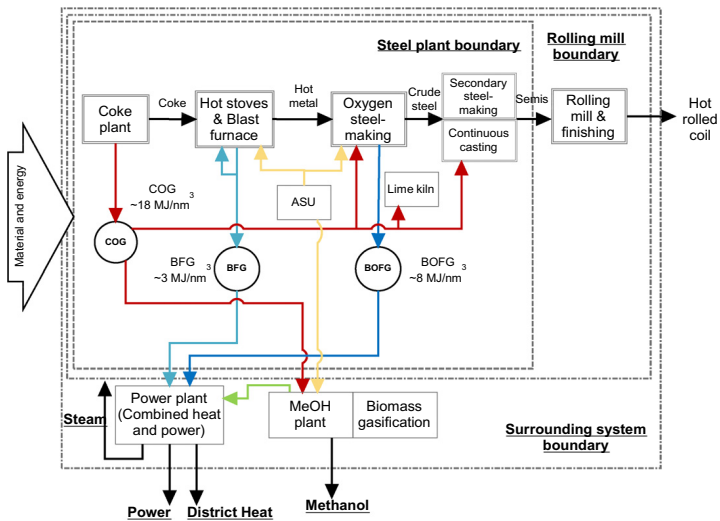

Fig. 2. System configuration in Case B.

methanol, heat and power. The total efficiency increases to 67% as the increased use of COG in methanol production decreases the flared gas amounts, see Table 6.

In Case B, significant amounts of HP steam is recovered from the methanol production, which is supplied the existing steam cycle at the CHP. The steel plant gases supplied to the CHP decreases to 1714 GW h, but the tail gas from the MeOH synthesis is instead added. The recovered HP steam from the synthesis influences the steam cycle of the power plant limiting the amount of off-gases possible to recover. This results in an increased flaring of the

Please cite this article in press as: Lundgren J et al. Methanol production from steel-work off-gases and biomass based synthesis gas. Appl Energy (2013), http://dx.doi.org/10.1016/j.apenergy.2013.03.010

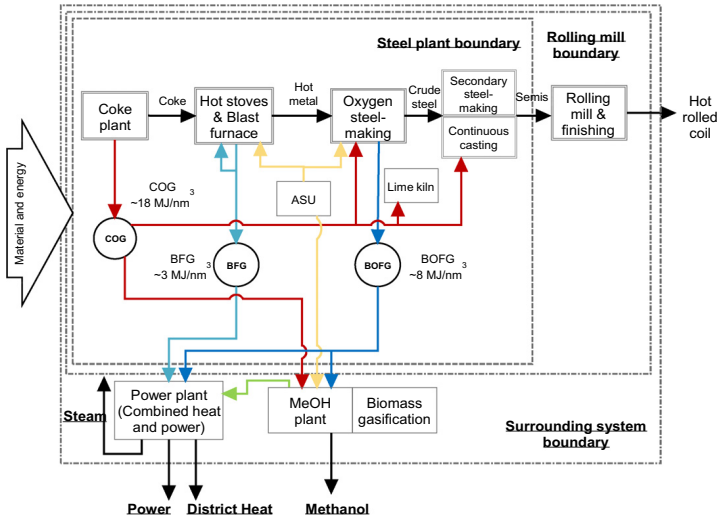

Fig. 3. System configuration in Case C.

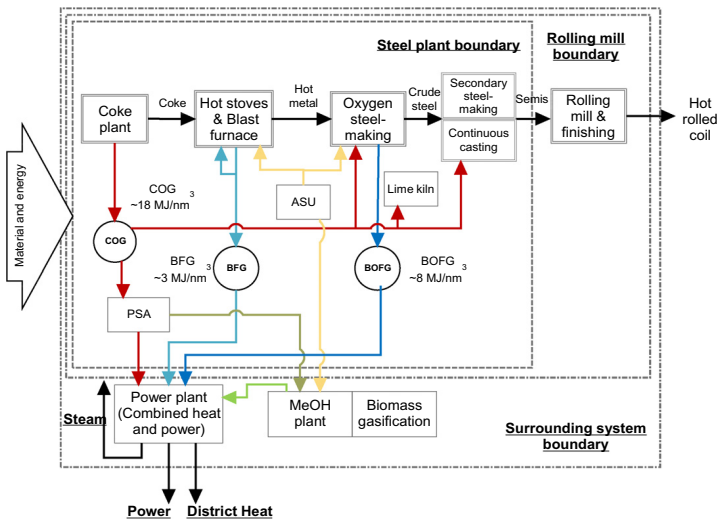

Fig. 4. System configuration in Case D.

off-gases, but anyway increased gas utilization efficiency compared to the reference system.

In Case C, an additional 492 GW h of BOFG is supplied for methanol production. In this case the largest amount of HP steam is supplied to the CHP. The effect of utilizing the BOFG in methanol production can be seen on the amount of gases flared. The total efficiency increases to 65%. The increased HP steam amount supplied to the power plant and the increased DH production from

Please cite this article in press as: Lundgren J et al. Methanol production from steel-work off-gases and biomass based synthesis gas. Appl Energy (2013), http://dx.doi.org/10.1016/j.apenergy.2013.03.010

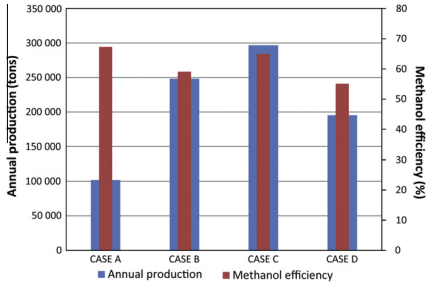

Fig. 5. Annual methanol production capacities and efficiencies. Blue bars show the production capacities and red bars illustrate the methanol production efficiencies. (For interpretation of the references to colour in this figure legend, the reader is referred to the web version of this article.)

Table 5
Steam, district heating and tail gas outputs of the different cases.

Case	HP steam (kg/s)	LP steam (kg/s)	District heating (MW)	Tail gas (MW)
A	3.9	3.7	3.5	17.8
B	15.5	8.1	30	52
C	19.8	10.1	28.4	54.7
D	13.6	6.2	29.1	41.6

Table 6
Gas utilization (GW h/yr).

	Ref. 2006	Case A	Case B	Case C	Case D
Power plant					
Fuel gas	2281	2128	2230	1956	2288
BFG	1655	1652	1652	1390	1472
BOFG	389	301	62	0	0
COG	237	0	0	0	207[b]
Tailgas MeOH	0	161	503	552	426
HP steam					
MeOH	0	99	418	558	389
Gases MeOH					
COG	0	656	656	617	207[a]
BOFG	0	191	0	492	0
BIOG	0	0	2006	2006	2006
Energy products					
DH MeOH	0	32	290	287	298
DHCHP	753	722	463	467	455
DH total	753	753	753	753	753
Power BP	331	326	204	205	200
Power Cond.	272	307	637	636	641
MeOH	0	704	1630	1985	1344
Losses					
Flared gases[b]					
Total	392	131	561	432	830
BFG	169	66	66	328	246
BOFG	157	55	485	55	546
COG	67	10	10	50	37
Efficiency[c]	50.7%	67.3%	59.1%	65.0%	55.1%

[a] H_2 free COG.
[b] H2 rich COG.
[c] For security reasons, also COG is needed when flaring BFG. (power + -DH + MeOH)/(gas flare + gas CHP + gas MeOH).

the MeOH synthesis results in higher condensing power production operation.

In Case D, the tail gas from the PSA mainly containing CH_4 and CO is fired in the CHP plant together with the tail gas from the MeOH synthesis. The DH production from the MeOH synthesis and the HP steam recovered results in increased condensing power production. The corresponding total efficiency decreases to 55%.

In Cases B, C and D, the total power production increases to a maximum, close to 840 GW h, resulting in limitation in the recovery of process gases. In Case A there is still possibility to utilize more process gases.

Taking into account the amount of flared gases, the overall gas utilization efficiencies become 67.3%, 59.1%, 65.0% and 55.1% for Cases A–D, respectively.

3.2. Economics

The investment cost has been based on an extensive in-house database with budget quotations, which have been updated to 2Q 2012 and scaled to the studied plant size. The investment cost for the parts has thus been assessed by using in-house information and applying accepted factor and index methods for updating. Due to the rapid fluctuations in steel material and engineering costs the last few years, scaling using relevant indices (CEPCI index, etc.) has been applied to include these changes.

The costs are presented for Cases A–D where every process island has been calculated as a turn-key delivery, i.e. including erection and civil works. In addition, the balance of plant completes the plant. This part includes all the adjacent parts of the plant which do not belong to a specific process island, for example buildings, pipe racks, power supply, etc. Table 7 shows a summary of the calculated investment costs.

The direct costs includes process equipment, bulk material as piping, electrical equipment, instrumentation, tracing and insulation, pipe racks and steel structures, painting, technology and license fees, civil works and erection works, roads and areas for handling of biofuels, spare parts to important process equipment and transportation to the construction site.

One of the most important economic factors is the production cost. It gives an evaluation of how profitable a production of methanol would be for a given capacity of the plant. The production cost has been calculated, where revenues, e.g. district heat which is exported have been accounted for. The production cost is given in EUR per petrol equivalent liter, where the unit cost is adjusted for the differences in the heating value and density of petrol and methanol. The cost of capital is calculated with an annuity of 7.60%. Table 8 shows the resulting production costs for the different cases.

As shown, Cases A, B and C show similar methanol production costs, while Case D is the most expensive case.

3.3. Environmental analysis

Converting all the incoming carbon of the different coal types into CO_2, 3.457 Mton of CO_2 is generated in the reference case, partly emitted in the steel plant partly in the CHP plant. The specific CO_2 emission (calculated as total carbon as CO_2 divided by

Table 7
Summary of calculated investment costs, in MEUR.

Investment cost	Case A	Case B	Case C	Case D
Direct costs	115	355	376	321
Indirect costs including unspecified[a]	48	138	150	118
Total costs	162	493	526	439

[a] Includes costs such as project administration and development, legal permits, engineering, interest during erection, insurance, working capital etc. Unspecified costs with own estimations includes startup, functional testing before commercial production, temporary equipment, spare parts and storages.

Please cite this article in press as: Lundgren J et al. Methanol production from steel-work off-gases and biomass based synthesis gas. Appl Energy (2013), http://dx.doi.org/10.1016/j.apenergy.2013.03.010

Table 8
Estimated production costs for the Cases A–D.

Production cost	Unit	Case A	Case B	Case C	Case D
Operational cost	MEUR/year	39	112	115	98
Capital cost	MEUR/year	16	49	52	43
Production cost	EUR/MW h	92	92	90	119
Production cost	EUR/ton	511	508	498	658
Petrol eq. liter	EUR/liter	0.82	0.82	0.80	1.06

the steel production) is 1.641 ton/ton of slabs. Summarized results of the different Cases A–D are shown in Table 9.

As shown in the table, the coal and iron-ore pellet use is more or less constant in all the cases. There is a slight reduction in coal demand and pellet use in the Cases A–D compared to the reference case due to that the new operation practice suggested with O_2 enriched combustion air in the hot stoves results in a minor efficiency improvement. In turn, this results in a small reduction in coal use and consequently reduced CO_2 emissions. The specific CO_2 emissions for the different cases are shown in Fig. 6 indicating that the emission for the system decreases slightly with the integration of methanol production. The specific CO_2 emission for the steel plant is as lowest in Case A as an effect of the decreased flaring of excess gases.

As the total emissions of CO_2 decreases from the system, at the same time as methanol is produced, the methanol product should be considered as carbon neutral.

4. Discussions

Integration of a biomass gasifier with a steel plant and its off-gases gives several possibilities and opportunities for adding value to the steel production with new revenues of a high value liquid methanol fuel product. One important integration benefit is that the steel production will not be influenced by operational interruptions in the gasification and synthesis plant. Similarly, the methanol production can partly continue even if the supply of off-gases is interrupted. At the same time it gives many variables and one of the distinguishing factors is to size the biorefinery, not only from a technical perspective but foremost for the economic performance and the competitiveness of the product on an emerging biofuel market. The first criterion is the fuel availability, which at Luleå is not a limiting parameter concerning biomass fuels, as the region is rich in forest fuels. Though, there is an integration on the capacity of available off-gases which then determines partly the size of both up- and downstream processes. It shall be stated that the gasifier capacity used in this study has not been optimized, which is apparent in the cases where the gas flaring actually increase.

The second criterion is to estimate the smallest possible size – justifying integration rather than having a stand-alone biorefinery – and still achieve a production cost which is competitive with

Table 9
Summary of main material flows.

	Ref. 2006	Case A	Case B	Case C	Case D
Coal (kton/a)	1393	1391	1391	1391	1391
Iron ore pellets (kton/a)	3196	3193	3193	3193	3193
External scrap (kton/a)	6	6	6	6	6
Biomass syngas (GW h/a)	0	0	2190	2190	2190
Slabs (kton/a)	2106	2106	2106	2106	2106
Power surplus (GW h/a)	60	0	0	58	99
Power (deficit) (GW h/a)	0	1	10	0	0
District heat (GW h/a)	753	753	753	753	753
Methanol (kton/a)	0	98	270	282	245
Surplus gas (GW h/a)	392	131	1395	1160	1444
CO_2 (kton/a)	3457	3392	3395	3392	3392

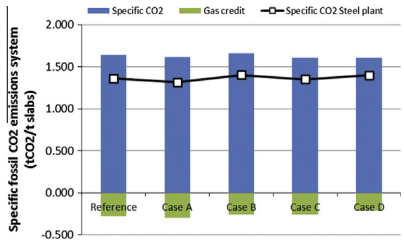

Fig. 6. Specific CO_2 emissions per ton of steel slabs (fossil sources).

other biofuels – and fossil fuels. The latter because the methanol product has highest value as a blend-component in petrol and if no tax exemption will be available then the fuel will compete with fossil based methanol and petrol. This is important as the new Renewable Energy Directive from EU demands declaration on sustainability, which then gives a decision on tax exemption. The current methanol price is about 320 EUR/ton [18] which translates into about 56 EUR/MW h. The value for heat is much smaller and in addition, the heat demand may also be less than 5000 h. The economic conclusion is therefore to focus on (large) methanol production.

Modern natural gas based methanol plants are so called mega plants with annual outputs of >1 Mton or about 2800 ton per day. In Case C roughly 1000 ton per day are produced corresponding to one third of the production of a mega plant. On the one hand, if the plant shall be competitive, it should be essentially larger. On the other, a larger plant will put strain on biomass logistics. A fuel input of 300 MW_{th} equals ca 1 Mton per year of wood – a substantial amount. In the case of full tax exemption, the sales value would be 134 EUR/MW h (including distribution cost and margins). With such value the biorefinery would not need to be super-large. However, bioethanol or other similar fuel would be closest competitor and ultimately it is the production cost of modern-sized bioethanol plants and the bioethanol market that gives the sales cost for the methanol.

For the steel plant the closest question is the current value of the gas with combustion in the CHP plant for power and heat production contra production of methanol. At the same time the steam cycle of the CHP plant must be balanced against the variations in heat load to minimize need for flaring when there is no use of the off-gases. In summary, there are too many variables and too little known information to make a decisive recommendation on even close optimum values. The export of carbon in coke oven and/or BOF gas can influence the need for emission rights and the economic evaluation.

Taking it from the biomass side of 300 MW_{th} fuel input and other studies for biorefinery production costs gives a production volume that is deemed tentatively feasible. This will give a starting point for a process that is iterative at best and also will depend on location and market.

5. Conclusions

The main objective of this project has been to carry out a techno-economic analysis of the production of methanol from steel-work off-gases, with and without synthesis gas from biomass gasification.

Depending on case, in the range of 102,000–287,000 ton of methanol can be produced per year to costs in the range of 498–658 EUR per ton under the assumed conditions. Translated

Please cite this article in press as: Lundgren J et al. Methanol production from steel-work off-gases and biomass based synthesis gas. Appl Energy (2013), http://dx.doi.org/10.1016/j.apenergy.2013.03.010

to petrol equivalents, the range is in between 0.80 and 1.06 EUR per liter. The lowest production cost is found in Case C, while the hydrogen separation case (Case D) results in the highest production cost. Case C also has the highest methanol production rate. Additionally Case A, where no biomass synthesis gas is involved, reaches the highest methanol efficiency, 70%. From an energy point of view, Case A may be considered as the most promising production case and compared to the current CHP production (reference case 2006), the overall energy efficiency increases by 13% points.

From a systems analysis perspective, the following conclusions can be drawn:

- Methanol synthesis integrated with the steel plant system (Cases A and C) is feasible and shows great potential to improve the total gas utilization in the steelwork system.
- The integration effect of a methanol synthesis unit based on the steelworks gases (Case A) shows more efficient gas utilization than the current situation for SSAB in Luleå.
- Integrating of biomass gasification technology will influence the utilization of the off-gases significantly. The flaring increases, although the total gas utilization efficiency is higher compared to the reference system with production of heat and power.

The main conclusion is therefore that integrating methanol production in steel plants can be made economically feasible and may result in energy efficiency improvements as well as CO_2-emission reductions. Case A (no biomass) and Case C (including biomass) are the most interesting production cases and deserve further investigations.

Acknowledgements

The authors greatly acknowledge the financial contribution of the Swedish Energy Agency and SSAB EMEA. The authors would also like to thank Bio4Energy, a strategic research environment appointed by the Swedish government, for supporting this work.

References

[1] Research In China. China Methanol Industry, Report, 2009–2010. TCY011; 2010.
[2] Li H, Hong H, Jin H, Cai R. Analysis of a feasible polygeneration system for power and methanol production taking natural gas and biomass as materials. Appl Energy 2010;87:2846–53.
[3] Ghanbari H, Helle M, Saxen H. Process integration of steelmaking and methanol production for suppressing CO_2 emissions – a study of different auxiliary fuels. Chem Eng Process: Process Intensificat 2012;61:58–68.
[4] Lundgren J, Asp B, Larsson M, Grip C-E. Methanol production at an integrated steel mill. In: Proc. of the 18th International congress of chemical and process engineering, 24–28 August, 2008, Prague, Czech Republic; 2008.
[5] Larsson M, Dahl J. Reduction of the specific energy use in an integrated steel plant: the effect of an optimisation model. Isl J Int 2003;43(10):1664–73.
[6] Wang C, Karlsson J, Hooey L, Bodén A. Application of oxygen enrichment in hot stoves and its potential influence on the energy system in an integrated steel plant. In: Proc. of the world renewable energy conference (WREC) 2011, May 8–13, Linköping, Sweden; 2011
[7] Ekbom T, Brandberg Å, Boding H, Ahlvik P. BioMeeT II – stakeholders for biomass based methanol/DME/power/heat energy combine. Swedish Energy Agency and European Commission, Altener II Report, Contract No. 4.1030/C/00-014, Stockholm; 2003.
[8] Albertazzi S, Basile F, Brandin J, Einvall J, Fornasari G, Hulteberg C, et al. Effect of fly ash and H_2S on a Ni-based catalyst for the upgrading of a biomass-generated gas. Biomass Bioenergy 2008;32:345.
[9] Albertazzi S, Basile F, Brandin J, Einvall J, Hulteberg C, Fornasari G, et al. The technical feasibility of biomass gasification for hydrogen production. Catal Today 2005;106:297–300.
[10] Ertl G, Knözinger H, Schüth F, Weitkamp J, editors. Handbook of heterogeneous catalysis. John Wiley & Sons; 2008. ISBN 978-3-527-31241-2.
[11] The Swedish Riksbank. Exchange rates; 2012 [accessed 03.15.12]
[12] Swedish Energy Agency. Wood fuel and peat prices. Statistical report ; 2012 [accessed April 2012].
[13] Nordpool. Electricty spot price; 2012. <http://www.nordpool.se>. [accessed April 2012].
[14] LuleKraft AB. Information from the district heating producer LUKAB;2012.
[15] Larson ED, Consonni S, Katofsky RE, Iisa K, Fredrick Jr. A cost-benefit assessment of gasification-based biorefining in the kraft pulp and paper industry. Princeton: Princeton Environmental Institute; 2006. p. 152, DE-FC26-04NT42260.
[16] Stahl K. The värnamo demonstration plant. Berling Skogs: Trelleborg; 2001. p. 133.
[17] Opcon powerbox – emission free electric power. Opcon AB; Cited February 2010 <www.opcon.se>.
[18] ICIS pricing, Reed business information limited. 2012. January report on methanol contract prices in Europe; 2012. <http://www.icispricing.com/> [accessed January 2012]

Please cite this article in press as: Lundgren J et al. Methanol production from steel-work off-gases and biomass based synthesis gas. Appl Energy (2013), http://dx.doi.org/10.1016/j.apenergy.2013.03.010